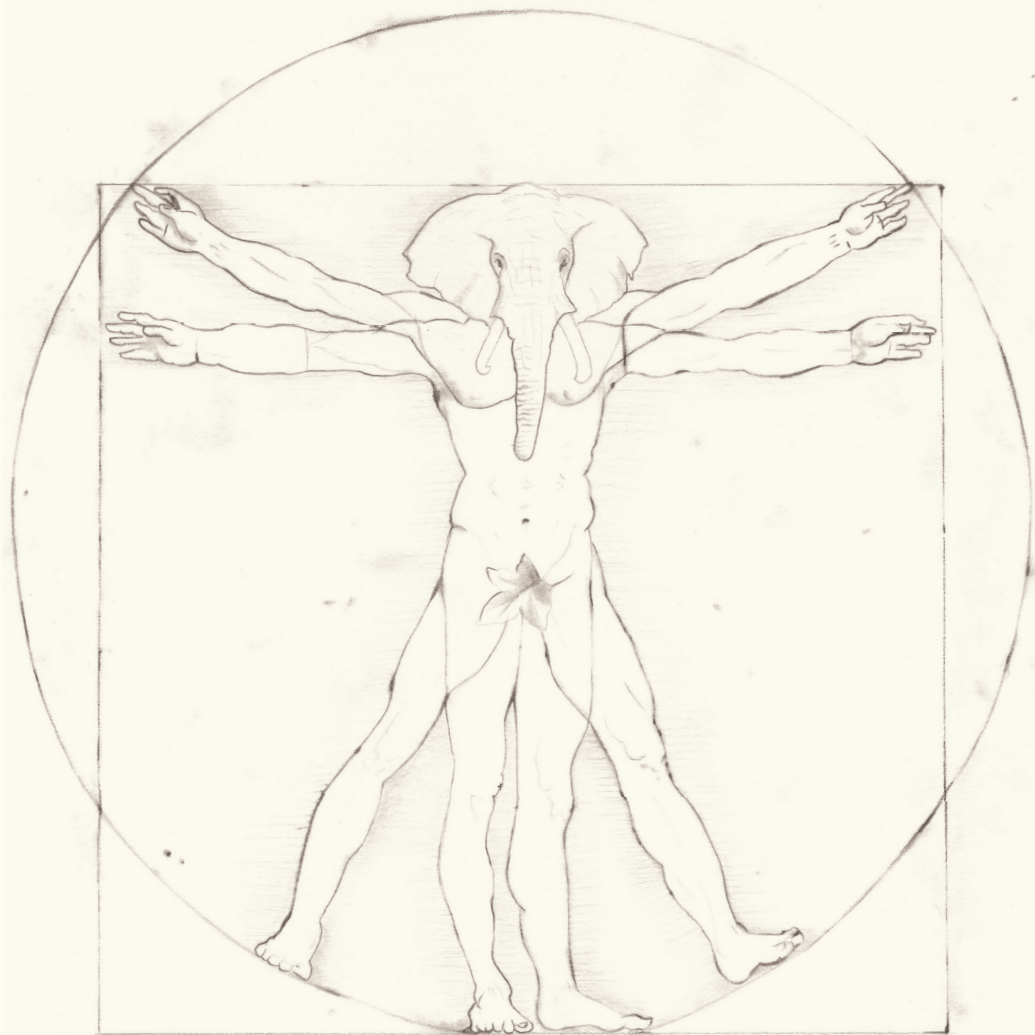


*The role of hypoxia and metabolism
in the pathogenesis of
systemic sclerosis*



Andrea Ottria

*The role of hypoxia and metabolism in the
pathogenesis of systemic sclerosis*

Andrea Ottria

ISBN: 978-94-6380-841-5

Design by: Andrea Ottria & Nadia Vazirpanah

Cover by: Nazanin Vaziranah, NazArtWorks

Printed by: ProefschriftMaken, www.proefschriftmaken.nl

© Andrea Ottria, 2020

All rights reserved. No part of this thesis may be reproduced or transmitted in any form or by any means without the prior permission of the author. The copyright of the articles that have been published have been transferred to the respective journals

The role of hypoxia and metabolism in the pathogenesis of systemic sclerosis

De rol van hypoxie en metabolisme in de pathogenese van sclerodermie

(met een samenvatting in het Nederlands)

Proefschrift

ter verkrijging van de graad van doctor aan de
Universiteit Utrecht
op gezag van de
rector magnificus, prof.dr. H.R.B.M. Kummeling,
ingevolge het besluit van het college voor promoties
in het openbaar te verdedigen op

woensdag 10 juni 2020 des ochtends te 10.30 uur

door

Andrea Ottria

geboren op 5 april 1987
te Genova, Italië

Promotor:

Prof. dr. T.R.D.J. Radstake

Copromotor:

Dr. W.K. Marut

Table of contents:

Chapter 1: Introduction (page 6)

Chapter 2: Hypoxia and TLR9 activation drive CXCL4 production in systemic sclerosis pDCs via mtROS and HIF-2a (page 26)

Chapter 3: Hypoxia and TLR3 activation drive CXCL4 production via HIFs in systemic sclerosis patient moDCs (page 56)

Chapter 4: Inhibition of HIF-2a reduces pro-inflammatory cytokine production in plasmacytoid dendritic cells (page 80)

Chapter 5: CXCL4 drives fibrosis by promoting several key cellular and molecular processes. (page 96)

Chapter 6: Fatty acid and carnitine metabolism are dysregulated in Systemic sclerosis patients (page 134)

Chapter 7: mTOR inhibition by metformin impacts monosodium urate crystal induced inflammation and cell death in gout: a prelude to a new add-on therapy? (page 160)

Chapter 8: Discussion (page 196)

Chapter 9: Summary (page 206)

Dankwoord (page 216)

List of publications (page 220)

Curriculum vitae (page 224)

Introduction

Systemic Sclerosis

Systemic sclerosis (SSc) is a rare and chronic pathological condition of which the aetiology is still poorly understood. SSc is clinically associated with fibrosis, vascular abnormalities and immune alterations. In addition to the skin, internal organs and in particular guts, lungs, heart and kidneys can be affected by the disease¹. The incidence of SSc varies around the world from 7 cases per 100.000 inhabitants in Norway to 44 cases per 100.000 inhabitants in Canada per year. Women are mostly affected with a ratio female/male of 3:1 in Norway and 15:1 in USA and most of the patients have an age at the time of the diagnosis between 30 and 60 years².

SSc was firstly described in Napoli in 1753 by Carlo Curzio³ while working at the Ospedale degli incurabili (hospital for untreatable) and later in 1836 named skleroderma generale by Giambattista Fantonetti⁴. Skleroderma is the combination of two Greek words: Sklerosis (=hard) and Dermis (=skin), as the main clinical characteristic of SSc is skin fibrosis¹.

Fibrosis is a process where the fibrotic connective component of a tissue (mainly collagen) exceeds the physiological quantity⁵. Fibrosis occurs mainly as a response to chronic inflammatory reaction, for example after persistent infections or tissue injury⁵. The response can also occur when the body identifies a foreign body (corpus alienum). Another example is the presence of prosthesis which could be recognized as a foreign body by the immune system and it will face a process of encapsulation until it is isolated in a “virtual” space outside of the body. The aim of fibrotic processes is to protect from “danger” by isolating “unrecognizable” and foreign bodies outside of the body. At the same time, a tissue that becomes fibrotic will lose its physiological function in exchange of serving solely as a “barrier”⁶.

In SSc, the extension of the skin fibrosis is used as a parameter to classify patients. The classification knows three different patterns:

- non-cutaneous (ncSSc),
- limited cutaneous (lcSSc) and
- diffuse cutaneous (dcSSc).

Patients with ncSSc do not have skin involvement, while lcSSc and dcSSc have skin involvement. In the case of lcSSc, the skin involvement regards the face and arms, and legs till the elbow and knee. The skin involvement of patients with dcSSc can involve all the skin of the body, including chest and back^{1,7}. In the majority of the patients with SSc, Raynaud phenomenon (RP) is the first visible symptom⁸. RP is a vasospasm that leads to whitening of the fingers (of hands or feet). Eventually, this can be followed by a blue phase, where the fingers become blue and finally the colour of the fingers become red as the vasospasm ends⁹. Generally, patients will start to develop skin fibrosis years after the RP. Each patient develops skin fibrosis with a different pattern, some will develop it immediately as dcSSc, while other will first develop a lcSSc-like pattern and eventually progress towards a dcSSc-like pattern; while others will never develop skin fibrosis. Given the disease heterogeneity and the distinct sequence in which the symptoms are manifested, diagnosis of the disease remains a challenge. Therefore, there are criteria set according to which the specialists can diagnose the disease. The last version of the criteria is the 2013 American College of Rheumatology (ACR) and European League Against Rheumatism (EULAR) criteria for SSc¹⁰ (resumed in table 1).

Table 1 ACR/EULAR criteria for SSc

Item	Sub-item	Score
Skin thickening of the fingers of both hands extending proximal to the metacarpophalangeal joints (sufficient criterion)	-	9
Skin thickening of the fingers (only count the highest score)	Puffy fingers	2
	Sclerodactyly of the fingers (distal to metacarpophalangeal but proximal to the proximal interphalangeal joints)	4
Fingertip lesions (only count the highest score)	Digital tip ulcers	2
	Fingertip pitting scars	3
Telangiectasia	-	2
Abnormal nailfold capillaries	-	2
Pulmonary arterial hypertension (PAH) and/or Interstitial lung Disease (ILD)* (*Maximum score is 2)	PAH ILD	2
Raynaud's phenomenon	-	3
Scleroderma related antibodies**(any of anti-centromere, anti-topoisomerase I [anti-Scl 70], anti-RNA polymerase III) (**Maximum score is 3)	Anti-centromere Anti-topoisomerase I Anti-RNA polymerase III	3

According to the 2013 ACR-EULAR criteria, a total score higher or equal to 9 or a skin involvement of the fingers of both hands proximal to the metacarpophalangeal joints are sufficient to make diagnosis of SSc.

As previously mentioned, vascular abnormalities are one of the main characteristics of SSc. In this regard, a comprehensive review regarding SSc pathogenesis has been published, with 100 articles only about vascular abnormalities in SSc. Pattanaik *et al.* resumed the typical vascular alterations present in SSc vasculopathy, as reduction and altered structure in capillaries, damaged endothelial cells and impaired microvasculature structure¹¹. The

cause of these alterations is still uncertain, but our study have suggested that CXCL4, a chemokine increased in SSc¹², may contribute to disease vasculopathy¹³.

Although the symptoms and presentation of SSc are very heterogeneous, one constant present condition that all SSc patients have in common is hypoxia¹⁴. Hypoxia is a condition where the oxygen concentration in the tissues is lower than the physiological level¹⁴. This condition can occur during inflammation or during RP due to vasoconstriction. Hypoxia occurs also due to impaired vascular structure or due to impaired oxygen supply through a fibrotic tissue. Taken together, aberrant immune activation (inflammation), vascular abnormalities and fibrosis all have hypoxia in common.

The immune system in SSc

The underlying events leading to SSc are still unknown, but as an autoimmune disease, it is generally accepted that a disturbed and aberrantly functioning immune system is the leading cause of the disease¹⁵. Furthermore, chronic endothelial cell activation, and recurrent immune cells infiltration e.g. lymphocytes, monocytes and dendritic cells (DC)^{16,17}, are considered as the earliest events in the pathogenesis of SSc¹⁸. Different studies have demonstrated that B cells, T cells and monocytes have an aberrant profile in SSc.

It has been shown that B cells contribute to SSc pathogenesis producing autoantibodies, activating other immune cells and/or by pro-inflammatory cytokine production¹⁹. Moreover, due to overexpression of CD19, B cells have a chronically hyper-reactive memory compartment and promote autoantibody production¹⁹. Therefore, anti B cell therapy has been considered in SSc treatment, even though there are no direct evidences explaining how B cells regulate SSc pathophysiology¹⁹.

T cells and in particular the regulatory (anti-inflammatory) compartment (Treg) have been associated to the pathogenesis of SSc²⁰⁻²². Circulating Treg have been found to have a decreased functional ability^{21,23}, but are increased in numbers during the episodes of disease

activity²⁴. Moreover, it has been shown that Treg are capable of converting to pathogenic effector T cells, Th17 and Th2 cytokine producing cells^{25–28}. This conversion of Treg depletes the anti-inflammatory immune forces even further and thereby contributes to a chronic inflammatory state of SSc^{20,28,29}.

Similarly, monocytes were observed to play a role in the pathogenesis of SSc. The presence of pro-fibrotic monocytes, in particular monocytes with M1- (pro-inflammatory) and M2-phenotype, signifies the effect of aberrant monocyte's behavior and their contribution in fibrotic pathology of SSc^{30,31}.

Another important key player in the pathogenesis of SSc are dendritic cells (DCs). As an important part of the immune system, DCs are the link between the innate and the adaptive immune response³² and express toll-like receptors (TLRs). These receptors are known to be highly preserved during the evolution and are able to recognize conserved domains of proteins and pathogens³³. One important role of DCs is to recognize pathogens after which they initiate an immune response and subsequently recruit and activate the adaptive immune system³². A common *in Vitro* model to study the behavior of DCs is monocyte derived dendritic cells (mo)DCs³⁴. *In Vivo*, the importance of DCs in SSc pathogenesis has been shown by many studies^{35–39}. In particular, plasmacytoid DCs (pDCs) has been recognized as fundamental cell type involved in the pathophysiology of SSc¹².

pDCs are mainly involved in viral response and therefore equipped with endosomal TLRs⁴⁰. Current literature pinpointed that in SSc, pDCs are dysregulated and migrate to the lungs and skin^{12,41,42}, where locally produce cytokines and initiate an immune response. Finally, pDCs are the major type I interferon (IFN) producing cells and the main source of C-X-C-motif ligand 4 (CXCL4) in SSc¹². IFN type I (composed by IFN α and IFN β) cytokines are involved in the anti-viral and microbial responses^{43,44}. Interestingly, various gene polymorphisms associated with SSc are involved in controlling type I IFN⁴⁵. Furthermore, in skin and blood of near half of the patients with SSc, an excessive production of type I IFN has been observed^{45–48}. An upregulation in IFN levels is considered as a relatively early

manifestation of SSc⁴⁷. Also, IFN-inducible chemokine has been shown to correlate with the involvement of the skin and lungs in SSc⁴⁹. Similarly, CXCL4 levels correlate with skin and lung fibrosis and it has been shown that CXCL4 mediates the TLR-induced type I IFN production¹².

CXCL4

CXCL4 is a cytokine originally isolated from platelets and therefore also known as platelet derived factor 4 (PF4). As an immune modulating cytokine, CXCL4 plays an important role in diseases such as intestinal inflammatory bowel disease (IBD), psoriasis, cystic fibrosis, liver fibrosis and cancer⁵⁰⁻⁵⁵. Furthermore, CXCL4 stimulation of monocytes orchestrates an increase in production level of interleukin (IL-) 6 and tumour necrosis factor α (TNF α)^{56,57}. Another study has shown that moDCs, when differentiated in the presence of CXCL4, develop a more mature phenotype with increase of responsiveness to TLRs, increased pro-inflammatory cytokine production and a higher capacity to stimulate the proliferation of T cells⁵⁸. In addition, CXCL4 promotes IL-17 production⁵⁹ and T-helper cell 2 (Th2) cytokines (IL-4, IL-5, and IL-13), and suppresses T-helper cell 1 (Th1) cytokines⁶⁰ in T lymphocytes. To date, a detailed mechanism of CXCL4 in SSc is rather unknown and requires further investigations. However, early studies performed by van Bon and colleagues have shown that pDCs are the main CXCL4 producers in patients with SSc and thereby emphasized CXCL4 might function as a potential biomarker of SSc¹². Furthermore, Kioon and collaborators pinpointed a potential role of phosphatidylinositol 3-kinase δ in CXCL4 secretion after TLR8 stimulation⁴¹ and Lande *et al.* showed that CXCL4 can create immune complexes with “self” DNA and the presence of these induced and correlated with type I IFN production in blood and skin⁶¹. Therefore, growing evidence suggests that CXCL4 increase in SSc might eventuate the chronic pro-inflammatory status of the disease.

Hypoxia and HIFs

SSc is a disease characterized by fibrosis, vascular abnormalities and immune alterations and hypoxia is interconnected with all these three aspects¹⁴. When hypoxia occurs within the cell, the level of mitochondrial reactive oxygen species (mtROS) rises and the hypoxia inducible factors (HIFs) get activated⁶². mtROS are highly reactive molecules that are physiologically produced inside the mitochondria⁶³ during the energy production from the oxidative phosphorylation process^{64,65}. Recent literature, in contrary to what have been assumed before, suggests that mtROS are not simply a side product of the energy machinery of the cell, but an oxygen sensor machine⁶⁴. In other words, mtROS level increases in a low oxygen level environment of the cell during hypoxia. Intriguingly, mtROS have been shown to be responsible for the production of pro-inflammatory cytokines^{66,67} and HIFs stabilization^{64,68}. Therefore, hypoxia and oxygen poor environment enhances mtROS production which further adds on into the inflammatory response.

There are three different HIFs and each type is more expressed in one cell-type as compared to the other⁶⁹. However, within the known HIF types, HIF1 is the most studied and HIF2 and HIF3 are poorly understood. In fact, HIFs were initially thought to have overlapping function⁷⁰. Generally, HIFs work as dimers with an alpha and a beta subunit⁷¹. The alpha subunits are constantly produced and degraded via proteasome by the cell in physiological conditions. When the alpha subunit of the HIFs is not degraded (and therefore stabilized) it can dimerize with the beta subunit and activate the transcription of its target genes. There are two systems that control the stabilization of the HIF alpha subunits, one oxygen-dependant and one oxygen-independent^{72,73}. In the oxygen-dependant manner the presence of oxygen, via prolyl hydroxylase (PHD) and von Hippel-Lindau protein (VHL) eventuates the ubiquitination and degradation of the HIF's alpha subunit. When hypoxia occurs, the ubiquitination pathway gets interrupted and results in stabilisation of the HIF alpha subunit. In the oxygen-independent manner, growth factors, deregulated oncogenes, tumour suppressors⁷⁴ and TLRs can all interfere with degradation of the alpha subunit and promote

the stabilisation of HIF alpha subunit, totally independent from the presence or absence of oxygen^{73,74}. This signifies that hypoxic environment and inflammation can stabilize HIF alpha subunit both in an oxygen-dependent as well as the oxygen independent manner in SSc and thereby create a vicious inflammatory circle where HIFs are chronically activated. Besides, HIFs are involved in multiple cellular processes such as metabolic pathways which allow the cell to adapt to low oxygen level (hypoxia). For example, one of the effects of HIFs stabilisation is the increase of the glucose uptake and promoting the anaerobic glycolysis⁷⁵. Furthermore, HIFs trigger the production of vascular endothelial growth factor (VEGF), erythropoietin, cell migration, proliferation and apoptosis⁷⁵. HIFs are also involved in the production of collagen⁷⁶, the main component of fibrotic tissues, and cytokine production by immune cells⁷⁷. In particular, in SSc, HIFs are recently considered as potential therapeutic targets, since HIFs are appeared to be involved in several inflammatory associated phases i.e. cytokine production, vascular cell activation and repair and finally scare tissue formation. Considering that chronic HIF activation subsequent extracellular matrix, vascular remodelling and futile angiogenesis, the combination of these factors eventuates the exacerbation of chronic hypoxia and promotes further fibrosis⁷⁸. Therefore, targeting these factors via HIF regulation might potentially contribute in treating chronic inflammation and fibrosis in SSc.

Metabolism in immune cells

The term cellular metabolism refers to all the reactions that happen inside the cell in order to maintain life. Those processes involve complex sequences of highly regulated biochemical reactions, called metabolic pathways. One emerging branch of cellular metabolism is the immunometabolism, that studies the interactions between the immunological and metabolic processes. Immunometabolism is a recent research area introduced here to assess the pathophysiology of SSc. An increase in glycolysis upon tumour growth factor- β (TGF- β) stimulation have been shown to enhance fibroblast differentiation and collagen

deposition⁷⁹⁻⁸². Further, it has been suggested that a disturbed fatty acid composition could promote a myofibroblast phenotype in mesangial cells⁸³. Also, an altered fatty acid metabolism due to decrease of relevant enzymes could promote fibrosis in renal cells⁸⁴. Activated immune cells experience drastic metabolic reprogramming fundamental for their function⁸⁵⁻⁹⁰. Nevertheless, assessing metabolism has recently pinpointed a link between metabolic status and redox balance. Interestingly, the redox balance and the oxidative stress have already been linked to pathogenesis of SSc by different studies⁹⁰⁻⁹⁶. Available literature signified that an aberrant immunometabolism could have significant effects on immune reaction and immune cell behaviour modulating fatty acid metabolism, fibrosis and oxidative stress. Given the fundamental role of immunometabolism in the immune response, eventual disfunctions occurring in metabolic pathways of immune cells can be involved in the pathogenesis of SSc^{97,98}.

Mass spectrometry and metabolomics

The gold standard technique used to study the metabolism is mass spectrometry (MS). This technique was developed between the last decades of the nineteenth century and the beginning of the twentieth century. MS is based on the analysis of the mass-to-charge ratio of ions. The results are presented as a spectrum and it is used to determine the elemental signature and thereby revealing the molecular structure and composition of a sample. One of the uses of mass spectrometry is metabolomics, the study of the processes regarding the small molecules involved in metabolism. Assessing the metabolic profile provides a snapshot of the physiological and non-physiological processes occurring inside and outside of the cell (plasma/serum). Therefore, stating the physiological state of an organism⁹⁹. These aspects make MS ideal in order to study the metabolism of the cells and can provide fundamental insights on the state of SSc at the time of the assessment and potentially help delineating the metabolical status of the immune cells in SSc.

Metabolomics in immune cells

Assessment of metabolomics in immune cells and subsequent reprogramming in immune diseases have shown promising results so far. In line with this, by assessing metabolomics, Yiming *et al.* demonstrated that autoreactive CD4⁺ T cells play an important role in Lupus using mice models. They showed that these cells rely on glycolysis and mitochondrial oxidative metabolism and that inhibition of these two metabolic pathways with 2-Deoxy-D-glucose (2DG) and metformin, “normalizes” the activated state of T cells and leads to remission of Lupus in mice model¹⁰⁰.

In line with findings of Yiming *et al.*, activated T cells and resting T cells are known to undergo drastic metabolic changes, relying on aerobic glycolysis and FAO respectively^{89,101,102,89,103}. Besides, it has been shown that blocking glycolysis via 2-DG can suppress the differentiation towards the T effector compartment (pro-inflammatory phenotype of T cells) and promotes the differentiation towards the T regulatory compartment (anti-inflammatory phenotype of T cells)^{104–106}. Since Treg are less active in SSc^{21,23} and T effector cells has been pinpointed as contributors in the pathogenesis of the disease^{107–109}, shifting the T cells phenotype from pro-inflammatory state to more anti-inflammatory compartment by blocking glycolysis in these cells could potentially be a beneficial strategy in treatment of patients with SSc.

Introduction to metabolism

The cellular metabolism is made by six major metabolic pathways, glycolysis, Krebs cycle, pentose phosphate pathway (PPP), the fatty acid (FA) oxidation (FAO), the FA synthesis and the amino acid (AA) metabolic pathway⁹⁸. All the six pathways are important for the cell as they all are the regulators and source of energy metabolism, represented by adenosine triphosphate (ATP). As mentioned before, the FA metabolism and therefore the FAO, is one of the pathways potentially involved and disturbed in SSc. Recently it has been shown that patients (and mice) with tubulointerstitial fibrosis had lower FAO enzymes and restoring the

fatty acid metabolism in those mice could protect them from the fibrotic process⁸⁴.

Normally, the FAO takes place in the mitochondria and converts FA into energy via intermediate molecules such as acetyl-coenzyme A (CoA), *reduced nicotinamide adenine dinucleotide* (NADH) and *reduced flavin adenine dinucleotide* (FADH₂). The first step of the FAO process is the “activation” of the FA by linking to acetyl-CoA which then will be differently processed depending on the length of the FA. If the FA is shorter than six carbons, it will directly/passively migrate to the mitochondria and get disassembled to generate ATP. A FA longer than six carbons, instead, will have to be first linked/conjugated to another molecule called carnitine before being able to migrate to the mitochondria where it will be “detached” from its chaperone carnitine and being dismantled into small molecules. This will be utilized within the Krebs cycle and the electron chain in order to generate ATP⁹⁸.

Carnitine is an interesting molecule with a structure similar to an AA⁹⁹ and is present in nearly every organism (vegetal and animal)¹¹⁰. Carnitine can derive from diet, but it is also endogenously produced. Furthermore, deficiencies of carnitine can lead to diseases such as cardiomyopathy, muscle-skeletal weakness and hypoglycaemia¹¹¹. Furthermore, acyl-carnitines has been observed to be altered in urine of SSc patients¹¹², suggesting a potential link to the disease.

Fatty acids immunometabolism

In both adaptive and innate immunity, FAO plays an important role. In particular, FAO is crucial for long living cells and cells that are not inflammatory by nature, such as macrophages M2 and T regulatory cells or T memory cells⁹⁸. Therefore, it is not surprising that in immune cells, FAO is widely driven by tolerogenic stimuli since FAO is required for the tolerogenic cytokines production⁹⁸. Also, the inflammatory function of macrophages is modulated by FAO. Excessive FA present within the macrophages stimulates pro-inflammatory cytokine (e.g. IL-1 α) production¹¹³. This while stimulation of the FAO have been shown to consequence a reduction of the pro-inflammatory cytokine production

level¹¹⁴. Furthermore, in an *in Vitro* experiment, it has been demonstrated that FAO can be decisive in the differentiation of macrophages towards an anti-inflammatory profile (M2)^{115,116}.

In T cells, FAO plays a fundamental role as the differentiation factor towards anti-inflammatory T regulatory cells. Also the inhibition of pro-inflammatory effector T cells is FAO dependant¹¹⁷. In addition, memory CD8 T cells rely on FAO in order to survive and to setup a rapid immune response towards antigens that they have had encountered before¹¹⁸. Wu *et al.* showed that TLR9 stimulation of mouse pDCs with CpG-A, induces FAO, needed for the production of type I IFN and pro-inflammatory cytokines such as IL-6 and TNF α . In the same study, IFN α was shown to induce FA synthesis and FAO in mouse pDCs whereby a vicious circle is created¹¹⁹. Therefore, it is likely to assume that this vicious circle is developed in SSc pDCs, where an increased type I IFN α , together with an aberrant TLR response, could accelerate and maintain FAO continuing the chronic inflammatory response in the disease.

mTOR and HIF

One key regulator of the cell metabolism is the mammalian target of rapamycin (mTOR) complex. As a protein kinase, mTOR is a protein that consumes ATP to attach a phosphate group to another protein and it controls many cellular functions, i.e. proliferation, protein synthesis, autophagy^{120,121} and HIF stabilization¹²². It has been shown that mTOR and HIF-1 can cooperate to modulate proliferation and glycolysis within the cells¹²³. Furthermore, mTOR has been shown to play an important regulatory role during the immune response. It governs and directs cell activation according to the intra- and extra-cellular nutritional status in order to regulate an inflammatory response¹²³. In gout, an autoinflammatory disease characterized by persistent painful joint inflammatory attacks, mTOR was shown to play a crucial role in suppressing the inflammatory response since its inhibition led to a reduction of pro-inflammatory mediators secretion¹²⁴. Furthermore, Soypaçacı *et al.* suggested that

mTOR could play a role in SSc pathogenesis¹²⁵. Also, Forestier *et al.* showed an altered B cell homeostasis referable to mTOR alteration¹²⁶ in SSc. In healthy pDCs mTOR induced production of type I IFN, TNF and IL-6 upon TLR9 triggering have been demonstrated¹²⁷. mTOR promotes *de novo* FA synthesis in immune cells¹²⁸ in order to feed FAO and thereby promote inflammation. Therefore, inhibition of mTOR could contribute in reducing the production of pro-inflammatory cytokines in pDCs by reducing the *de novo* FA synthesis and counteracting the IFN self-promoting vicious circle and diminishing chronic inflammation.

Aim of this thesis

The aim of my thesis was to identify the mechanism underling aberrant CXCL4 production and to study the metabolical status in pathophysiology of SSc.

In the first part of this thesis we focused mainly on the underlying mechanism substantiating CXCL4 production and its effect on fibrotic processes. In **Chapter 2** we studied the mechanism responsible for CXCL4 production in pDCs from patients with SSc. Further, the effect of the combination of hypoxia and TLR9 on CXCL4 production by increasing mitochondrial ROS and HIF-2 α stabilization in pDCs is discussed in this chapter. In **Chapter 3**, we demonstrated that moDCs are also capable to produce CXCL4. Similar to pDCs, also in moDCs HIF-2 α played an important role in CXCL4 production. However, it seemed that also HIF-1 α was involved in the secretion of CXCL4. Given the importance of HIF-2 α in the production of CXCL4, in **Chapter 4** we demonstrated the role of this transcription factor in the production of pro-inflammatory cytokine such as IFN α , TNF α , IL-6 and IL-8. In **Chapter 5** the role of CXCL4 in fibrosis and endothelial dysfunction was explored and thereby the potential and beneficial therapeutic effect of blocking CXCL4 was discussed.

In the second part of this thesis, we focused on the immunometabolism of SSc patients. In **Chapter 6** we showed how carnitine and the fatty acid metabolism are altered in plasma of patients with SSc and play a role in the production of pro-inflammatory mediators such

as IL-6 in moDCs and peripheral blood mononucleate cells (PBMCs). In **Chapter 7** the effect of metformin and mTOR inhibition was studied. In an *in Vitro* model, the effect of mTOR activation in substantiating immune response on activated monocytes challenged by monosodium urate (MSU) crystals was studied. As a key player in metabolism, mTOR regulates immune metabolism and therefore downregulation of mTOR might potentially provide therapeutic target in treatment of auto-immune and autoinflammatory disease.

All the findings of this thesis are further summarized and discussed in **Chapter 8**, together with future perspectives in SSc field.

References:

1. Sobolewski P, Maślińska M, Wieczorek M, et al. Systemic sclerosis - Multidisciplinary disease: Clinical features and treatment. *Reumatologia*. 2019;57(4):221–233.
2. Bergamasco A, Hartmann N, Wallace L, Verpillat P. Epidemiology of systemic sclerosis and systemic sclerosis-associated interstitial lung disease. *Clin. Epidemiol.* 2019;Volume 11:257–273.
3. Curzio C. Discussioni Anatomico-Pratiche di un raro e stravagante morbo cutaneo in una giovane Donna felicemente curato in questo grande Ospedale degl' Incurabili. 1753;
4. Abbot S, Bossingham D, Proudman S, de Costa C, Ho-Huynh A. Risk factors for the development of systemic sclerosis: A systematic review of the literature. *Rheumatol. Adv. Pract.* 2018;2(2):1–12.
5. Wynn TA. Cellular and molecular mechanisms of fibrosis. *J. Pathol.* 2008;214(2):199–210.
6. Tang L, Eaton JW. Inflammatory responses to biomaterials. *Am. J. Clin. Pathol.* 1995;103(4):466–471.
7. Hachulla E, Launay D. Diagnosis and classification of systemic sclerosis. *Clin. Rev. Allergy Immunol.* 2011;40(2):78–83.
8. Pauling JD, Saketkoo LA, Matucci-Cerinic M, Ingegnoli F, Khanna D. The patient experience of Raynaud's phenomenon in systemic sclerosis. *Rheumatol. (United Kingdom)*. 2018;58(1):18–26.
9. Cooke JP, Marshall JM. Mechanisms of Raynaud's disease. *Vasc. Med.* 2005;10(4):293–307.
10. Van Den Hoogen F, Khanna D, Fransen J, et al. 2013 classification criteria for systemic sclerosis: An american college of rheumatology/European league against rheumatism collaborative initiative. *Arthritis Rheum.* 2013;65(11):2737–2747.
11. Pattanaik D, Brown M, Postlethwaite BC, Postlethwaite AE. Pathogenesis of systemic sclerosis. *Front. Immunol.* 2015;6(JUN):272.
12. van Bon L, Affandi AJ, Broen J, et al. Proteome-wide Analysis and CXCL4 as a Biomarker in Systemic Sclerosis. *N. Engl. J. Med.* 2014;370(5):433–443.
13. Aidoudi-Ahmed S, Bikfalvi A. Interaction of PF4 (CXCL4) with the vasculature: A role in atherosclerosis and angiogenesis. *Thromb. Haemost.* 2010;104(5):941–948.
14. Beyer C, Schett G, Gay S, Distler O, Distler JHW. Hypoxia. Hypoxia in the pathogenesis of systemic sclerosis. *Arthritis Res. Ther.* 2009;11(2):220.
15. Fullard N, O'Reilly S. Role of innate immune system in systemic sclerosis. *Semin. Immunopathol.* 2015;37(5):511–517.
16. Takehara K. Pathogenesis of systemic sclerosis. *J. Rheumatol.* 2003;30(4):755–759.
17. Allanore Y, Simms R, Distler O, et al. Systemic sclerosis. *Nat. Rev. Dis. Prim.* 2015;1(1):15002.
18. Altorok N, Wang Y, Kahaleh B. Endothelial dysfunction in systemic sclerosis. *Curr. Opin. Rheumatol.* 2014;26(6):615–620.
19. Yoshizaki A. Pathogenic roles of B lymphocytes in systemic sclerosis. *Immunol. Lett.* 2018;195:76–82.
20. Frantz C, Auffray C, Avouac J, Allanore Y. Regulatory T cells in systemic sclerosis. *Front. Immunol.* 2018;9(OCT):
21. Wang YY, Wang Q, Sun XH, et al. DNA hypermethylation of the forkhead box protein 3 (FOXP3) promoter in CD4+ T cells of patients with systemic sclerosis. *Br. J. Dermatol.* 2014;171(1):39–47.
22. Shu Y, Hu Q, Long H, et al. Epigenetic Variability of CD4+CD25+ Tregs Contributes to the Pathogenesis of Autoimmune Diseases. *Clin. Rev. Allergy Immunol.* 2017;52(2):260–272.
23. Broen JCA, Wolvers-Tettero ILM, Geurts-van Bon L, et al. Skewed X chromosomal inactivation impacts T regulatory cell function in systemic sclerosis. *Ann. Rheum. Dis.* 2010;69(12):2213–2216.
24. Radstake TRDJ, van Bon L, Broen J, et al. Increased Frequency and Compromised Function of T Regulatory Cells in Systemic Sclerosis (SSc) Is Related to a Diminished CD69 and TGFβ Expression. *PLoS One.* 2009;4(6):e5981.
25. Yang XO, Nurieva R, Martinez GJ, et al. Molecular Antagonism and Plasticity of Regulatory and Inflammatory T Cell Programs. *Immunity.* 2008;29(1):44–56.

26. Osorio F, LeibundGut-Landmann S, Lochner M, et al. DC activated via dectin-1 convert Treg into IL-17 producers. *Eur. J. Immunol.* 2008;38(12):3274–3281.
27. Koenen HJPM, Smeets RL, Vink PM, et al. Human CD25^{high}Foxp3^{pos} regulatory T cells differentiate into IL-17 producing cells. *Blood.* 2008;112(6):2340–2352.
28. Macdonald KG, Dawson NAJ, Huang Q, et al. Regulatory T cells produce profibrotic cytokines in the skin of patients with systemic sclerosis. *J. Allergy Clin. Immunol.* 2015;135(4):946–955.e9.
29. Antiga E, Quaglini P, Bellandi S, et al. Regulatory T cells in the skin lesions and blood of patients with systemic sclerosis and morphea. *Br. J. Dermatol.* 2010;162(5):1056–1063.
30. Mathai SK, Gulati M, Peng X, et al. Circulating monocytes from systemic sclerosis patients with interstitial lung disease show an enhanced profibrotic phenotype. *Lab. Investig.* 2010;90(6):812–823.
31. Cutolo M, Trombetta AC, Soldano S. Monocyte and macrophage phenotypes: a look beyond systemic sclerosis. Response to: “M1/M2 polarisation state of M-CSF blood-derived macrophages in systemic sclerosis” by Lescoat et al. *Ann. Rheum. Dis.* 2019;78(11):e128–e128.
32. Lu TT. Dendritic cells: Novel players in fibrosis and scleroderma. *Curr. Rheumatol. Rep.* 2012;14(1):30–38.
33. Iwasaki A, Medzhitov R. Toll-like receptor control of the adaptive immune responses. *Nat. Immunol.* 2004;5(10):987–95.
34. Van Den Heuvel MM, Vanhee DDC, Postmus PE, Hoefsmit ECM, Beelen RHJ. Functional and phenotypic differences of monocyte-derived dendritic cells from allergic and nonallergic patients. *J. Allergy Clin. Immunol.* 1998;101(1):90–95.
35. Mehta H, Goulet PO, Nguyen V, et al. Topoisomerase I peptide-loaded dendritic cells induce autoantibody response as well as skin and lung fibrosis. *Autoimmunity.* 2016;49(8):503–513.
36. Gerber EE, Gallo EM, Fontana SC, et al. Integrin-modulating therapy prevents fibrosis and autoimmunity in mouse models of scleroderma. *Nature.* 2013;503(7474):126–130.
37. Takahashi T, Asano Y, Nakamura K, et al. A potential contribution of antimicrobial peptide LL-37 to tissue fibrosis and vasculopathy in systemic sclerosis. *Br. J. Dermatol.* 2016;175(6):1195–1203.
38. Mathes AL, Christmann RB, Stifano G, et al. Global chemokine expression in systemic sclerosis (SSc): CCL19 expression correlates with vascular inflammation in SSc skin. *Ann. Rheum. Dis.* 2014;73(10):1864–1872.
39. Broen JCA, Bossini-Castillo L, Van Bon L, et al. A rare polymorphism in the gene for Toll-like receptor 2 is associated with systemic sclerosis phenotype and increases the production of inflammatory mediators. *Arthritis Rheum.* 2012;64(1):264–271.
40. Takagi H, Arimura K, Uto T, et al. Plasmacytoid dendritic cells orchestrate TLR7-mediated innate and adaptive immunity for the initiation of autoimmune inflammation. *Sci. Rep.* 2016;6(1):24477.
41. Kioon MDA, Tripodo C, Fernandez D, et al. Plasmacytoid dendritic cells promote systemic sclerosis with a key role for TLR8. *Sci. Transl. Med.* 2018;10(423):eaam8458.
42. Kafaja S, Valera I, Divekar AA, et al. pDCs in lung and skin fibrosis in a bleomycin-induced model and patients with systemic sclerosis. *JCI insight.* 2018;3(9):.
43. Ivashkiv LB, Donlin LT. Regulation of type I interferon responses. *Nat. Rev. Immunol.* 2014;14(1):36–49.
44. McNab F, Mayer-Barber K, Sher A, Wack A, O’Garra A. Type I interferons in infectious disease. *Nat. Rev. Immunol.* 2015;15(2):87–103.
45. Skaug B, Assassi S. Type I interferon dysregulation in Systemic Sclerosis. *Cytokine.* 2019;154635.
46. Higgs BW, Liu Z, White B, et al. Patients with systemic lupus erythematosus, myositis, rheumatoid arthritis and scleroderma share activation of a common type I interferon pathway. *Ann. Rheum. Dis.* 2011;70(11):2029–2036.
47. Brkic Z, Van Bon L, Cossu M, et al. The interferon type i signature is present in systemic sclerosis before overt fibrosis and might contribute to its pathogenesis through high BAFF gene expression and high collagen synthesis. *Ann. Rheum. Dis.* 2016;75(8):1567–1573.

48. Tan FK, Zhou X, Mayes MD, et al. Signatures of differentially regulated interferon gene expression and vasculotrophism in the peripheral blood cells of systemic sclerosis patients. *Rheumatology*. 2006;45(6):694–702.
49. Liu X, Mayes MD, Tan FK, et al. Correlation of interferon-inducible chemokine plasma levels with disease severity in systemic sclerosis. *Arthritis Rheum*. 2013;65(1):226–235.
50. Burstein SA, Malpass TW, Yee E, et al. Platelet factor-4 excretion in myeloproliferative disease: implications for the aetiology of myelofibrosis. *Br. J. Haematol*. 1984;57(3):383–392.
51. Van Raemdonck K, Van den Steen PE, Liekens S, Van Damme J, Struyf S. CXCR3 ligands in disease and therapy. *Cytokine Growth Factor Rev*. 2015;26(3):311–327.
52. Schwarz KB, Rosensweig J, Sharma S, et al. Plasma markers of platelet activation in cystic fibrosis liver and lung disease. *J. Pediatr. Gastroenterol. Nutr*. 2003;37(2):187–91.
53. Tamagawa-Mineoka R, Katoh N, Ueda E, Masuda K, Kishimoto S. Elevated platelet activation in patients with atopic dermatitis and psoriasis: increased plasma levels of beta-thromboglobulin and platelet factor 4. *Allergol. Int*. 2008;57(4):391–6.
54. Yeo L, Adlard N, Biehl M, et al. Expression of chemokines CXCL4 and CXCL7 by synovial macrophages defines an early stage of rheumatoid arthritis. *Ann. Rheum. Dis*. 2016;75(4):763–771.
55. Zaldivar MM, Pauels K, Von Hundelshausen P, et al. CXC chemokine ligand 4 (CXCL4) is a platelet-derived mediator of experimental liver fibrosis. *Hepatology*. 2010;51(4):1345–1353.
56. Kasper B, Winoto-Morbach S, Mittelstädt J, et al. CXCL4-induced monocyte survival, cytokine expression, and oxygen radical formation is regulated by sphingosine kinase 1. *Eur. J. Immunol*. 2010;40(4):1162–1173.
57. Scheuerer B, Ernst M, Dürrbaum-Landmann I, et al. The CXC-chemokine platelet factor 4 promotes monocyte survival and induces monocyte differentiation into macrophages. *Blood*. 2000;95(4):1158–66.
58. Silva-Cardoso SC, Affandi AJ, Spel L, et al. CXCL4 Exposure Potentiates TLR-Driven Polarization of Human Monocyte-Derived Dendritic Cells and Increases Stimulation of T Cells. *J. Immunol*. 2017;199(1):253–262.
59. Affandi AJ, Silva-Cardoso SC, Garcia S, et al. CXCL4 is a novel inducer of human Th17 cells and correlates with IL-17 and IL-22 in psoriatic arthritis. *Eur. J. Immunol*. 2018;48(3):522–531.
60. Romagnani P, Maggi L, Mazzinghi B, et al. CXCR3-mediated opposite effects of CXCL10 and CXCL4 on TH1 or TH2 cytokine production. *J. Allergy Clin. Immunol*. 2005;116(6):1372–9.
61. Lande R, Lee EY, Palazzo R, et al. CXCL4 assembles DNA into liquid crystalline complexes to amplify TLR9-mediated interferon- α production in systemic sclerosis. *Nat. Commun*. 2019;10(1):1731.
62. Kelly B, O'Neill LAJ. Metabolic reprogramming in macrophages and dendritic cells in innate immunity. *Cell Res*. 2015;25(7):771–84.
63. Reichart G, Mayer J, Zehm C, et al. Mitochondrial complex IV mutation increases reactive oxygen species production and reduces lifespan in aged mice. *Acta Physiol*. 2019;225(4):e13214.
64. Mansfield KD, Guzy RD, Pan Y, et al. Mitochondrial dysfunction resulting from loss of cytochrome c impairs cellular oxygen sensing and hypoxic HIF- α activation. *Cell Metab*. 2005;1(6):393–399.
65. Li X, Fang P, Yang WY, et al. Mitochondrial ROS, uncoupled from ATP synthesis, determine endothelial activation for both physiological recruitment of patrolling cells and pathological recruitment of inflammatory cells. *Can. J. Physiol. Pharmacol*. 2016;95(3):247–252.
66. Li X, Wang X, Zheng M, Luan QX. Mitochondrial reactive oxygen species mediate the lipopolysaccharide-induced pro-inflammatory response in human gingival fibroblasts. *Exp. Cell Res*. 2016;347(1):212–221.
67. Agod Z, Fekete T, Budai MM, et al. Regulation of type I interferon responses by mitochondria-derived reactive oxygen species in plasmacytoid dendritic cells. *Redox Biol*. 2017;13:633–645.

68. Sanjuán-Pla A, Cervera AM, Apostolova N, et al. A targeted antioxidant reveals the importance of mitochondrial reactive oxygen species in the hypoxic signaling of HIF-1 α . *FEBS Lett.* 2005;579(12):2669–2674.
69. Talks KL, Turley H, Gatter KC, et al. The expression and distribution of the hypoxia-inducible factors HIF-1 α and HIF-2 α in normal human tissues, cancers, and tumor-associated macrophages. *Am. J. Pathol.* 2000;157(2):411–421.
70. Hu C-J, Wang L-Y, Chodosh LA, Keith B, Simon MC. Differential Roles of Hypoxia-Inducible Factor 1 (HIF-1) and HIF-2 in Hypoxic Gene Regulation. *Mol. Cell. Biol.* 2003;23(24):9361–9374.
71. Semenza GL. Hypoxia-inducible factors in physiology and medicine. *Cell.* 2012;148(3):399–408.
72. Haeberle HA, Dürrstein C, Rosenberger P, et al. Oxygen-independent stabilization of hypoxia inducible factor (HIF)-1 during RSV infection. *PLoS One.* 2008;3(10):e3352.
73. Welsh SJ, Dale AG, Lombardo CM, et al. Inhibition of the hypoxia-inducible factor pathway by a G-quadruplex binding small molecule. *Sci. Rep.* 2013;3(1):2799.
74. Agani F, Jiang B-H. Oxygen-independent Regulation of HIF-1: Novel Involvement of PI3K/ AKT/mTOR Pathway in Cancer. *Curr. Cancer Drug Targets.* 2013;13(3):245–251.
75. Liu W, Shen SM, Zhao XY, Chen Dr. GQ. Targeted genes and interacting proteins of hypoxia inducible factor-1. *Int. J. Biochem. Mol. Biol.* 2012;
76. Chowdhury R, Hardy A, Schofield CJ. The human oxygen sensing machinery and its manipulation. *Chem. Soc. Rev.* 2008;37(7):1308–1319.
77. Jeong HJ, Chung HS, Lee BR, et al. Expression of proinflammatory cytokines via HIF-1 α and NF- κ B activation on desferrioxamine-stimulated HMC-1 cells. *Biochem. Biophys. Res. Commun.* 2003;306(4):805–811.
78. Xiong A, Liu Y. Targeting hypoxia inducible factors-1 α as a novel therapy in Fibrosis. *Front. Pharmacol.* 2017;8(MAY):
79. Goodwin J, Choi H, Hsieh MH, et al. Targeting hypoxia-inducible factor-1 α / pyruvate dehydrogenase kinase 1 axis by dichloroacetate suppresses bleomycin-induced pulmonary fibrosis. *Am. J. Respir. Cell Mol. Biol.* 2018;58(2):216–231.
80. Cho SJ, Moon JS, Lee CM, Choi AMK, Stout-Delgado HW. Glucose transporter 1-dependent glycolysis is increased during aging-related lung fibrosis, and phloretin inhibits lung fibrosis. *Am. J. Respir. Cell Mol. Biol.* 2017;56(4):521–531.
81. Zhao H, Dennery PA, Yao H. Metabolic reprogramming in the pathogenesis of chronic lung diseases, including BPD, COPD, and pulmonary fibrosis. *Am. J. Physiol. - Lung Cell. Mol. Physiol.* 2018;314(4):L544–L554.
82. Xie N, Tan Z, Banerjee S, et al. Glycolytic reprogramming in myofibroblast differentiation and lung fibrosis. *Am. J. Respir. Crit. Care Med.* 2015;192(12):1462–1474.
83. Mishra R, Simonson MS. Oleate Induces a Myofibroblast-Like Phenotype in Mesangial Cells. *Arterioscler. Thromb. Vasc. Biol.* 2008;28(3):541–547.
84. Kang HM, Ahn SH, Choi P, et al. Defective fatty acid oxidation in renal tubular epithelial cells has a key role in kidney fibrosis development. *Nat. Med.* 2015;21(1):37–46.
85. Bettencourt IA, Powell JD. Targeting Metabolism as a Novel Therapeutic Approach to Autoimmunity, Inflammation, and Transplantation. *J. Immunol.* 2017;198(3):999–1005.
86. MacIver NJ, Michalek RD, Rathmell JC. Metabolic Regulation of T Lymphocytes. *Annu. Rev. Immunol.* 2013;31(1):259–283.
87. Buck MD, O'Sullivan D, Pearce EL. T cell metabolism drives immunity. *J. Exp. Med.* 2015;212(9):1345–1360.
88. Pearce EL, Pearce EJ. Metabolic pathways in immune cell activation and quiescence. *Immunity.* 2013;38(4):633–643.
89. Pearce EL, Poffenberger MC, Chang CH, Jones RG. Fueling immunity: Insights into metabolism and lymphocyte function. *Science (80-.).* 2013;342(6155):1242454–1242454.
90. Zhu H, Chen W, Liu D, Luo H. The role of metabolism in the pathogenesis of systemic sclerosis. *Metabolism.* 2019;93:44–51.

91. Ogawa F, Shimizu K, Muroi E, et al. Serum levels of 8-isoprostane, a marker of oxidative stress, are elevated in patients with systemic sclerosis. *Rheumatology*. 2006;45(7):815–818.
92. Böger RH, Maas R, Schulze F, Schwedhelm E. Elevated levels of asymmetric dimethylarginine (ADMA) as a marker for cardiovascular disease and mortality. *Clin. Chem. Lab. Med.* 2005;43(10):1124–1129.
93. Riccieri V, Spadaro A, Fuksa L, et al. Specific oxidative stress parameters differently correlate with nailfold capillaroscopy changes and organ involvement in systemic sclerosis. *Clin. Rheumatol.* 2008;27(2):225–230.
94. Tikly M, Channa K, Theodorou P, Gulumian M. Lipid peroxidation and trace elements in systemic sclerosis. *Clin. Rheumatol.* 2006;25(3):320–324.
95. Luo JY, Liu X, Jiang M, Zhao HP, Zhao JJ. Oxidative stress markers in blood in systemic sclerosis: A meta-analysis. *Mod. Rheumatol.* 2017;27(2):306–314.
96. Murrell DF. A radical proposal for the pathogenesis of scleroderma. *J. Am. Acad. Dermatol.* 1993;28(1):78–85.
97. Colamatteo A, Micillo T, Bruzzaniti S, et al. Metabolism and autoimmune responses: The microRNA connection. *Front. Immunol.* 2019;10(AUG):
98. O'Neill LAJ, Kishton RJ, Rathmell J. A guide to immunometabolism for immunologists. *Nat. Rev. Immunol.* 2016;16(9):553–565.
99. Hollywood K, Brison DR, Goodacre R. Metabolomics: Current technologies and future trends. *Proteomics*. 2006;6(17):4716–4723.
100. Yin Y, Choi SC, Xu Z, et al. Normalization of CD4+ T cell metabolism reverses lupus. *Sci. Transl. Med.* 2015;7(274):274ra18.
101. Wang R, Dillon CP, Shi LZ, et al. The Transcription Factor Myc Controls Metabolic Reprogramming upon T Lymphocyte Activation. *Immunity*. 2011;35(6):871–882.
102. Pollizzi KN, Powell JD. Integrating canonical and metabolic signalling programmes in the regulation of T cell responses. *Nat. Rev. Immunol.* 2014;14(7):435–446.
103. Pearce EL, Walsh MC, Cejas PJ, et al. Enhancing CD8 T-cell memory by modulating fatty acid metabolism. *Nature*. 2009;460(7251):103–7.
104. Berod L, Friedrich C, Nandan A, et al. De novo fatty acid synthesis controls the fate between regulatory T and T helper 17 cells. *Nat. Med.* 2014;20(11):1327–1333.
105. Gerriets VA, Kishton RJ, Nichols AG, et al. Metabolic programming and PDHK1 control CD4+ T cell subsets and inflammation. *J. Clin. Invest.* 2015;125(1):194–207.
106. Shi LZ, Wang R, Huang G, et al. HIF1 α -dependent glycolytic pathway orchestrates a metabolic checkpoint for the differentiation of TH17 and Treg cells. *J. Exp. Med.* 2011;208(7):1367–1376.
107. Kurasawa K, Hirose K, Sano H, et al. Increased interleukin-17 production in patients with systemic sclerosis. *Arthritis Rheum.* 2000;43(11):2455–2463.
108. Rodríguez-Reyna TS, Furuzawa-Carballeda J, Cabiedes J, et al. Th17 peripheral cells are increased in diffuse cutaneous systemic sclerosis compared with limited illness: A cross-sectional study. *Rheumatol. Int.* 2012;32(9):2653–2660.
109. Truchetet ME, Brembilla NC, Montanari E, Allanore Y, Chizzolini C. Increased frequency of circulating Th22 in addition to Th17 and Th2 lymphocytes in systemic sclerosis: Association with interstitial lung disease. *Arthritis Res. Ther.* 2011;13(5):R166.
110. Bremer J. Carnitine. Metabolism and functions. *Physiol. Rev.* 1983;63(4):1420–1480.
111. Stanley CA. Carnitine deficiency disorders in children. *Ann. N. Y. Acad. Sci.* 2004;1033(1):42–51.
112. Fernández-Ochoa Á, Quirantes-Piné R, Borrás-Linares I, et al. Urinary and plasma metabolite differences detected by HPLC-ESI-QTOF-MS in systemic sclerosis patients. *J. Pharm. Biomed. Anal.* 2019;162:82–90.
113. Freigang S, Ampenberger F, Weiss A, et al. Fatty acid-induced mitochondrial uncoupling elicits inflammasome-independent IL-1 α and sterile vascular inflammation in atherosclerosis. *Nat. Immunol.* 2013;14(10):1045–1053.

114. Malandrino MI, Fucho R, Weber M, et al. Enhanced fatty acid oxidation in adipocytes and macrophages reduces lipid-induced triglyceride accumulation and inflammation. *Am. J. Physiol. - Endocrinol. Metab.* 2015;308(9):E756–E769.
115. Huang SCC, Everts B, Ivanova Y, et al. Cell-intrinsic lysosomal lipolysis is essential for alternative activation of macrophages. *Nat. Immunol.* 2014;15(9):846–855.
116. Vats D, Mukundan L, Odegaard JI, et al. Oxidative metabolism and PGC-1 β attenuate macrophage-mediated inflammation. *Cell Metab.* 2006;4(1):13–24.
117. Michalek RD, Gerriets VA, Jacobs SR, et al. Cutting Edge: Distinct Glycolytic and Lipid Oxidative Metabolic Programs Are Essential for Effector and Regulatory CD4⁺ T Cell Subsets. *J. Immunol.* 2011;186(6):3299–3303.
118. Van Der Windt GJW, O’Sullivan D, Everts B, et al. CD8 memory T cells have a bioenergetic advantage that underlies their rapid recall ability. *Proc. Natl. Acad. Sci. U. S. A.* 2013;110(35):14336–14341.
119. Wu D, Sanin DE, Everts B, et al. Type 1 Interferons Induce Changes in Core Metabolism that Are Critical for Immune Function. *Immunity.* 2016;44(6):1325–1336.
120. Hay N, Sonenberg N. Upstream and downstream of mTOR. *Genes Dev.* 2004;18(16):1926–1945.
121. Lipton JO, Sahin M. The Neurology of mTOR. *Neuron.* 2014;84(2):275–291.
122. Land SC, Tee AR. Hypoxia-inducible factor 1 α is regulated by the mammalian target of rapamycin (mTOR) via an mTOR signaling motif. *J. Biol. Chem.* 2007;282(28):20534–20543.
123. Pan C, Liu Q, Wu X. Hif1 α /mir-520a-3p/akt1/mTOR feedback promotes the proliferation and glycolysis of gastric cancer cells. *Cancer Manag. Res.* 2019;11:10145–10156.
124. Vazirpanah N, Otrria A, Van Der Linden M, et al. MTOR inhibition by metformin impacts monosodium urate crystal-induced inflammation and cell death in gout: A prelude to a new add-on therapy? *Ann. Rheum. Dis.* 2019;78(5):663–671.
125. Soypaçacı Z, Gümüş ZZ, Çakaloğlu F, et al. Role of the mTOR pathway in minor salivary gland changes in Sjogren’s syndrome and systemic sclerosis. *Arthritis Res. Ther.* 2018;20(1):170.
126. Forestier A, Guerrier T, Jouvray M, et al. Altered B lymphocyte homeostasis and functions in systemic sclerosis. *Autoimmun. Rev.* 2018;17(3):244–255.
127. Cao W, Manicassamy S, Tang H, et al. Toll-like receptor-mediated induction of type I interferon in plasmacytoid dendritic cells requires the rapamycin-sensitive PI(3)K-mTOR-p70S6K pathway. *Nat. Immunol.* 2008;9(10):1157–1164.
128. Weichhart T, Hengstschlager M, Linke M. Regulation of innate immune cell function by mTOR. *Nat. Rev. Immunol.* 2015;15(10):599–614.

Hypoxia and TLR9 activation drive CXCL4 production in systemic sclerosis pDCs via mtROS and HIF-2a

Andrea Ottria^{1,2}, Maili Zimmermann^{1,2}, Laurent M. Paardekooper³, Tiago Carvalheiro^{1,2}, Nadia Vazirpanah^{1,2}, Sandra Silva-Cardoso^{1,2}, Alsja J. Affandi^{1,2}, Eleni Chouri^{1,2}, Maarten v.d Kroef^{1,2}, Ralph G. Tieland^{1,2}, Cornelis P.J. Bekker^{1,2}, Catharina G.K. Wichers^{1,2}, Marzia Rossato^{1,2}, Enric Mocholi-Gimeno^{1,2}, Janneke Tekstra², Evelien Ton², Jaap M. van Laar², Marta Cossu^{1,2}, Lorenzo Beretta⁴, Samuel Garcia Perez^{1,2}, Aridaman Pandit^{1,2}, Femke Bonte-Mineur⁵, Kris A. Reedquist^{1,2}, Geert van den Bogaart^{3,6}, Timothy R.D.J. Radstake^{1,2}, Wioleta Marut^{1,2*}

Affiliations

¹Laboratory of Translational Immunology, University Medical Center Utrecht, Utrecht University, Utrecht, the Netherlands

²Department of Rheumatology and Clinical Immunology, University Medical Center Utrecht, Utrecht University, Utrecht, the Netherlands

³Department of Tumor Immunology, Radboud Institute for Molecular Life Sciences, Radboud University Medical Center, Nijmegen, the Netherlands

⁴Referral Center for Systemic Autoimmune Diseases, University of Milan & Fondazione IRCCS Ospedale Maggiore Policlinico, Mangiagalli e Regina Elena, Via Pace 9, Milan, Italy

⁵ Department of Rheumatology and Clinical Immunology Maasstad Hospital, Rotterdam, the Netherlands

⁶Department of Molecular Immunology, Groningen Biomolecular Sciences and Biotechnology Institute, University of Groningen, Groningen, the Netherlands

* Materials and Correspondence

Wioleta Marut, PhD, University Medical Centre Utrecht | Heidelberglaan 100 | Tel: +31 88 75 535 68 | w.k.marut@umcutrecht.nl

Manuscript under revision by Cell Reports

Summary

Systemic sclerosis (SSc) is a complex disease characterized by vascular abnormalities and inflammation culminating in hypoxia and excessive fibrosis. Previously, we identified CXCL4 as a novel predictive biomarker in SSc. Although CXCL4 is well-studied, the mechanisms driving its production are unclear.

Plasmacytoid dendritic cells (pDCs) from healthy controls and SSc patients were cultured in the presence of hypoxia or atmospheric oxygen level and/or stimulated with several TLR-agonists. CXCL4 release was potentiated only when pDCs were co-cultured under hypoxia and TLR9 agonist. Here, we demonstrated that CXCL4 production is dependent on the overproduction of mitochondrial reactive oxygen species (mtROS) leading to stabilization of HIF-2 α . In addition, we show that hypoxia is fundamental for CXCL4 production by umbilical cord (uc)CD34 derived pDCs.

TLR-mediated activation of immune cells in the presence of hypoxia underpins the pathogenic production of CXCL4 in SSc. Blocking either, mtROS or HIF-2 α pathways may therapeutically attenuate the contribution of CXCL4 to SSc and other inflammatory diseases driven by CXCL4.

Keywords: CXCL4, pDCs, Hypoxia, TLRs, mtROS, HIF-2 α

Introduction

Systemic sclerosis (SSc) is an auto-immune disease characterized by vascular alteration, immune dysregulation and fibrosis of the skin and internal organs (Gabrielli et al., 2009). Vascular alterations are manifested by reduced density and loss of capillaries, which lead to impaired oxygenation in the tissue of SSc patients. Oxygen flow is even further reduced by excessive deposition of extracellular matrix, making low oxygen level (hypoxia) one of the characteristic features of SSc (Fuschiotti, 2016). Previously, we identified CXCL4 as a new biomarker for SSc (van Bon et al., 2014), and we demonstrated that CXCL4 in these patients is mainly produced by plasmacytoid dendritic cells (pDCs) (van Bon et al., 2014). CXCL4 is largely viewed as a pro-inflammatory chemokine, which in monocytes can boost the production of IL-6 and TNF α cytokines (Kasper et al., 2010; Scheuerer et al., 2000). In T cells, CXCL4 induces the production of IL-17 (Affandi et al., 2018) and drives the production of Th2 cytokines (IL-4, IL-5, and IL-13), while suppressing Th1 cytokines (Romagnani et al., 2005). CXCL4 is involved in several inflammatory and fibrotic diseases such as intestinal inflammatory bowel disease (IBD), psoriasis, cystic fibrosis, liver fibrosis and cancer (Burstein et al., 1984; Van Raemdonck et al., 2015; Schwarz et al., 2003; Tamagawa-Mineoka et al., 2008; Yeo et al., 2016; Zaldivar et al., 2010).

Interestingly, the level of CXCL4 in SSc patients was found to be the highest in a very progressive subset of the disease (van Bon et al., 2014), where impaired tissue oxygenation and inflammation are the highest, indicating that hypoxia could be a relevant factor for CXCL4 release. Furthermore, these patients have high release of endogenous toll like receptor (TLR) agonists. These locally produced TLR agonists play an important role in SSc pathogenesis by driving inflammation and fibrosis (Kioon et al., 2018; Pattanaik et al., 2015). Together, accumulating evidence implicates a role for CXCL4 in inflammatory and fibrotic diseases such as SSc which makes CXCL4 an attractive therapeutic target. One way of blocking the side effects of CXCL4 is inhibiting its production. Here we explored several potential mechanisms of CXCL4 production by systematically testing the effects of hypoxia and TLR activation on pDCs.

Results

pDC's CXCL4 production is dependent upon hypoxia and TLR9

pDCs were exposed to hypoxia and/or TLR agonists after which CXCL4 production was quantified. The exposure to hypoxia alone or to individual TLR agonists alone did not induce CXCL4 production at protein or RNA level (**Fig1b, 1d**). However, the production of CXCL4 was increased upon co-exposure of hypoxia and TLR9 agonist, CpG-C ($P<0.0001$ on protein level, $P=0.0057$ on mRNA level) (**Fig1b, 1d**). CXCL4 production was not increased when the cells were co-exposed to hypoxia and other TLR agonists (**Fig1b**). Therefore, in the following experiments, pDCs were stimulated only with CpG-C.

Our data confirmed a high level of CXCL4 production by unstimulated pDCs from SSc patients both at protein (**Fig1c**) and mRNA level (**Fig1d**) compared to HC pDCs in atmospheric conditions ($P=0.0021$). In addition, CXCL4 production of SSc pDCs was not further increased after hypoxia, TLR9 stimulation or the combination of them, neither at mRNA nor protein level (**Fig1c,1d**).

Hypoxia and TLR9 specifically regulates the production of CXCL4 by pDCs but not other cytokines

To examine the specificity of production of CXCL4 in response to hypoxia and TLR9 stimulation, we also assessed the production of other cytokines relevant to SSc such as IFN α , TNF α , IL6, IL8 for pDCs (**Fig2a-2d**). TLR stimulation alone was sufficient to significantly increase the production of these cytokines (IFN α $P<0.0001$; TNF α $P=0.0051$; IL6 $P<0.0001$; IL8 $P<0.0001$) by HC pDCs, while hypoxia alone and co-exposure to hypoxia with TLR9 had no further effect on the production of these cytokines (**Fig2a-2d**). Hence the concerted action of hypoxia and endosomal TLR9 signalling was specific in inducing CXCL4 production.

Figure 1

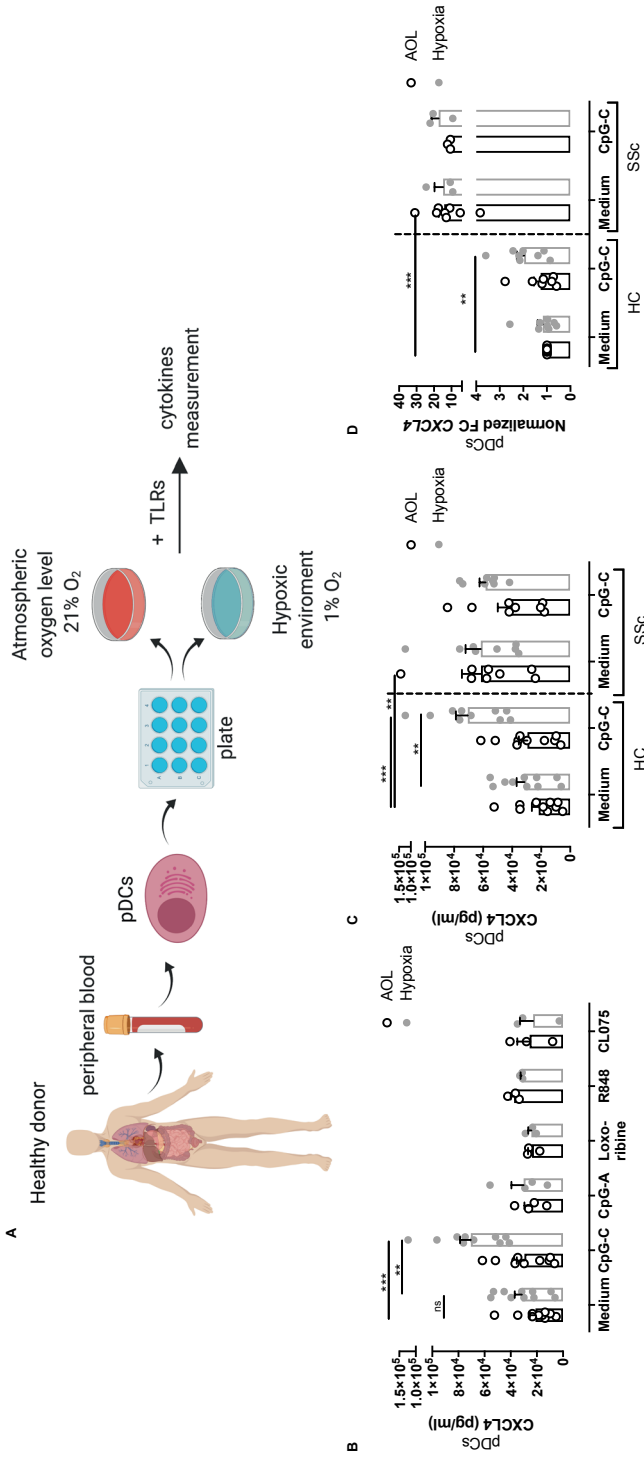


Figure 1. Hypoxia and TLR9 are the factors leading to increased CXCL4 production in pDCs. **A**) Schematic layout of the experimental design created with Biorender. **B**) CXCL4 levels quantified in the supernatant of pDCs isolated from healthy participants upon hypoxia or atmospheric oxygen level (AOL) and challenged with either TLR9 agonist (CpG-C, N=12 or CpG-A, N=4), TLR7/8 (R848, N=3), TLR7/8 (R848, N=3) or TLR8 agonist (CL075, N=3) during 16 hours. **C**) Supernatant CXCL4 levels secreted by pDCs of healthy participants (N=17) and patients with SSx (N=8) triggered with TLR9 agonist (CpG-C) incubated under hypoxic or normoxic conditions for 16 hours. **D**) CXCL4 mRNA expression level represented as normalized fold change (FC) in healthy participants (N=8) and SSx (N=8) pDCs, incubated in hypoxic or atmospheric condition, that were challenged with TLR9 (CpG-C) for 16 hours. Bars are represented as mean \pm SEM. Grey and white edge respectively represent hypoxic and atmospheric conditions. **= $P \leq 0.01$, ***= $P \leq 0.001$, using Mann-Whitney test.

Figure 2

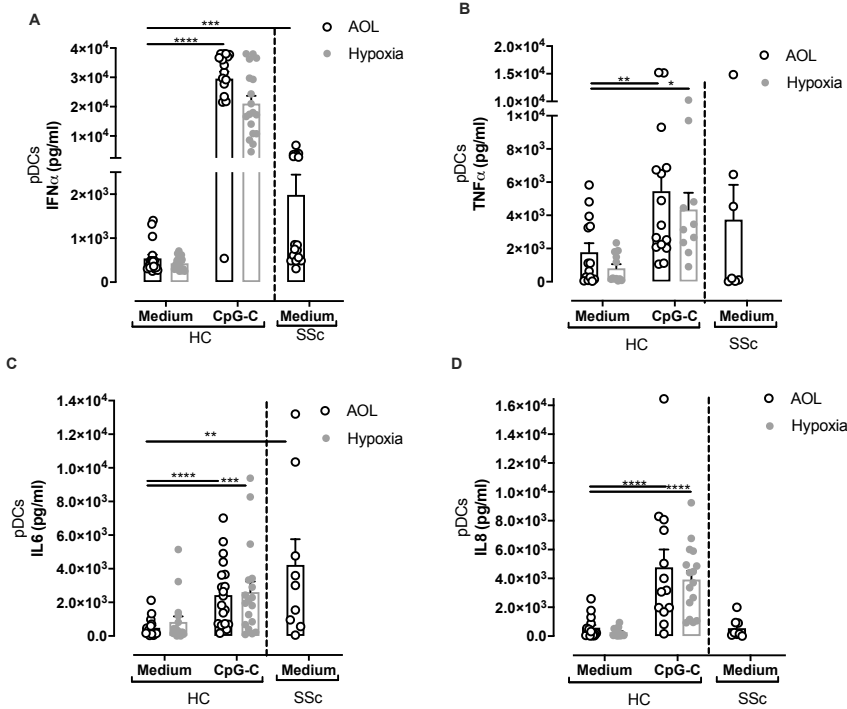


Figure 2. Hypoxia is an important factor for CXCL4 production but not for other cytokines produced by pDCs. Measurement of **A)** interferon (IFN) α , **B)** tumour necrosis factor (TNF) α , **C)** interleukin 6 (IL6) and **D)** interleukin 8 (IL8) in the supernatant of healthy pDCs (N=17 IFN α , N=15 TNF α , N=20 IL6, N=15 IL8) cultured in AOL or hypoxic conditions and co-stimulated with TLR9 agonist CPG-C and SSc pDCs (N=17 IFN α , N=7 TNF α , N=9 IL6, N=8 IL8) for 16hrs. Bars are represented as mean \pm SEM. *= $P \leq 0.05$, **= $P \leq 0.01$, ***= $P \leq 0.001$, ****= $P \leq 0.0001$ using Mann-Whitney test.

Increased mtROS production in SSc patient pDCs is associated with instability of mtDNA and is essential for CXCL4 production

It has previously been demonstrated that hypoxia increases the production of ROS from mitochondria (Chandel et al., 2000). We identified an increased basal level of mtROS in SSc pDCs ($P=0.0007$) (**Fig3a**). Increased production of mtROS may result in the progressive destruction of mitochondrial DNA (mtDNA) and consequent loss of mitochondrial function (Ide et al., 2001). We found a significant overall reduction in the mtDNA copy number, expressed as the ratio between *B2M/CYB*, in SSc patient pDCs ($P=0.0011$) (**Fig3b**). In addition, we looked at the expression of genes that act as antioxidants to clear mtROS, such as

SOD2 (superoxide dismutase 2), *PRDX3* (thioredoxin-dependent peroxide reductase), *NRF2* (nuclear factor erythroid-derived 2, that regulates antioxidant gene transcription) and *BCL2* (B-cell lymphoma 2) in different subsets of SSc. Accordingly to the literature (Clements et al., 1993; Goh et al., 2008; LeRoy et al., 1988), patients were classified as ncSSc (non-cutaneous SSc), lcSSc (limited cutaneous SSc) and dcSSc (diffuse cutaneous SSc) and schematically represented in **Supplemental Figure 1**. We found a significant reduction in the expression of *NRF2* in lcSSc ($P=0.0001$) and dcSSc ($P=0.043$), *PRDX3* in lcSSc ($P=0.0325$) and dcSSc ($P=0.0356$), *BCL2* in lcSSc ($P=0.0087$) and dcSSc ($P=0.0197$) and *SOD2* in lcSSc ($P=0.0402$) (**Fig3c**). In HC pDCs we observed an increased production of mtROS after exposure to hypoxia and TLR9 ($P=0.0079$), which mimicked the high levels of mtROS observed in SSc pDCs ($P=0.0007$) (**Fig3a**). In order to assess the role of mtROS in CXCL4 production, HC pDCs were incubated in the presence of mitoQ, a specific mtROS inhibitor. We observed a reduction of the CXCL4 production in cells co-exposed to hypoxia and TLR agonist in the presence of mitoQ, demonstrating an important role of mtROS in CXCL4 production in HC pDCs ($P=0.029$) (**Fig3d**). Also, in pDCs from SSc patients, mitoQ reduced the production of CXCL4 ($P=0.028$). Furthermore, mitoQ did not affect cell viability (**Supplemental Figure 3**).

2

Figure 3

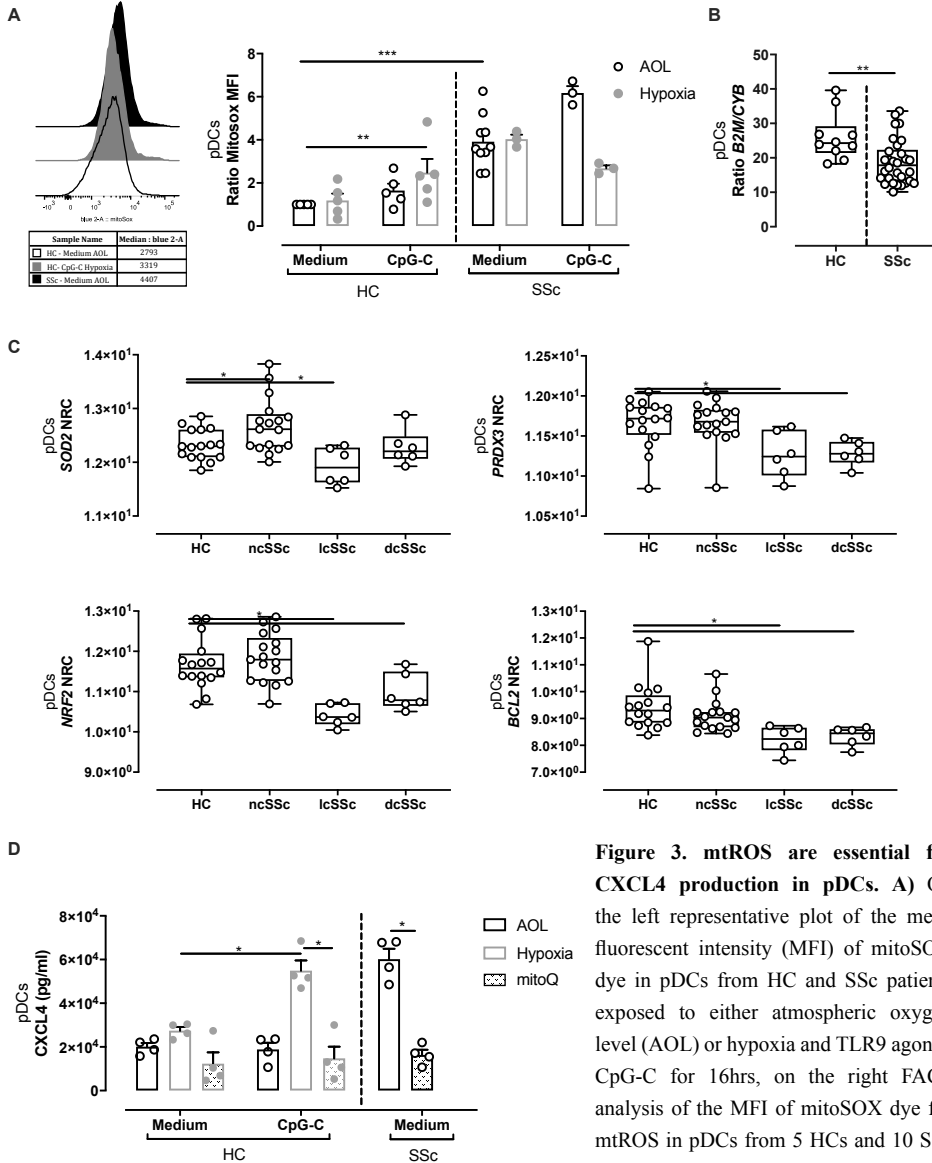


Figure 3. mtROS are essential for CXCL4 production in pDCs. **A)** On the left representative plot of the mean fluorescent intensity (MFI) of mitoSOX dye in pDCs from HC and SSc patients exposed to either atmospheric oxygen level (AOL) or hypoxia and TLR9 agonist CpG-C for 16hrs, on the right FACS analysis of the MFI of mitoSOX dye for mtROS in pDCs from 5 HCs and 10 SSc patients exposed to either AOL or hypoxia

and TLR9 agonist CpG-C for 16hrs. **B)** Quantification of mitochondrial DNA copies expressed as ratio between beta 2 macroglobulin (B2M) and cytochrome B (CYB) in freshly isolated pDCs of HC and SSc patients. **C)** RNA sec analysis of SOD2, PRDX3, NRF2 and BCL2 in pDCs from HC and SSc patients. **D)** ELISA measurement of CXCL4 in pDCs (4HC and 4SSc patients) exposed to either AOL or hypoxia and TLR9 agonist CpG-C +/- MitoQ for 16hrs. Bars are represented as mean \pm SEM. Grey and white edges respectively represent hypoxic and atmospheric conditions. Abbreviations: NRC= normalized read count, ncSSc = non-cutaneous SSc, lcSSc = limited cutaneous SSc, dcSSc = diffuse cutaneous SSc. *= $P \leq 0.05$, **= $P \leq 0.01$, ***= $P \leq 0.001$, using ordinary one-way ANOVA (C) and Mann-Whitney test (A, B, D, E).

HIF-2 α expression is increased in SSc pDCs and is essential for CXCL4 production

The hypoxia inducible factors (HIFs) are stabilized upon exposure to hypoxia, TLR triggering and/or increased production of mtROS (Spirig et al., 2010). Therefore, we first measured the expression of HIFs in pDCs from SSc patients, where we found an increased expression of *HIF-2 α* mRNA ($P < 0.0001$) (**Fig4a**). We observed no differences in *HIF-1 α* RNA level in any of the disease subsets (**Fig4b**). To confirm this observation, we measured the ratio of HIF-2 α and HIF-1 α protein in SSc pDCs, where we confirmed the higher ratio of HIF-2 α in patients ($P = 0.0062$), suggesting that hypoxia responses in SSc patient pDCs are due to HIF-2 α rather than HIF-1 α (**Fig4c, Supplemental Figure 2**). We observed no expression of HIF3 α in pDCs (data not shown). Next, we measured the protein level of HIF-2 α and HIF-1 α in pDCs exposed to hypoxia and TLR9 agonist, where we found HIF-2 α to be increased ($P = 0.028$), in contrary to HIF-1 α (**Fig4d,4e**).

In order to confirm the link between mtROS and HIFs we measured the RNA expression of *HIF-1 α* and *HIF-2 α* in pDCs from HC co-exposed to hypoxia and TLR9 and SSc patients, both in the presence of mtROS inhibitor mitoQ. We observed reduction of *HIF-2 α* RNA expression in pDCs from HC exposed to hypoxia and TLR9 as in pDCs from SSc patients when mitoQ was added to the mediums ($P = 0.029$). Further, we observed no differences in *HIF-1 α* RNA level (**Fig4f**).

To further assess the importance of HIF-2 α in CXCL4 production, specific inhibitors for HIF-2 α or HIF-1 α were added to the culture. Inhibition of HIF-2 α , but not HIF-1 α , in both, HC ($P = 0.007$) and SSc ($P = 0.038$) pDCs resulted in a reduction of CXCL4 production (**Fig4g**), with no effect on cell viability (**Supplemental Figure 3**).

In order to confirm the obligatory role of HIF-2 α in CXCL4 production, HIF-2 α or HIF-1 α were silenced in HCs pDCs and subsequently exposed to hypoxia and TLR9 agonist. We observed that HIF-2 α silencing in pDCs led to a significant reduction in CXCL4 production ($P = 0.0022$), while HIF-1 α silencing did not (**Fig4h**). The efficiency of the silencing was 54.7% for HIF-2 α and 58.8% for HIF-1 α (**Supplemental Figure 4**)

Figure 4

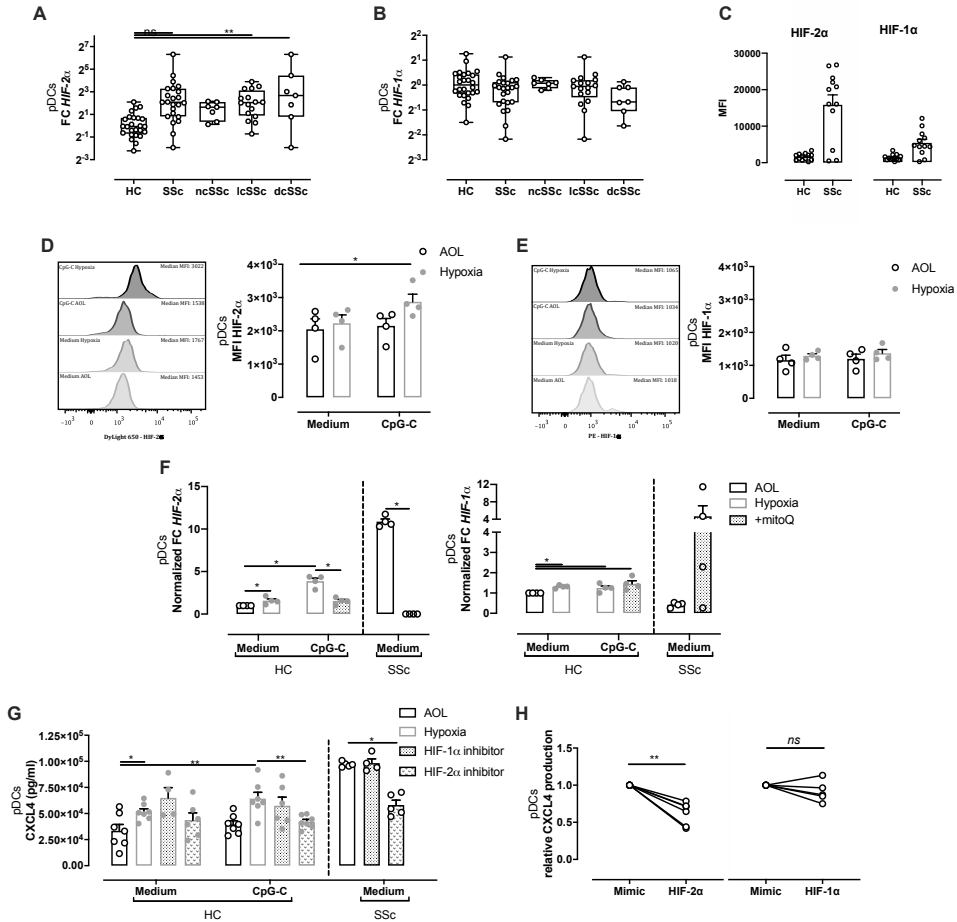


Figure 4. HIF-2 α is essential for the production of CXCL4 by pDCs. **A)** qPCR quantification of HIF-2 α and **B)** HIF-1 α genes in freshly isolated pDCs from HCs and SSc patients. **C)** Quantification of HIF-2 α and HIF-1 α protein expression as mean fluorescent unit (MFI) in freshly isolated pDCs from 13 HC and 12 SSc patients. **D)** On the left, representative plot, on the right analysis of intracellular FACS staining of HIF-2 α and **E)** HIF-1 from pDCs in 4 HCs, cultured in either atmospheric oxygen level (AOL) or hypoxic condition and TLR9 agonist CpG-C for 16hrs. **F)** qPCR quantification of *HIF-2 α* and *HIF-1 α* genes in pDCs (4HC and 4SSc patients) exposed to either AOL or hypoxia and TLR9 agonist CpG-C +/- MitoQ for 16hrs **G)** ELISA measurement of CXCL4 in pDCs from 7 HC and 5 SSc patients cultured in atmospheric or hypoxic condition +/- CpG-C with the addition of either HIF-1 α inhibitor or HIF-2 α inhibitor to the culture medium for 16hrs. **H)** Measurement of CXCL4 production in pDCs from 5 HCs exposed to hypoxia and CpG-C and transfected with a non-targeting (mimic) siRNA or either HIF-2 α or HIF-1 α siRNA, expressed as relative production compared to mimic. All data represents mean \pm SEM. Grey edges represent hypoxic condition and white bars AOL. Abbreviations: ncSSc = non-cutaneous SSc, lcSSc = limited cutaneous SSc, dcSSc = diffuse cutaneous SSc. *= $P \leq 0.05$, **= $P \leq 0.01$, ***= $P \leq 0.001$, ****= $P \leq 0.0001$ using unpaired Kruskal-Wallis test (A, B) and Mann-Whitney test (C, D, E, F, G).

Hypoxia is fundamental for the production of CXCL4 in CD34+ derived pDCs

Umbilical cord derived (uc)CD34+ derived pDCs were differentiated for 14 days either in atmospheric oxygen level (AOL) or hypoxia, and after exposed to TLR9 ligand CpG-C for 16hrs (**Fig5a**). We screened the cytokines production of the ucCD34 derived pDCs that were differentiated in AOL and observed that they were able to produce IFN α ($P=0.0093$), TNF α ($P=0.081$) and IL-6 ($P=0.04$) but no CXCL4 after TLR9 exposure (**Fig5b**). Interestingly, ucCD34 derived pDCs differentiated under hypoxia (5%) were able to produce CXCL4 (**Fig5c**). These results indicate that hypoxia plays a fundamental role for not only the production but also the ability to produce CXCL4 by pDCs.

2

Figure 5

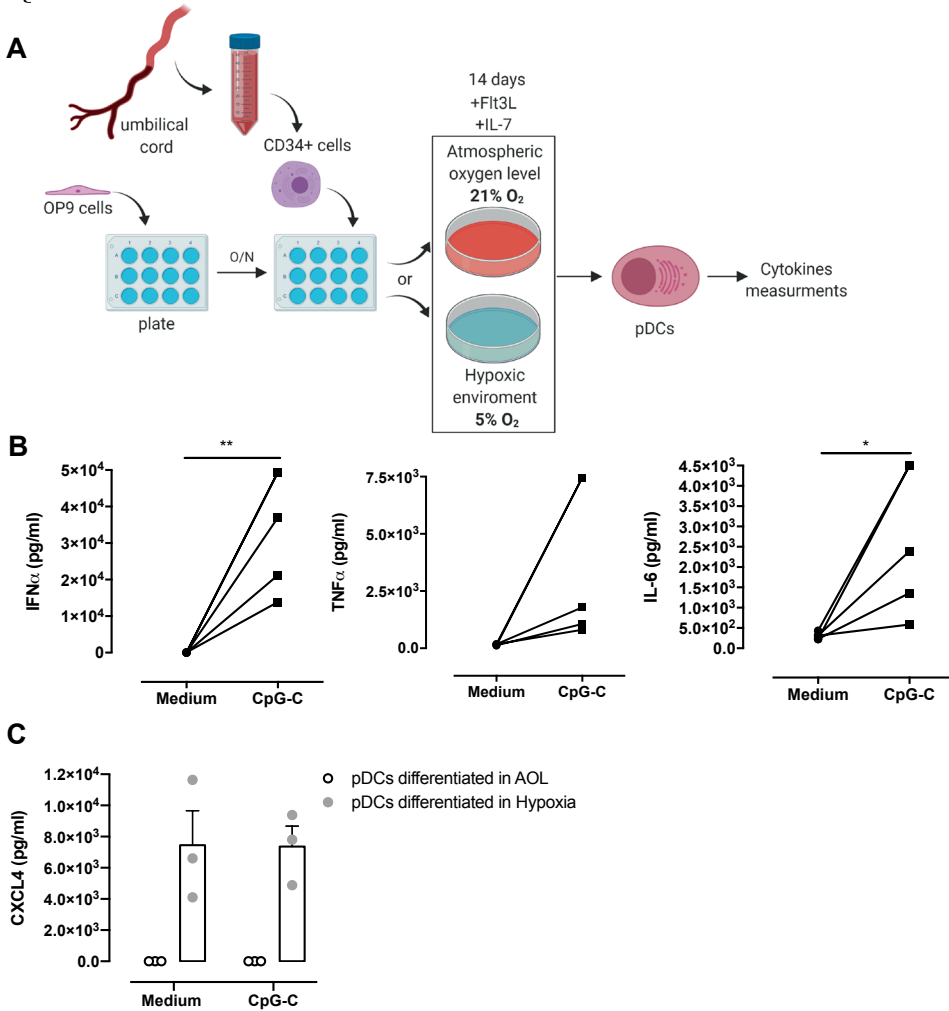


Figure 5. Hypoxia is the fundamental factor to enable CXCL4 production by pDCs. (A) Schematic representation of the experimental layout of the ucCD34 derived pDCs, created with Biorender (B). Luminex measurement of IL6, TNF α and IFN α production in ucCD34 derived pDCs differentiated in AOL and stimulated with TLR9 ligand CpG-C. (C) CXCL4 Elisa measurement in ucCD34 derived pDCs, differentiated either in AOL or hypoxia and subsequently exposed to TLR9 ligand CpG-C either in AOL or hypoxia. Bars are represented as mean \pm SEM. Grey and white edges respectively represent hypoxic and atmospheric conditions.

Discussion

We identified hypoxia as a key factor responsible for the production of CXCL4 by pDCs. Hypoxia is often considered a driving force behind many pathological hallmarks of SSc (Beyer et al., 2009). Our results suggest that the hypoxic environment makes pDCs more prone to respond to viral or bacterial infection or endogenous ligands via TLR signalling, culminating in high CXCL4 production and acceleration of disease progression. Recently our group observed that CXCL4 promotes genetic imprinting of DCs making them more prone to TLR stimulation and changes DCs in pro-fibrotic cells via direct matrix production as well as indirectly by inducing myofibroblast transition (manuscript in revision). Together with the observations presented here this suggests that CXCL4 plays an essential role in the vicious circle of inflammation, hypoxia and fibrosis as observed in SSc. Hence, for the first time we provide a link between hypoxia and disease progression which is orchestrated by CXCL4, an observation with great therapeutic relevance.

Hypoxia could be seen as a generalized phenomenon in SSc patients, due to the Raynaud Phenomenon and the vasculopathy responsible of the typical vascular alteration of SSc (Pattanaik et al., 2015). Therefore, we speculated that this vasculopathy is responsible of a condition of chronic hypoxia in SSc. Also, the events responsible of the Raynaud Phenomenon could take place in organs different from the skin, affecting the circulatory cells. Furthermore, it has been shown that hypoxia leads to oxidative stress via excessive production of ROS in dendritic cells (Paardekooper et al., 2019). Recently it has been shown that mitochondrial ROS (mtROS), rather than other sources of ROS, are responsible for the production of inflammatory cytokines (Agod et al., 2017; Li et al., 2013). In this study, we found increased basal levels of mtROS being produced by pDCs isolated from SSc patients. Increased production of mtROS in the cell can lead to alteration in mitochondria such as a decrease in mtDNA copy numbers (Vidoni et al., 2013). In fact, we observed a reduction in mtDNA copy numbers in pDCs from SSc patients consistent with their exposure to excessive mtROS production. To further explore the involvement of mtROS in

SSc pDCs, we investigated the expression of genes that play a crucial role in maintaining cellular redox homeostasis in the mitochondria, such as SOD2 or NRF2. These genes were significantly reduced in SSc pDCs, especially in patients with fibrotic involvement (lcSSc, dcSSc). Targeting one of these genes could restore mtROS homeostasis in SSc patients. For instance, pharmacological activation of NRF2 with the naturally occurring NRF2 activator sulforaphane could be a valid approach (Noh et al., 2015). Interestingly, blocking mtROS with a specific mtROS inhibitor (mitoQ), significantly reduced the production of CXCL4 in pDCs.

HIFs are transcriptional activators that function as master regulators of oxygen homeostasis in the cell and are capable of influencing cell metabolism, vascular neogenesis, metabolic changes, cell proliferation and survival (Semenza, 2003). HIFs are stabilized upon exposure to hypoxia, TLR triggering, and production of mtROS (Sanjuán-Pla et al., 2005; Schroedl et al., 2002).

Our data show an increased expression of HIF-2 α in SSc pDCs, while no significant changes were observed in the expression of HIF-1 α . Interestingly, we found that blocking mtROS with mitoQ, specifically blocks the expression of HIF-2 α but not HIF-1 α . in pDCs. Furthermore, we were able to induce high HIF-2 α expression in HC pDCs, through hypoxia and TLR9 agonist exposure. In stimulated HC pDCs and pDCs of SSc patients, inhibiting as well as silencing HIF-2 α diminished the production of CXCL4 significantly. This observation is in line with the findings of Ryu *et al.*, where, although not showing the mechanism, fibroblast like synoviocytes from rheumatoid arthritis patients overexpressing HIF-2 α showed that the production of different pro-inflammatory mediators, including CXCL4 was significantly increased on RNA level (Ryu et al., 2014). Furthermore, we observed that ucCD34 derived pDCs differentiated under AOL are able to produce cytokines such as IL6, TNF α and IFN α , but not CXCL4. Interestingly, ucCD34 derived pDCs differentiated under hypoxia (5% O₂) were able to produce CXCL4, further highlighting the fundamental role of hypoxia in CXCL4 production.

Taken together, as CXCL4 plays an important role in inflammation and fibrosis, prevention of its excessive production and/or inhibition of its function provides an attractive target for a plethora of medical conditions. As clinically grade monoclonal antibodies against CXCL4 are not yet available an alternative way to block the effects of CXCL4 is the prevention of its release.

Our study identifies hypoxia and TLR9 stimulation as a crucial factor driving CXCL4 release via increased production of mtROS leading to HIF-2 α stabilization, all thus potentially interesting molecular processes for therapeutic targeting (**Fig.6**). Interestingly, a few successful clinical trials were already performed by using MitoQ to block mtROS production in aging (Rossman et al., 2018). Also HIF-2 α antagonist (PT2385) was recently successfully used for a phase 1 clinical trial for the treatment of clear cell renal carcinoma (Courtney et al., 2018). Further studies are warranted to assess the potential clinical relevance of blocking the detrimental effects of hypoxia by interference with the responsible downstream molecular processes.

Our study thus reveals new insight into the pathogenesis of SSc in identifying metabolic changes in SSc pDCs, including increase of mtROS and alterations in mitochondria. This study is the first to show significant changes in the expression of HIFs in SSc patients, where HIF-2 α plays an essential role.

Figure 6

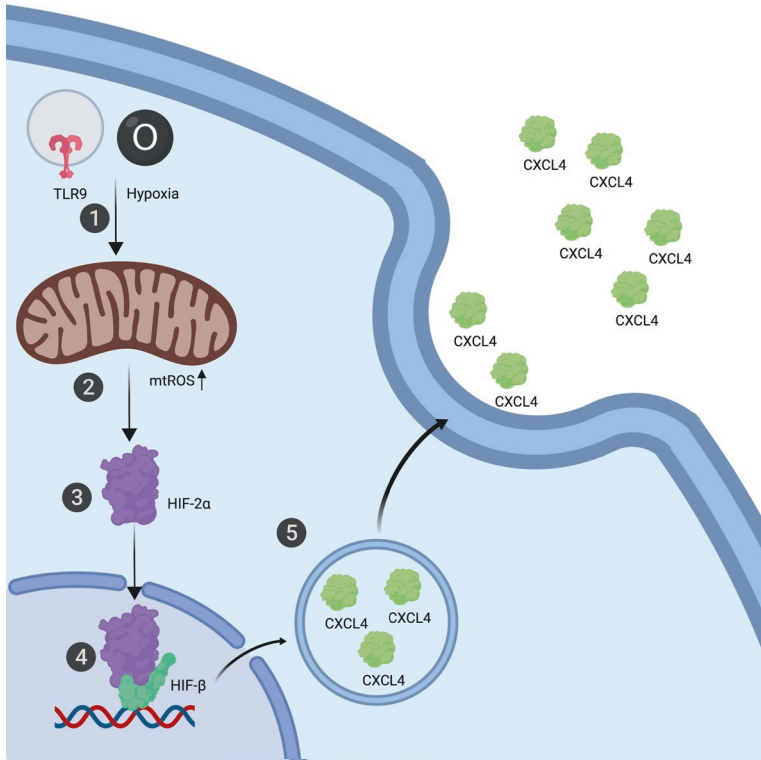


Figure 6. Model of CXCL4 production upon exposure to hypoxia and TLR9 in HCs and SSc pDCs. (1) The co-exposure to hypoxia and TLR9 agonist leads to increase of mtROS production (2). mtROS stabilize HIF-2 α (3) that can dimerize with HIF- β and induce CXCL4 expression (4). CXCL4 is then transported to the plasma membrane and released (5). Created with Biorender.

2

Supplemental Tables

Supplemental Table 1. Base-line characteristics of patients with SSc, categorized according to the ACR (2013) criteria.

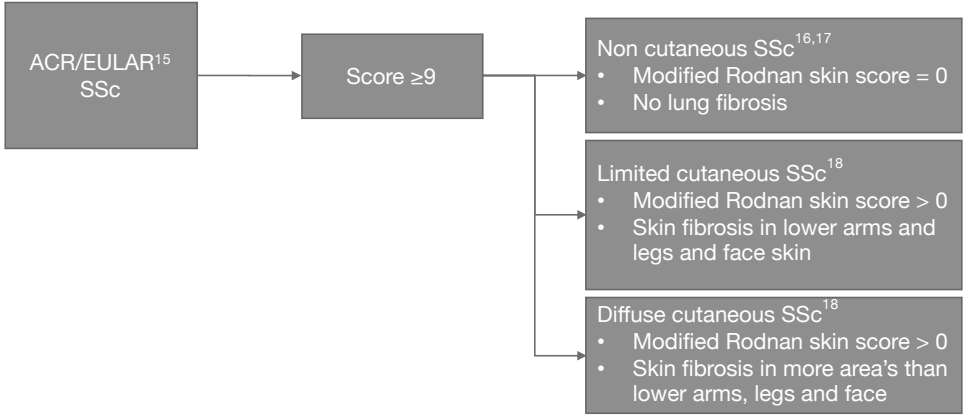
	Healthy participants (n=97)	SSc (n=70)
Age (years) (min-max)	44 (33–62)	59 (30–80)
Female (%)	80	81
ANA (Antinuclear Antibody) (%)	–	63 (90%)
ACA (Anticentromere Antibody) (%)	–	32 (46%)
Scl70 (Anti topoisomerase I) (%)	–	37 (54%)
mRSS (modified Rodnan skin score) (min-max)	–	7 (0-36)
ILD (Interstitial lung disease) (%)	–	21 (30%)
Disease Duration (years) (min-max)	–	12 (2-35)

The values are represented as mean + min-max.

2

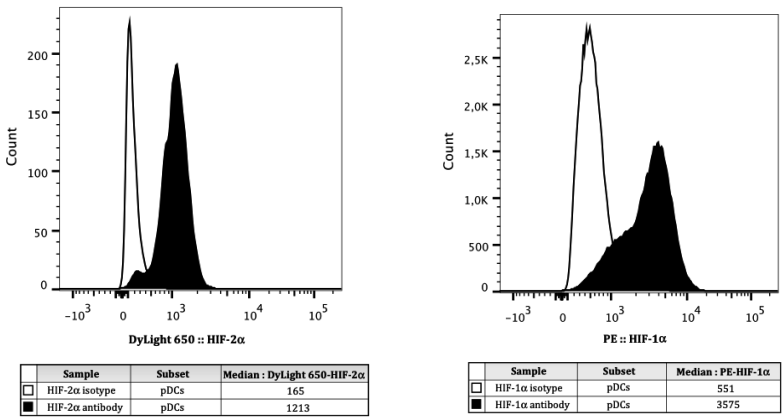
Supplemental Figures

Supplemental Figure 1



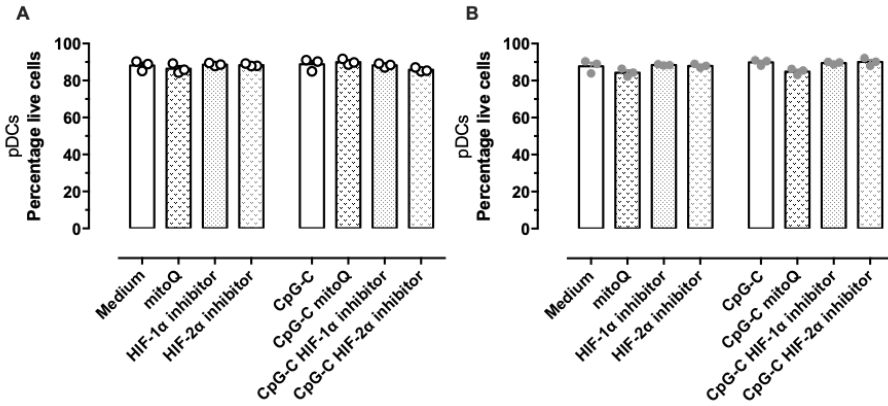
Supplemental Figure 1. SSc Classification criteria

Supplemental Figure 2



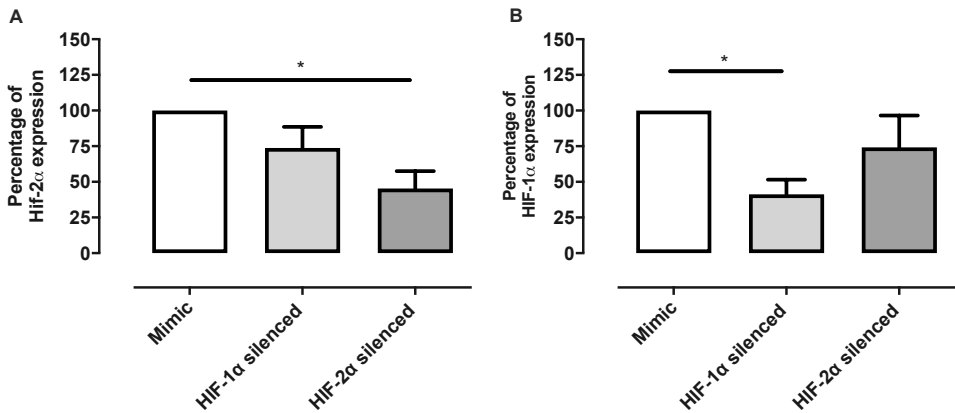
Supplemental Figure 2. HIF-2 α and HIF-1 α isotope staining. Flow analysis of the staining of pDCs with anti HIF-2 α A) and HIF-1 α B) antibodies and the respective isotypes.

Supplemental Figure 3



Supplemental Figure 3. Percentage of live cells. FACS analysis expressed as percentage of live cells in annexin V, 7-AAD dead staining of pDCs cultured in either atmospheric **A**) or hypoxic **B**) condition and TLR9 agonist CpG-C for 16hrs, both, exposed to different inhibitors (mitoQ, HIF-1 α and HIF-2 α inhibitor). All data represents mean \pm SEM. Grey and white circles respectively represent hypoxic and atmospheric conditions.

Supplemental Figure 4



Supplemental Figure 4. Silencing efficiency. qPCR quantification of **A**) HIF-2 α and **B**) HIF-1 α after silencing represented as percentage of expression compared to Mimic transfection. All data represents mean \pm SEM

STAR METHODS

LEAD CONTACT AND MATERIALS AVAILABILITY

Key resource Table 1

	Reagent	Cat#	Company
Cell isolation	10 mL Li-Hep vacutainer	#367526,	BD Biosciences
	Ficoll gradient	#17-1440-02	GE Healthcare
	pDCs beads (CD304 (BDCA-4/Neuropilin-1) MicroBead Kit, human)	#130-090-532	Miltenyi Biotec
	RPMI 1640 GlutaMAX medium	#61870-010	Thermo Fisher Scientific
	Fetal Bovine Serum (FBS)	#S181A	Biowest
	Penicillin-Streptomycin	#15070063	Thermo Fisher Scientific
Cell culturing and stimulation	IL3	#11340033	Immnotools
	CpG-C	#tlrl-m362-1	Invivogen
	CpG-A	#tlrl-2216-1	Invivogen
	CL075	#tlrl-c75	Invivogen
	R848	#tlrl-r848	Invivogen
	Loxoribine	#tlrl-lox	Invitrogen
Inhibitors	mitoQ (provided by Dr Mike Murphy)		
	HIF-1 α	# CAS 1568-83-8	Santa Cruz Biotechnology
	HIF-2 α	#SML0883	Sigma-Aldrich
Cell transfection	Lipofectamine® 2000 Transfection Reagent	#11668-019	Invitrogen
	HIF-1 α specific small interfering RNA (siRNA)		Thermo Scientific
	HIF-2 α specific small interfering RNA (siRNA)		Thermo Scientific
	control non-targeting siRNA		Thermo Scientific
mtROS measurement	MitoSOX™ Red	# M36008	Thermo Fisher
Cytokine quantification	CXCL4 ELISA kit	#DY795	R&D Systems
	INF α ELISA kit	#BMS216MST	Thermo Fischer
RNA extraction and cDNA synthesis	Allprep RNA/DNA Micro Kit	# 80284	Qiagen
	SuperScript™ II RT	#18064014	Thermo Fisher Scientific

qPCR	SYBR green Master Mix	# 4309155	Applied Biosystems
	TaqMan Master Mix	# 4369016	Applied Biosystems
Intracellular staining	Fix-Perm	# 88-8824-00	eBioscience

Key resource Table 2. Primer's sequence description

Target	Forward primer	Reverse primer	TaqMan Assay ID
CXCL4	-	-	Hs00236998_m1
HIF-1α	TGCTCATCAGTTGCCACTTC	TATCCAAATCACCAGCATCC	-
HIF-2α	GGAGACGGAGGTGTTCTATGAG	CAGAGCAAACCTGAGGAGAGG	-
B2M	-	-	Hs00939627_m1
GUSB	CACCAGGGACCATCCAATACC	GCAGTCCAGCGTAGTTGAAAAA	-
CYTB	GCCTGCCTGATCCTCAAAT	AAGGTAGCGGATGATTCAGCC	-

Key resource Table 3. Antibodies utilized for FACS analysis in pDCs

Marker	Colour	Cat#
CD123	BV510	306022, Biolegend
CD303	FITC	130-090-510, Miltenyi Biotec
HIF-1α	PE	359704, Biolegend
HIF-2α	DyLight 650	MA5-16021, Thermofisher

Lead Contact and Materials Availability

This study did not generate new unique reagents. Further information and requests for resources and reagents should be directed to and will be fulfilled by the Lead Contact, Dr. Wioleta Marut (w.k.marut@umcutrecht.nl).

Experimental model and subject details

Patient Cohort

Blood from patients and sex- and age-matched healthy controls (HC) was obtained from the University Medical Center Utrecht and the Maastad Hospital Rotterdam (The Netherlands). All patients provided informed written consent approved by the local institutional medical ethics review boards prior to inclusion in this study. Samples and clinical information were treated anonymously immediately after collection. Patients fulfilled the ACR/EULAR 2013 classification criteria for SSc (Van Den Hoogen et al., 2013) and the demographics and clinical characteristics of the patients are detailed in **Supplemental Table 1**. Briefly, we will refer to ncSSc (Non-cutaneous SSc) as patients with no skin fibrosis involvement and to lcSSc (Limited cutaneous SSc) and dcSSc (Diffuse cutaneous SSc) as patients with skin fibrosis involvement (schematically represented in **Supplemental Figure 1** (Clements et al., 1993; Goh et al., 2008; LeRoy et al., 1988)). The study was performed according to the guidelines of the Declaration of Helsinki and the local ethical and Review committee from each centre approved the study.

Reagents, catalogue numbers and company name are listed in **Key resource table 1**.

Method details

Cell isolation

Peripheral blood mononuclear cells (PBMCs) from HC and SSc patients were isolated by Ficoll gradient. pDCs were isolated using an autoMACS Pro Separator according to the manufacturer's instructions. Purity was routinely assessed by flow cytometry and above 92% for pDCs.

pDCs stimulation

Half million pDCs per ml were cultured in RPMI-GlutaMAX supplemented with 10% fetal

bovine serum (FBS), 10,000 I.E. penicillin-streptomycin and interleukin-3 (IL-3, 10ng/ml), and then incubated either in atmospheric (21% O₂) or hypoxic conditions (1% O₂ - in a Rasquinn invivO2 1000 hypoxic chamber). Cells were acclimated for 30 minutes before being exposed to different stimuli and/or inhibitors. Cells were stimulated with the TLR agonists CpG-C (TLR9, 1μM), CpG-A (TLR9, 1μM), Loxoribine (TLR7, 1μg/ml), R848 (TLR7/8, 2μg/ml) or CL075 (TLR8, 5mM) for 16 hours in an incubator at 37°C and 5% CO₂.

Inhibition of mitochondrial reactive oxygen species (mtROS) and HIFs

To inhibit mtROS we used mitoQ (10nM) (provided by Dr Mike Murphy, MRC Mitochondrial Biology Unit, University of Cambridge, UK), and HIF-1α and HIF-2α were inhibited using HIF-1α (Bisphenol A dimethyl ether, 10nM) and HIF-2α (HIF-2 Antagonist 2, 10nM) inhibitors.

Transfection of pDCs using siRNA

Transfection of pDCs was done using Lipofectamine® 2000 Transfection Reagent. HIF-1α, HIF-2α or control non-targeting silencing RNA (siRNA) (5nM) were mixed with Optimem and Plus reagent and incubated for 20 minutes at room temperature prior to transfection for 6 hours. After transfection cells were incubated either under atmospheric or hypoxic conditions as described above.

RNA sequencing

RNA sequencing was performed by Beijing Genomics Institute (Hong Kong) using 100ng RNA per sample to prepare RNAseq libraries (TruSeq Stranded kit, Illumina) after poly(A) capture according to the manufacturer's instructions. Pooled libraries of equimolar concentration were sequenced according to manufacturer's protocols using the Illumina HiSeq 2000 sequencer. Each sample generated approximately 2x10⁷paired-end (100bp) reads. FastQC was used to perform quality check and, using STAR aligner (Dobin et al., 2013), samples were aligned to a reference human genome (GRCh38 build 79). HTSeq-

count was used to calculate the read counts per gene (Anders et al., 2015). DESeq2 was used to perform the differential gene expression analysis of HCs and SSc patients as described before. To obtain normalized read counts, variance stabilizing transformation was used (Love et al., 2014).

mtROS measurement

mtROS production was quantified using MitoSOX™ Red Mitochondrial Superoxide Indicator according to the manufacturer's protocol, measured in FACS CANTO II Flow cytometer and analysed with BD FACSDiva software.

Quantification of cytokine production level

Cell-free supernatants were analyzed by ELISA for CXCL4 and interferon (IFN) α . Tumor necrosis factor (TNF) α , IL6 and IL8 were measured using human single-plex assays (Bio-Rad) and read on a Bio-Plex 200 system (Bio-Rad).

RT-PCR and quantitative (q)PCR

RNA from pDCs was isolated using the Allprep RNA/DNA kit. Total RNA was reverse-transcribed using SuperScript™ II RT. Duplicate PCR reactions were performed using SYBR green or TaqMan with a Quantstudio Real-Time PCR detection system. cDNA was amplified using specific primers (**Key resource Table 2**). Relative levels of gene expression were calculated by normalizing to *GUSB* or *B2M* housekeeping genes. Fold changes (FC) of mRNA were calculated by using the formulas $2^{-\Delta C_t}$ and $2^{-\Delta\Delta C_t}$.

Intracellular Flow cytometry in pDCs

pDCs were stained extracellularly first with CD123 and CD303 at 4°C using optimized concentrations of antibody for 15 minutes. After being fixed and permeabilized using Fix-Perm according to manufacturer's protocol, pDCs were stained with either anti-HIF-1 α or anti-HIF-2 α antibody. Data were acquired using a Fortessa flow cytometer and analyzed using FlowJo Software. Protein levels were quantified and represented as mean fluorescence intensity. Antibodies used are listed in **Key resource Table 3**.

OP9 cells harvest and culture

On day 0 OP9 cells, a cell line derived from mouse bone marrow stromal cell (Nakano et al., 1994), were seeded on a 24 well plate at a final concentration of 20.000 cells per well in 750 μ l of MEM α medium enriched with 20% FCS and 1% penicillin and streptomycin. Cells were kept at 37°C and 5%CO₂ overnight.

CD34+ cell culture

Umbilical cord derived CD34 cells, isolated from cord blood donated to the UMC Utrecht hospital, were thawed in a 37°C water bath, diluted in PBS and loaded on FBS. After one wash in PBS, cells were re-suspended in MEM α enriched with 20% FBS, 1% penicillin and streptomycin. Cells were plated on top of OP9 cells, at a final concentration of 25000 cells per well. Medium was supplemented with IL-7 (15ng/ml) (Peprotech) and Flt-3L (15ng/ml) (Cellgenix). Cells were then incubated for 14 days either in Hypoxia (5% O₂) or in AOL (21% O₂) at 5%CO₂. Every 2 days complete MEM α medium enriched with IL7 and Flt-3L was added. On day 14 the cells were stimulated with CpG-C either in hypoxia (5% O₂) or AOL (21% O₂) with 5% CO₂.

Viability assessment on pDCs

Cell death was assessed by Annexin V-7AAD staining. Cells were stained with Annexin V (1:100 dilution, BD Pharmingen) and 7AAD (1:100 dilution, BD Pharmingen) and measured using a FACS Canto Flow Cytometer. The data were further analysed with BD FACS DIVA software.

Quantification and statistical analysis

Where appropriate, Mann–Whitney test, unpaired Kruskal–Wallis test or paired one-way ANOVA test, were assessed using Graph Pad Prism7.0 Software. *P* values smaller than 0.05 were considered to be statistically significant.

Acknowledgements

This study was supported by research funding Marie Curie Intra-European Fellowship (Proposal number: 624871), the NWO VENI (grant number 91919149) and Gravitation (grant number 2013 ICI-024.002.009).

All the authors listed have made substantial, direct, and intellectual contribution to the work and approved it for publication. We thank Wilco de Jager (MultiPlex Core Facility, University Medical Center Utrecht) for performing Luminox assays. We thank *Dr Mike Murphy MRC Mitochondrial Biology Unit Wellcome Trust/MRC Building Hills Road, Cambridge CB2 0XY, UK for providing us mitoQ.*

Author contribution

All authors approved the final version after being involved in drafting and revising the article for important intellectual content. A. Ottria and W. Marut had full access to the data and takes responsibility for the accuracy of the performed analysis and the integrity of the data. A. Ottria, T.R.D.J. Radstake and W. Marut were involved in design of the study. Execution and analysis of the results was performed by A. Ottria. A. Ottria, M. Zimmermann, T. Carneiro, N. Vazirpanah, S. Silva-Cardoso, A.J. Affandi, E. Chouri, M.v.d Kroef, E. Mocholi-Gimeno, M. Rossato, S. Garcis Perez, R.G. Tieland, C.P.J. Bekkers and R.G.K. Wichers were involved in performing experiments. A. Pandit was involved in analyzing the gene array seq. A. Ottria and M. Cossu were involved in selection of the patients. J. Tekstra, E. Ton, J. van Laar, L. Beretta, F. Bonte-Mineur and T.R.D.J. Radstake were involved in inclusion of SSc patients. All the authors contributed to the review of the manuscript.

Declaration of interests:

The authors declare no competing interests.

Ethical approval information

This study was performed according to the guidelines of the Declaration of Helsinki and study meets the approval of Ethical and Review committee of the Institutional Review

and Ethical Board of University medical centre of Utrecht and Maastad Ziekenhuis of Rotterdam and University of Milan & Fondazione IRCCS Ospedale Maggiore Policlinico, Italy. The Ethical Committee approval was obtained in November 2011 (Ethical approval number 12-466 and 13-697). Moreover, in this study, all participants gave their informed consent before the inclusion.

References

- Affandi, A.J., Silva-Cardoso, S.C., Garcia, S., Leijten, E.F.A., van Kempen, T.S., Marut, W., van Roon, J.A.G., and Radstake, T.R.D.J. (2018). CXCL4 is a novel inducer of human Th17 cells and correlates with IL-17 and IL-22 in psoriatic arthritis. *Eur. J. Immunol.* *48*, 522–531.
- Agod, Z., Fekete, T., Budai, M.M., Varga, A., Szabo, A., Moon, H., Boldogh, I., Biro, T., Lanyi, A., Bacsı, A., et al. (2017). Regulation of type I interferon responses by mitochondria-derived reactive oxygen species in plasmacytoid dendritic cells. *Redox Biol.* *13*, 633–645.
- Anders, S., Pyl, P.T., and Huber, W. (2015). HTSeq—a Python framework to work with high-throughput sequencing data. *Bioinformatics* *31*, 166–169.
- Beyer, C., Schett, G., Gay, S., Distler, O., and Distler, J.H. (2009). Hypoxia. Hypoxia in the pathogenesis of systemic sclerosis. *Arthritis Res. Ther.* *11*, 220.
- van Bon, L., Affandi, A.J., Broen, J., Christmann, R.B., Marijnissen, R.J., Stawski, L., Farina, G.A., Stıfano, G., Mathes, A.L., Cossu, M., et al. (2014). Proteome-wide Analysis and CXCL4 as a Biomarker in Systemic Sclerosis. *N. Engl. J. Med.* *370*, 433–443.
- Burstein, S.A., Malpass, T.W., Yee, E., Kadin, M., Brigden, M., Adamson, J.W., and Harker, L.A. (1984). Platelet factor-4 excretion in myeloproliferative disease: implications for the aetiology of myelofibrosis. *Br. J. Haematol.* *57*, 383–392.
- Chandel, N.S., McClintock, D.S., Feliciano, C.E., Wood, T.M., Melendez, J.A., Rodriguez, A.M., and Schumacker, P.T. (2000). Reactive oxygen species generated at mitochondrial Complex III stabilize hypoxia-inducible factor-1 α during hypoxia: A mechanism of O₂sensing. *J. Biol. Chem.* *275*, 25130–25138.
- Clements, P.J., Lachenbruch, P.A., Seibold, J.R., Zee, B., Steen, V.D., Brennan, P., Silman, A.J., Allegar, N., Varga, J., and Massa, M. (1993). Skin thickness score in systemic sclerosis: an assessment of interobserver variability in 3 independent studies. *J. Rheumatol.* *20*, 1892–1896.
- Courtney, K.D., Infante, J.R., Lam, E.T., Figlin, R.A., Rini, B.I., Brugarolas, J., Zojwalla, N.J., Lowe, A.M., Wang, K., Wallace, E.M., et al. (2018). Phase I Dose-Escalation Trial of PT2385, a First-in-Class Hypoxia-Inducible Factor-2 α Antagonist in Patients With Previously Treated Advanced Clear Cell Renal Cell Carcinoma. *J. Clin. Oncol.* *36*, 867–874.
- Dobin, A., Davis, C.A., Schlesinger, F., Drenkow, J., Zaleski, C., Jha, S., Batut, P., Chaisson, M., and Gingeras, T.R. (2013). STAR: ultrafast universal RNA-seq aligner. *Bioinformatics* *29*, 15–21.
- Fuschiotti, P. (2016). Current perspectives on the immunopathogenesis of systemic sclerosis. *ImmunoTargets Ther.* *5*, 21–35.
- Gabrielli, A., Avvedimento, E. V. and Krieg, T. (2009). Scleroderma. *N. Engl. J. Med.* *360*, 1989–2003.
- Goh, N.S.L., Desai, S.R., Veeraraghavan, S., Hansell, D.M., Copley, S.J., Maher, T.M., Corte, T.J., Sander, C.R., Ratoff, J., Devaraj, A., et al. (2008). Interstitial lung disease in systemic sclerosis: a simple staging system. *Am. J. Respir. Crit. Care Med.* *177*, 1248–1254.
- Van Den Hoogen, F., Khanna, D., Fransen, J., Johnson, S.R., Baron, M., Tyndall, A., Matucci-Cerinic, M., Naden, R.P., Medsger, T.A., Carreira, P.E., et al. (2013). 2013 classification criteria for systemic sclerosis: An american college of rheumatology/ European league against rheumatism collaborative initiative. *Arthritis Rheum.*
- Ide, T., Tsutsui, H., Hayashidani, S., Kang, D., Suematsu, N., Nakamura, K., Utsumi, H., Hamasaki, N., and Takeshita, A. (2001). Mitochondrial DNA damage and dysfunction associated with oxidative stress in failing hearts after myocardial infarction. *Circ. Res.* *88*, 529–535.
- Kasper, B., Winoto-Morbach, S., Mittelstädt, J., Brandt, E., Schütze, S., and Petersen, F. (2010). CXCL4-induced monocyte survival, cytokine expression, and oxygen radical formation is regulated by sphingosine kinase 1. *Eur. J. Immunol.* *40*, 1162–1173.
- Kioon, M.D.A., Tripodo, C., Fernandez, D., Kirou, K.A., Spiera, R.F., Crow, M.K., Gordon, J.K., and Barrat, F.J. (2018). Plasmacytoid dendritic cells promote systemic sclerosis with a key role for TLR8. *Sci. Transl. Med.* *10*.
- LeRoy, E.C., Black, C., Fleischmajer, R., Jablonska,

- S., Krieg, T., Medsger, T.A., Rowell, N., and Wollheim, F. (1988). Scleroderma (systemic sclerosis): classification, subsets and pathogenesis. *J. Rheumatol.* *15*, 202–205.
- Li, X., Fang, P., Mai, J., Choi, E.T., Wang, H., and Yang, X.-F. (2013). Targeting mitochondrial reactive oxygen species as novel therapy for inflammatory diseases and cancers. *J. Hematol. Oncol.* *6*, 19.
- Love, M.I., Huber, W., and Anders, S. (2014). Moderated estimation of fold change and dispersion for RNA-seq data with DESeq2. *Genome Biol.* *15*, 550.
- Nakano, T., Kodama, H., and Honjo, T. (1994). Generation of lymphohematopoietic cells from embryonic stem cells in culture. *Science* *265*, 1098–1101.
- Noh, J.-R., Kim, Y.-H., Hwang, J.H., Choi, D.-H., Kim, K.-S., Oh, W.-K., and Lee, C.-H. (2015). Sulforaphane protects against acetaminophen-induced hepatotoxicity. *Food Chem. Toxicol.* *80*, 193–200.
- Paardekooper, L.M., Vos, W., and van den Bogaart, G. (2019). Oxygen in the tumor microenvironment: effects on dendritic cell function. *Oncotarget* *10*, 883–896.
- Pattanaik, D., Brown, M., Postlethwaite, B.C., and Postlethwaite, A.E. (2015). Pathogenesis of Systemic Sclerosis. *Front. Immunol.* *6*, 272.
- Van Raemdonck, K., Van den Steen, P.E., Liekens, S., Van Damme, J., and Struyf, S. (2015). CXCR3 ligands in disease and therapy. *Cytokine Growth Factor Rev.* *26*, 311–327.
- Romagnani, P., Maggi, L., Mazzinghi, B., Cosmi, L., Lasagni, L., Liotta, F., Lazzeri, E., Angeli, R., Rotondi, M., Fili, L., et al. (2005). CXCR3-mediated opposite effects of CXCL10 and CXCL4 on TH1 or TH2 cytokine production. *J. Allergy Clin. Immunol.* *116*, 1372–1379.
- Rossmann, M.J., Santos-Parker, J.R., Steward, C.A.C., Bispham, N.Z., Cuevas, L.M., Rosenberg, H.L., Woodward, K.A., Chonchol, M., Gioscia-Ryan, R.A., Murphy, M.P., et al. (2018). Chronic Supplementation With a Mitochondrial Antioxidant (MitoQ) Improves Vascular Function in Healthy Older Adults. *Hypertension* *71*, 1056–1063.
- Ryu, J.-H.H., Chae, C.-S.S., Kwak, J.-S.S., Oh, H., Shin, Y., Huh, Y.H., Lee, C.-G.G., Park, Y.-W.W., Chun, C.-H.H., Kim, Y.-M.M., et al. (2014). Hypoxia-Inducible Factor-2 α Is an Essential Catabolic Regulator of Inflammatory Rheumatoid Arthritis. *PLoS Biol.* *12*, 1–16.
- Sanjuán-Pla, A., Cervera, A.M., Apostolova, N., Garcia-Bou, R., Víctor, V.M., Murphy, M.P., and McCreath, K.J. (2005). A targeted antioxidant reveals the importance of mitochondrial reactive oxygen species in the hypoxic signaling of HIF-1 α . *FEBS Lett.* *579*, 2669–2674.
- Scheuerer, B., Ernst, M., Dürrbaum-Landmann, I., Fleischer, J., Grage-Griebenow, E., Brandt, E., Flad, H.D., and Petersen, F. (2000). The CXCL-chemokine platelet factor 4 promotes monocyte survival and induces monocyte differentiation into macrophages. *Blood* *95*, 1158–1166.
- Schroedl, C., McClintock, D.S., Budinger, G.R.S., and Chandel, N.S. (2002). Hypoxic but not anoxic stabilization of HIF-1 α requires mitochondrial reactive oxygen species. *Am. J. Physiol. Cell. Mol. Physiol.* *283*, L922–L931.
- Schwarz, K.B., Rosensweig, J., Sharma, S., Jones, L., Durant, M., Potter, C., and Narkewicz, M.R. (2003). Plasma markers of platelet activation in cystic fibrosis liver and lung disease. *J. Pediatr. Gastroenterol. Nutr.* *37*, 187–191.
- Semenza, G.L. (2003). Targeting HIF-1 for cancer therapy. *Nat. Rev. Cancer* *3*, 721–732.
- Spirig, R., Djafarzadeh, S., Regueira, T., Shaw, S.G., von Garnier, C., Takala, J., Jakob, S.M., Rieben, R., and Lepper, P.M. (2010). Effects of TLR agonists on the hypoxia-regulated transcription factor HIF-1 α and dendritic cell maturation under normoxic conditions. *PLoS One* *5*.
- Tamagawa-Mineoka, R., Katoh, N., Ueda, E., Masuda, K., and Kishimoto, S. (2008). Elevated platelet activation in patients with atopic dermatitis and psoriasis: increased plasma levels of beta-thromboglobulin and platelet factor 4. *Allergol. Int.* *57*, 391–396.
- Vidoni, S., Zanna, C., Rugolo, M., Sarzi, E., and Lenaers, G. (2013). Why mitochondria must fuse to maintain their genome integrity. *Antioxid. Redox Signal.* *19*, 379–388.
- Yeo, L., Adlard, N., Biehl, M., Juarez, M., Smallie, T., Snow, M., Buckley, C.D., Raza, K., Filer, A., and Scheel-Toellner, D. (2016). Expression of chemokines CXCL4 and CXCL7 by synovial macrophages defines an early stage of rheumatoid arthritis. *Ann. Rheum. Dis.* *75*,

763–771.

Zaldivar, M.M., Pauels, K., Von Hundelshausen, P., Berres, M.L., Schmitz, P., Bornemann, J., Kowalska, M.A., Gassler, N., Streetz, K.L., Weiskirchen, R., et al. (2010). CXC chemokine ligand 4 (CXCL4) is a platelet-derived mediator of experimental liver fibrosis. *Hepatology* 51, 1345–1353.

Hypoxia and TLR3 activation drive CXCL4 production via HIFs in systemic sclerosis patient moDCs

Andrea Ottria^{1,2}, Maili Zimmermann^{1,2}, Tiago Carneiro^{1,2}, Nadia Vazirpanah^{1,2}, Alsya J. Affandi^{1,2}, Ralph G. Tieland^{1,2}, Cornelis P.J. Bekker^{1,2}, Janneke Tekstra², Evelien Ton², Samuel Garcia Perez^{1,2}, Femke Bonte-Mineur³, Kris A. Reedquist^{1,2}, Timothy R.D.J. Radstake^{1,2}, Wioleta Marut^{1,2*}

Affiliations

¹Center for Translational Immunology, University Medical Center Utrecht, Utrecht University, Utrecht, the Netherlands

²Department of Rheumatology and Clinical Immunology, University Medical Center Utrecht, Utrecht University, Utrecht, the Netherlands

³Department of Rheumatology and Clinical Immunology, Maastad Hospital, Rotterdam, the Netherlands

*Materials and Correspondence

Wioleta Marut, PhD, University Medical Centre Utrecht | Heidelberglaan 100 | Tel: +31 88 75 535 68 | w.k.marut@umcutrecht.nl

Manuscript submitted

Abstract

Systemic sclerosis (SSc) is a complex autoimmune disease characterized by inflammation and vascular aberrancies leading to hypoxia and fibrosis of skin and multiple internal organs. Patients with SSc have increased proinflammatory cytokine production such as interleukin (IL)-8, IL-6, tumour necrosis factor (TNF) α , and chemokine (C-X-C motif) ligand 4 (CXCL4) that has been shown to play an essential role in SSc pathogenesis. In the current study, we assessed the potential role of monocyte derived dendritic cells (moDCs) and the underlying mechanism of action in the production of IL-8, IL-6, TNF α and CXCL4 and as such the pathophysiology of SSc.

moDCs were cultured in hypoxic or normoxic environment in presence/absence of several Toll-Like receptor (TLR) agonists stimulation. Cytokines production was determined by ELISA and qPCR. The level of mitochondrial reactive oxygen species (mtROS) was determined by flow cytometry. Fundamental role of hypoxia inducible factors (HIFs α) on cytokine production was assessed by inhibition of HIF-1 α and HIF-2 α .

After 6 days of differentiating moDCs, a persistent elevated level of IL-8 and CXCL4 were observed in unstimulated SSc moDCs when compared to moDCs from healthy controls (HCs). Co-stimulation of HCs moDCs by TLR3 agonist under hypoxia mimicked high production of IL-8 and CXCL4 found in SSc moDCs, but also led to increased IL-6 and TNF α . Furthermore, we demonstrated that the persisting elevated CXCL4 level in HCs moDCs is a result of increased production of mtROS and stabilization of HIF-1 α and HIF-2 α are responsible for persistent elevated CXCL4 level in HCs moDCs. Further, we showed that the production of CXCL4, IL-8, IL-6 and TNF α was downregulated by blocking the HIFs in moDCs.

The activation of immune cells via TLR alone in particular, and a combination of TLR and hypoxic environment establish the pathogenic persistent production of IL-8, IL-6, TNF α , and CXCL4 in SSc. Therefore, suppression of these pro-inflammatory cytokines production by blocking either mtROS, HIF-1 α or HIF-2 α pathways might provide a therapeutic tool in downregulation of chronic inflammation in SSc.

Introduction

Systemic sclerosis (SSc) is an auto-immune disease characterized by vascular modifications, immune aberrations and fibrosis of the skin and internal organs (1). One of the main hallmarks of SSc is hypoxia (low oxygen level) which is induced upon vascular abnormalities and excessive deposition of extracellular matrix (2). Hypoxia induces the production of mitochondrial reactive oxygen species (mtROS) (3) which are important molecules capable of inducing pro-inflammatory cytokine production, such as type I interferon (3,4). Also, hypoxia stabilizes the hypoxia inducible factors (HIFs) which are responsible for modulation of metabolic and functional adaptations in the cell (3). In particular, HIFs are able to promote the expression of genes such as vascular endothelial growth factor (VEGF) and glucose transporter 1 (GLUT1), but also pro-inflammatory mediators such as C-C motif chemokine ligand (CCL) 5, C-X-C motif chemokine ligand (CXCL) 12 and tumour necrosis factor (TNF) α (5,6). Additionally, an aberrant immune response in SSc is hypothesized to originate from an impaired response to Toll-like receptors (TLRs) (7). TLRs are highly conserved receptors specialized in recognition of conserved patterns in pathogens (8,9). Interestingly, TLR activation initiates proinflammatory reaction by inducing cytokine production and promoting the immune response via HIF stabilization (10,11). TLRs are prominent players in innate response and are expressed on immune cells, i.e. dendritic cells (DCs) and non-immune cells such as endothelial cells, fibroblasts and epithelial cells (9). Interestingly, DCs are the initiators and modulators in immune responses and play an important role in the immune pathogenesis of SSc (12,13).

Previously, our group has demonstrated an elevated level of CXCL4 in patients with SSc and identified plasmacytoid DCs (pDCs) as the main producers of CXCL4 (14). CXCL4 is a pro-inflammatory chemokine that impacts wide range of immune cells. In monocytes, CXCL4 boosts the production of proinflammatory mediators (9,10). CXCL4 induces the production of IL-17 (15) and Th2 cytokines, while it suppresses Th1 cytokines production in T cells (10). In addition, CXCL4 has been implicated in other inflammatory and fibrotic

diseases such as intestinal inflammatory bowel disease, psoriasis, cystic fibrosis, liver fibrosis and even cancer (17–22). Importantly, in our previous study, we showed that CXCL4 production in pDCs is orchestrated upon mtROS and HIF-2 α stabilization through hypoxia and TLR9 stimulation (23).

Here, we demonstrate that monocyte derived (mo)DCs, which is a commonly used *in vitro* model of conventional DCs, are also persistent producers of CXCL4 upon simultaneous stimulation of hypoxia and TLR3. Furthermore, the combination of hypoxia and TLR3 potentiated not only the production of CXCL4, but also showed also to be implicated in the production of pro-inflammatory cytokines such as interleukin (IL-) 8, IL-6 and TNF α . Moreover, we explored the potential role of mtROS and HIFs in the production of pro-inflammatory cytokines by systematically testing the effects of hypoxia and TLR activation on moDCs.

Patients and methods

Patient Cohort

Blood from patients and (sex- and age-matched) healthy controls (HC) was obtained from the University Medical Center Utrecht and the Maastad Hospital Rotterdam (The Netherlands). All patients provided written informed consent approved by the local institutional medical ethics review boards prior to inclusion in this study. Samples and clinical information were treated anonymously immediately after collection. Patients fulfilled the ACR/EULAR 2013 classification criteria for SSc (24) and the demographics and clinical characteristics of the patients are detailed in **Table 1**. The study was performed according to the guidelines of the Declaration of Helsinki and the local ethical and Review committee from each centre approved the study.

Table 1. Baseline characteristics of patients with SSc.

	Healthy Participants (N=40)	SSc (N=20)
Age (years) (min-max)	40 (28–60)	56 (34–78)
Female (%)	78	80
ANA (antinuclear antibody) (%)	–	18 (90%)
ACA (anticentromere antibody) (%)	–	9 (45%)
Scl70 (anti topoisomerase I) (%)	–	11 (55%)
MRSS (modified Rodnan skin score) (min-max)	–	7 (0-36)
ILD (Interstitial lung disease) (%)	–	6 (30%)
Disease duration (years) (min-max)	–	15 (4-35)

The values are represented as mean + min-max or absolute number + percentage.

Cell isolation

Peripheral blood mononuclear cells (PBMCs) from HC and SSc patients were isolated by Ficoll gradient. Monocytes were isolated using an autoMACS Pro Separator according the manufacturer's instructions. Purity was routinely assessed by flow cytometry and above

94%.

Monocyte-derived dendritic cells (moDC) differentiation and stimulation

One million monocytes per ml were cultured in RPMI-GlutaMAX supplemented with 10% FBS and 10,000 I.E. penicillin-streptomycin and differentiated to moDCs by adding recombinant human granulocyte-macrophage colony-stimulating factor (GM-CSF, 800 IU/mL) and recombinant human interleukin-4 (IL-4, 500 IU/mL), as previously described (25). At day 6, cells were harvested, re-plated and acclimated for 30 minutes either in atmospheric or hypoxic (Rasquinn invivO2 1000 hypoxic chamber set at in 1% O₂ and 5% CO₂) conditions prior stimulation with the TLR agonists LPS (TLR4, 100ng/ml), Poly(I:C) (TLR3, 25µg/ml) or R848 (TLR7/8, 2µg/ml) for 24 hours.

Inhibition of mitochondrial reactive oxygen species (mtROS) and hypoxia inducible factors (HIFs)

To inhibit mtROS we used mitoQ (10nM) (provided by Dr Mike Murphy, MRC Mitochondrial Biology Unit, University of Cambridge, UK), and HIF-1 α and HIF-2 α were inhibited using HIF-1 α (Bisphenol A dimethyl ether, 10nM) and HIF-2 α (HIF-2 Antagonist 2, 10nM) inhibitors.

mtROS measurement

mtROS production was quantified using MitoSOX™ Red Mitochondrial Superoxide Indicator according to the manufacturer's protocol, measured in FACS CANTO II Flow cytometer and analysed with BD FACS Diva software.

Quantification of cytokine production level

Cell-free supernatants were analysed by ELISA for CXCL4. TNF α , IL-6 and IL-8 were measured using human single-plex assays (Bio-Rad) and read on a Bio-Plex 200 system (Bio-Rad).

RT-PCR and quantitative (q)PCR

RNA from moDCs was isolated using the Allprep RNA/DNA kit. Total RNA was reverse-

transcribed using SuperScript™ II RT. Duplicate PCR reactions were performed using TaqMan with a Quantstudio Real-Time PCR detection system. cDNA was amplified using specific primers. Relative level of CXCL4 (Hs00236998_m1) gene expression was calculated by normalizing to *B2M* (Hs00939627_m1) housekeeping genes. Fold changes (FC) of mRNA were calculated by using the formulas and $2^{-\Delta\Delta C}$.

Western Blot

moDCs were lysed in Laemmli's buffer and content quantified with a BCA Protein Assay Kit (Pierce). Equal amounts of total protein were subjected to electrophoresis on NuPAGE™ 4-12% Bis-Tris gels (Invitrogen) and proteins were transferred to PVDF membranes (Millipore). Blocking was performed using milk (5%). Membranes were incubated overnight at 4°C with primary specific antibodies against HIF-1 α (NOVUNB100-105SS, Novus Biological), HIF-2 α (NB100-122SS, Novus Biologicals) and α -Tubulin (T5168, Sigma-Aldrich), then washed and incubated in TBS/T containing horseradish peroxidase-conjugated secondary antibody. Protein was detected with Lumi-lightplus Western Blotting Substrate (Roche Diagnostics) using a ChemiDoc™ MP System (Biorad). Relative protein expression was normalized to tubulin.

Viability assessment

Cell death was assessed by Annexin V-7AAD staining. Cells were stained with Annexin V (1:100 dilution, BD Pharmingen) and 7AAD (1:100 dilution, BD Pharmingen) and measured using a FACS Canto Flow Cytometer. The data were further analysed with BD FACS DIVA software.

Reagents and Statistical analysis

Reagents, catalogue numbers and company name are listed in **Supplementary reagent table 1**. Where appropriate, Mann-Whitney test or Paired t test was assessed using Graph Pad Prism 8.0 Software. *P* values smaller than 0.05 were considered to be statistically significant.

Results

Hypoxia induces CXCL4 production in moDCs

We compared the production of CXCL4 at protein and mRNA level in healthy and SSc moDCs. When compared to healthy moDCs, SSc moDCs after 6 days of culture produced higher level of CXCL4 at protein ($P<0.0001$) and mRNA ($P=0.0003$) level (**Figure 1A**). CXCL4 production, both at protein and mRNA level, upon stimulation with hypoxia, TLR3, or a combination of both, remained unchanged in SSc moDCs (**Supplementary Figure 1A, 1B**).

Next, CXCL4 production was quantified in healthy moDCs after hypoxia and/or TLR agonists exposure. Exposure to hypoxia solely was sufficient to induce CXCL4 production at protein ($P=0.0068$) and mRNA level ($P=0.0003$) (**Figure 1B, Supplementary Figure 1A, 1B**). In contrary to SSc moDCs, the production of CXCL4 in healthy moDCs was further potentiated upon co-exposure to hypoxia and TLR3 agonists Poly(I:C) ($P=0.0192$ on protein level, $P=0.0087$ on mRNA level). CXCL4 production remained unchanged upon moDCs exposure to hypoxia and other TLR agonists (**Figure 1B**). Therefore, in the following experiments moDCs were stimulated solely with Poly(I:C). Stimulation of healthy moDCs with TLRs alone in atmospheric conditions had no effect on CXCL4 production (**Figure 1B**).

Production of CXCL4 by moDCs is specifically regulated by hypoxic condition

To examine the specificity of CXCL4 production upon hypoxia and TLR3 stimulation, we assessed the production of other cytokines relevant to SSc such as IL-8, IL-6, and TNF α under the same conditions (**Figure 1C**). As expected, TLR stimulation alone was sufficient to significantly increase the production of IL-8 ($P=0.026$), IL-6 ($P=0.0082$), and TNF α ($P=0.0012$). Hypoxia alone had no effect on the production of these cytokines. Co-exposure to hypoxia and TLR3 stimulation induced a clear trend for increase, although not statistically significant (**Figure 1C**), indicating that hypoxia and endosomal TLR signalling induce the production of CXCL4 in healthy moDCs. We also observed that moDCs from SSc patients produced IL-8 ($P=0.0221$) in absence of any stimulation when compared to healthy moDCs

(Figure 1C), suggesting that moDCs from SSc are more pro-inflammatory prone.

Figure 1

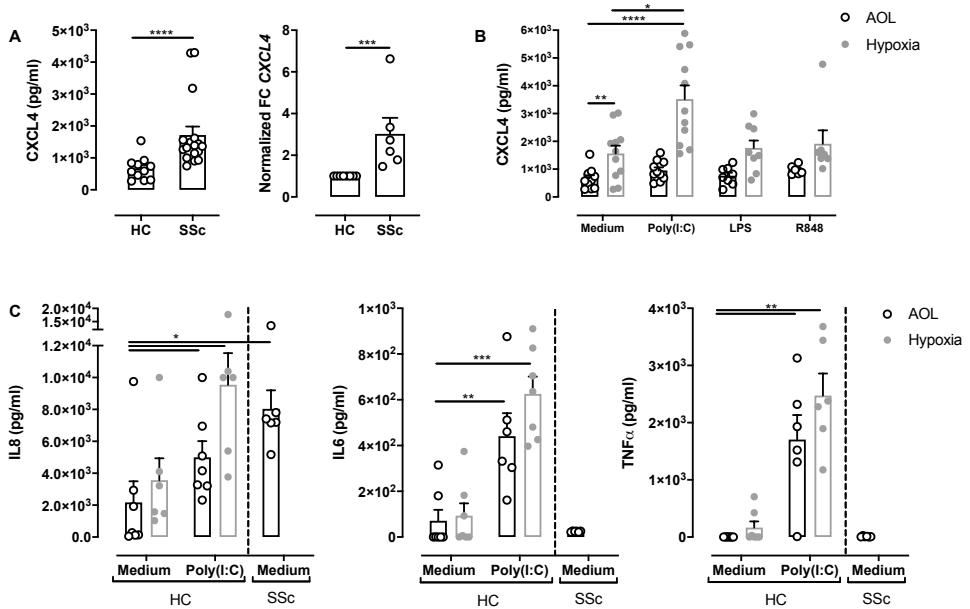


Figure 1. Hypoxia leads to increased CXCL4 production in moDCs. **A)** On the left CXCL4 level quantification in healthy participants (N=11) and SSc (N=17) moDCs incubated in medium conditions during 24 hours. On the right mRNA expression level of CXCL4 in healthy participants (N=6) and SSc (N=6) moDCs incubated in medium conditions during 24 hours. **B)** Level of CXCL4 release in supernatant of healthy participants moDCs cultured in hypoxic or atmospheric conditions and challenged with either TLR3 ligand (Poly I:C, N=11), TLR4 ligand (LPS, N=8) or TLR7/8 ligand (R848, N=6) for 24 hours. **C)** Measurement of interleukin 8 (IL-8), interleukin 6 (IL-6) and tumour necrosis factor (TNF) α in the supernatant from moDCs (7 HC and 6 SSc patients), cultured in atmospheric oxygen level (AOL) or hypoxic conditions and co-stimulated with TLR3 agonist Poly(I:C) for 24 hours. Bars are represented as mean \pm SEM. Grey and white edge respectively represent hypoxic and atmospheric conditions. *= $P \leq 0.05$, **= $P \leq 0.01$, ***= $P \leq 0.001$, ****= $P \leq 0.0001$ using Mann-Whitney test.

Increased mitochondrial ROS (mtROS) production in moDCs is essential for CXCL4 production in healthy moDCs

To assess the impact of hypoxia and TLR3 stimulation on mtROS production in moDCs, cells were exposed to hypoxia (1%) and stimulated with TLR3 ligand Poly(I:C). Hypoxia alone induced mtROS production in healthy moDCs ($P=0.046$) (Figure 2A, left panel). This was not the case when the cells were stimulated with Poly(I:C) alone. The combination

of Poly(I:C) and hypoxia potentiated an increased mtROS production level as compared to the medium condition ($P=0.0012$) and led to elevated levels of CXCL4 production ($P=0.0047$), as compared to the medium condition (**Figure 2A**, left panel). In order to assess whether mtROS has a role in CXCL4 production by healthy moDCs, moDCs were incubated in the presence of mitoQ, a specific mtROS inhibitor. As a result, we observed a reduction in CXCL4 production by healthy moDCs after hypoxia ($P=0.0411$) alone and after co-exposure to hypoxia and TLR3 agonist ($P=0.002$) in the presence of mitoQ (**Figure 2A**, right panel). We observed no effect of mitoQ alone on IL-6, IL-8, and TNF α production in healthy moDCs (data not shown). This demonstrates the important role of mtROS in CXCL4 production by healthy moDCs exposed to hypoxia. Interestingly, in moDCs from SSc patients, mitoQ had no effect on CXCL4 production, suggesting differences in the role of mtROS in regulating CXCL4 production in SSc moDCs compared to healthy moDCs. Furthermore, these differences were excluded to be caused by mitoQ affecting moDCs viability (**Supplementary Figure 2**).

HIFs are essential for CXCL4 production in moDCs

HIFs are stabilized upon hypoxic environment, TLR activation and/or mtROS increase (11). In order to delineate the role of HIFs in CXCL4 production by moDCs, we quantified the expression of HIF-1 α and HIF-2 α at protein level in moDCs upon hypoxia exposure and TLR3 ligand stimulation. We observed, on one hand, an increase in HIF-2 α ($P=0.041$) protein after exposure of moDCs to hypoxia and TLR3 ligand stimulation (**Figure 2B**). HIF-1 α , on the other hand, was increased only after moDCs exposure to hypoxia alone ($P=0.026$) (**Figure 2B**). The role of HIFs in CXCL4 production was also investigated by adding HIFs inhibitors to moDCs culture medium. We observed that in healthy moDCs, both HIF-2 α ($P=0.0022$) and HIF-1 α ($P=0.0022$) inhibitors were able to significantly suppress CXCL4 production in cells co-exposed to hypoxia and TLR3 agonist (**Figure 2C**). Next, we looked at the effect of HIFs inhibition on IL-6, IL-8, and TNF α . We observed that both

HIF-2 α and HIF-1 α inhibitors were able to significantly reduce IL-6 (HIF-2 α $P=0.013$, HIF-1 α $P=0.013$) and TNF α (HIF-2 α $P=0.0036$, HIF-1 α $P=0.0034$) production in healthy moDCs exposed to TLR3 agonist only (**Supplementary Figure 3**). Further, HIF-2 α and HIF-1 α inhibition reduced IL-6 (HIF-2 α $P=0.063$, HIF-1 α $P=0.033$) and TNF α (HIF-2 α $P=0.029$, HIF-1 α $P=0.0051$) production in HCs moDCs co-exposed to hypoxia and TLR3 ligand (**Supplementary Figure 3A, 3B**). The exposure to HIFs inhibitor had no effect on IL-8 production in healthy moDCs (**Supplementary Figure 3C**).

Similarly to healthy moDCs, the inhibition of HIFs substantiate reduction in CXCL4 production in moDCs from SSc patients (HIF-2 α $P=0.026$; HIF-1 α $P=0.026$) (**Figure 2C**). This suggests CXCL4 production in SSc moDCs is regulated by HIF pathway independent from mtROS signalling.

The inhibition of HIF-2 α in SSc moDCs, similarly to healthy moDCs, induced reduction of IL-6 production ($P<0.0001$) and a non-significant but hence clear trend in TNF α in five out of six donors, but no effect was observed on IL-8 production. Interestingly, the inhibition of HIF-1 α instead, augmented the production of IL-6 ($P=0.0005$) and IL-8 ($P<0.0001$), but had no effect on TNF α in SSc moDCs, indicating there are differences in the role of HIF-1 α regulating pro-inflammatory cytokines in healthy and SSc moDCs. All in all, these results underline the fundamental roles of both HIF-1 α and HIF-2 α in the modulation of CXCL4, IL-6, and TNF α by both healthy and SSc moDCs.

3

Figure 2

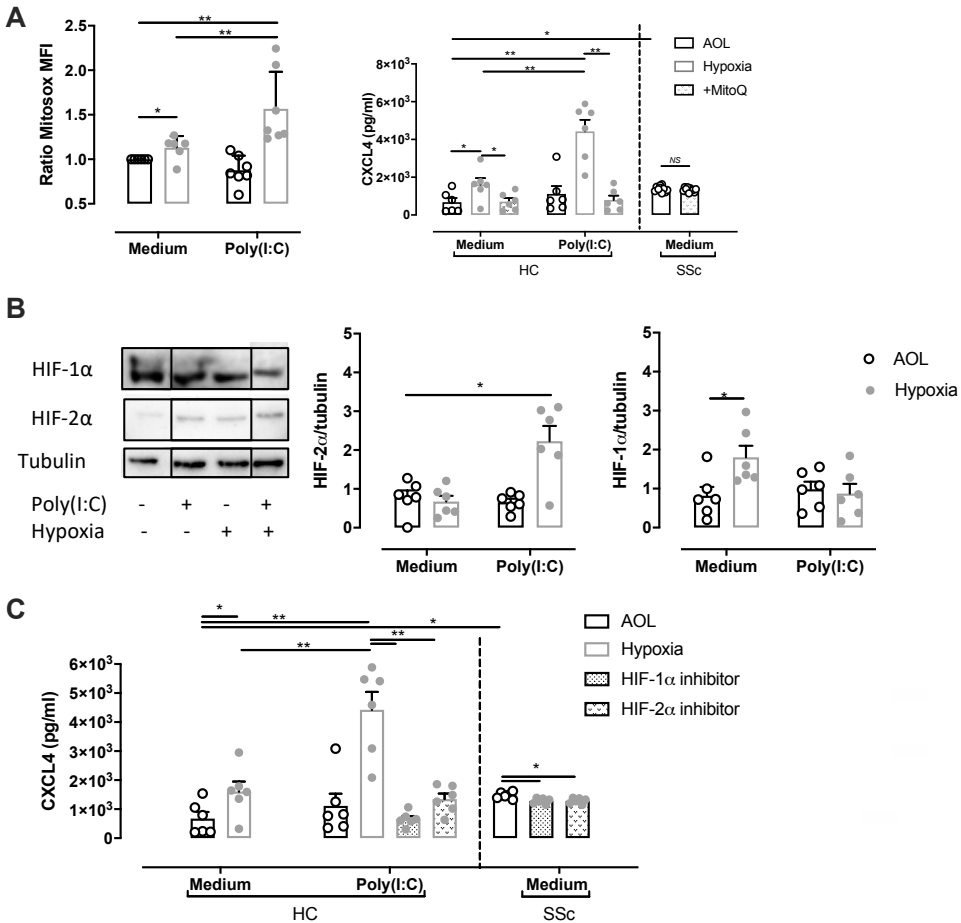


Figure 2. mtROS and HIFs are essential for CXCL4 production in pDCs and moDCs. A) On the left FACS analysis of the MFI of mitoSOX dye for mtROS in moDCs from 6 HCs exposed to either AOL or hypoxia and TLR3 agonist Poly(I:C) for 24hrs. On the right ELISA measurement of CXCL4 in moDCs (6HC and 6SSc patients) exposed to either AOL or hypoxia and TLR3 agonist Poly(I:C) +/- MitoQ for 24hrs. **B)** On the left representative blot of 4 Western Blot gels for HIF-1α, HIF-2α and tubulin. In the middle quantification of HIF-2α and (on the right) HIF-1α in moDCs from 6 HC cultured either in AOL or exposed to hypoxia and TLR3 agonist Poly(I:C). Samples were run in the same gel but the lines are not congruent as another TLR agonist was tested in between. **C)** Elisa measurement of CXCL4 in moDCs from 6 HC cultured in AOL or hypoxia +/- Poly(I:C) and 10 SSc patients cultured in atmospheric condition with the addition of either HIF-1α inhibitor or HIF-2α inhibitor to the culture medium for 24hrs. Bars are represented as mean ±SEM. Grey and white edges respectively represent hypoxic and atmospheric conditions. *= $P \leq 0.05$, **= $P \leq 0.01$, ***= $P \leq 0.001$, ****= $P \leq 0.0001$ using and Mann-Whitney test.

Discussion

3

In this study we revealed that moDCs are able to produce CXCL4 after hypoxia and TLR3 co-exposure with a mechanism similar to what we previously observed in pDCs (23). Furthermore, we demonstrate that IL-6 and TNF α , but not IL-8 production, in HCs moDCs is HIFs dependent. Hypoxia is recognized as the leading force behind various pathological characteristics of SSc (26). Here, by demonstrating the role of hypoxia substantiating CXCL4 production by moDCs, our results confirm hypoxia as a key modulator involved in the pathophysiology of SSc by modulating moDCs' TLR response and cytokine production. In addition, our results demonstrate the role of hypoxia substantiating CXCL4 production by moDCs.

In line with the literature (23,27), we observed that hypoxia stimulation orchestrates the production of mtROS in healthy moDCs. Also, TLR stimulation is known to induce mtROS production (23,28). Accordingly, co-exposure with TLR and hypoxia led to an increase in mtROS production in HC moDCs. Similarly to what we previously observed in pDCs (23), the inhibition of mtROS led to a reduction of CXCL4 production in healthy moDCs. In contrary, the inhibition of mtROS had no effect on the production of IL-8, IL-6, and TNF α in healthy moDCs. In contrast to our observations in HCs moDCs, suppression of mtROS in SSc moDCs had no effect on CXCL4 production, suggesting SSc moDCs have become resistant to the changes in mtROS.

Interestingly, unstimulated moDCs of SSc patients were able to spontaneously produce high levels of CXCL4 and IL-8 after a period of at least 6 days in culture, when compared to healthy moDCs. Chronic exposure to hypoxic and highly inflammatory *in vivo* environment present in SSc patients might potentiate epigenetic modifications and thereby implicate a deviating regulatory mechanism in SSc moDCs. For example, hypoxia is known to induce epigenetic modifications in fibroblasts through HIFs stabilization and to promote the construction of a pro-fibrotic profile in these cells (29). Similarly, hypoxia, via HIFs, is capable to epigenetically reprogram monocytes. These modifications are responsible for

the long-term memory of the innate immunity. In addition, hypoxia leads to a shifting in the monocyte's metabolism, preparing them for a prompt and rapid immune response (30).

Epigenetic modifications could lead to hypermethylation of promotor regions that suppresses gene expression. For instance, *SOCS1*, is a gene regulated by HIF-1 α and is known to be involved in processes such as proliferation, apoptosis and cytokine production (31). In macrophages hypermethylation of *SOCS1* leads to overproduction of TNF α and IL-6 (32). Therefore, our results could be explained by epigenetic modifications induced by chronic hypoxia that lead to hypermethylation of a promotor region, and thereby modifying the SSc moDCs with a "chronically proinflammatory signature". Thereby, it is tempting to assume that hypoxia induces chronically active sets of immune cells that are primed to orchestrate overproduction of pro-inflammatory cytokines i.e. CXCL4 and IL-8 as observed in SSc moDCs. Moreover, these findings could signify an imprinted altered regulatory epigenetic mechanism in SSc moDCs which potentially leads to the persistent production of CXCL4 and IL-8, even in absence of hypoxia and TLR stimulation *ex vivo*. Hence, since inhibition of mtROS in healthy moDCs substantiates a reduction of CXCL4 production upon hypoxia and TLR stimulation, mtROS machinery pathways might entail the potential epigenetic imprinting which eventuates persistent CXCL4 production in SSc moDCs.

Recent studies in our group describe the presence of a feedback loop whereby CXCL4 is able to promote the genetic imprinting of DCs (25). Cardoso *et al.* demonstrated in moDCs, that CXCL4 is able to reprogram the cells and thereby priming a more mature cell-phenotype and augment the TLR responsiveness in these cells. CXCL4 primed moDCs had a higher production level of IL-12 and TNF α upon TLR3 stimulation. These moDCs were also proficient inducers of proliferation and cytokine production of CD4⁺ T (and CD8⁺) cells. Moreover, moDCs matured upon CXCL4 exposure had excessive superior ability to present antigens derived from endocytosis. This underlines the important involvement of TLR3 as an endosomal TLR and thereby explains CXCL4 production prominently upon TLR3 stimulation in SSc moDCs. Therefore, we speculate that, the high concentrations of

CXCL4 observed in circulation of SSc patients (14) could already implicate epigenetically modified moDCs and which eventuate an altered inflammatory response in patients with SSc. The potential imprinting of SSc moDCs has to be confirmed in future studies.

Further assessing our findings, we were also interested to enquire the role of HIFs on CXCL4, IL-6, IL-8, and TNF α production in healthy moDCs. We observed that the expression of HIF-1 α was induced through hypoxia alone while HIF-2 α was expressed after hypoxia and TLR3 agonist co-exposure. However, since inhibiting HIF-1 α and HIF-2 α in healthy and SSc moDCs diminished CXCL4 production, one could speculate that the epigenetic modification upon chronic hypoxia and CXCL4 exposure might be implemented by chronic stabilization of HIFs. According to the literature, HIFs have been shown to be involved in regulating immune responses. For instance, while the available literature on HIF-2 α and its working mechanism is rather poor, HIF-1 α is known to be involved in the production of pro-inflammatory cytokines such as IL-8, IL-1 β and TNF α (33–35), however limited is known about the role HIF-2 α and its working mechanism on immune processes. To our knowledge there is only one study delineating the relevance of HIF-2 α in mouse macrophages and production of proinflammatory cytokines such as IL-1 β , IL-12, TNF α and IFN γ (36). Therefore, and in line with this, our study is providing the first indications on crucial distinct modulatory roles of both HIF-1 α and HIF-2 α in CXCL4 production by healthy and SSc moDCs, and HIF-2 α in IL-6 and TNF α production by healthy moDCs.

In SSc patients, HIF-1 α inhibition increased the production level of IL-8 and TNF α and decreased CXCL4 production, whereas the inhibition of HIF-2 α reduced IL-6 and TNF α as well as CXCL4 production level. Therefore, we believe that HIF-2 α plays an important role in SSc moDCs similar to what we observed in SSc pDCs (23).

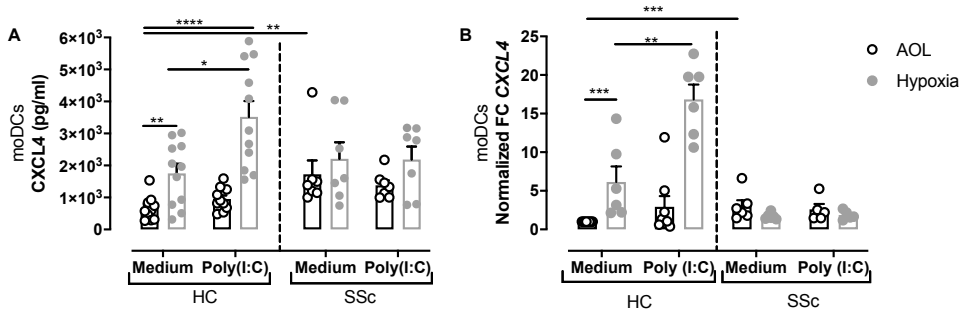
In conclusion, CXCL4 is a cytokine known to contribute to chronic inflammation in SSc. In this study we demonstrated how hypoxia and mtROS via HIFs stabilization are responsible for elevated CXCL4 production level and that unstimulated SSc moDCs produce high levels of pro-inflammatory cytokines such as CXCL4. Since CXCL4 is a

cytokine known to contribute to chronic inflammation in autoimmune diseases such as SSc (14,37–39), in a clinical setting, suppressing CXCL4 production maybe beneficial for therapeutic intervention: by intervening the vicious circle of TLR triggering, mtROS release and HIFs activation, might potentially inhibit chronic inflammation in moDCs and subsequently diminish the extent of hypoxia and prevent SSc patients from a prognosis of further worsening. Our study provides prominent evidences on novel potential treatment target points in order to diminish hypoxia and chronic inflammation through intervening this pathogenic feedback loop. Future studies are required to further translate and validate these findings in *in vivo* studies and to prove the proposed epigenetic modifications leading to the proinflammatory signature of moDCs in patients with SSc.

Supplementary Figures

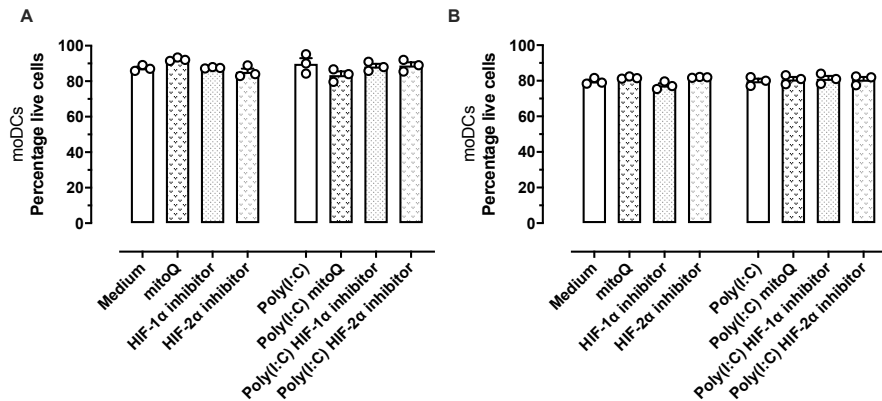
Supplementary Figure 1

Supplementary Figure 1. Hypoxia leads to increased CXCL4 production in moDCs. **A)** CXCL4 level quantification in healthy participants (N=11) and SSc (N=7) moDCs incubated in hypoxic or atmospheric conditions that were triggered with TLR3 ligand (Poly (I:C)) during 24 hours. **B)** mRNA expression level of CXCL4 in healthy participants (N=6) and SSc (N=6) moDCs incubated upon hypoxic and atmospheric conditions



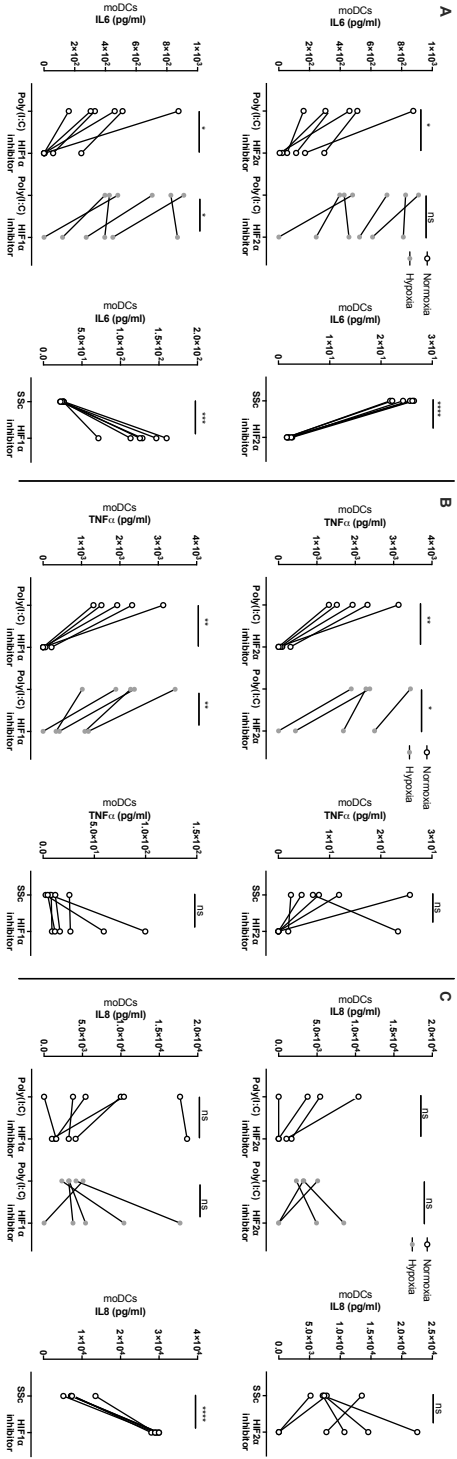
and triggered with TLR3 agonist (Poly I:C) during 24 hours. Bars are represented as mean \pm SEM. Grey and black edge respectively represent hypoxic and atmospheric conditions. *= $P \leq 0.05$, **= $P \leq 0.01$, ***= $P \leq 0.001$, ****= $P \leq 0.0001$ using Mann-Whitney test.

Supplementary Figure 2



Supplementary Figure 2. Percentage of live cells. FACS analysis expressed as percentage of live cells in annexin V, 7-AAD dead staining of moDCs cultured in either atmospheric A) or hypoxic B) condition and TLR3 agonist Poly(I:C) for 24 hours, exposed to different inhibitors (mitoQ, HIF-1 α and HIF-2 α inhibitor). All data represents mean \pm SEM.

Supplementary Figure 3



Supplementary Figure 3. Effect of HIF inhibition on pro-inflammatory cytokine production in moDCs. Measurement of interleukin 6 (IL-6) (A), interleukin 8 (IL-8) (C) and tumour necrosis factor (TNF) α (B) in the supernatant from healthy moDCs (N=6), cultured in atmospheric oxygen level (AOL) or hypoxic conditions and co-stimulated with TLR3 agonist Poly(I:C) in the presence of HIF-2 α (top left panel) or HIF-1 α (bottom left panel) for 24 hours. On the right panel measurement SSc patients moDCs (N=6) cultured in AOL and exposed to HIF-2 α (top right panel) or HIF-1 α (bottom right panel) for 24 hours. Bars are represented as mean \pm SEM. Grey and black edge respectively represent hypoxic and atmospheric conditions. *= $P \leq 0.05$, **= $P \leq 0.01$, ***= $P \leq 0.0001$, ****= $P \leq 0.00001$ using paired test.

Supplementary reagent table 1,

	Reagent	Cat#	Company
Cell isolation	10 mL Li-Hep vacutainer	#367526,	BD Biosciences
	Ficoll gradient	#17-1440-02	GE Healthcare
	Monocyte beads (CD14 MicroBeads, human)	#130-050-201	Miltenyi Biotec
	RPMI 1640 GlutaMAX medium	#61870-010	Thermo Fisher Scientific
	Fetal Bovine Serum (FBS)	#S181A	Biowest
	Penicillin-Streptomycin	#15070063	Thermo Fisher Scientific
Cell culturing and stimulation	CpG-C	#t1rl-m362-1	Invivogen
	CpG-A	#t1rl-2216-1	Invivogen
	CL075	#t1rl-c75	Invivogen
	R848	#t1rl-r848	Invivogen
	Loxoribine	#t1rl-lox	Invitrogen
Inhibitors	mitoQ (provided by Dr Mike Murphy)		
	HIF-1a	# CAS 1568-83-8	Santa Cruz Biotechnology
	HIF-2a	#SML0883	Sigma-Aldrich
mtROS measurement	MitoSOX™ Red	# M36008	Thermo Fisher
Cytokine quantification	CXCL4 ELISA kit	#DY795	R&D Systems
RNA extraction and cDNA synthesis qPCR	Allprep RNA/DNA Micro Kit	#80284	Qiagen
	SuperScript™ II RT	#18064014	Thermo Fisher Scientific
	TaqMan Master Mix	#4369016	Applied Biosystems
Intracellular staining	Fix-Perm	#88-8824-00	eBioscience

Ethical approval information

This study was performed according to the guidelines of the Declaration of Helsinki and study meets the approval of Ethical and Review committee of the Institutional Review and Ethical Board of University medical centre of Utrecht and Maastad Ziekenhuis of Rotterdam. The Ethical Committee approval was obtained in November 2011 (Ethical approval number 12-466 and 13-697). Moreover, in this study, all participants gave their informed consent before the inclusion.

Acknowledgements

This study was supported by research funding Marie Curie Intra-European Fellowship (Proposal number: 624871), the NWO VENI (grant number 91919149) and Gravitation (grant number 2013 ICI-024.002.009).

All the authors listed have made substantial, direct, and intellectual contribution to the work and approved it for publication. We thank Wilco de Jager (MultiPlex Core Facility, University Medical Center Utrecht) for performing Luminex assays. We thank *Dr Mike Murphy MRC Mitochondrial Biology Unit Wellcome Trust/MRC Building Hills Road, Cambridge CB2 0XY, UK for providing us mitoQ.*

Author contribution

All authors approved the final version after being involved in drafting and revising the article for important intellectual content. A. Ottria and W. Marut had full access to the data and take responsibility for the accuracy of the performed analysis and the integrity of the data. A. Ottria, T.R.D.J. Radstake and W. Marut were involved in design of the study. Execution and analysis of the results was performed by A. Ottria. A. Ottria, M. Zimmermann, T. Carvalheiro, N. Vazirpanah, A.J. Affandi, S. Garcis Perez, R.G. Tieland and C.P.J. Bekker were involved in performing experiments. A. Ottria was involved in selection of the patients. J. Tekstra, E. Ton, F. Bonte-Mineur and T.R.D.J. Radstake were involved in inclusion of SSc patients. All the authors contributed to the review of the manuscript.

References

1. Gabrielli A, Avvedimento E V, Krieg T. Scleroderma. *N Engl J Med* 2009;360:1989–2003. Available at: <http://www.ncbi.nlm.nih.gov/pubmed/19420368>.
2. Fuschiotti P. Current perspectives on the immunopathogenesis of systemic sclerosis. *ImmunoTargets Ther* 2016;5:21–35. Available at: <http://www.ncbi.nlm.nih.gov/pubmed/27529059>.
3. Li X, Fang P, Mai J, Choi ET, Wang H, Yang X-F. Targeting mitochondrial reactive oxygen species as novel therapy for inflammatory diseases and cancers. *J Hematol Oncol* 2013;6:19. Available at: <http://jhoonline.biomedcentral.com/articles/10.1186/1756-8722-6-19>.
4. Agod Z, Fekete T, Budai MM, Varga A, Szabo A, Moon H, et al. Regulation of type I interferon responses by mitochondria-derived reactive oxygen species in plasmacytoid dendritic cells. *Redox Biol* 2017;13:633–645.
5. Palazon A, Goldrath AW, Nizet V, Johnson RS. HIF Transcription Factors, Inflammation, and Immunity. *Immunity* 2014;41:518–528.
6. Peyssonnaud C, Datta V, Cramer T, Doedens A, Theodorakis EA, Gallo RL, et al. HIF-1 α expression regulates the bactericidal capacity of phagocytes. *J Clin Invest* 2005;115:1806–1815. Available at: <http://www.jci.org/articles/view/23865>.
7. Bhattacharyya S, Varga J. Emerging Roles of Innate Immune Signaling and Toll-Like Receptors in Fibrosis and Systemic Sclerosis. *Curr Rheumatol Rep* 2015;17.
8. Iwasaki A, Medzhitov R. Toll-like receptor control of the adaptive immune responses. *Nat Immunol* 2004;5:987–995.
9. Delneste Y, Beauvillain C, Jeannin P. Immunité naturelle. *Médecine/Sciences* 2007;23:67–74. Available at: <http://www.medicinesciences.org/10.1051/medsci/200723167>.
10. Han S, Xu W, Wang Z, Qi X, Wang Y, Ni Y, et al. Crosstalk between the HIF-1 and Toll-like receptor/nuclear factor- κ B pathways in the oral squamous cell carcinoma microenvironment. *Oncotarget* 2016;7. Available at: <http://www.oncotarget.com/fulltext/9329>.
11. Spirig R, Djafarzadeh S, Regueira T, Shaw SG, Garnier C von, Takala J, et al. Effects of TLR agonists on the hypoxia-regulated transcription factor HIF-1 α and dendritic cell maturation under normoxic conditions. *PLoS One* 2010;5.
12. Dumoitier N, Lofek S, Mouthon L. Pathophysiology of systemic sclerosis: State of the art in 2014. *Press Medicale* 2014;43:e267–e278. Available at: <https://www.sciencedirect-com.proxy.library.uu.nl/science/article/pii/S0755498214003741>. Accessed June 30, 2018.
13. Haniffa M, Collin M, Ginhoux F. Ontogeny and Functional Specialization of Dendritic Cells in Human and Mouse. In: *Advances in Immunology*. Vol 120.; 2013:1–49. Available at: <https://linkinghub.elsevier.com/retrieve/pii/B9780124170285000016>.
14. Bon L van, Affandi AJ, Broen J, Christmann RB, Marijnissen RJ, Stawski L, et al. Proteome-wide Analysis and CXCL4 as a Biomarker in Systemic Sclerosis. *N Engl J Med* 2014;370:433–443. Available at: <http://www.nejm.org/doi/10.1056/NEJMoa1114576>.
15. Affandi AJ, Silva-Cardoso SC, Garcia S, Leijten EFA, Kempen TS van, Marut W, et al. CXCL4 is a novel inducer of human Th17 cells and correlates with IL-17 and IL-22 in psoriatic arthritis. *Eur J Immunol* 2018;48:522–531. Available at: <http://www.ncbi.nlm.nih.gov/pubmed/29193036>.
16. Romagnani P, Maggi L, Mazzinghi B, Cosmi L, Lasagni L, Liotta F, et al. CXCR3-mediated opposite effects of CXCL10 and CXCL4 on TH1 or TH2 cytokine production. *J Allergy Clin Immunol* 2005;116:1372–9. Available at: <http://www.ncbi.nlm.nih.gov/pubmed/16337473>.
17. Raemdonck K Van, Steen PE Van den, Liekens S, Damme J Van, Struyf S. CXCR3 ligands in disease and therapy. *Cytokine Growth Factor Rev* 2015;26:311–327. Available at: <https://linkinghub.elsevier.com/retrieve/pii/S1359610114001634>.
18. Tamagawa-Mineoka R, Katoh N, Ueda E, Masuda K, Kishimoto S. Elevated platelet activation in patients with atopic dermatitis and psoriasis: increased plasma levels of beta-thromboglobulin and platelet factor 4. *Allergol Int* 2008;57:391–6. Available at: <http://www.ncbi.nlm.nih.gov/pubmed/18797178>.
19. Yeo L, Adlard N, Biehl M, Juarez M, Smallie

- T, Snow M, et al. Expression of chemokines CXCL4 and CXCL7 by synovial macrophages defines an early stage of rheumatoid arthritis. *Ann Rheum Dis* 2016;75:763–771. Available at: <http://ard.bmj.com/lookup/doi/10.1136/annrheumdis-2014-206921>.
20. Schwarz KB, Rosensweig J, Sharma S, Jones L, Durant M, Potter C, et al. Plasma markers of platelet activation in cystic fibrosis liver and lung disease. *J Pediatr Gastroenterol Nutr* 2003;37:187–91. Available at: <http://www.ncbi.nlm.nih.gov/pubmed/12883307>.
 21. Burstein SA, Malpass TW, Yee E, Kadin M, Brigden M, Adamson JW, et al. Platelet factor-4 excretion in myeloproliferative disease: implications for the aetiology of myelofibrosis. *Br J Haematol* 1984;57:383–392. Available at: <http://doi.wiley.com/10.1111/j.1365-2141.1984.tb02912.x>.
 22. Zaldivar MM, Pauels K, Hundelshausen P Von, Berres ML, Schmitz P, Bornemann J, et al. CXC chemokine ligand 4 (CXCL4) is a platelet-derived mediator of experimental liver fibrosis. *Hepatology* 2010;51:1345–1353.
 23. Ottria, Andrea et al. Hypoxia and TLR9 activation drive CXCL4 production in systemic sclerosis pDCs via mtROS and HIF-2a. *Cell Rep* 2019.
 24. Hoogen F Van Den, Khanna D, Fransen J, Johnson SR, Baron M, Tyndall A, et al. 2013 classification criteria for systemic sclerosis: An american college of rheumatology/ European league against rheumatism collaborative initiative. *Arthritis Rheum* 2013;65:2737–2747.
 25. Silva-Cardoso SC, Affandi AJ, Spel L, Cossu M, Roon JAG van, Boes M, et al. CXCL4 Exposure Potentiates TLR-Driven Polarization of Human Monocyte-Derived Dendritic Cells and Increases Stimulation of T Cells. *J Immunol* 2017;199:253–262. Available at: <http://www.jimmunol.org/lookup/doi/10.4049/jimmunol.1602020>.
 26. Beyer C, Schett G, Gay S, Distler O, Distler JH. Hypoxia. Hypoxia in the pathogenesis of systemic sclerosis. *Arthritis Res Ther* 2009;11:220. Available at: <http://arthritis-research.biomedcentral.com/articles/10.1186/ar2598>.
 27. Mansfield KD, Guzy RD, Pan Y, Young RM, Cash TP, Schumacker PT, et al. Mitochondrial dysfunction resulting from loss of cytochrome c impairs cellular oxygen sensing and hypoxic HIF- α activation. *Cell Metab* 2005;1:393–399. Available at: <http://www.ncbi.nlm.nih.gov/pubmed/16054088>.
 28. West AP, Brodsky IE, Rahner C, Woo DK, Erdjument-Bromage H, Tempst P, et al. TLR signalling augments macrophage bactericidal activity through mitochondrial ROS. *Nature* 2011;472:476–480. Available at: <http://www.nature.com/articles/nature09973>.
 29. Watson CJ, Collier P, Tea I, Neary R, Watson JA, Robinson C, et al. Hypoxia-induced epigenetic modifications are associated with cardiac tissue fibrosis and the development of a myofibroblast-like phenotype. *Hum Mol Genet* 2014;23:2176–2188. Available at: <https://academic.oup.com/hmg/article-lookup/doi/10.1093/hmg/ddt614>. Accessed June 30, 2018.
 30. Cheng SC, Quintin J, Cramer RA, Shephardson KM, Saeed S, Kumar V, et al. mTOR- and HIF-1 α -mediated aerobic glycolysis as metabolic basis for trained immunity. *Science (80-)* 2014;345.
 31. Wan J, Ma J, Mei J, Shan G. The effects of HIF-1 α on gene expression profiles of NCI-H446 human small cell lung cancer cells. *J Exp Clin Cancer Res* 2009;28:150. Available at: <http://jccr.biomedcentral.com/articles/10.1186/1756-9966-28-150>.
 32. Cheng C, Huang C, Ma TT, Bian EB, He Y, Zhang L, et al. SOCS1 hypermethylation mediated by DNMT1 is associated with lipopolysaccharide-induced inflammatory cytokines in macrophages. *Toxicol Lett* 2014;225:488–497. Available at: <https://linkinghub.elsevier.com/retrieve/pii/S0378427414000137>.
 33. Bosco MC, Varesio L. Dendritic cell reprogramming by the hypoxic environment. *Immunobiology* 2012;217:1241–1249. Available at: <http://dx.doi.org/10.1016/j.imbio.2012.07.023>.
 34. Blengio F, Raggi F, Pierobon D, Cappello P, Eva A, Giovarelli M, et al. The hypoxic environment reprograms the cytokine/chemokine expression profile of human mature dendritic cells. *Immunobiology* 2013;218:76–89. Available at: <https://linkinghub.elsevier.com/retrieve/pii/S0171298512000381>.
 35. Paardekooper LM, Bendix MB, Ottria A, Haer LW de, Beest M Ter, Radstake TRDJDJ, et

al. Hypoxia potentiates monocyte-derived dendritic cells for release of tumor necrosis factor α via MAP3K8. *Biosci Rep* 2018;38. Available at: <http://www.ncbi.nlm.nih.gov/pubmed/30463908>.

36. Imtiyaz HZ, Williams EP, Hickey MM, Patel SA, Durham AC, Yuan LJ, et al. Hypoxia-inducible factor 2 α regulates macrophage function in mouse models of acute and tumor inflammation. *J Clin Invest* 2010;120:2699–2714. Available at: <http://www.jci.org/articles/view/39506>.
37. Lande R, Lee EY, Palazzo R, Marinari B, Pietraforte I, Santos GS, et al. CXCL4 assembles DNA into liquid crystalline complexes to amplify TLR9-mediated interferon- α production in systemic sclerosis. *Nat Commun* 2019;10:1731. Available at: <http://www.ncbi.nlm.nih.gov/pubmed/31043596>.
38. Kioon MDA, Tripodo C, Fernandez D, Kirou KA, Spiera RF, Crow MK, et al. Plasmacytoid dendritic cells promote systemic sclerosis with a key role for TLR8. *Sci Transl Med* 2018;10:eaam8458. Available at: <http://stm.sciencemag.org/lookup/doi/10.1126/scitranslmed.aam8458>.
39. Mehta H, Goulet P-O, Nguyen V, Pérez G, Koenig M, Senécal J-L, et al. Topoisomerase I peptide-loaded dendritic cells induce autoantibody response as well as skin and lung fibrosis. *Autoimmunity* 2016;49:503–513. Available at: <http://www.ncbi.nlm.nih.gov/pubmed/7808577>.

Inhibition of HIF-2 α reduces pro-inflammatory cytokine production in plasmacytoid dendritic cells

Andrea Ottria^{1,2}, Maili Zimmermann^{1,2}, Tiago Carneiro^{1,2}, Nadia Vazirpanah^{1,2}, Alsya J. Affandi^{1,2}, Ralph G. Tieland^{1,2}, Cornelis P.J. Bekker^{1,2}, Janneke Tekstra², Evelien Ton², Samuel Garcia Perez^{1,2}, Femke Bonte-Mineur³, Kris A. Reedquist^{1,2}, Timothy R.D.J. Radstake^{1,2}, Wioleta Marut^{1,2*}

Affiliations

¹*Center of Translational Immunology, University Medical Center Utrecht, Utrecht University, Utrecht, the Netherlands*

²*Department of Rheumatology and Clinical Immunology, University Medical Center Utrecht, Utrecht University, Utrecht, the Netherlands*

³*Department of Rheumatology and Clinical Immunology Maastad Hospital, Rotterdam, the Netherlands*

***Materials and Correspondence**

Wioleta Marut, PhD, University Medical Centre Utrecht | Heidelberglaan 100 | Tel: +31 88 75 535 68 | w.k.marut@umcutrecht.nl

Manuscript ready for submission

Abstract

Systemic sclerosis (SSc) is an autoimmune disease characterized by hypoxia, immune activation, vascular aberrances and fibrosis. An increased level of proinflammatory cytokine production such as interferon (IFN) α , tumour necrosis factor (TNF) α , interleukin (IL)-8 and IL-6 has been shown in patients with SSc. In line with this, hypoxia has been implicated in the production of those cytokines via hypoxia inducible factors (HIFs). We assessed the potential role of HIFs in the production of IFN α , TNF α , IL-6 and IL-8 by plasmacytoid dendritic cells (pDCs) from healthy and SSc.

Primary healthy pDCs were cultured in hypoxic or atmospheric environment in presence and or absence of Toll like receptor 9 (TLR9) agonist stimulation followed by quantification of cytokines production level by ELISA. The level of HIFs protein was determined by flow cytometry. Fundamental role of HIFs on cytokine production was further assessed by inhibition of HIFs.

We demonstrated that inhibition of HIF-2 α and HIF-1 α reduces the production level of IFN α and TNF α in healthy pDCs. Furthermore, in SSc pDCs we demonstrate the positive correlation between both HIF-2 α and HIF-1 α stabilization with the production of IFN α , TNF α and IL-8, while HIF-2 α solely correlated IL-6 production.

In conclusion, suppression of IFN α , TNF α , IL-6 and IL-8 production by blocking HIF-2 α pathway might provide a therapeutic tool in downregulation of chronic inflammation and thereby the subsequent disease hallmarks of SSc.

Introduction

Systemic sclerosis (SSc) is one of the most complex known systemic autoimmune diseases with an unpredictable course and is characterized by hypoxia and immune dysregulation (1). According to the literature, aberrant Toll like receptor (TLR) signalling (2–4) and an excessive secretion level of pro-inflammatory cytokines i.e. interferon (IFN-) α , tumour necrosis factor (TNF-) α interleukin (IL-) 6, IL-8 and C-X-C motif ligand (CXCL) 4 (4–9), are the main hallmarks of the dysregulated immune response in SSc. As one of the most conserved receptors, TLRs are specialized pathogen recognition receptors. Once triggered, TLR receptors eventuate activation of the innate immune system followed by production and secretion of proinflammatory cytokines. TLR triggering also activates adaptive immunity and orchestrates cell survival and proliferation (10). Hypoxia, which is the key player in persistent inflammation in SSc, is known to induce the expression of TLRs (11) on immune cells (i.e. leukocytes, dendritic cells, macrophages, natural killer cells, and T cells and B cells) and non-immune cells (i.e. epithelial and endothelial cells) (12).

Hypoxia is a condition whereby the oxygen level is lower than the physiological level and therefore occurs typically during inflammation whereby cells are forced to change their energetic metabolism from aerobic (oxygen-dependant) to anaerobic (oxygen-independent). Upon hypoxic conditions, hypoxia inducible factors (HIFs) are activated. HIFs are dimeric proteins formed by an α and β subunit that act as transcription factors for various pro-inflammatory associated genes such as CXCL4 (13), CXCL5 and CXCL12, nuclear factor kappa-light-chain-enhancer of activated B cells (NF κ B), TNF α and cytokine-inducible Nitric oxide synthases (iNOS) (14,15). Therefore, activation of HIFs in a hypoxic environment is decisive for further modulation and direction of (pro-) inflammatory responses. Notably, in order for HIFs to be activated, HIF- α subunit requires to be stabilized and dimerized with HIF- β subunit. In a physiological scenario HIF- α subunit is stabilized in an oxygen depending manner. In an inflammatory or hypoxic scenario however, HIF- α subunit is stabilized in an oxygen independent manner via growth factors, cytokines, metabolites

and TLRs signalling (12–16). Once the HIF- α subunit is stabilized, it dimerizes with the HIF- β subunit and interacts with the DNA to promote the expression of target genes. There are 3 different HIF- α subunits, HIF-1, 2 and 3 α , from which only the first two are the most studied. The combination of HIF- α subunits is differently present and expressed in various tissues and upon activation maintains different physiological mechanisms (16). For instance, HIF-1 α seems to be more involved in the acute response to hypoxia, while HIF-2 α appears to be more involved in the chronic response to hypoxia (17). Finally, recent literature pinpoint the role of HIF-1 α in autoimmune diseases such as rheumatoid arthritis, intestinal bowel disease, psoriasis and SSc (18) and recently, we showed that CXCL4, potential biomarker for SSc which is mainly produced by pDCs (9), is elevated upon HIF-2 α stabilization as a consequence of hypoxia and TLR9 stimulation (13).

Overlooking the evidence, since HIFs activation orchestrate inflammatory response and thereby consequence a vicious proinflammatory circle through TLR activation (19,20) and a dysregulated cytokine profile (13,21,22), we gauge the implication of this synergy in SSc. In this setup, we studied the role of HIFs activation in plasmacytoid dendritic cells (pDCs) as a prominent affected immune cell type in SSc (9,13). Therefore, we hypothesized that the HIFs overactivation might potentially induce secretion of pro-inflammatory cytokines in DCs of patients with SSc.

Methods

Patients cohort

Blood from patients and sex- and age-matched healthy controls (HC) was obtained from the University Medical Center Utrecht (The Netherlands). All patients provided informed written consent approved by the local institutional medical ethics review boards prior to inclusion in this study. Samples and clinical information were treated anonymously immediately after collection. All patients fulfilled the ACR/EULAR 2013 classification criteria for SSc (23). The study was performed according to the guidelines of the Declaration of Helsinki and the local ethical and Review committee from each centre approved the study. Demographics and clinical characteristics of the patients are detailed in **Table 1**.

Table 1 patients characteristics

	Healthy participants (n=18)	SSc (n=14)
Age (years) (min-max)	39 (26–58)	49 (43–78)
Female (%)	15 (83%)	10 (71%)
ANA (antinuclear antibody) (%)	–	13 (93%)
ACA (anticentromere antibody) (%)	–	3 (21%)
Scl70 (anti topoisomerase I) (%)	–	3 (21%)
MRSS (modified Rodnan skin score) (min-max)	–	24 (0-39)
ILD (Interstitial lung disease) (%)	–	2 (14%)
Disease duration (years) (min-max)	–	12 (1-23)

The values are represented as mean + min-max or absolute number + percentage.

Cell isolation and stimulation

Peripheral blood mononuclear cells (PBMCs) from HC and SSc patients were isolated by Ficoll gradient (cat# 17-1440-02, GE Healthcare). According the manufacturer's instructions, pDCs were isolated using an autoMACS Pro Separator. Purity was routinely assessed by flow cytometry and above 92%.

Following, pDCs were seeded to a final concentration of half million per ml in RPMI-GlutaMAX (cat# 61870-010, ThermoFisher) supplemented with 10% fetal bovine serum (FBS) (cat# S181A, Biowest), 10.000 I.E. penicillin-streptomycin (cat# 15070063, ThermoFisher) and interleukin-3 (IL-3, 10ng/ml) (cat# 11340033, Immunotools), and then incubated either in atmospheric (21% O₂) or hypoxic conditions (1% O₂ - in a Rasquinn invivO2 1000 hypoxic chamber). Cells were acclimated for 30 minutes before being exposed to different stimuli and/or inhibitors. Cells were stimulated with the TLR agonists CpG-C (TLR9, 1 μ M) (cat# tlr1-m362-1, Invivogen) and HIF-1 α and HIF-2 α were inhibited using HIF-1 α (Bisphenol A dimethyl ether, 10nM) (cat# CAS 1568-83-8, Santa Cruz Biotechnology) and HIF-2 α (HIF-2 Antagonist 2, 10nM) (cat# SML0883, Sigma-Aldrich) inhibitors during 16 hours in an incubator at 37°C and 5% CO₂.

Intracellular HIFs protein quantification

Using optimized concentration of antibodies, pDCs were stained extracellularly with CD123 (cat# 306022, Biolegend) and CD303 (cat# 130-090-510, Miltenyi Biotec) antibodies at 4°C for 15 minutes. After, cells were fixed and permeabilized using Fix-Perm (cat# 88-8824-00, eBioscience) according to manufacturer's protocol. Antibody against HIF-1 α (cat# 359704, Biolegend) or HIF-2 α (cat# MA5-16021, ThermoFisher) was then added. Data were acquired using a Fortessa flow cytometer and analysed using FlowJo Software. Protein levels were quantified and represented as mean fluorescence intensity (MFI).

Cytokine quantification

Cell-free supernatants were analysed by ELISA for interferon α (IFN α) (cat# BMS216MS, ThermoFisher). TNF α and interleukin 6 (IL-6) and interleukin 8 (IL-8) were measured using human single-plex assays (Bio-Rad) and read on a Bio-Plex 200 system (Bio-Rad).

Statistical analysis

Where appropriate, Mann-Whitney test or Wilcoxon test were assessed using Graph Pad Prism 8.0 Software. *P* values smaller than 0.05 were considered as statistically significant.

Results

TLR induced cytokine expression in pDCs

In our previous research we demonstrated that TLR9 is an important factor in secretion of CXCL4 and other pro-inflammatory cytokines such as IFN α , TNF α , IL-6 and IL-8 in SSc (13). Here, in order to study the effect of TLR on cytokine production, pDCs from healthy individuals were cultured with TLR9 ligand CpG-C in atmospheric oxygen level (AOL) or hypoxia during 16 hours. After, supernatants free of cells were analysed for IFN α , TNF α , IL-6 and IL-8. We observed that TLR9 stimulation led to increment of IFN α ($P=0.031$), TNF α ($P=0.031$), IL-6 ($P=0.031$) and IL-8 ($P=0.031$) in AOL. Hypoxia alone or in combination with TLR9 didn't induce any further significant increase in production level of pro-inflammatory cytokines i.e. IFN α , TNF α , IL-6 and IL-8 in healthy pDCs. Furthermore, spontaneous production of IFN α ($P=0.0022$) was observed in SSc pDCs. This was not observed in TNF α , IL-6 and IL-8 (**Figure 1A**).

Figure 1

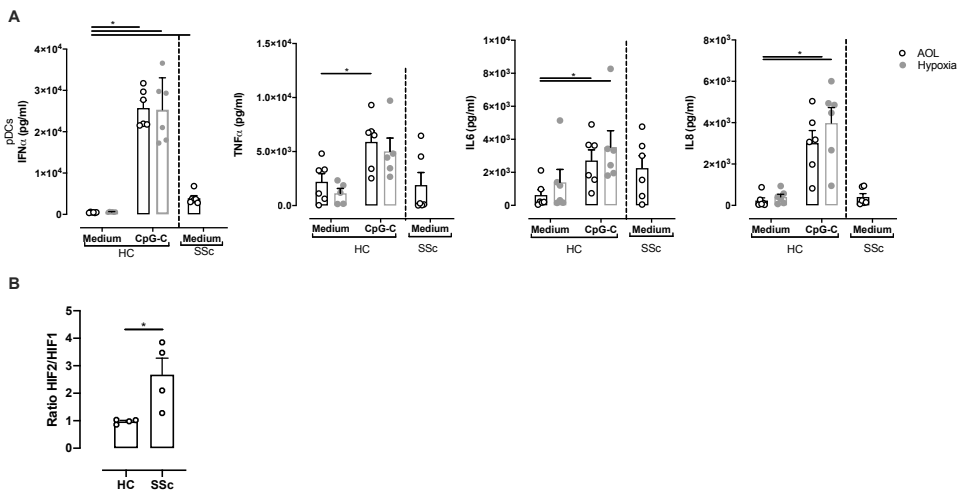


Figure 1. TLR9 triggering leads to increased IFN α , TNF α , IL-6 and IL-8 production in moDCs. A) From the left IFN α , TNF α , IL-6 and IL-8 level quantification in healthy participants (N=6) and SSc (N=6) pDCs incubated with or without TLR9 ligand CpG-C and in AOL or hypoxic conditions during 16 hours. **B)** HIFs protein level expressed as ratio HIF-2 α /HIF-1 α of mean fluorescent of healthy participants (N=4) and SSc (N=4). Bars are represented as mean \pm SEM. Grey and white edge respectively represent hypoxic and atmospheric conditions (AOL). *= $P \leq 0.05$, **= $P \leq 0.01$, ***= $P \leq 0.001$, ****= $P \leq 0.0001$ using Wilcoxon and Mann-Whitney test.

HIF-2 α is increased in pDCs from SSc patients

Next, TLR are known to induce HIFs stabilisation and in our previous research we demonstrated that HIF-2 α was increased in SSc patients (13). We therefore measured the HIF-2 α and HIF-1 α protein expression level in pDCs from healthy and SSc patients. We observed an increased ratio of HIF-2 α expression in SSc as compared to healthy ($P=0.0286$) (**Figure 1B**)

HIF-2 α inhibition reduces pro-inflammatory cytokine production in stimulated healthy pDCs

In order to study the effect of HIFs inhibition after TLR stimulation on cytokine production in a physiological setting, pDCs from healthy individuals were cultured with TLR9 ligand CpG-C during 16 hours in the presence of HIF-2 α or HIF-1 α inhibitor in AOL or hypoxia. After, supernatants free of cells were assessed for presence of IFN α , TNF α , IL-6 and IL-8. After HIF-2 α inhibition, we observed a significant reduction in IFN α production level in AOL ($P=0.0046$) and hypoxia ($P=0.031$) (**Figure 2A**). The inhibition of HIF-1 α failed to significantly reduce IFN α in AOL and hypoxia (**Figure 2B**). Similarly, TNF α secretion was reduced after HIF-2 α inhibition in AOL ($P=0.016$) and hypoxia ($P=0.049$) (**Figure 2C**). HIF-1 α inhibition had no effect both in AOL and hypoxia on TNF α production (**Figure 2D**). Further, the inhibition of HIF-2 α or HIF-1 α had no diminishing effect on IL-6 and IL-8 production level in healthy pDCs both in AOL and hypoxia. Interestingly, the inhibition of HIF-1 α led to increase of IL-8 production ($P=0.024$) in hypoxia (**Figure 2E-2H**).

HIF-2 α and HIF-1 α inhibition reduces pro-inflammatory cytokine production in stimulated pDCs from SSc patients

In order to study the effect of HIF-2 α and HIF-1 α inhibition and the concomitant modulatory mechanisms in which they operate unstimulated pDCs from SSc patient were cultured with or without HIF-2 α or HIF-1 α inhibitor in AOL during 16 hours. After, we quantified the production level of IFN α , TNF α , IL-6 and IL-8. We observed that IFN α secretion was

reduced after inhibition of both HIF-2 α ($P=0.011$) and HIF-1 α ($P=0.029$) (**Figure 2I, 2J**). Similarly, TNF α secretion was reduced by both HIF-2 α ($P=0.021$) and HIF-1 α ($P=0.043$) (**Figure 2K, 2L**). The inhibition of HIF-2 α led to a reduction trend in IL-6 production ($P=0.0536$) (**Figure 2M**), while HIF-1 α inhibition had no effect (**Figure 2N**). Finally, IL-8 secretion was reduced by both HIF-2 α ($P=0.037$) and HIF-1 α ($P=0.035$) inhibitors (**Figure 2O, 2P**).

Figure 2

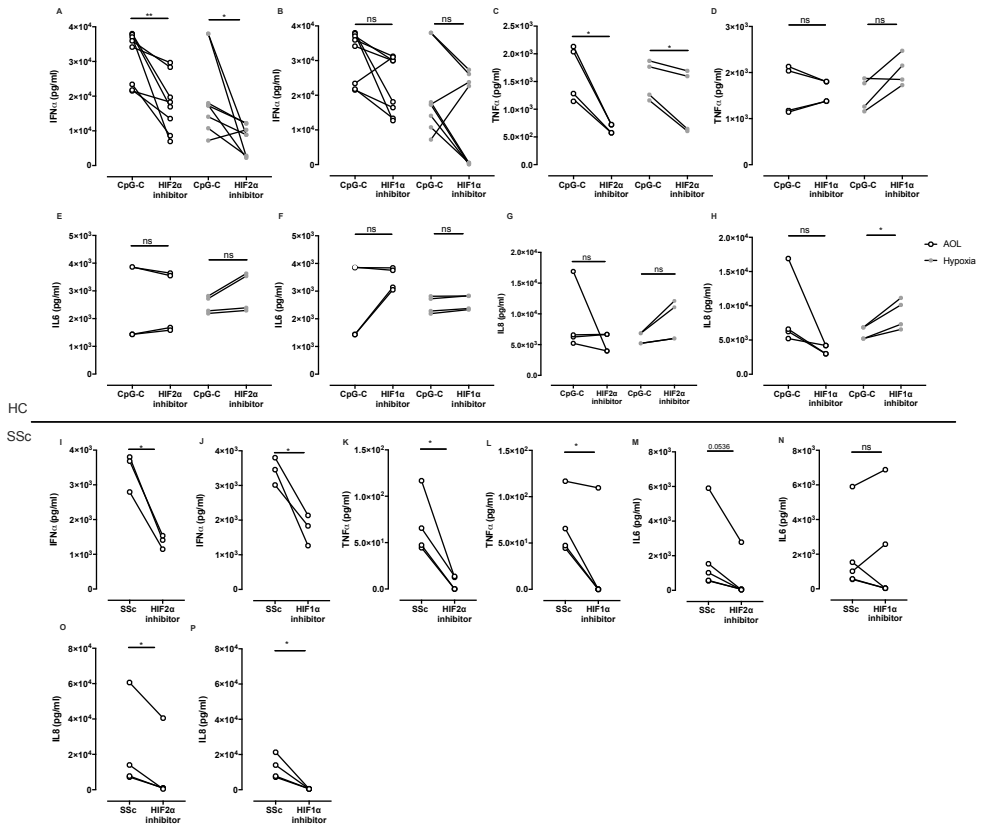


Figure 2. HIF-2 α and HIF-1 α regulatory effect on IFN α , TNF α , IL-6 and IL-8. On the top cytokine quantification in cell free supernatant of **A, E**) IFN α , **B, F**) TNF α , **C, G**) IL-6 and **D, H**) IL-8 in pDCs from healthy participants (N=8 IFN α , N=4 TNF α , IL-6, IL-8) cultured in either AOL or hypoxia and exposed to TLR9 ligand CpG-C in the presence of HIF-2 α inhibitor (**A, B, C, D**) or HIF-1 α inhibitor (**E, F, G, H**) for 16 hours. On the bottom cytokine quantification in cell free supernatant of **I, M**) IFN α , **J, N**) TNF α , **K, O**) IL-6 and **L, P**) IL-8 in pDCs from SSc patients (N=4) cultured in AOL in the presence of HIF-2 α inhibitor (**I, J, K, L**) or HIF-1 α inhibitor (**M, N, O, P**) for 16 hours. Grey and white dots respectively represent hypoxic and atmospheric conditions (AOL). *= $P\leq 0.05$, **= $P\leq 0.01$, ***= $P\leq 0.001$, ****= $P\leq 0.0001$ using and Wilcoxon test.

Discussion

In this study, mimicking the SSc like conditions, we demonstrated that *in Vitro* stimulation of TLR9 in healthy pDCs orchestrate a significant increase in the production levels of pro-inflammatory cytokines such as IFN α , TNF α , IL-8 and IL-6 via HIF-2 α stabilization. Furthermore, we underline the importance of HIFs in downregulation of basal high levels of pro-inflammatory cytokines such as IFN α , TNF α , IL-8 and IL-6 *ex Vivo* in unstimulated pDCs of SSc patients. In our previous studies, we pinpointed HIF-2 α as a key player in CXCL4 production by pDCs from SSc patients (13). Here, for the first time, we demonstrate preliminary data on the fundamental role of HIF-2 α in pro-inflammatory cytokine production by pDCs of patients with SSc. Furthermore, we confirmed our previous observation showing significant disbalance in HIFs ratio in SSc pDCs (13).

We hypothesised whether inhibition of HIF stabilization in SSc pDCs, could reduce the production of pro-inflammatory cytokines in SSc. Confirming our hypothesis, our results demonstrate that TLR stimulated HIF-2 α stabilization alone is sufficient to orchestrate pro-inflammatory cytokine production in healthy pDCs. This is in line with the findings of Spirig *et al.*, who have shown that TLR activation stabilizes HIFs in dendritic cells (24). Following, other similar studies underlined that HIF-1 α stabilisation is positively associated with cytokine production upon TLR4 triggering using LPS stimulation in monocytes (25–27). HIF-1 α has been considered to play an important modulatory role in proinflammatory response and inflammation (28). In our study, inhibition of HIF-1 α had no suppressing effect on IFN α , TNF α , IL-6 and IL-8 in healthy pDCs. Our observations do not entirely exclude HIF-1 α involvement in the immune response, but confirm our previous results pinpointing a major role of HIF-2 α , rather than solely HIF-1 α in pDCs' immune response (13) Remarkably, in freshly isolated healthy pDCs, basal ratio of HIF-2 α /HIF-1 α protein was around one, indicating an equal proportion of HIF-2 α and HIF-1 α as compared to this ratio in SSc pDCs. Overlooking our results, we speculate that it is less likely for HIF-1 α solely to orchestrate TLR9 ligand CpG-C induced immune response in healthy pDCs.

In our study downregulation of only HIF-2 α eventuated a reduction in IFN α and TNF α cytokine production of healthy pDCs. This observation is in line with what Imtiyas *et al.*, showed in mouse macrophages, where HIF-2 α plays a fundamental role in TNF α cytokine production (29). Even though limited number of studies have been stipulating the specific downstream pathways upon which TLRs act (26), yet we believe that TLR9, as an endosomal receptor, is highly sensitive to hypoxia and therefore an important factor in inducing cytokine production by pDCs in autoimmune and inflammatory diseases with hypoxia as a main hallmark (30).

4

Intriguingly, we observed that HIF-1 α inhibition in healthy pDCs exposed to hypoxia led to an increase in IL-8 production level. IL-8 is a pro-inflammatory chemokine with pro-angiogenic effects (31). We speculate that, when suppressing HIF-1 α , HIF-2 α is responsible for an induction of IL-8 level. This mechanism would further support our speculation that HIF-2 α plays a major pro-inflammatory role upon TLR9 triggering in healthy pDCs.

Interestingly, in SSc we observed that both HIF-1 α and HIF-2 α inhibition substantiate a significant reduction in IFN α , TNF α and IL-8 production levels in pDCs. However, inhibition of HIF-1 α and HIF-2 α stabilization had no significant effect on IL-6 production levels. Literature regarding the effect of HIF-1 α in IL-6 production is contradictory. In mice DCs deletion of HIF-1 α showed no alteration in IL-6 production as this remained similar to wildtype controls (32). However, other studies culturing cell-lines have described the inhibitory effect of HIF-1 α suppression on IL-6 production levels (33). We believe that IL-6 production in SSc pDCs is HIF-1 α independent, since its suppression had no effect on production level of this cytokine. Inhibition of HIF-2 α however, showed a non-significant but clear IL-6 lowering trend. Hence, HIF-2 α working mechanism requires further in-depth studies since there is very little known about its regulatory pathway and this information is even more limited on HIF-2 α inhibitory effect on IL-6 production in pDCs (15).

When assessing the role of hypoxia in cytokine secretion level of SSc pDCs, one could presuppose that in contrast to the healthy setting, implicated epigenetic modification

eventuated by *in Vivo* chronic exposure to hypoxic environment could explain the high HIF-2 α /HIF-1 α ratio at basal level in SSc patients. In line with this, it is likely to assume that the epigenetically modified pDCs with proinflammatory-like phenotype continue producing cytokines even in absence of specific triggers as a consequence of chronically activated and stabilized HIFs. In line with this, Wippf and colleagues have pinpointed the association between HIF-1 α gene polymorphism with SSc in a French European Caucasian population (34). In addition, inhibition of HIFs as a treatment target has been already considered in cancer therapy (35). Unfortunately, literature about the role of HIF-2 α in SSc is poor. In a more pathological setting, it has been shown that hypoxia can inflict epigenetic modification in cells, such as in fibroblasts, leading to a more fibrotic profile (36). Similarly, hypoxia inflicted cellular metabolic alterations in SSc has been described before (37,38). Such alterations might originate from epigenetic modification, either directly or indirectly in a HIF-associated mechanism of action (39,40). To our knowledge, our study provides the first observations on the effect of HIF-1 α and HIF-2 α inhibition on cytokine biology i.e. IFN α , TNF α , IL-6 and IL-8 in healthy and SSc pDCs. Even though our study shows a trend evidencing IL-6 reduction upon HIF-2 α inhibition, these results remain preliminary and are therefore a promising foundation for further investigations on anti-inflammatory treatment therapies.

Taken together, combination of targeting HIF-2 α and HIF-1 α as potential key producers of pro-inflammatory cytokines upon hypoxia and TLR stimulation in SSc, might provide an inflammatory mitigating option in this disease. While HIF-1 α has already been addressed as a potential target in SSc, according to our preliminary results, we believe that the potentials of HIF-2 α suppression in SSc should not be excluded. Further studies are required to elucidate the role of HIFs and in particular HIF-2 α subunit as a target therapy in SSc to diminish hypoxia induced inflammation and subsequent disease prognosis.

References

1. Pattanaik D, Brown M, Postlethwaite BC, Postlethwaite AE. Pathogenesis of systemic sclerosis. *Front Immunol* (2015) **6**:272. doi:10.3389/fimmu.2015.00272
2. Bhattacharyya S, Varga J. Emerging Roles of Innate Immune Signaling and Toll-Like Receptors in Fibrosis and Systemic Sclerosis. *Curr Rheumatol Rep* (2015) **17**: doi:10.1007/s11926-014-0474-z
3. Fullard N, O'Reilly S. Role of innate immune system in systemic sclerosis. *Semin Immunopathol* (2015) **37**:511–517. doi:10.1007/s00281-015-0503-7
4. Fuschiotti P. Current perspectives on the immunopathogenesis of systemic sclerosis. *ImmunoTargets Ther* (2016) **5**:21–35. doi:10.2147/ITT.S82037
5. Baraut J, Michel L, Verrecchia F, Farge D. Relationship between cytokine profiles and clinical outcomes in patients with systemic sclerosis. *Autoimmun Rev* (2010) **10**:65–73. doi:10.1016/j.autrev.2010.08.003
6. Trojanowska M. Role of PDGF in fibrotic diseases and systemic sclerosis. *Rheumatology* (2009) **47**:v2–v4. doi:10.1093/rheumatology/ken265
7. Sato S, Hasegawa M, Takehara K. Serum levels of interleukin-6 and interleukin-10 correlate with total skin thickness score in patients with systemic sclerosis. *J Dermatol Sci* (2001) **27**:140–146. doi:10.1016/S0923-1811(01)00128-1
8. Holcombe RF, Baethge BA, Stewart RM, Betzing K, Hall VC, Fukuda M, Wolf RE. Cell Surface Expression of Lysosome-Associated Membrane Proteins (LAMPs) in Scleroderma: Relationship of lamp2 to Disease Duration, Anti-Sc170 Antibodies, Serum Interleukin-8, and Soluble Interleukin-2 Receptor Levels. *Clin Immunol Immunopathol* (1993) **67**:31–39. doi:10.1006/clin.1993.1042
9. Van Bon L, Affandi AJ, Broen J, Christmann RB, Marijnissen RJ, Stawski L, Farina GA, Stifano G, Mathes AL, Cossu M, et al. 433-443 Proteome-wide analysis and CXCL4 as a biomarker in systemic sclerosis. *N Engl J Med* (2014) **370**:433–443. doi:10.1056/NEJMoa1114576
10. Medzhitov R, Preston-Hurlburt P, Janeway CA. A human homologue of the *Drosophila* toll protein signals activation of adaptive immunity. *Nature* (1997) **388**:394–397. doi:10.1038/41131
11. Kuhlicke J, Frick JS, Morote-Garcia JC, Rosenberger P, Eltzschig HK. Hypoxia inducible factor (HIF)-1 coordinates induction of toll-like receptors TLR2 and TLR6 during hypoxia. *PLoS One* (2007) **2**:e1364. doi:10.1371/journal.pone.0001364
12. Delneste Y, Beauvillain C, Jeannin P. Immunité naturelle. *Médecine/Sciences* (2007) **23**:67–74. doi:10.1051/medsci/200723167
13. Ottria, Andrea et al. Hypoxia and TLR9 activation drive CXCL4 production in systemic sclerosis pDCs via mtROS and HIF-2 α . *Cell Rep* (2019)
14. Jeong HJ, Chung HS, Lee BR, Kim SJ, Yoo SJ, Hong SH, Kim HM. Expression of proinflammatory cytokines via HIF-1 α and NF- κ B activation on desferrioxamine-stimulated HMC-1 cells. *Biochem Biophys Res Commun* (2003) **306**:805–811. doi:10.1016/S0006-291X(03)01073-8
15. Palazon A, Goldrath AW, Nizet V, Johnson RS. HIF Transcription Factors, Inflammation, and Immunity. *Immunity* (2014) **41**:518–528. doi:10.1016/j.immuni.2014.09.008
16. Patel SA, Simon MC. Biology of hypoxia-inducible factor-2 α in development and disease. *Cell Death Differ* (2008) **15**:628–634. doi:10.1038/cdd.2008.17
17. Fitzpatrick SF. Immunometabolism and Sepsis: A Role for HIF? *Front Mol Biosci* (2019) **6**: doi:10.3389/fmolb.2019.00085
18. Deng W, Feng X, Li X, Wang D, Sun L. Hypoxia-inducible factor 1 in autoimmune diseases. *Cell Immunol* (2016) **303**:7–15. doi:10.1016/j.cellimm.2016.04.001
19. Van Bon L, Cossu M, Loof A, Gohar F, Wittkowski H, Vonk M, Roth J, Van Den Berg W, Van Heerde W, Broen JCA, et al. Proteomic analysis of plasma identifies the Toll-like receptor agonists S100A8/A9 as a novel possible marker for systemic sclerosis phenotype. *Ann Rheum Dis* (2014) **73**:1585–1589. doi:10.1136/annrheumdis-2013-205013
20. Broen JCA, Bossini-Castillo L, Van Bon L, Vonk MC, Knaapen H, Beretta L, Rueda B, Hesselstrand R, Herrick A, Worthington

- J, et al. A rare polymorphism in the gene for Toll-like receptor 2 is associated with systemic sclerosis phenotype and increases the production of inflammatory mediators. *Arthritis Rheum* (2012) **64**:264–271. doi:10.1002/art.33325
21. van Bon L, Affandi AJ, Broen J, Christmann RB, Marijnissen RJ, Stawski L, Farina GA, Stifano G, Mathes AL, Cossu M, et al. Proteome-wide Analysis and CXCL4 as a Biomarker in Systemic Sclerosis. *N Engl J Med* (2014) **370**:433–443. doi:10.1056/NEJMoa1114576
22. Cossu M, van Bon L, Preti C, Rossato M, Beretta L, Radstake TRDJ. Earliest Phase of Systemic Sclerosis Typified by Increased Levels of Inflammatory Proteins in the Serum. *Arthritis Rheumatol* (2017) **69**:2359–2369. doi:10.1002/art.40243
23. Van Den Hoogen F, Khanna D, Fransen J, Johnson SR, Baron M, Tyndall A, Matucci-Cerinic M, Naden RP, Medsger TA, Carreira PE, et al. 2013 classification criteria for systemic sclerosis: An american college of rheumatology/European league against rheumatism collaborative initiative. *Arthritis Rheum* (2013) **65**:2737–2747. doi:10.1002/art.38098
24. Spirig R, Djafarzadeh S, Regueira T, Shaw SG, von Garnier C, Takala J, Jakob SM, Rieben R, Lepper PM. Effects of TLR agonists on the hypoxia-regulated transcription factor HIF-1 α and dendritic cell maturation under normoxic conditions. *PLoS One* (2010) **5**: doi:10.1371/journal.pone.0010983
25. Winning S, Fandrey J. Dendritic Cells under Hypoxia: How Oxygen Shortage Affects the Linkage between Innate and Adaptive Immunity. *J Immunol Res* (2016) **2016**: doi:10.1155/2016/5134329
26. Frede S, Stockmann C, Freitag P, Fandrey J. Bacterial lipopolysaccharide induces HIF-1 activation in human monocytes via p44/42 MAPK and NF- κ B. *Biochem J* (2006) **396**:517–527. doi:10.1042/BJ20051839
27. Paardekooper LM, Bendix MB, Ottria A, de Haer LW, Ter Beest M, Radstake TRDJ, Marut W, van den Bogaart G. Hypoxia potentiates monocyte-derived dendritic cells for release of tumor necrosis factor α via MAP3K8. *Biosci Rep* (2018) **38**: doi:10.1042/BSR20182019
28. Nizet V, Johnson RS. Interdependence of hypoxic and innate immune responses. *Nat Rev Immunol* (2009) **9**:609–617. doi:10.1038/nri2607
29. Imtiyaz HZ, Williams EP, Hickey MM, Patel SA, Durham AC, Yuan LJ, Hammond R, Gimotty PA, Keith B, Simon MC. Hypoxia-inducible factor 2 α regulates macrophage function in mouse models of acute and tumor inflammation. *J Clin Invest* (2010) **120**:2699–2714. doi:10.1172/JCI39506
30. Peng S, Li C, Wang X, Liu X, Han C, Jin T, Liu S, Zhang X, Zhang H, He X, et al. Increased toll-like receptors activity and TLR ligands in patients with autoimmune thyroid diseases. *Front Immunol* (2016) **7**:578. doi:10.3389/fimmu.2016.00578
31. Takamori H, Oades ZG, Hoch RC, Burger M, Schraufstatter IU. Autocrine growth effect of IL-8 and GRO α on a human pancreatic cancer cell line, Capan-1. *Pancreas* (2000) **21**:52–56. doi:10.1097/00006676-200007000-00051
32. Köhler T, Reizis B, Johnson RS, Weighardt H, Förster I. Influence of hypoxia-inducible factor 1 α on dendritic cell differentiation and migration. *Eur J Immunol* (2012) **42**:1226–1236. doi:10.1002/eji.201142053
33. Jeong HJ, Hong SH, Park RK, Shin T, An NH, Kim HM. Hypoxia-induced IL-6 production is associated with activation of MAP kinase, HIF-1, and NF- κ B on HEI-OC1 cells. *Hear Res* (2005) **207**:59–67. doi:10.1016/j.heares.2005.04.003
34. Wipff J, Dieude P, Avouac J, Tiev K, Hachulla E, Granel B, Diot E, Sibilia J, Mouthon L, Meyer O, et al. Association of hypoxia-inducible factor 1A (HIF1A) gene polymorphisms with systemic sclerosis in a French European Caucasian population. *Scand J Rheumatol* (2009) **38**:291–294. doi:10.1080/03009740802629432
35. Burroughs SK, Kaluz S, Wang D, Wang K, Van Meir EG, Wang B. Hypoxia inducible factor pathway inhibitors as anticancer therapeutics. *Future Med Chem* (2013) **5**:553–572. doi:10.4155/fmc.13.17
36. Watson CJ, Collier P, Tea I, Neary R, Watson JA, Robinson C, Phelan D, Ledwidge MT, McDonald KM, McCann A, et al. Hypoxia-induced epigenetic modifications are associated with cardiac tissue fibrosis and the development of a myofibroblast-like

- phenotype. *Hum Mol Genet* (2014) **23**:2176–2188. doi:10.1093/hmg/ddt614
37. Julià A, Vinaixa M, Domènech E, Fernández-Nebro A, Cañete JD, Ferrándiz C, Tornero J, Gisbert JP, Nos P, Casbas AG, et al. Urine metabolome profiling of immune-mediated inflammatory diseases. *BMC Med* (2016) **14**:133. doi:10.1186/s12916-016-0681-8
38. Murgia F, Svegliati S, Poddighe S, Lussu M, Manzin A, Spadoni T, Fischetti C, Gabrielli A, Atzori L. Metabolomic profile of systemic sclerosis patients. *Sci Rep* (2018) **8**:7626. doi:10.1038/s41598-018-25992-7
39. Cheng SC, Quintin J, Cramer RA, Shepardson KM, Saeed S, Kumar V, Giamarellos-Bourboulis EJ, Martens JHA, Rao NA, Aghajani A, et al. MTOR- and HIF-1 α -mediated aerobic glycolysis as metabolic basis for trained immunity. *Science* (80-) (2014) **345**: doi:10.1126/science.1250684
40. Zhang S, Bories G, Lantz C, Emmons R, Becker A, Liu E, Abecassis MM, Yvan-Charvet L, Thorp EB. Immunometabolism of Phagocytes and Relationships to Cardiac Repair. *Front Cardiovasc Med* (2019) **6**: doi:10.3389/fcvm.2019.00042

Ethical approval information

This study was performed according to the guidelines of the Declaration of Helsinki and study meets the approval of Ethical and Review committee of the Institutional Review and Ethical Board of University medical centre of Utrecht. The Ethical Committee approval was obtained in November 2011 (Ethical approval number 12-466). Moreover, in this study, all participants gave their informed consent before the inclusion.

Acknowledgements

This study was supported by research funding Marie Curie Intra-European Fellowship (Proposal number: 624871), the NWO VENI (grant number 91919149) and Gravitation (grant number 2013 ICI-024.002.009).

All the authors listed have made substantial, direct, and intellectual contribution to the work and approved it for publication. We thank Wilco de Jager (MultiPlex Core Facility, University Medical Center Utrecht) for performing Luminex assays.

Author contribution

All authors approved the final version after being involved in drafting and revising the article for important intellectual content. A. Ottria and W. Marut had full access to the data and takes responsibility for the accuracy of the performed analysis and the integrity of the data. A. Ottria, T.R.D.J. Radstake and W. Marut were involved in design of the study. Execution and analysis of the results was performed by A. Ottria. A. Ottria, M. Zimmermann, T. Carvalheiro, N. Vazirpanah, A.J. Affandi, S. Garcis Perez, R.G. Tieland, C.P.J. Bekkers were involved in performing experiments. A. Ottria was involved in selection of the patients. J. Tekstra, E. Ton and T.R.D.J. Radstake were involved in inclusion of SSc patients. All the authors contributed to the review of the manuscript.

CXCL4 drives fibrosis by promoting several key cellular and molecular processes.

Alsya J. Affandi^{1,2,11*}, Tiago Carneiro^{1,2*}, Andrea Ottria^{1,2}, Judith J. de Haan³, Maïke A.D. Brans³, Maarten M. Brandt⁴, Ralph G. Tieland^{1,2}, Beatriz Malvar Fernández^{1,2}, Cornelis P.J. Bekker^{1,2}, Maarten van der Linden^{1,2}, Maili Zimmermann^{1,2}, Barbara Giovannone^{1,5}, Catharina G.K. Wichers^{1,2}, Samuel Garcia^{1,2}, Yan Juan Xu⁶, M. Anna Kowalska^{7,8}, Maaïke Waasdorp⁹, Caroline Cheng⁶, Susan Gibbs^{9,10}, Saskia C.A. de Jager³, Joel A.G. van Roon^{1,2}, Timothy R.D.J. Radstake^{1,2}, Wioleta Marut^{1,2,#}

Affiliations

¹Center for Translational Immunology, University Medical Center Utrecht, Utrecht University, Utrecht, The Netherlands.

²Department of Rheumatology and Clinical Immunology, University Medical Center Utrecht, Utrecht University, Utrecht, The Netherlands.

³Department of Experimental Cardiology, University Medical Center Utrecht, Utrecht University, Utrecht, The Netherlands.

⁴Experimental Cardiology, Department of Cardiology, Thoraxcenter Erasmus University Medical Center, Rotterdam, The Netherlands

⁵Department of Dermatology, University Medical Center Utrecht, Utrecht University, Utrecht, The Netherlands.

⁶Department of Nephrology and Hypertension, University Medical Center Utrecht, Utrecht University, The Netherlands.

⁷Department of Hematology, Children's Hospital of Philadelphia, Philadelphia, PA, USA.

⁸Institute of Medical Biology, Polish Academy of Science, Lodz, Poland.

⁹Department of Molecular Cell Biology and Immunology, Amsterdam University Medical Center, Vrije Universiteit Amsterdam, Amsterdam, The Netherlands.

¹⁰Department of Oral Cell Biology, Academic Centre for Dentistry (ACTA), University of Amsterdam and Vrije Universiteit Amsterdam, Amsterdam, The Netherlands.

¹¹Present address: Department of Molecular Cell Biology and Immunology, Amsterdam University Medical Center, Vrije Universiteit Amsterdam, Amsterdam, The Netherlands.

*Equal contribution

Corresponding Author

Dr. Wioleta Marut, PhD University Medical Centre Utrecht, Heidelberglaan 100, Tel: +31 88 75 535 68 W.K.Marut@umcutrecht.nl

Manuscript submitted

Abstract

Fibrosis, characterized by excessive deposition of extracellular matrix (ECM) by myofibroblasts, is a major cause of mortality worldwide. With few treatments available, understanding the pathways involved in myofibroblast activation is crucial to develop novel treatment strategies. Systemic sclerosis (SSc) is a prototypic fibrotic disease in which CXCL4 has been identified to strongly correlate with skin and lung fibrosis. Here we aimed to elucidate the role of CXCL4 in fibrosis development. We observed that CXCL4 levels were increased in multiple mouse inflammatory and fibrotic models. Using CXCL4-deficient mice, we demonstrated the essential role of CXCL4 in promoting fibrotic events in the skin, lung, and heart using two independent fibrosis models. Overexpressing human CXCL4 in mice aggravated bleomycin-induced skin fibrosis, whereas blocking CXCL4 abrogated fibrosis development. Using *in vitro* assays, we confirmed CXCL4 directly induced myofibroblast differentiation and collagen synthesis in different precursor cells. Our findings identify a pivotal role of CXCL4 in fibrosis, further substantiating the potential role for neutralizing CXCL4 as a novel therapeutic strategy.

Introduction

In fibrotic disorders, an excessive deposition of extra cellular matrix (ECM) leads to the obliteration of the original tissue architecture and function¹. During this process, a large amount of ECM components is produced by activated myofibroblasts, characterized by *de novo* α -smooth muscle actin (α -SMA) expression². Although myofibroblasts are required during physiological tissue repair mechanisms such as wound healing, their persistence can lead to the development of fibrosis. The origin of these cells was initially assumed to be tissue resident fibroblasts, but other cell types can also give rise to the formation of myofibroblasts (myofibroblast transformation, MT). For instance, the conversion of cells from endothelial (EndMT) or epithelial (EMT) origins towards mesenchymal-like cells, is likely to play an essential role in systemic sclerosis (SSc) and other chronic fibrotic disorders^{2,3}. The transformation of myofibroblasts from precursor cells is thought to be driven mainly by TGF β , but other fibrogenic cytokines derived from immune cells can also contribute to this process^{4,5}.

SSc is a prototypical fibrotic disease manifested by fibrosis in the skin and multiple internal organs, that is often preceded by chronic inflammation and vascular alterations^{6,7}. With the purpose of delineating the underlying causes of the disease, we previously found the chemokine CXCL4 to be increased in the circulation and skin of SSc patients, predicting the progression of both skin and lung fibrosis⁸. CXCL4 is a multifunctional chemokine that can target virtually all cells in the vasculature, and it is involved in numerous biological processes including the modulation of immune responses and angiogenesis⁸⁻¹⁰. CXCL4 has a pro-inflammatory role for multiple cells including promoting the production of IL-6 and TNF α in monocytes^{11,12}, priming toll-like receptor (TLR) responses of monocyte-derived dendritic cells¹³, as well as boosting IL-17 production in CD4 T cells¹⁴. CXCL4 has been shown to be increased in inflammatory diseases, including inflammatory bowel disease, psoriasis, atherosclerosis, and rheumatoid arthritis^{10,15,16}, as well as fibrotic disorders, such as chronic liver fibrosis, cystic fibrosis, and myelofibrosis¹⁷⁻¹⁹. Its importance

in disease pathogenesis has been shown in animal studies where CXCL4-deficient mice were protected from disease development in atherosclerosis, acute lung injury, and liver fibrosis models¹⁹⁻²¹. Furthermore, CXCL4 could directly suppress endothelial cell proliferation and their expression of the transcription factor FLI1, a negative regulator of collagen synthesis⁸. Although this series of observations is suggestive for the potential pro-fibrotic properties of CXCL4, it is currently unclear whether CXCL4 could play a direct role in initiating the fibrotic processes via myofibroblast precursor cells, which is a crucial void in information given the lack of effective therapies for fibrosis.

Here, we demonstrate increased levels of CXCL4 in multiple experimental models of inflammation and fibrosis, and we show proof of concept for CXCL4 as a therapeutic target, as genetic knockdown of CXCL4 in mice almost completely abolish fibrosis in the skin, lungs and the heart. Importantly, we show that blocking CXCL4 abrogates skin fibrosis, while overexpression of CXCL4 aggravates disease. In addition, we reveal the direct role of CXCL4 in the formation of myofibroblasts from different human precursor cells *in vitro* and delineate the mechanisms involved. Our study establish CXCL4 as a key component in fibrosis development and the potential of blocking CXCL4 as a novel therapeutic strategy.

Results

CXCL4 is increased in inflammatory and fibrotic conditions

CXCL4 has been shown to be increased in SSc skin and bleomycin-induced skin fibrosis model, the most widely accepted animal model for SSc²². Upon subcutaneous bleomycin treatment for 7 days, *Cxcl4* mRNA expression was indeed increased in the skin of mice as compared to saline controls (**Fig. 1a,b**). Whereas changes in serum CXCL4 levels were undetectable after 7 days of treatment, CXCL4 levels were clearly increased after 28 days (**Supplementary Fig. 1a**). We further examined CXCL4 levels in other *in vivo* experimental models mimicking SSc or other forms of fibrosis. We performed chronic stimulation with TLR ligands poly(I:C) and lipopolysaccharide, using a subcutaneously implanted mini-osmotic pump, to induce skin inflammation and fibrosis^{23,24} and we observed increased expression of *Cxcl4* mRNA in the skin in both models (**Supplementary Fig. 1b,c**). Since CXCL4 has been implicated in other fibrotic disease¹⁹, we utilized the scleroderma-like graft-versus-host disease model (Scl-GvHD) to induce skin fibrosis, and the model of pressure overload-induced cardiac fibrosis by transverse aortic constriction (TAC), to further examine the notion that increased levels of CXCL4 are a generalized phenomenon in fibrosis. In line with this thought, CXCL4 levels were found to be increased in the serum and heart of the Scl-GvHD and TAC models, respectively (**Supplementary Fig. 1d,e**).

CXCL4 deficiency abrogates fibrosis in skin and lung

We next aimed to elucidate the role of CXCL4 in bleomycin-induced fibrosis development using *Cxcl4*^{-/-} mice. Subcutaneous injection of bleomycin led to the anticipated skin thickening and increase of dermal thickness in wild-type C57BL/6 (WT) mice, whereas in the *Cxcl4*^{-/-} counterparts the effects of bleomycin was almost fully abrogated (**Fig. 1c-e**). In line with these observations, the amount of bleomycin-induced collagen in the skin was significantly reduced in *Cxcl4*^{-/-} mice (**Fig. 1f**). The increase of dermal myofibroblasts (α SMA⁺) was also diminished in *Cxcl4*^{-/-} mice, indicating the myofibroblast formation

Fig. 1

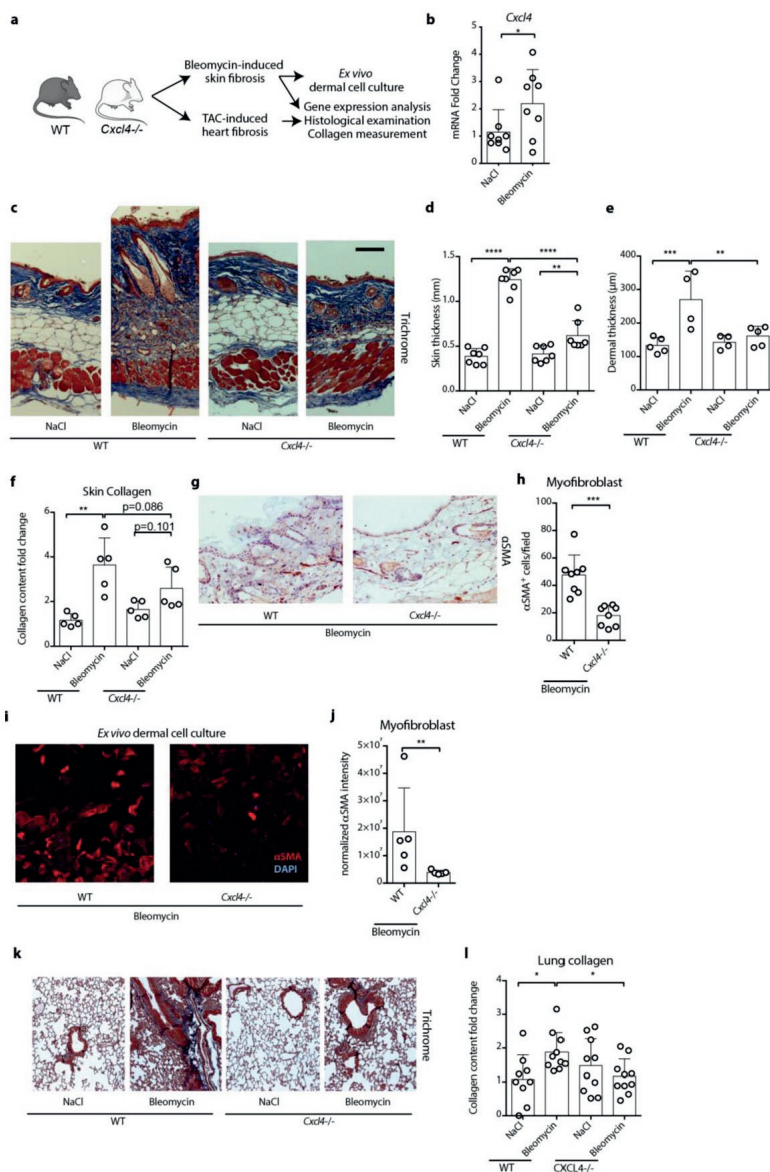


Figure 1. CXCL4 is a critical factor required for bleomycin-induced skin and lung fibrosis. (a) C57BL/6 wild type (WT) or *Cxcl4*^{-/-} mice were injected subcutaneously with bleomycin or saline (NaCl) control and further processed as described. (b) Total RNA was isolated from the skin, and *Cxcl4* mRNA expression was quantified by qPCR. (*n* = 8 per group) (c) Representative skin histological analysis after bleomycin or NaCl treatment, stained with Masson's Trichrome (blue for collagen), is displayed. Quantification of (d) caliper-measured skin thickness or (e) histologically-measured dermal thickness is shown (*n* = 4-7 per group). (f) Collagen content upon bleomycin treatment in skin after bleomycin was measured by hydroxyproline assay (*n* = 5 per group). (g) Representative histological analysis for αSMA⁺ immune cells in the dermis, and (h) their quantification, after bleomycin or NaCl

5

control treatment are shown ($n = 8$ per group). (i,j) Skin was digested after four weeks of treatment and harvested cells were cultured at 37°C for a week for assessment of dermal myofibroblasts. (i) Representative images of α SMA-(red) expressing myofibroblast are displayed, and (j) quantification of α SMA normalized to cell number by nuclei staining (DAPI, blue) is shown ($n = 5$ per group). (k) Representative lung histological analysis stained with Masson's Trichrome staining is shown. (l) Collagen content in the lung after bleomycin exposure was measured by hydroxyproline assay ($n = 9-10$ per group). Bars represent mean \pm SD. One-way ANOVA with FDR correction for multiple testing or two-tailed Mann-Whitney test was used as appropriate. * (adj.) $p < 0.05$, ** $p < 0.01$, *** $p < 0.001$, **** $p < 0.0001$.

to be inhibited in *Cxcl4* deficient mice (Fig. 1g,h). Furthermore, *ex vivo* cultures of dermal fibroblasts isolated from bleomycin-treated mice, revealed a higher expression level of α SMA when compared to untreated mice (Fig. 1i,j). Subcutaneous bleomycin treatment is known to also induce a systemic inflammatory and fibrotic process in distal organs²⁵. Commensurate to these observations, the lungs of *Cxcl4*^{-/-} mice were almost completely protected against the bleomycin-induced fibrosis (Fig. 1k,l). Therefore, these data suggest that CXCL4 deficiency protects mice from bleomycin-induced skin and lung fibrosis.

CXCL4 promotes inflammatory and fibrotic processes

Next, we further investigated the mechanisms that conferred protection to *Cxcl4*^{-/-} mice against bleomycin exposure. We found increased mRNA expression of the ECM components *Colla1*, *Col3a1* and the pro-fibrotic *Tgfb1* following bleomycin treatment in the skin of WT mice. The increase of these pro-fibrotic factors was abolished in *Cxcl4*^{-/-} mice (Supplementary Fig. 2a). A decrease of SMAD2/3 expression in the skin of *Cxcl4*^{-/-} mice following bleomycin treatment, as compared to WT mice (Supplementary Fig. 2b,c), further indicated that TGF- β signaling might be affected. With respect to inflammation, the number of dermal-infiltrating CD45⁺ immune cells recruited after bleomycin-treatment was drastically decreased in *Cxcl4*^{-/-} mice (Supplementary Fig. 2d,e). As observed in SSc, the bleomycin-treated WT mice showed systemic signs of inflammation such as increased levels of circulating E-selectin, P-selectin and the chemokine KC (murine homologue of IL-8), which were reduced in their *Cxcl4*^{-/-} counterparts (Supplementary Fig. 2f). Furthermore, it has been proposed that pericytes link vascular damage to fibrosis in SSc

patients, via their trans-differentiation into myofibroblasts²⁶. We found a high number of PDGFR- β^+ pericytes in the skin of bleomycin-treated WT mice (**Supplementary Fig. 2g,h**). On the contrary, *Cxcl4*^{-/-} mice displayed significantly reduced numbers of pericytes, more resembling control, NaCl-treated WT mice (**Supplementary Fig. 2g,h**). Thus, these findings further support a crucial role of CXCL4 in fibrosis development through multiple mechanisms.

CXCL4-deficiency abrogates heart fibrosis

Further support for the role of CXCL4 in fibrosis was sought in the non-SSc-related pressure-overload TAC model *in vivo*. Collagen accumulation appeared in the perivascular and interstitial regions of the heart from WT mice 7 days post-TAC as revealed by Trichrome staining, whereas almost none was observed in their *Cxcl4*^{-/-} counterparts (**Fig. 2a**). Moreover, the myofibroblast markers α SMA and collagen I were significantly decreased in *Cxcl4*^{-/-} mice when compared to WT mice post-TAC (**Fig. 2b,c**). Next, gene expression profiling of fibrosis-associated genes revealed overexpression of genes involved in ECM synthesis and processing (*Acta2*, *Fnl1*, *Colla2*, *Col3a1*, *Mmp14*, *Lox*), TGF β signaling (*Tgfb3*, *Ctgf*, *Thbs1*, *Serpine1*), and the Smad pathway in the hearts of TAC-treated WT mice, but not in *Cxcl4*^{-/-} mice (**Fig. 2d,e**). This shows that the effect of bleomycin and TAC in initiating inflammation and fibrosis in the skin, lungs and circulation is crucially dependent upon CXCL4.

8). (b) Representative histological analysis of α SMA⁺ myofibroblasts (red), collagen (green), and nuclei staining (DAPI, blue) in the dermis after TAC or sham control treatment. (c) Quantification of myofibroblasts and collagen is shown ($n = 4-6$ per group). (d,e) Total RNA was isolated from the heart after TAC or sham surgery, and mRNA expression was quantified by qPCR. (d) A qPCR array of fibrotic genes from representative mice (sham $n = 2$, TAC $n = 3$ from each WT and *Cxcl4*^{-/-} mice) was performed. Significantly upregulated genes in WT TAC group compared to WT sham group are indicated by asterisks. Genes were clustered using correlation distance with complete linkage by ClustVis. (e) Quantitative single PCRs of selected genes in an enlarged cohort was performed to validate the identified genes (sham $n = 3$, TAC $n = 7-8$). Bars represent mean \pm SD. One-way ANOVA with FDR correction for multiple testing or two-tailed t test was used as appropriate. * adj. $p < 0.05$, ** $p < 0.01$, *** $p < 0.001$.

CXCL4 blocking ameliorates while CXCL4 overexpression aggravates fibrosis in bleomycin-induced skin fibrosis

Since CXCL4 mediated bleomycin-induced inflammatory and fibrotic processes, next we determined the potential therapeutic effect of blocking CXCL4 using a monoclonal antibody. Remarkably, when mice were administered with anti-CXCL4, the increase of dermal thickness after bleomycin treatment was completely suppressed (**Fig. 3a,b**), concomitant with reduced numbers of α SMA⁺ myofibroblasts (**Fig. 3c,d**). This highly suggests that blocking CXCL4 inhibits fibrosis development induced by bleomycin.

Additionally, to confirm the pathogenic properties of CXCL4, we used mice deficient of mouse CXCL4 but overexpressing human CXCL4 (*huCXCL4*⁺). In these *huCXCL4* mice, we found a significant increase of skin fibrosis as compared to WT mice following 2 weeks of bleomycin treatment, as demonstrated by hydroxyproline staining and skin thickness measurement (**Fig. 3e-f**). Of note, untreated *huCXCL4*⁺ mice did not spontaneously develop skin fibrosis, implying that CXCL4 alone is not sufficient to develop fibrosis (data not shown).

Fig. 3

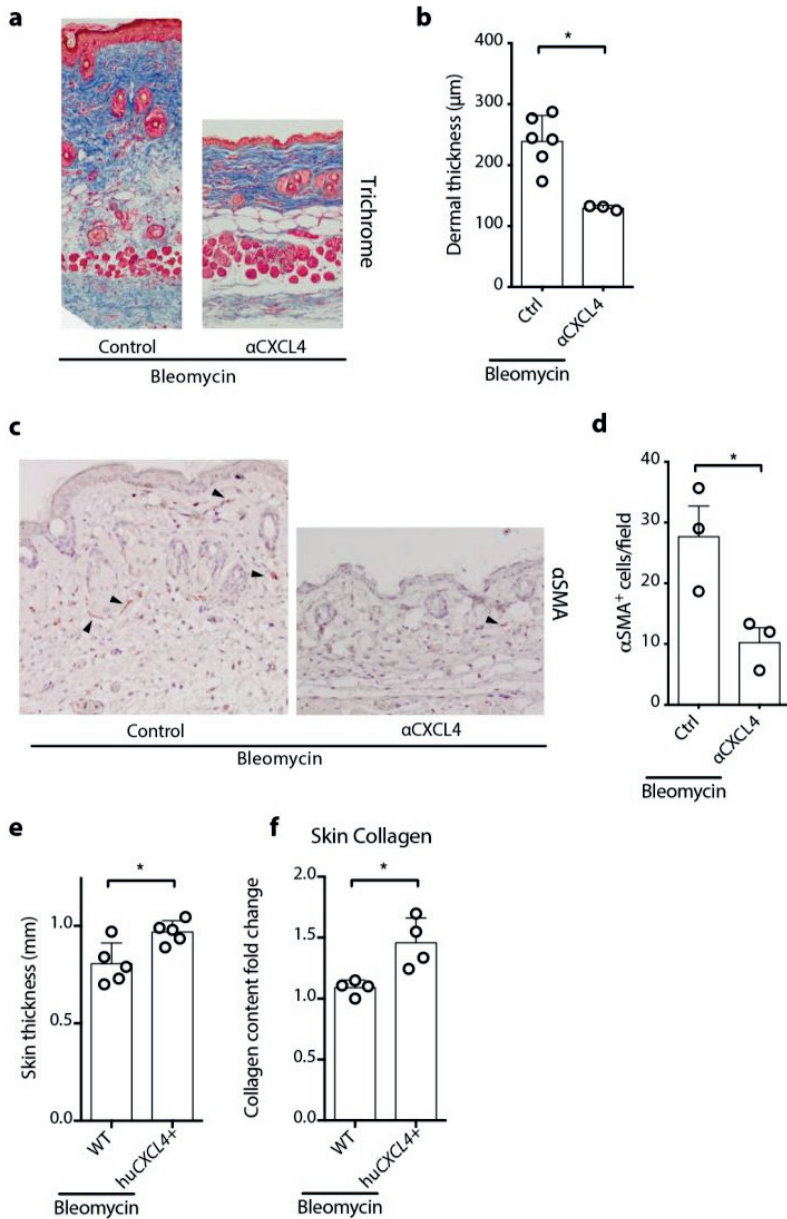


Figure 3. Blocking CXCL4 suppresses and overexpression human CXCL4 promotes bleomycin-induced skin fibrosis. C57BL/6 wild type (WT) or *Cxcl4*^{-/-} overexpressing human *CXCL4* (*huCXCL4*⁺) mice were injected subcutaneously with bleomycin or saline (NaCl) control, or with anti-CXCL4 antibody. **(a)** Representative skin histological analysis after bleomycin only or with additional anti-CXCL4 antibody treatment, stained with Masson's Trichrome (blue for collagen), is displayed. **(b)** Quantification of histologically-measured dermal thickness is shown ($n = 3-6$ per group). **(c)** Representative histological analysis for αSMA^+ cells in the dermis, and **(d)** their quantification, after bleomycin treatment with or without anti-CXCL4 antibody are shown ($n = 3$ per

group). (e,f) WT or huCXCL4⁺ mice were treated with bleomycin and (f) caliper-measured skin thickness was measured and (f) collagen was measured by hydroxyproline assay ($n = 4-5$ per group). Bars represent mean \pm SD. Two-tailed t test was used. * $p < 0.05$, ** $p < 0.01$, *** $p < 0.001$, **** $p < 0.0001$.

CXCL4 stimulates myofibroblast transition of human skin stromal cells

To investigate which cell types are involved in CXCL4-driven fibrotic processes, we assessed CXCL4 role on myofibroblasts-differentiation in a variety of primary human precursor cells. First, we determined whether CXCL4 had an effect on human skin-derived stromal cells, by separating dermis and adipose layer from normal human skin, to isolate dermal fibroblasts and adipose-derived stromal cells (ASCs), respectively (**Fig. 4a**). We cultured these cells with CXCL4 and tested changes in contractile properties of these cells using gel contraction assay. After 7 days of culture, CXCL4 treated ASCs induced higher gel contraction as compared to control medium (**Fig. 4d-f**), but only minimal changes were seen on dermal fibroblasts (**Fig. 4b,c**). This CXCL4-induced contractility was maintained until at least 14 days of culture. This is accompanied by the increased expression of myofibroblast markers α -SMA (*ACTA2*), smooth muscle 22 alpha (*SM22 α /TAGLN*), collagen I (*COL1A1*) upon CXCL4 exposure (**Fig. 4g, supplementary Fig. 3**). These findings reveal that CXCL4 clearly induced myofibroblast-like phenotype in ASCs.

We then determined collagen production cultured normal human dermal fibroblasts in collagen deposition assay. CXCL4 treatment led to an increased amount of deposited collagen by fibroblasts as compared to medium control (**Fig. 6h,i**). Furthermore, the expression of myofibroblast markers α -SMA (*ACTA2*), smooth muscle 22 alpha (*SM22 α /TAGLN*), collagen I and vimentin, was increased by CXCL4 in most donor fibroblasts (**Fig. 6j-l**). However, the effects were modest and CXCL4 seems to only partially promote transition from fibroblast into myofibroblast.

Fig.4

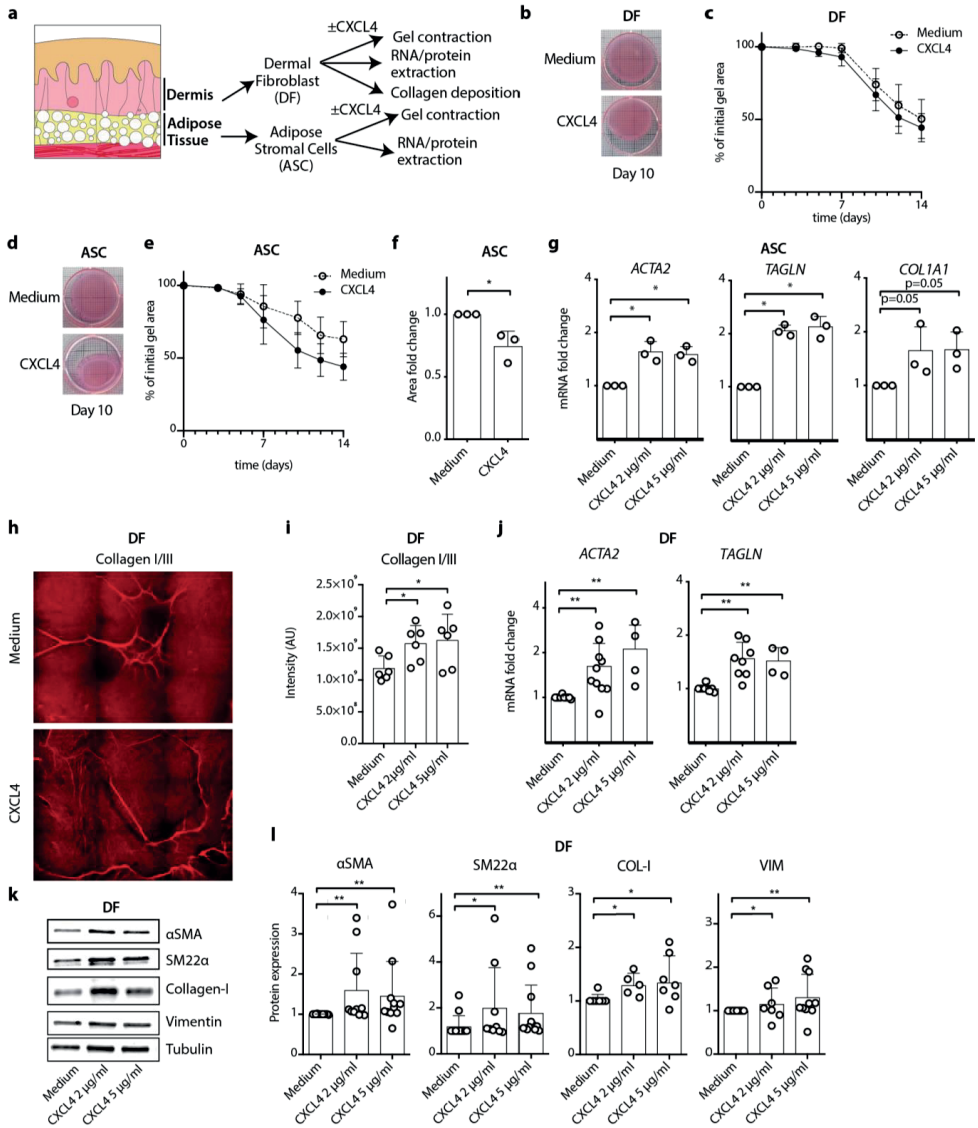


Figure 4. CXCL4 induces myofibroblast phenotype in primary normal human adipose-derived stromal cells (ASCs) and dermal fibroblasts. (a) Human skin was processed and adipose-derived stromal cells (ASCs) and dermal fibroblasts (DF) were isolated for further treatment with CXCL4. (b-e) ASCs or fibroblasts were cultured in collagen gel matrix in the presence or absence of 5 μ g/ml CXCL4 for the indicated time points, and the area of gel was measured for contractility. ($n = 3$ per group). (f) The quantification of contracted area normalized to control for ASCs at day 14 is shown ($n = 3$ per group). (g) ASCs were stimulated with different doses of CXCL4 for 24 h, mRNA was isolated and gene expression was quantified using qPCR ($n = 3$ per group). (h) Fibroblasts were cultured in the presence or absence of 5 μ g/ml CXCL4 for 7 d, then cells were lysed and ECM deposited on culture

vessel was imaged using immunofluorescence. Representative images (h) are shown and collagen I/III amount as measured by intensity (i) was quantified ($n = 6$ per group). (j) Fibroblasts were stimulated with different doses of CXCL4 for 24 h, mRNA was isolated and gene expression was quantified using qPCR ($n = 4-10$ per group). (k,l) Fibroblasts were stimulated with different doses of CXCL4 for 24 h and whole cell lysate was isolated and protein expression was assessed by western blot analysis ($n = 7-12$ per group). Representative images (k) are shown and protein level (l) was quantified. Bars represent mean \pm SD. One-way ANOVA with FDR correction for multiple testing was used. * adj. $p < 0.05$, ** $p < 0.01$, *** $p < 0.001$, **** $p < 0.0001$.

CXCL4 stimulates pericyte-mesenchymal transition and impairs tubular formation in pericytes-endothelial cells co-culture

Pericytes, which function as vessel-associated (mural) support cells, have been implicated to be myofibroblast progenitors in fibrotic process in different organs²⁷. Since we observed increased number of pericytes after bleomycin treatment (**supplementary Fig. 2**), we further assessed the effect of CXCL4 on human primary pericytes. Pericytes treated with CXCL4 displayed an increased RNA and protein expression of the myofibroblast markers α SMA, SM22 α , and collagen I (**Fig. 5a,b**). Similar to endothelial cells, the expression of *FLII* was also downregulated in pericytes in the presence of CXCL4 (**Fig. 5a**). These data indicate that CXCL4 induces pericytes-mesenchymal transition and production of collagen by these cells.

By directly interacting with endothelial cells, pericytes play an important role in blood vessel maintenance in homeostatic condition²⁸. Since EndMT has also been shown to coincide with an increased endothelial cell migration and a loss of capillary formation^{29,30}, we sought to investigate the effect of CXCL4 in angiogenesis using pericyte-endothelial cell co-culture to evaluate endothelial cell tubular formation. Addition of CXCL4 drastically reduced both the number as well as the length of the tubules formed by endothelial cells in a dose-dependent manner (**Fig. 5c,d**). Consistent with previous reports³¹, increased levels of CXCL4 impaired the endothelial capacity to form an appropriate tissue vasculature.

Fig. 5

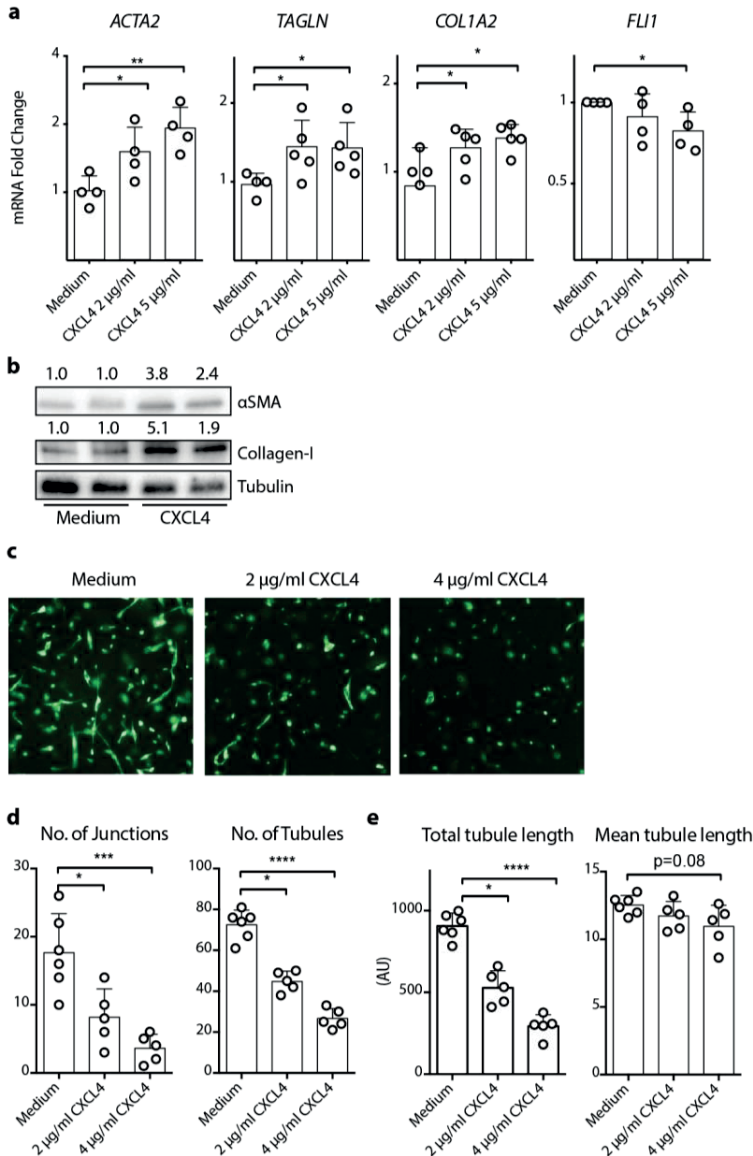


Figure 5. CXCL4 induces myfibroblast differentiation in human pericytes and reduces endothelial cell tubular formation in a 3D co-culture with pericytes. (a-c) Normal human brain pericytes were cultured in the presence or absence of CXCL4 for 24 h and processed for RNA and protein analysis. (a) Total RNA was isolated and gene expression was quantified using qPCR ($n = 4$ per group). (b) Whole cell lysate was isolated and protein expression was assessed by western blot analysis. Values from densitometric analysis normalized to tubulin are shown ($n = 4-5$ per group). (c-e) Human umbilical vein endothelial cells (HUVEC) transduced with green fluorescent protein were co-cultured with human brain pericytes in a collagen matrix. (c) After 48 h stimulation

with CXCL4 or medium alone, images were acquired. Representative images from 1 out of 3 experiments are shown. (d,e) Endothelial cell tubular formation was quantified by assessment of numbers of junctions and tubules, total length of all tubules and mean length of the formed tubules ($n = 5-6$ per group). Bars represent mean \pm SD. One-way ANOVA with FDR correction for multiple testing was used. * adj. $p < 0.05$, ** $p < 0.01$.

CXCL4 induces a myfibroblast phenotype in human endothelial cells via metabolic reprogramming

EndMT is a common process in fibrotic conditions^{2,3,32,33}. CXCL4 was previously shown to inhibit endothelial cell proliferation and expression of FLI1^{8,34}, the main regulator of ECM production and a suppressor of EndMT. Hence, we postulated that CXCL4 could directly promote fibrosis through promoting EndMT. In line with this, we observed significant reduction in the number of lectin⁺ α SMA⁺ cells *Cxcl4*^{-/-} mice when compared to WT mice after bleomycin treatment, indicating decrease of EndMT in *Cxcl4*^{-/-} mice (**Fig. 6a,b**).

To better understand the role of CXCL4 in EndMT, we performed CXCL4 treatment on human pulmonary arterial endothelial cells and analyzed transcriptional changes using qPCR fibrosis array. The expression of myofibroblast marker α -SMA (*ACTA2*), collagens (*COL1A2*, *COL3A1*), and pro-fibrotic/TGF β pathways (*SERPINI1*, *TGFB2*) were increased after CXCL4 treatment (**Fig. 6c**). We further confirmed CXCL4-induced upregulation of myofibroblast markers such as α -SMA, SM22 α , and collagen-I at both RNA (**Fig. 6d**) and protein level (**Fig. 6e,f**) with additional experiments. Additionally, changes in cell morphology were observed when endothelial cells were treated with CXCL4, with many cells acquiring a fibroblast-like spindle shape (**Fig. 6g**). Moreover, addition of CXCL4 also reduced the expression of the collagen negative regulator *FLII* as we saw previously, while increasing expression of *COL4A1* and *SNAIL1*, a key transcription factor in EndMT³⁵ (**Fig. 6d**). There were no significant changes in the expression of the endothelial cell lineage marker *CDH1* upon CXCL4 treatment (data not shown). These data demonstrate that CXCL4 mediates EndMT and the subsequent increase of collagen synthesis. Furthermore, metabolic changes have been shown to occur during EndMT process³⁶. Here we found that endothelial cells treated with CXCL4 had an increased oxygen consumption rate (OCR)

as compared to medium control (**Fig. 6h,i**). Blocking oxidative phosphorylation with oligomycin inhibited expression of myofibroblast markers such as α SMA and collagen I upon CXCL4 treatment (**Fig. 6j**). In contrast, blocking glycolysis with 2-deoxy-D-glucose (2DG) did not suppress the expression of myofibroblast markers. These data indicate that oxidative phosphorylation is required for CXCL4-induced EndMT.

Fig. 6

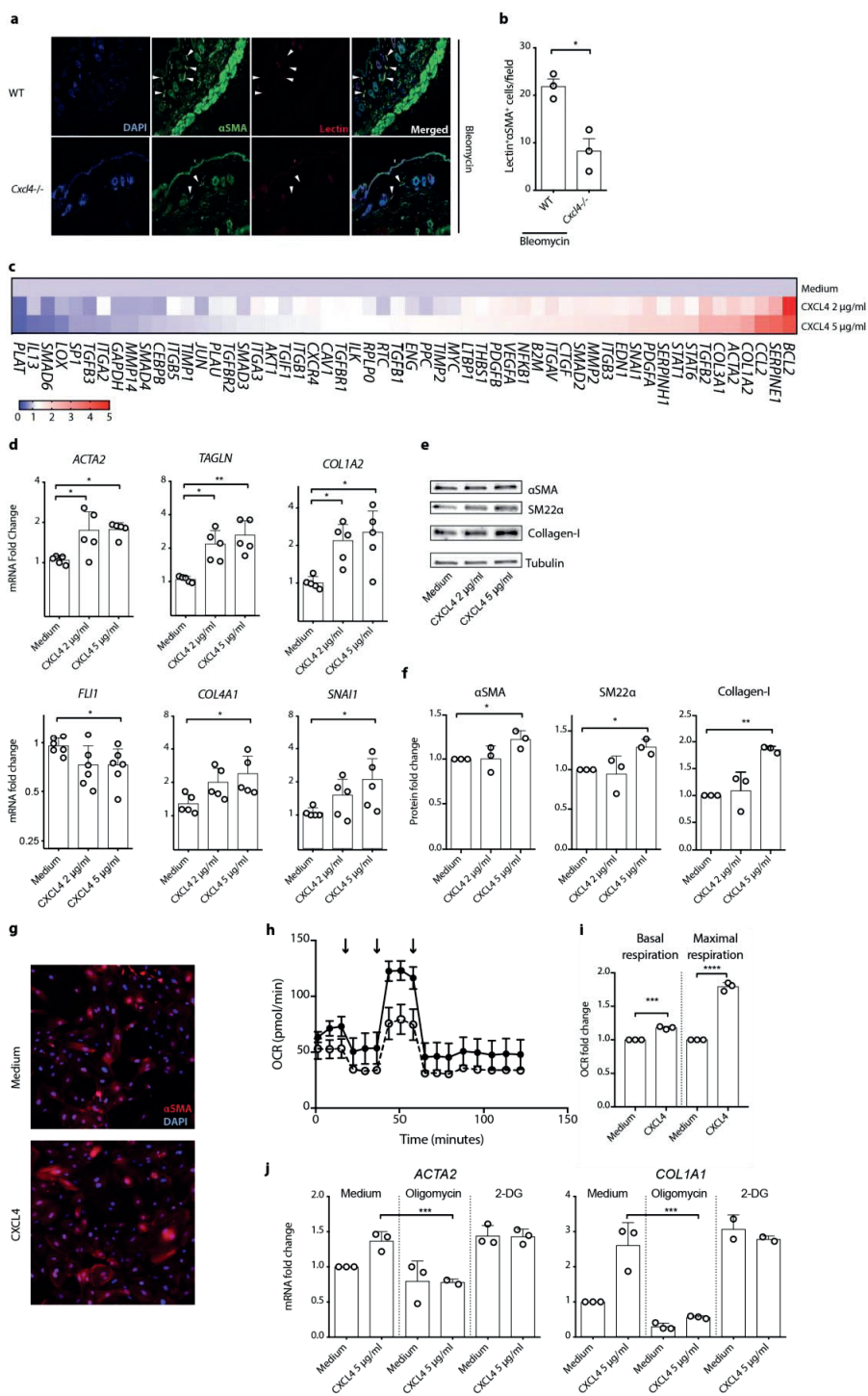


Figure 6. CXCL4 stimulates myofibroblast differentiation in endothelial cells via metabolic changes. (a,b) Skin from C57BL/6 wild type (WT) or *Cxcl4*^{-/-} mice injected with bleomycin were stained for α SMA⁺ myofibroblasts (green), lectin (red), and nuclei staining (DAPI, blue). (a) Representative immunostaining and (b) quantification of lectin⁺ α SMA⁺ cells are shown. (c-f) Normal human pulmonary endothelial cells (HPAEC) were cultured in the presence or absence of CXCL4 for 24 h and processed for RNA, protein, and metabolic analysis. Total RNA was isolated and gene expression was determined using (c) qPCR fibrosis array (n = 3 per group) and further validated by (d) qPCR by including additional experiments (n = 5 per group). (e,f) Whole cell lysate were isolated and protein expression was assessed by western blot analysis. (e) Representative blot and (f) quantification are shown (n = 3 per group). (g) HPAEC were cultured in the presence or absence of CXCL4 for 24 h and fixed and permeabilized prior to staining of α SMA (red) and nuclei (Hoechst, blue). Representative immunofluorescence images from one out of 3 independent experiments are shown. (h,i) After 24 h CXCL4 (open circle) or control (closed circle) treatment, HPAEC were cultured in XF basal medium and OCR was measured in response to oligomycin, FCCP, and rotenone, as indicated by the arrows. (h) Representative OCR measurement (i) quantification of basal and maximal respiration are shown. (j) HPAEC were cultured in the presence or absence of CXCL4, 1 μ M Oligomycin, and 100 mM 2DG, for 24 h, and RNA was isolated and gene expression was quantified using qPCR (n = 2-3 per group). Bars represent mean \pm SD. One-way ANOVA with FDR correction for multiple testing or two-tailed t test was used as appropriate. * (adj.) p < 0.05, ** p < 0.01, *** p < 0.001, **** p < 0.0001.

Discussion

Fibrosis is a process that is initiated by soluble factors produced by immune cells that, when uncontrolled, disrupts the original tissue architecture and leads to organ dysfunction, as observed in many chronic inflammatory diseases such as SSc³⁷. It is thought that TGF β is the principal mediator of fibrosis formation, but earlier attempts targeting TGF β were unsuccessful in fibrotic diseases, and only recently a new pan-TGF β neutralizing antibody has shown some clinical benefits in patients with SSc^{4,38}. More recently, IL-11, TLR signaling, and neutrophil extracellular traps have been identified as novel components in fibrosis³⁹⁻⁴¹. As effective therapies for fibrotic diseases are still lacking¹, the discovery of factors driving fibrogenesis is crucial to the development of new therapeutic modalities. Here we identify CXCL4 as a key component in fibrosis development, and the first proof of concept of targeting CXCL4 in fibrotic diseases.

We observed an increase of CXCL4 in multiple mouse models of inflammation and fibrosis, including in bleomycin- and TLR-induced SSc, Scl-GvHD, and TAC-mediated fibrosis models. The exact mechanism responsible for this pathological increase of CXCL4 is still unknown, although TLR triggering, inflammasome activation, as well as hypoxia may be involved (^{22,42,43}, unpublished observation). More recently, CXCL4 was shown to be increased in a newly developed mouse model of skin and lung fibrosis, using DC loaded with topoisomerase I autoantigen, as well as in bleomycin model^{22,44}. Our knockout study revealed that mice deficient for CXCL4 are protected from bleomycin-induced skin and lung fibrosis. Moreover, transgenic overexpression of human CXCL4 aggravated bleomycin-induced skin fibrosis. As bleomycin treatment is a widely used pre-clinical model in research related to dermal and lung fibrosis^{45,46}, this provides evidence for CXCL4 to be a crucial determinant of fibrosis in these diseases.

In the bleomycin model, the presence of inflammation, in particular early in the disease, is crucial for fibrosis development. We found a major reduction of immune cells in the skin of *Cxcl4*^{-/-} mice as compared to WT mice following bleomycin injections. These

5

data indicate that the presence of CXCL4 is crucial for chemotaxis of immune cells towards the site of injury, and this reveals another layer of possible mechanisms via which CXCL4 leads to fibrosis development. Additionally, CXCL4 is known to have the capacity to promote inflammation by amplifying TLR signaling on immune cells^{8,13,47}. Next to this, we demonstrate that CXCL4 is also required for the development of TAC-induced heart fibrosis. Cardiac involvement is the second leading cause of death behind pulmonary complications in SSc patients⁴⁸. The pathogenic role of CXCL4 has been shown in atherosclerosis and ischemia/reperfusion models^{20,49}, and a recent report suggests that CXCL4 might promote cardiac dilation and mortality in a mouse model of myocardial-infarction⁵⁰. The role of CXCL4 in coronary artery disease remains unclear^{51,52} and CXCL4 contribution to cardiac fibrosis development in humans still needs to be verified. The pro-fibrotic role of CXCL4 has been indicated in animal models of liver fibrosis. Upon treatment with CCL4 or thioacetamide¹⁹, *Cxcl4*^{-/-} mice showed amelioration of liver fibrosis as compared to controls. In a rat model of chronic liver allograft dysfunction, blocking CXCL4 could significantly protect rats from liver fibrosis⁵³. Indeed, in this study we demonstrate that blocking CXCL4 abrogates bleomycin-induced skin fibrosis. Taken together, our data on experimental models of skin, lung, and cardiac fibrosis, further corroborate the notion of CXCL4 as a central mediator of fibrosis *in vivo*.

Myofibroblasts, as identified by the high expression of α SMA and the production of ECM proteins, is a defining feature of tissue fibrosis. Although it was initially thought that resident fibroblasts were the source of myofibroblasts, it is becoming clear that they can be derived from multiple precursors, including endothelial cells and pericytes^{2,3,6,37}. Here we have demonstrated that CXCL4 induced myofibroblast-like properties in endothelial cells, pericytes, adipose-derived stromal cells, and dermal fibroblasts. In the bleomycin model, the majority of α SMA positive myofibroblasts were shown to express pericyte markers⁵⁴. Our *in vivo* data confirmed these findings, showing that pericytes were present in high numbers in fibrotic skin of these mice. On the contrary, in *Cxcl4*^{-/-} mice pericytes presence were significantly reduced, resembling more the control mice. An increased number of

activated PDGF β R⁺ pericytes has also been found in the fibrotic skin of SSc patients⁵⁵. These activated pericytes were positive for myofibroblast markers such as, α SMA, ED-A FN and Thy-1 in SSc skin²⁶. The crucial role of pericytes as a source for myofibroblasts present in the skin is further supported by another study demonstrating that the majority of collagen-producing α SMA⁺ myofibroblasts were generated from a PDGFR β ⁺ NG2⁺ perivascular subpopulation following acute dermal injury⁵⁶. Our data showed that α SMA staining in the bleomycin-treated skin from *Cxcl4*^{-/-} mice to be reduced, and that skin fibroblasts isolated from *Cxcl4*^{-/-} mice following bleomycin injection, expressed lower α SMA, as compared to WT mice. Thus, our data suggests that CXCL4 plays a pivotal role in myofibroblast differentiation, in which pericytes were among the source, leading to fibrosis development *in vivo*. This is in line with our *in vitro* observations, where CXCL4 stimulation of pericytes leads to transdifferentiation into myofibroblast.

Another potential source of myofibroblasts are adipocytes, and this has been described in bleomycin-induced SSc models^{57,58}. In this respect increased dermal CXCL4 could be one of the factors that drives intradermal fat loss at the expense of increased fibrosis, and this needs further evaluation⁵⁹. We observed that adipose-derived stromal cells showed increased myofibroblast markers and acquired contractility when exposed to CXCL4, indicating these cells to also contribute to CXCL4-driven tissue fibrosis. Interestingly, this CXCL4 effect on myofibroblasts differentiation was more pronounced in adipose-derived stromal cells as compared to dermal fibroblast.

Previously, sera-derived from SSc patients has been shown to induce EndMT in dermal microvascular endothelial cells⁶⁰. On account of the high amount of CXCL4 in the circulation of these patients⁶¹⁻⁶⁴, it is likely that CXCL4 might be a driving force in myofibroblast transformation from cells in the vasculature. We observed a lower number of lectin⁺ α SMA⁺ endothelial-derived myofibroblasts in *Cxcl4*^{-/-} mice upon bleomycin treatment, indicating CXCL4 role in inducing EndMT *in vivo*. Indeed, our *in vitro* experiments with endothelial cells confirmed that CXCL4 stimulation directly

initiated myofibroblast differentiation and induced collagen synthesis. This transition depends upon a metabolic shift to oxidative phosphorylation induced by CXCL4, confirming previous findings that increased oxygen consumption rate is required for myofibroblast differentiation^{65,66}. Furthermore, CXCL4 is known for its angiogenic property on endothelial cells⁶⁷. Using a 3D co-culture of pericytes and endothelial cells, a system closer to physiological conditions, we confirmed that CXCL4 inhibited endothelial tubular formation. Therefore, CXCL4 increase could directly promote EndMT and suppress vasculogenesis, both prominent features of SSc⁶⁸.

To summarize, we present evidence of CXCL4 as a novel fibrogenic molecule that directly promotes myofibroblast transformation in a variety of precursor cells essential for fibrosis development across multiple organs *in vivo* (**Fig. 7**). Furthermore, CXCL4 also plays an important role in mediating innate and adaptive immune responses^{13,14,69,70}, inducing vascular changes^{71,72}, and it is required in other inflammatory models *in vivo*^{20,21,49,73}. As a key upstream molecule linking multiple processes, CXCL4 is a promising target for intervention in SSc and many other inflammatory and fibrotic disorders.

Fig. 7

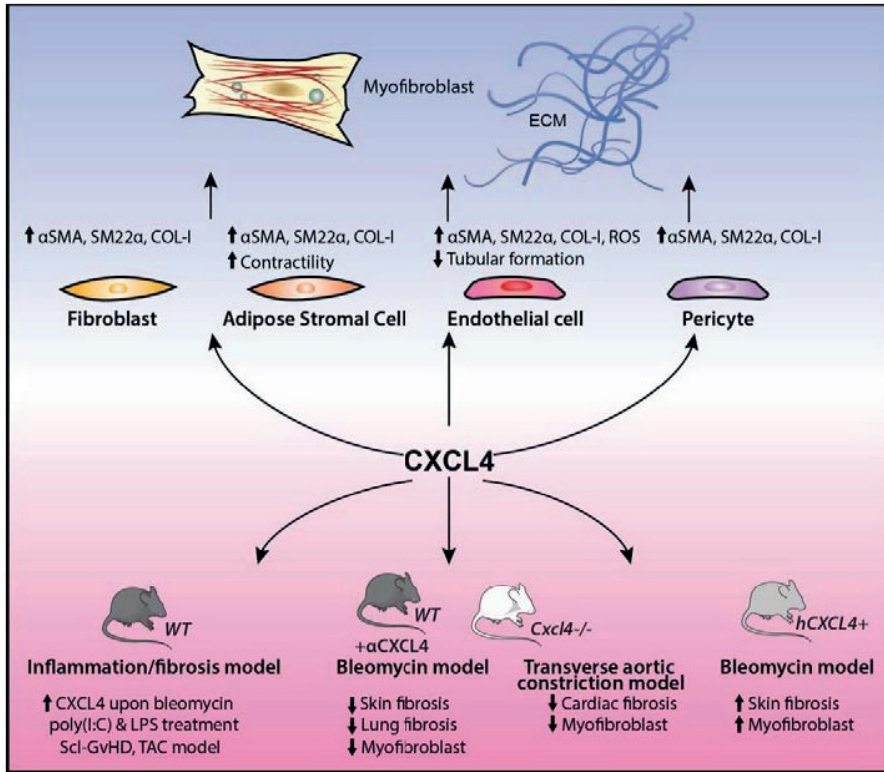


Figure 7. CXCL4 as a key pro-fibrogenic molecule. Using genetic approach (knockout, overexpression) and blocking antibody, we show the essential role of CXCL4 in fibrosis development in the skin, lung, and heart using two independent fibrosis models, and the therapeutic potential of targeting CXCL4 against fibrosis. Our study also demonstrates that CXCL4 directly induces myofibroblast differentiation from different precursors cells including stromal cells and endothelial cells.

5

Methods

Cell culture

Normal human dermal fibroblasts were isolated as described before⁷⁴ and cultured in DMEM medium (Thermo Fisher Scientific) supplemented with 10% fetal bovine serum (FBS, Biowest) and 1% penicillin-streptomycin (pen/strep). For adipose stromal cells, fat was removed from the dermis and epidermis and cut into small pieces. The epidermis was removed from the dermis after dispase incubation. Both dermis and adipose tissue were incubated in collagenase type II (Gibco, Invitrogen, Paisly, UK)/dispase II (Roche, Mannheim, Germany) solution for 2h at 37°C, passed through a 40 µm cell strainer, and cultured⁷⁵. Human pulmonary arterial endothelial cells (HPAEC) and human umbilical vein endothelial cells (HUVEC, both from Thermo Fisher Scientific) were cultured in EBM-2 media supplemented with EGM-2 bullet kit (both Lonza) and 10% FBS, in 0.2% bovine skin gelatin-coated (Sigma Aldrich) culture vessels. Human brain pericytes (Sciencell) were cultured in DMEM medium supplemented with 10% FBS, 1% pen/strep in 0.1% gelatin-coated (Costar) culture plates. Cells were cultured at 37°C in humidified atmosphere containing 5% CO₂. Fibroblasts, endothelial cells and pericytes were prestarved prior to stimulation with recombinant human CXCL4 (Peprotech) in basal media with low serum for 24 - 48 h.

RNA isolation and quantitative PCR

Total RNA was isolated from cell lysates using the RNeasy MiniPrep Kit (Qiagen), followed by retrotranscription with iScript reverse transcriptase kit (Biorad), or superscript IV (Life Technologies) according to the manufacturer's instructions. Expression of protein-coding genes was analysed by real-time quantitative-PCR (qPCR) using SybrSelect mastermix with 300-500 nM primer pairs, or Taqman reactions on a StepOne Plus or QuantStudio 12k flex (Thermo Fisher Scientific). qPCR data were normalized to the expression of *GUSB* (human) or *Rpl13* and *B2m* (mouse) housekeeping genes. The mouse fibrosis PCR array (Qiagen) was used according to manufacturer's instructions and normalized to *Gapdh*

and *Hsp90* using QuantStudio software. Heatmap was generated using ClustVis software (<http://biit.cs.ut.ee/clustvis/>) clustered using correlation distance with complete linkage.

Western blotting

Cells were lysed in RIPA buffer (Sigma Aldrich) with Complete Protease inhibitor (Roche). Protein content was determined by BCA assay (Pierce) and samples were denatured in Laemmli buffer (Bio-Rad) at 95°C for 10 min. 5-10 µg of protein was loaded to Mini-PROTEAN TGX 4-20% gels (Bio-Rad), separated by electrophoresis, and blotted with a nitrocellulose Trans-blot Turbo transfer pack, according to manufacturer's instructions (all from Bio-Rad). After blocking for 1 h in 5% (m/v) milk, blots were incubated with primary antibody at 4°C overnight, followed with secondary antibody for 1 h at room temperature (RT), and washed in Tris-buffered saline with 0.2% Tween-20 in between steps. Protein bands were developed using ECL (GE Healthcare) and measured on Molecular Imager GelDoc (Bio-Rad) or were detected using infrared fluorescence detection on Odyssey imager (Li-Cor).

Extracellular matrix deposition assay

1,500 human dermal fibroblasts were seeded and cultured on 384-well black imaging plate (Greiner) in Fibroblast Basal Medium supplemented with Fibroblast Growth Kit, Low serum (2% (v/v) FBS, ATCC) at 37°C for one week with medium replenishment every two days. Presto Blue was used to monitor cell viability (Thermo Fisher Scientific). Recombinant human CXCL4 was added as indicated. After decellularization, matrices were fixed with 100% ice-cold methanol at -20°C for 30 min, blocked with 1% (v/v) normal goat serum in phosphate-buffered saline (PBS) for 30 min at RT, incubated with primary antibody in PBS for 1.5 h at RT, followed by secondary antibody in PBS for 1 h at RT, with PBS washes in between steps. Matrices were imaged at the Pathway 855 bio-imaging system (BD Biosciences) using the AttoVision software, and quantified with ImageJ software.

Collagen gel contraction assay

Collagen I was isolated from rat tails and reconstituted in 0.1% acetic acid (4 mg/ml). Fibroblasts and ASCs were seeded in 4 mg/ml collagen I solution at 2×10^5 cells/ml and 1 ml gel/well was poured into 12 wells plates. Gels were allowed to polymerize for 2 hours at 37°C. Gels were detached from the well surface to allow contraction and normal culture medium was added to the wells. Medium (including CXCL4) was replaced 3 times per week. Pictures were taken using a Canon Powershot G12 camera and gel surface was measured using ImageJ software.

Endothelial tubule formation assay

Collagen-based 3D co-cultures were performed as described previously⁷⁶. Lenti-GFP-transduced human umbilical vein endothelial cells (HUVECs) and lenti-dsRED-transduced human brain vascular pericytes were suspended in endothelial basal medium (Lonza) at a respective 5:1 ratio in collagen type I (2.0 mg/ml). Using NaOH, pH was set to 7.5, after which the cells were seeded in flat-bottomed 96 well plates followed by 1 h incubation at 37°C to enable collagen solidification. Next, 100 μ l medium was added after which the co-cultures were incubated at 37°C for another 24 h. Subsequently, medium containing CXCL4 was added to final concentrations of 0, 2 and 4 μ g/ml CXCL4. After 72 h of culture, fluorescently labeled co-cultures were imaged and analyzed using Angiosys software.

Metabolic Assays

OCRs were measured in HPAEC activated for 24 h using XF media (non-buffered RPMI 1640 containing 10 mM glucose, 2 mM L-glutamine, and 1 mM sodium pyruvate) under basal conditions and in response to 1 μ M oligomycin, 5 μ M FCCP, and 1 μ M rotenone on XF-96 Extracellular Flux Analyzers (Seahorse Bioscience). Maximal respiration was the OCR difference between uncoupler FCCP and rotenone.

Animal Experiments

Animal experiments were approved by the Committee on Animal Experiments of the University of Utrecht and experiments were performed at the Central Animal Laboratory, Utrecht University, The Netherlands, unless stated otherwise. *Cxcl4*^{-/-} and *huCXCL4*⁺ mice were generated in the laboratory of Dr. Mortimer Poncz⁷⁷.

Bleomycin-induced skin and lung fibrosis

Bleomycin-induced SSc was developed using daily subcutaneous injections of bleomycin (200 μ l, 500 μ g/ml, Bleomedac, Medac) into the back of adult female mice (either WT, *Cxcl4*^{-/-} or *huCXCL4*⁺ on C57BL/6 background) for the duration of two to four weeks ($n = 12$ per group or $n = 6$ per group per each time point). When indicated, mice were treated 10 days with 200 μ g of rabbit anti-murine CXCL4 (Bethyl Laboratories, Montgomery, TX, USA) delivered subcutaneously every other day. Two days after the last treatment, mice were treated with 200 μ l, 0.15 mg/kg, of buprenorphine (Temgesic), anesthetized with 5% isoflurane for blood collection, and sacrificed by cervical dislocation. Serum was collected after centrifugation at 1700 \times g for 10 min. Skin biopsies were obtained from the back region using biopsy punch (4 mm diameter). Tissues were stored in medium for cell culture, homogenized in RLT buffer for RNA isolation, frozen in RIPA buffer for immunoblotting, or snap frozen for collagen quantification. For histology, cannula was inserted into trachea and fixed with ligature, and lungs were instilled with 4% formalin. Skin biopsies were placed in between two foam pads in a histology cassette and fixed with 4% formalin. Following formalin fixation, tissues were embedded in paraffin and cut into 5 μ m sections for further analysis. Dermal fibroblasts were extracted from minced skin biopsies after digestion with 2.5 mg/ml collagenase from *Clostridium histolyticum* (Sigma Aldrich) at 37° C for 2 h with agitation. Debris were removed by 70 μ m cell strainer and cells were washed in medium. Cells were cultured in DMEM/F-12 supplemented with 10% FBS at 37°C until near confluency.

In vivo administration of TLR ligands

Mini osmotic pumps (Alzet), were implanted to adult mice (C57BL/6) ($n = 3-4$) under

anesthesia as described previously²⁴. Osmotic pumps were designed to deliver 1 μ l of PBS or stimuli per h over 7 days in a total of 200 μ l volume. 500 μ g/ml of poly(I:C) or lipopolysaccharide (LPS-EB ultrapure, both Invivogen) were used. After 7 days, mice were sacrificed and the skin (\sim 1 cm²) surrounding or distal to the pump outlet was homogenized in TRIzol (Invitrogen) for total RNA preparation.

Experimental procedure for induction of GvHD in BALB/c mice

Scl-GvHD was induced following splenocyte and bone marrow transplantation from male B10.D2 (H-2d; Jackson Laboratory) to female BALB/c mice (Janvier Laboratory) as described previously⁷⁸. Briefly, recipient mice were lethally irradiated with 750cGy from a Gammacel [¹³⁷Cs] source. After 3 h, they were injected intravenously with donor spleen cells (2×10^6 per mouse) and bone marrow cells (1×10^6 per mouse) that were previously removed of red blood cells using ammonium chloride solution and suspended in RPMI-1640 (Gibco). The control group received syngeneic BALB/c spleen and bone marrow cells. We used 9 mice per group. Mice were sacrificed by cervical dislocation after four weeks and blood was collected for serum preparation.

Transverse aortic constriction

WT ($n = 8$) or *Cxcl4*^{-/-} ($n = 8$) mice on a C57BL/6 background were subjected to transverse aortic constriction (TAC) or sham surgery as previously described⁷⁹. Briefly, mice were anaesthetized, intubated, and connected to a respirator with a 1:1 oxygen-air ratio. A core body temperature of 37° C was maintained during surgery by an experienced surgeon. Using a minimally invading approach, the aortic arch was reached between two ribs after midline incision in the anterior neck. Transverse aortic constriction was placed between the brachiocephalic artery and the left common artery against a blunt 27-gauge needle with a 7–0 silk suture followed by prompt removal of the needle. Sham operated mice underwent the same procedure without aortic constriction. After the indicated time points, mice were euthanized using sodium pentobarbital, blood was collected for serum measurement of cytokines, hearts were perfused with saline and fixed in formalin for histological analysis,

or snap frozen for RNA isolation.

Immunofluorescence of mouse fibroblasts ex vivo

Mouse fibroblasts were seeded at equal number on clear bottom 96-wells black imaging plate (Ibidi) and rested overnight. Cells were fixed with 50 μ l 4% paraformaldehyde, and blocked and permeabilized with 5% (v/v) normal donkey serum, 5% (v/v) normal goat serum, 0.3% (v/v) Triton X-100, in PBS for 1 h at RT. Cells were incubated with anti- α SMA (Sigma Aldrich) in antibody diluent (PBS with 10% (v/v) bovine serum albumin (BSA) and 0.3% (v/v) Triton X-100) for overnight at 4°C, followed by incubation with secondary antibody in antibody diluent for 1 h at RT, with PBS washes in between steps. Cell nuclei were visualized by Hoechst staining. Fibroblasts were imaged at the Pathway 855 bioimaging system (BD Biosciences) using AttoVision software, and quantified with ImageJ software.

Tissue Immunohistochemistry and Immunofluorescence

Formalin-fixed, paraffin-embedded skin and heart sections or 4% PFA-fixed, 0.25% Triton X 100-permeabilized cells were stained with appropriate primary antibodies, including rabbit anti- α SMA 1 h (Abcam), goat anti-collagen I 1 h, (Southern biotech), mouse anti-PDGFR- β overnight incubation (Santa Cruz), rabbit anti-SMAD2/3 overnight incubation (Abcam), and rabbit anti-CD31 overnight incubation, (Abcam). Counter staining of cell nuclei was performed using DAPI (Santa Cruz Biotechnology). Both tissue sections and cultured cells and were incubated with isotype control antibodies (Santa Cruz Biotechnology). Stained sections and cells were visualized using a bright field or fluorescence microscope (BH2 and BX41 Olympus). For quantification, integrated density was analyzed using ImageJ Software.

Measurement of secreted proteins

The level of CXCL4 in mouse sera was measured by enzyme-linked immunosorbent assay (R&D). Levels of soluble KC, E-selectin, and L-selectin, were measured by multiplex

immunoassay (Millipore) based on xMAP technology (Luminex) at the MultiPlex Core Facility of the Center for Translational Immunology, University Medical Center Utrecht⁸⁰. For the Luminex-based assay, acquisition was performed with a Bio-Rad FlexMap3D system using Xponent 4.2 software and analyzed using Bio-Plex Manager 6.1.1.

Histochemical Analysis

Consecutive 5- μ m skin, lung, and heart sections of paraffin-embedded tissue were stained with Mason's trichrome, to evaluate collagen content and organization. Dermal thickness was determined at five different locations per slide for each mouse by two blinded, experienced researchers using ImageJ.

Quantification of Tissue Collagen

Collagen content was quantified by colorimetric assays from 4 mm skin punch biopsies. Skin sections were transferred into a microcentrifuge tube and upon addition of 150 μ l 6M HCl hydrolyzed by overnight incubation at 95°C in a heat block, and collagen content was determined in supernatants by QuickZyme total collagen assay (QuickZyme Bioscience).

Statistical analysis

Mann Whitney's test or one-way ANOVA corrected for multiple comparison by controlling false discovery rate (FDR) were calculated using GraphPad Prism Software as appropriate. Differences of (adjusted) p value < 0.05 were considered significantly different.

Acknowledgements

Alsya J. Affandi was supported by the Dutch Arthritis Association (Reumafonds grant NR-10-1- 301) and the Netherlands Organization for Scientific Research (Mosaic grant 017.008.014). Tiago Carvalheiro was supported by a grant from the Portuguese national funding agency for science, research and technology: Fundação para a Ciência e a Tecnologia [SFRH/BD/93526/2013]. Wioleta Marut obtained funding from Marie Curie Intra-European Fellowship (Proposal number: 624871) and from the NWO VENI grant number 91919149. Timothy R.D.J. Radstake and Joel A.G. van Roon received funding from ERC Starting Grant (ERC-2011-StG, Circumvent). We thank Mike DiMarzio, Giuseppina Stifano, Giuseppina A. Farina (Boston University School of Medicine), Aniek Meijers, Karin de Cortie, Wouter van Leeuwen, Dirk-Jan Heijnen, Enric Mocholi-Gimeno, and Christian van Dijk (University Medical Center Utrecht) for their technical advice, support, and expertise. We also thank Kris A. Reedquist for critical review of the manuscript.

Author Contributions

A.J.A., T.C., T.R.D.J.R., W.M. conceived the experiments, drafted and revised the manuscript. A.J.A., T.C., C.C., M.A.K., S.Gibbs., S.C.A.dJ., J.A.G.vR., T.R.D.J.R., W.M., designed the experiments. A.O., J.J.dH., M.A.D.B., M.M.B., R.G.T., B.M.F., C.P.J.B., M.vdL., B.G., C.G.K.W., S.Garcia., M.W., Y.J.X. carried out the experiments. C.P.J.B., M.A.K., J.A.G.vR., S.Garcia., M.W., revised the manuscript. J.A.G.vR., T.R.D.J.R., W.M. supervised the study. All authors have made substantial, direct, and intellectual contribution to the work and approved the final version of the manuscript. All authors have agreed both to be personally accountable for the author's own contributions and to ensure that questions related to the accuracy or integrity of any part of the work, even ones in which the author was not personally involved, are appropriately investigated, resolved, and the resolution documented in the literature.

Correspondence

Correspondence to Dr. Wioleta Marut at W.K.Marut@umcutrecht.nl.

Competing interests

The authors reported no conflict of interests for the work described here.

References

1. Rockey, D. C., Bell, P. D. & Hill, J. A. Fibrosis — A Common Pathway to Organ Injury and Failure. *N. Engl. J. Med.* **372**, 1138–1149 (2015).
2. Hinz, B. *et al.* The Myofibroblast. *Am. J. Pathol.* **170**, 1807–1816 (2007).
3. Mack, M. & Yanagita, M. Origin of myofibroblasts and cellular events triggering fibrosis. *Kidney Int.* **87**, 297–307 (2015).
4. Lafyatis, R. Transforming growth factor β -at the centre of systemic sclerosis. *Nat. Rev. Rheumatol.* (2014). doi:10.1038/nrrheum.2014.137
5. Kendall, R. T. & Feghali-Bostwick, C. a. Fibroblasts in fibrosis: novel roles and mediators. *Front. Pharmacol.* **5**, 123 (2014).
6. Ho, Y. Y., Lagares, D., Tager, A. M. & Kapoor, M. Fibrosis - A lethal component of systemic sclerosis. *Nat. Rev. Rheumatol.* **10**, 390–402 (2014).
7. Varga, J. & Abraham, D. Systemic sclerosis: a prototypic multisystem fibrotic disorder. *J. Clin. Invest.* **117**, 557–67 (2007).
8. van Bon, L. *et al.* Proteome-wide analysis and CXCL4 as a biomarker in systemic sclerosis. *N. Engl. J. Med.* **370**, 433–43 (2014).
9. Duan, H. *et al.* Combined analysis of monocyte and lymphocyte messenger RNA expression with serum protein profiles in patients with scleroderma. *Arthritis Rheum.* **58**, 1465–1474 (2008).
10. Van Raemdonck, K., Van den Steen, P. E., Liekens, S., Van Damme, J. & Struyf, S. CXCR3 ligands in disease and therapy. *Cytokine Growth Factor Rev.* **26**, 311–327 (2015).
11. Scheuerer, B. *et al.* The CXC-chemokine platelet factor 4 promotes monocyte survival and induces monocyte differentiation into macrophages. *Blood* **95**, 1158–66 (2000).
12. Kasper, B. *et al.* CXCL4-induced monocyte survival, cytokine expression, and oxygen radical formation is regulated by sphingosine kinase 1. *Eur. J. Immunol.* **40**, 1162–73 (2010).
13. Silva-Cardoso, S. C. *et al.* CXCL4 Exposure Potentiates TLR-Driven Polarization of Human Monocyte-Derived Dendritic Cells and Increases Stimulation of T Cells. *J. Immunol.* **199**, 253–262 (2017).
14. Affandi, A. J. *et al.* CXCL4 is a novel inducer of human Th17 cells and correlates with IL- 17 and IL-22 in psoriatic arthritis. *Eur. J. Immunol.* **48**, 522–531 (2018).
15. Tamagawa-Mineoka, R., Katoh, N., Ueda, E., Masuda, K. & Kishimoto, S. Elevated platelet activation in patients with atopic dermatitis and psoriasis: increased plasma levels of beta-thromboglobulin and platelet factor 4. *Allergol. Int.* **57**, 391–6 (2008).
16. Yeo, L. *et al.* Expression of chemokines CXCL4 and CXCL7 by synovial macrophages defines an early stage of rheumatoid arthritis. *Ann. Rheum. Dis.* **75**, 763–71 (2016).
17. Schwarz, K. B. *et al.* Plasma markers of platelet activation in cystic fibrosis liver and lung disease. *J. Pediatr. Gastroenterol. Nutr.* **37**, 187–91 (2003).
18. Burstein, S. A. *et al.* Platelet factor-4 excretion in myeloproliferative disease: implications for the aetiology of myelofibrosis. *Br. J. Haematol.* **57**, 383–92 (1984).
19. Zaldivar, M. M. *et al.* CXC chemokine ligand 4 (Cxcl4) is a platelet-derived mediator of experimental liver fibrosis. *Hepatology* **51**, 1345–53 (2010).
20. Koenen, R. R. *et al.* Disrupting functional interactions between platelet chemokines inhibits atherosclerosis in hyperlipidemic mice. *Nat. Med.* **15**, 97–103 (2009).
21. Grommes, J. *et al.* Disruption of platelet-derived chemokine heteromers prevents neutrophil extravasation in acute lung injury. *Am. J. Respir. Crit. Care Med.* **185**, 628–36 (2012).
22. Ah Kioon, M. D. *et al.* Plasmacytoid dendritic cells promote systemic sclerosis with a key role for TLR8. *Sci. Transl. Med.* **10**, 1–14 (2018).
23. Farina, G. A. *et al.* Poly(I:C) drives type I IFN- and TGF β -mediated inflammation and dermal fibrosis simulating altered gene expression in systemic sclerosis. *J. Invest. Dermatol.* **130**, 2583–93 (2010).
24. Stifano, G. *et al.* Chronic Toll-like receptor 4 stimulation in skin induces inflammation, macrophage activation, transforming growth factor beta signature gene expression, and fibrosis. *Arthritis Res. Ther.* **16**, R136 (2014).
25. Liang, M. *et al.* A modified murine model of systemic sclerosis: Bleomycin given by pump infusion induced skin and pulmonary inflammation and fibrosis. *Lab. Investig.* **95**,

- 342–350 (2015).
26. Rajkumar, V. S. *et al.* Shared expression of phenotypic markers in systemic sclerosis indicates a convergence of pericytes and fibroblasts to a myofibroblast lineage in fibrosis. *Arthritis Res. Ther.* **7**, R1113-23 (2005).
 27. Sundberg, C., Ivarsson, M., Gerdin, B. & Rubin, K. Pericytes as collagen-producing cells in excessive dermal scarring. *Lab. Invest.* **74**, 452–66 (1996).
 28. Ferland-McCollough, D., Slater, S., Richard, J., Reni, C. & Mangialardi, G. Pericytes, an overlooked player in vascular pathobiology. *Pharmacol. Ther.* **171**, 30–42 (2017).
 29. Lee, S.-W. *et al.* Snail as a potential target molecule in cardiac fibrosis: paracrine action of endothelial cells on fibroblasts through snail and CTGF axis. *Mol. Ther.* **21**, 1767–77 (2013).
 30. Zhang, W., Chen, G., Ren, J.-G. & Zhao, Y.-F. Bleomycin induces endothelial mesenchymal transition through activation of mTOR pathway: a possible mechanism contributing to the sclerotherapy of venous malformations. *Br. J. Pharmacol.* **170**, 1210–1220 (2013).
 31. Vandercappellen, J., Van Damme, J. & Struyf, S. The role of the CXC chemokines platelet factor-4 (CXCL4/PF-4) and its variant (CXCL4L1/PF-4var) in inflammation, angiogenesis and cancer. *Cytokine Growth Factor Rev.* **4**, 1–18 (2010).
 32. Kovacic, J. C., Mercader, N., Torres, M., Boehm, M. & Fuster, V. Epithelial-to-mesenchymal and endothelial to-mesenchymal transition: from cardiovascular development to disease. *Circulation* **125**, 1795–808 (2012).
 33. Piera-Velazquez, S. & Jimenez, S. A. Molecular mechanisms of endothelial to mesenchymal cell transition (EndoMT) in experimentally induced fibrotic diseases. *Fibrogenesis Tissue Repair* **5**, S7 (2012).
 34. Dubrac, A. *et al.* Functional divergence between 2 chemokines is conferred by single amino acid change. *Blood* **116**, 4703–11 (2010).
 35. Kokudo, T. *et al.* Snail is required for TGF- β -induced endothelial-mesenchymal transition of embryonic stem cell-derived endothelial cells. *J. Cell Sci.* **121**, 3317–3324 (2008).
 36. Xiong, J. *et al.* A Metabolic Basis for Endothelial-to-Mesenchymal Transition. *Mol. Cell* **69**, 689-698.e7 (2018).
 37. Hinz, B. *et al.* Recent developments in myofibroblast biology: Paradigms for connective tissue remodeling. *Am. J. Pathol.* **180**, 1340–1355 (2012).
 38. Rice, L. M. *et al.* Fresolimumab treatment decreases biomarkers and improves clinical symptoms in systemic sclerosis patients. *J. Clin. Invest.* **125**, 2795–807 (2015).
 39. Bhattacharyya, S. & Varga, J. Endogenous ligands of TLR4 promote unresolving tissue fibrosis: Implications for systemic sclerosis and its targeted therapy. *Immunol. Lett.* (2017). doi:10.1016/j.imlet.2017.09.011
 40. Martinod, K. *et al.* Peptidylarginine deiminase 4 promotes age-related organ fibrosis. *J. Exp. Med.* **214**, 439–458 (2017).
 41. Schafer, S. *et al.* IL11 is a crucial determinant of cardiovascular fibrosis. *Nature* **1–30** (2017). doi:10.1038/nature24676
 42. Schaffner, A., Rhyn, P., Schoedon, G. & Schaefer, D. J. Regulated expression of platelet factor 4 in human monocytes—role of PARs as a quantitatively important monocyte activation pathway. *J. Leukoc. Biol.* **78**, 202–9 (2005).
 43. Vandercappellen, J. *et al.* Stimulation of angiostatic platelet factor-4 variant (CXCL4L1/PF-4var) versus inhibition of angiogenic granulocyte chemotactic protein-2 (CXCL6/GCP-2) in normal and tumoral mesenchymal cells. *J. Leukoc. Biol.* **82**, 1519–30 (2007).
 44. Mehta, H. *et al.* Topoisomerase I peptide-loaded dendritic cells induce autoantibody response as well as skin and lung fibrosis. *Autoimmunity* **49**, 503–513 (2016).
 45. Williamson, J. D., Sadofsky, L. R. & Hart, S. P. The pathogenesis of bleomycin-induced lung injury in animals and its applicability to human idiopathic pulmonary fibrosis. *Exp. Lung Res.* **41**, 57–73 (2015).
 46. Beyer, C., Schett, G., Distler, O. & Distler, J. H. W. Animal models of systemic sclerosis: prospects and limitations. *Arthritis Rheum.* **62**, 2831–44 (2010).
 47. Lande, R. *et al.* CXCL4 assembles DNA into liquid crystalline complexes to amplify TLR9-mediated interferon- α production in systemic sclerosis. *Nat. Commun.* **10**, 1731 (2019).
 48. Tyndall, A. J. *et al.* Causes and risk factors for death in systemic sclerosis: A study from the EULAR Scleroderma Trials and Research

- (EUSTAR) database. *Ann. Rheum. Dis.* **69**, 1809–1815 (2010).
49. Lapchak, P. H. *et al.* The role of platelet factor 4 in local and remote tissue damage in a mouse model of mesenteric ischemia/reperfusion injury. *PLoS One* **7**, e39934 (2012).
 50. Lindsey, M. L. *et al.* CXCL4 Aggravates Cardiac Dilation and Mortality after Myocardial Infarction by Inducing Pro-inflammatory M1 Macrophages and Inhibiting Macrophage Phagocytosis [Abstract]. *FASEB J.* **31**, (2017).
 51. Levine, S. P., Lindenfeld, J., Ellis, J. B., Raymond, N. M. & Krentz, L. S. Increased plasma concentrations of platelet factor 4 in coronary artery disease: a measure of in vivo platelet activation and secretion. *Circulation* **64**, 626–32 (1981).
 52. Erbel, C. *et al.* CXCL4 Plasma Levels Are Not Associated with the Extent of Coronary Artery Disease or with Coronary Plaque Morphology. *PLoS One* **10**, e0141693 (2015).
 53. Li, J. *et al.* CXCL4 Contributes to the Pathogenesis of Chronic Liver Allograft Dysfunction. *J. Immunol. Res.* **2016**, 9276986 (2016).
 54. Liu, S., Taghavi, R. & Leask, A. Connective tissue growth factor is induced in bleomycin-induced skin scleroderma. *J. Cell Commun. Signal.* **4**, 25–30 (2010).
 55. Rajkumar, V. S., Sundberg, C., Abraham, D. J., Rubin, K. & Black, C. M. Activation of microvascular pericytes in autoimmune Raynaud's phenomenon and systemic sclerosis. *Arthritis Rheum.* **42**, 930–941 (1999).
 56. Dulauroy, S., Di Carlo, S. E., Langa, F., Eberl, G. & Peduto, L. Lineage tracing and genetic ablation of ADAM12(+) perivascular cells identify a major source of profibrotic cells during acute tissue injury. *Nat. Med.* **18**, 1262–70 (2012).
 57. Marangoni, R. G. *et al.* Myofibroblasts in murine cutaneous fibrosis originate from adiponectin-positive intradermal progenitors. *Arthritis Rheumatol.* **67**, 1062–1073 (2015).
 58. Martins, V. *et al.* FIZZ1-Induced Myofibroblast Transdifferentiation from Adipocytes and Its Potential Role in Dermal Fibrosis and Lipotrophy. *Am. J. Pathol.* **185**, 2768–2776 (2015).
 59. Onuora, S. Connective tissue diseases: Adipocyte-myofibroblast transition: linking intradermal fat loss to skin fibrosis in SSc. *Nat. Rev. Rheumatol.* **11**, 63 (2015).
 60. Manetti, M. *et al.* Endothelial-to-mesenchymal transition contributes to endothelial dysfunction and dermal fibrosis in systemic sclerosis. *Ann. Rheum. Dis.* **76**, 924–934 (2017).
 61. Haddon, D. J. *et al.* Proteomic Analysis of Sera from Individuals with Diffuse Cutaneous Systemic Sclerosis Reveals a Multianalyte Signature Associated with Clinical Improvement during Imatinib Mesylate Treatment. *J. Rheumatol.* **44**, 631–638 (2017).
 62. Valentini, G. *et al.* CXCL4 in undifferentiated connective tissue disease at risk for systemic sclerosis (SSc) (previously referred to as very early SSc). *Clin. Exp. Med.* **17**, 411–414 (2017).
 63. Volkmann, E. R. *et al.* Changes in plasma CXCL4 levels are associated with improvements in lung function in patients receiving immunosuppressive therapy for systemic sclerosis-related interstitial lung disease. *Arthritis Res. Ther.* **18**, 305 (2016).
 64. van Bon, L. *et al.* Proteomic analysis of plasma identifies the Toll-like receptor agonists S100A8/A9 as a novel possible marker for systemic sclerosis phenotype. *Ann. Rheum. Dis.* **73**, 1585–9 (2014).
 65. Bernard, K. *et al.* Metabolic reprogramming is required for myfibroblast contractility and differentiation. *J. Biol. Chem.* **290**, 25427–25438 (2015).
 66. Negmadjanov, U. *et al.* TGF- β 1-mediated differentiation of fibroblasts is associated with increased mitochondrial content and cellular respiration. *PLoS One* **10**, 1–12 (2015).
 67. Sarabi, a *et al.* CXCL4L1 inhibits angiogenesis and induces undirected endothelial cell migration without affecting endothelial cell proliferation and monocyte recruitment. *J. Thromb. Haemost.* **9**, 209–19 (2011).
 68. Trojanowska, M. Cellular and molecular aspects of vascular dysfunction in systemic sclerosis. *Nat. Rev. Rheumatol.* **6**, 453–60 (2010).
 69. Gouwy, M. *et al.* CXCL4 and CXCL4L1 Differentially Affect Monocyte Survival and Dendritic Cell Differentiation and Phagocytosis. *PLoS One* **11**, e0166006 (2016).
 70. Gleissner, C. a. Macrophage Phenotype Modulation by CXCL4 in Atherosclerosis. *Front. Physiol.* **3**, 1 (2012).
 71. Aidoudi-Ahmed, S. & Bikfalvi, A. Interaction

- of PF4 (CXCL4) with the vasculature: A role in atherosclerosis and angiogenesis. *Thromb. Haemost.* **104**, 941–948 (2010).
72. Van Raemdonck, K., Gouwy, M., Lepers, S. A., Van Damme, J. & Struyf, S. CXCL4L1 and CXCL4 signaling in human lymphatic and microvascular endothelial cells and activated lymphocytes: Involvement of mitogen-activated protein (MAP) kinases, Src and p70S6 kinase. *Angiogenesis* **17**, 631–640 (2014).
 73. von Hundelshausen, P. *et al.* Chemokine interactome mapping enables tailored intervention in acute and chronic inflammation. *Sci Transl Med* **9**, 1–15 (2017).
 74. Kabala, P. A. *et al.* Endoplasmic reticulum stress cooperates with Toll-like receptor ligation in driving activation of rheumatoid arthritis fibroblast-like synoviocytes. *Arthritis Res. Ther.* **19**, 1–11 (2017).
 75. Kroeze, K. L. *et al.* Chemokine-mediated migration of skin-derived stem cells: predominant role for CCL5/RANTES. *J. Invest. Dermatol.* **129**, 1569–81 (2009).
 76. Chrifi, I. *et al.* CMTM3 (CKLF-Like Marvel Transmembrane Domain 3) Mediates Angiogenesis by Regulating Cell Surface Availability of VE-Cadherin in Endothelial Adherens Junctions. *Arterioscler. Thromb. Vasc. Biol.* **37**, 1098–1114 (2017).
 77. Eslin, D. E. *et al.* Transgenic mice studies demonstrate a role for platelet factor 4 in thrombosis: dissociation between anticoagulant and antithrombotic effect of heparin. *Blood* **104**, 3173–80 (2004).
 78. Kavian, N. *et al.* Arsenic trioxide prevents murine sclerodermatous graft-versus-host disease. *J. Immunol.* **188**, 5142–9 (2012).
 79. de Haan, J. J. *et al.* Complement 5a Receptor deficiency does not influence adverse cardiac remodeling after pressure-overload in mice. *Sci. Rep.* **7**, 17045 (2017).
 80. de Jager, W., Prakken, B. J., Bijlsma, J. W. J., Kuis, W. & Rijkers, G. T. Improved multiplex immunoassay performance in human plasma and synovial fluid following removal of interfering heterophilic antibodies. *J. Immunol. Methods* **300**, 124–35 (2005).

Fatty acid and carnitine metabolism are dysregulated in Systemic sclerosis patients

A. Ottria^{1,2}, A.T. Hoekstra³, M. Zimmermann^{1,2}, M. van der Kroef^{1,2}, N. Vazirpanah^{1,2}, M. Cossu^{1,2}, E. Chouri^{1,2}, M. Rossato^{1,2}, L. Beretta⁴, R.G. Tieland^{1,2}, C.G.K. Wichers^{1,2}, E. Stigter⁵, C. Gulersonmez⁵, F. Bonte-Mineur⁶, C.R. Berkers^{3,7}, T.R.D.J. Radstake^{1,2}, W. Marut^{1,2*}

¹Center for Translational Immunology, University Medical Center Utrecht, Utrecht University, Utrecht, the Netherlands

²Department of Rheumatology and Clinical Immunology, University Medical Center Utrecht, Utrecht University, Utrecht, the Netherlands

³Biomolecular Mass Spectrometry and Proteomics, Bijvoet Center for Biomolecular Research, Utrecht University, Utrecht, the Netherlands

⁴Referral Center for Systemic Autoimmune Diseases, University of Milan & Fondazione IRCCS Ospedale Maggiore Policlinico, Mangiagalli e Regina Elena, Milan, Italy

⁵Department of Molecular Cancer Research, Center Molecular Medicine, Oncode Institute, University Medical Center Utrecht, Utrecht, The Netherlands

⁶Department of Rheumatology and Clinical Immunology, Maastad Hospital, Rotterdam, the Netherlands

⁷Department of Biochemistry and Cell Biology, Faculty of Veterinary Medicine, Utrecht University, Utrecht, the Netherlands

* Correspondence:

Wioleta Marut, PhD, University Medical Centre Utrecht | Heidelberglaan 100 | Tel: +31

88 75 535 68

w.k.marut@umcutrecht.nl

Keywords: Fatty Acid Oxidation, Carnitines, Dendritic cells, Systemic sclerosis, Metabolomics.

Manuscript published in Frontiers Immunology DOI: 10.3389/fimmu.2020.00822

Abstract

Systemic sclerosis (SSc) is a rare chronic disease of unknown pathogenesis characterized by fibrosis of the skin and internal organs, vascular alteration and dysregulation of the immune system. In order to better understand the immune system and its perturbations leading to diseases, the study of the mechanisms regulating cellular metabolism has gained a wide interest. Here we assessed the metabolical status of plasma and dendritic cells (DCs) in patients with SSc. We identified a dysregulated metabolomic signature in carnitine in both, circulation (plasma) and intracellularly in DCs of SSc patients. In addition, we confirmed carnitine alteration in the circulation of SSc patients in three independent plasma measurements and identified dysregulation of fatty acids. We hypothesized that fatty acid and carnitine alterations contribute to potentiation of inflammation in SSc. Incubation of healthy and SSc dendritic cells with etoposide, a carnitine transporter inhibitor, inhibited the production of pro-inflammatory cytokines such as IL-6 through inhibition of fatty acid oxidation. These findings shed light on the altered metabolic status of the immune system in SSc patients and opens potential novel avenues to reduce inflammation.

Introduction

Systemic Sclerosis (SSc) is an auto-immune disease with an unknown pathogenesis and unpredictable course. SSc is characterized by vascular lesions, immune cell activation, fibrosis of the skin and internal organs and loss of the hypodermal fat layer (1). As fat cells are important energy reservoirs, the loss of the fat layer in the fibrotic lesions suggests a role of metabolic changes in SSc. In the last years, metabolomics has shown rapid growth in its application to human health research. The aim of a metabolomics approach is to investigate the complete sets of metabolites within a given sample, in order to achieve a global view of the biological processes within the body (2). Many metabolomics studies already underlined the importance of metabolism in auto-immune diseases and the metabolomics approach has been applied to identify a fingerprint in diseases such as systemic lupus erythematosus (SLE), Sjögren's syndrome (3), multiple sclerosis and rheumatoid arthritis (2,4–6). In SSc, metabolomics pinpoints a distinct metabolic pattern between healthy controls and SSc patients. For instance, a distinct metabolic profile was identified in endothelial cells of SSc patients with pulmonary arterial hypertension (PAH) (7). Other studies have shown a dysregulated fatty acid beta oxidation and amino acid pathway in the urine profile of SSc patients (2,7–9).

6

Our group has been investigating the role of dendritic cells (DCs) in the pathogenesis of SSc. Previously, we have observed pathological behaviors of DCs in SSc patients, such as a downregulation of RUNX3 expression (10) or overproduction of pro-inflammatory cytokine CXCL4 in plasmacytoid DCs (pDCs) (11).

It has been shown that activated DCs have a different metabolic profile that supports their pro-inflammatory status (12). In the current study we investigated whether metabolomics assessments in the circulation and intracellularly in DCs of SSc patients, could reveal any metabolic aberrances that might contribute to the pathophysiology of SSc. Therefore, we explored the metabolic profile of plasma of a large cohort of SSc patients followed by a translational experimental setup. Our results indicate changes in the level of carnitine and

subsequently fatty acids metabolism, to be altered in circulation and DCs of patients with SSc. Finally, we demonstrated that etoposide, a drug used in cancer therapy, is able to downregulate inflammation in SSc.

Methods and patient's cohort

Patients Cohort

In compliance with the guidelines of the Declaration of Helsinki and following the approval of the local Institutional Ethical Review Board, peripheral blood was collected after receiving written informed consent of the patients. The criteria for selecting patients with SSc was performed according to the 2013 American College of Rheumatology (ACR) (13) Classification. **Table 1a** represents the characteristics of involved patients from Italian discovery cohort from which the plasma was utilized to perform mass spectrometry assessments. **Table 1b** represents the characteristics of involved patients from Dutch validation cohort from which the immune cells and fibroblasts were utilized to perform in vitro assessments.

Table 1a. Baseline and clinical characteristics of patients with SSc from the discovery cohort, categorized according to the ACR (2013) criteria (The data are presented as mean \pm SD or min-max)

Discovery cohort	HC (N=7)	SSc (N=20)	ncSSc (N=7)	lcSSc (N=6)	dcSSc (N=7)
Age	59 \pm 14	57 \pm 12	60 \pm 9	59 \pm 10	52 \pm 17
Disease duration (years)	-	13 \pm 11	9 \pm 5	26 \pm 7	7 \pm 7
Sex (n females)	7 (100%)	17 (85%)	7 (35%)	6 (30%)	4 (20%)
ACR/EULAR score	-	10 \pm 2	11 \pm 1	12 \pm 2	10 \pm 2
Raynaud's phenomenon (RP)	-	20 (100%)	7	6	7
Puffy fingers (PF)	-	7 (35%)	7	0	0
Sclerodactyly	-	12 (60%)	0	5	7
Digital ulcers (DU) (anamnestic)	-	5 (25%)	1	3	1
Modified rodnan skin score (MRSS)	-	4 (0-27)	0	4 (2-6)	12 (5-27)
Telangiectasia	-	10 (50%)	1	5	4
NVC pattern (nailfold video capillaroscopy)	-	9 (45%)	7	-	2
Anti-nucleus antibodies (ANA)	-	20 (100%)	7	6	7
Serum anticontromere (ACA)	-	11 (55%)	6	4	6

Autoantibodies against topoisomerase I (scl70)	-	5 (25%)	0	2	3
RVSP (right ventricular systolic pressure)	-	25,4 ±5,5	25,3 ±4,9	25,2 ±5	24,6 ±7,3
ILD (interstitial lung disease)	-	4 (20%)	0	1	3
Forced vital capacity (FVC) (% of predicted)	-	106 ±19	116 ±18	104 ±17	96 ±20
Lung diffusing capacity for carbon monoxide (DLCO) (% of predicted)	-	72 ±18	71 ±22	69 ±12	76 ±23
Nifedipine	-	19 (95%)	6	6	7
Disease-modifying antirheumatic drugs (DMARDs)	-	5 (25%)	1	1	3

Table 1b. Baseline and clinical characteristics of patients with SSc from the validation cohort, categorized according to the ACR (2013) criteria (The data are presented as mean ±SD or min-max)

Validation cohort	HC	SSc			
	(N=14)	validation (N=12)	ncSSc (N=3)	lcSSc (N=7)	dcSSc (N=2)
Age	42 ±10	53 ±9	43 ±4	56 ±9	55 ±3
Disease duration (years)	-	11 ±10	8 ±7	14 ±13	6 ±9
Sex (n females)	12 (86%)	11 (92%)	3 (100%)	7 (100%)	1 (50%)
ACR/EULAR score	-	12 ±2	12 ±1	11 ±2	14 ±2
Raynaud's phenomenon (RP)	-	12 (100%)	3	7	2
Puffy fingers (PF)	-	7 (50%)	1	3	2
Sclerodactyly	-	5 (42%)	0	3	2
Digital ulcers (DU) (anamnestic)	-	4 (33%)	0	2	2
Modified rodnan skin score (MRSS)	-	7 (0-19)	0	8 (4-10)	16 (14-19)
Telangiectasia	-	6 (50%)	1	4	1
NVC pattern (nailfold video capillaroscopy)	-	9 (75%)	1	4	2
Anti-nucleus antibodies (ANA)	-	12 (100%)	3	7	2
Serum anticentromere (ACA)	-	3 (25%)	1	2	0



Autoantibodies against topoisomerase I (scl70)	-	6 (50%)	1	4	1
ILD (interstitial lung disease)	-	2 (16%)	0	1	1
Disease-modifying antirheumatic drugs (DMARDs)	-	7 (58%)	0	5	2

Plasma collection and isolation

Venous blood was collected in a 6 mL ACD vacutainer (#364816, BD Biosciences). Blood was further centrifuged for 10 minutes at 1500 RPM at room temperature in order to obtain plasma. Next, plasma was aliquoted in sterile Micronics tubes and stored in at -80 Celsius degrees freezer until the experiment date.

Untargeted analysis methods

Direct-Infusion High resolution Mass Spectrometry (DIMS)

Extraction of dried blot spot samples (\varnothing 3mm) was performed by ultrasonification for 20 minutes in 140 μ L NSK-AB internal standard solution prepared according to the manufacturer's instructions (Cambridge Isotope Laboratories, Tewksbury, MA USA). After dilution with 60 μ L 0.3% formic acid, the samples were filtered over a 0.2 μ m cut-off filter plate (Acroprep, Pall Corporation, Ann Arbor, MI USA). The samples were collected in a 96 wells plate, sealed to avoid evaporation and subjected to DIMS using an Advion TriVersa NanoMate (Advion, Ithaca, NY USA) with 5 μ m ID chip-based infusion and a Q-Exactive Plus mass spectrometer (Thermo Scientific, Bremen, Germany). Mass spectrometry data were acquired in the scan range of m/z 70 to 600. The system was operated at 140000 mass resolution in both positive and negative mode (1.5 minutes each at 1.6 kV). For high mass accuracy, mass calibration was performed before each experiment and internal lock masses were used (14). Raw data files were converted to mzXML format using MS Convert and processed using an in-house-developed untargeted metabolomics pipeline as well as the HMDB database (accurate mass, isotopic pattern).

Liquid Chromatography Mass Spectrometry (LC-MS)

A volume of 50 μ L sample was subjected to water-methanol-chloroform extraction (Folch-method 3). After phase separation by centrifugation, both the aqueous and the organic phase containing all lipids were transferred to clean vials and dried under a gentle stream of nitrogen gas at 40°C.

Prior to analysis, the residue of the aqueous phase was dissolved in 100 μ L 10% acetonitrile in ultrapure water. Analysis was conducted with a Thermo Scientific Acella UHPLC system and an Acquity BEH C-8 column (1 \times 150mm, 1.7 μ m) kept at 40°C. The column outlet was coupled to a Thermo Scientific Orbitrap XL equipped with an electrospray ion source using both positive and negative ionization. The mass spectrometer was operated in data directed tandem MS mode. The mobile phases consisted of 6.5mM ammonium carbonate pH 8 (solvent A), and 6.5mM ammonium carbonate in methanol (solvent B) in negative mode. For positive mode analysis the solvents were 0.1% formic acid in ultrapure water and 0.1% formic acid in methanol, respectively. Analysis was started upon injection of 5 μ L of sample. A 10 minutes linear gradient of 0–100% B was started 3 minutes after the injection of the sample. The system was kept at 100% B for the next 4 minutes, after which the system returned to its starting situation. Total runtime was 22 minutes and the flow rate was 150 μ L per minute (15).

For lipidomic analysis the residue of the organic phase was dissolved in 100 μ L 80% acetonitrile-20% isopropanol. Analysis was conducted with the system described above using an Acquity BEH C18 column (1 \times 100mm, 1.7 μ m) kept at 60°C. The system was operated at a flow rate of 100 μ L per minute. The mobile phases consisted of 40% acetonitrile also containing 10mM ammonium acetate (solvent A), and 10% acetonitrile – 90% isopropanol also containing 10mM ammonium acetate (solvent B) for both negative and positive mode. A 12minute linear gradient of 40–100% B was started after the injection of 5 μ L of the sample. The system was kept at 100% B for the next 5 minutes, after which the system returned to its starting situation. Total runtime was 20 minutes.

For both the analysis of polar and apolar (lipid) metabolites, the acquired MS-data was

processed using MZMine 2 open source software 4 and searched against available databases.

Targeted analysis methods

Acylcarnitine analysis

For each analysis a volume of 50 μ L NSK-B internal standard solution was mixed with 50 μ L of plasma and 300 μ L acetonitrile, according to the manufacturer's instructions. The sample was centrifuged at 4° at 14000xg for 5 minutes and the supernatant was transferred to a GC vial and evaporated to dryness at 40°C under a gentle stream of nitrogen. A volume of 100 μ L freshly prepared butylation reagent was added to the residue. The vial was then vortexed, incubated at 60°C for 15 minutes and evaporated to dryness at 40°C under a gentle stream of nitrogen. The residue was dissolved in 100 μ L acetonitrile and subjected to analysis. Standards and quality control samples were prepared similarly (16).

Samples were analysed on a Waters XEVO Triple Quadrupole mass spectrometer using an Acquity UPLC system for sample delivery (Waters, Milford, MA USA). For the analysis of the samples, 5 μ L of the derivatised sample was injected via the systems bypass via a restrictor into an 400 μ L per minute acetonitrile flow. The MS system was operated in the positive ionization mode using MRM scanning (parent-daughter masses) with analyte dependent collision energy for acetyl-carnitine identification and quantification.

Fatty acid analysis

Arachidonic acid-D8 in methanol (10 μ L) was added to a sample (20 μ L) and subjected to water-methanol-chloroform extraction (Folch-method). After phase separation by centrifugation, the organic phase containing all lipids was removed from the vial and dried under a gentle stream of nitrogen gas at 40°C. The residue was dissolved in chloroform and subjected to clean-up by solid phase extraction (SPE) on amino-silica columns (17). After SPE, the fraction containing the FFA was dried under a stream of nitrogen at 37°C. The residue was dissolved in 100 μ L acetonitrile and subjected to LC-MS analysis using an Acella UHPLC coupled to a LTQ-Orbitrap XL MS. The LC was equipped with an

Acquity BEH-C18 column (2.1x5cm, 1.7 μ m) and guard column. Fatty acids were separated by means of 20 minutes 10 – 95% acetonitrile gradient in 0.1% acetic acid at 300 μ L per minutes and 60°C. FFA identification and response quantification was performed using retention time (\pm 0.1 minutes) and ion m/z values (\leq 5ppm).

Monocyte-derived DCs (moDCs) differentiation and stimulation

Peripheral blood mononuclear cells (PBMCs) from HC and SSc patients were isolated by Ficoll (GE Healthcare) gradient. Monocytes were isolated using an autoMACS Pro Separator (Miltenyi Biotec) according the manufacturer's instructions. Purity was routinely assessed by flow cytometry and above 94%. Monocytes were seeded at a final concentration of one million per ml and cultured in RPMI-GlutaMAX (Thermo Fisher Scientific). Medium was supplemented with 10% FBS (Biowest), 10.000 I.E. penicillin-streptomycin (Thermo Fisher Scientific), recombinant human granulocyte-macrophage colony-stimulating factor (GM-CSF, 800IU/mL) (R&D Systems) and recombinant human interleukin-4 (IL-4, 500IU/mL) (R&D Systems), as previously described (18).

Mass Spectrometry on moDCs

After 3 and 24 hours, moDCs were harvested and centrifuged for 5 minutes at 1000G. Medium samples were collected and cell pellet was washed with ice-cold PBS. Metabolites were extracted by adding 50 μ l of ice-cold MS lysis buffer (methanol/acetonitrile/ULC/MS grade water (2:2:1)) to the cell pellet. Samples were shaken for 10 minutes at 4°C and centrifuged at 14000G for 15 minutes, after which the supernatants were collected for LC-MS analysis. LC-MS analysis was performed on an Exactive mass spectrometer (Thermo Scientific) coupled to a Dionex Ultimate 3000 autosampler and pump (Thermo Scientific). The MS operated in polarity-switching mode with spray voltages of 4.5 kV and -3.5 kV. Metabolites were separated using a Sequant ZIC-pHILIC column (2.1 x 150mm, 5 μ m, guard column 2.1 x 20mm, 5 μ m; Merck) using a linear gradient of acetonitrile and eluent A (20mM (NH₄)₂CO₃, 0.1% NH₄OH in ULC/MS grade water (Biosolve)). Flow rate was set at 150 μ l/minute. Metabolites were identified and quantified using Lcquan

software (Thermo Scientific) on the basis of exact mass within 10ppm and further validated by concordance with retention times of standards. Peak intensities were normalized based on total intensities per time point.

Interleukin 6 quantification using ELISA

Interleukin (IL-)6 was quantified in Cell-free supernatants using ELISA based PeliKine compact™ human IL-6 kit (Sanquin, Amsterdam, The Netherlands) and was performed following the manufacturer's instructions.

Viability assessment on pDCs

Annexin V-7AAD staining was used to assess cell death. Cells were stained with Annexin V (1:100 dilution, BD Pharmingen) and 7AAD (1:100 dilution, BD Pharmingen) and measured using a FACS Canto Flow Cytometer. The data were further analysed with BD FACS DIVA software.

Statistical analysis

Statistical analysis was performed via website platformed base pipeline tool: <https://www.metaboanalyst.ca>. Distance between samples was measured with Pearson. Where appropriate, Mann–Whitney test or Paired t test was assessed using Graph Pad Prism 8.0 Software. P values smaller than 0.05 were considered as statistically significant.

Results

Different metabolic pattern between HC and SSc

After screening the spectra obtained from the plasma of 27 individuals, a total of 157 compounds were identified. Using the online platform from Metaboanalyst.ca, we performed t-test statistical analysis and a total of 56 compounds were identified having a different level in plasma from SSc patients compared to HC (**Table 2**). Next, a heatmap of the 56 identified metabolites was generated and is shown in **Figure 1a**. Briefly, the heatmap reveals different levels of metabolites involved in processes such as fatty acid oxidation (FAO) (L-carnitine and acyl-carnitines) or kidney function (such as urea and creatinine) were observed in patients compared to HC. With the same tool we generated a principal component analysis (PCA) and a Partial Least Squares Discriminant Analysis (PLS-DA) (**Supplementary Figure 1, Figure 1**). The result of the PCA and PLS-DA revealed clear separation between HC and SSc patients based on the levels of metabolites detected in plasma (**Figure 1b**). In order to identify the variable most efficient in separating the HC from the SSc patients, the variable importance in projection (VIP) score was generated. The results are shown in **Figure 1c**. The VIP score showed that L-carnitine and acyl-carnitines were relevant for the distinction between HC and SSc patients.

Table 2. T-test results of the features with different level in plasma from SSc compared to HC.

Compound	T STAT	P VALUE	-LOG10(P)	FDR
4-Aminobutyraldehyde	20.626	1.71E-16	15.768	2.70E-14
N-Methylethanolamine phosphate	15.732	4.30E-13	12.367	3.39E-11
Anandamide	8.5994	6.34E-09	8.1982	2.55E-07
L-Carnitine	-9.4886	6.46E-09	8.1895	2.55E-07
9Z_11E-13S-13-Hydroperoxyoctadeca-9_11-dienoic acid	8.6604	4.88E-08	7.3119	1.33E-06
3-Methyldioxyindole	-7.7001	5.05E-08	7.2965	1.33E-06
7-Methyluric acid	-7.5374	1.07E-07	6.9727	2.40E-06

Arachidonate	-6.9706	3.04E-07	6.5172	6.00E-06
3-Methyl-2-oxobutanoic acid	6.9281	4.30E-07	6.3665	7.55E-06
Urea	-6.6387	6.69E-07	6.1745	1.06E-05
Phenylacetaldehyde	6.7867	7.84E-07	6.1059	1.13E-05
5-Hydroxyindoleacetate	5.8472	1.08E-05	4.9657	0.00014249
Creatine	5.6352	1.19E-05	4.9227	0.00014522
Cortisone	-5.5075	2.19E-05	4.6593	0.00024732
Palmitoylglycerone phosphate	5.6637	2.56E-05	4.5917	0.00026969
Allantoate	-5.145	2.80E-05	4.553	0.00027639
N-Acetyl-L-aspartate	4.938	4.39E-05	4.3579	0.00040771
2-Phenylacetamide	-6.016	7.02E-05	4.154	0.00061579
LL-2_6-Diaminoheptanedioate	5.233	0.00010047	3.998	0.00083545
Tetralin	4.5971	0.0001385	3.8585	0.0010942
trans-Cinnamate	4.5062	0.00017441	3.7584	0.0013122
4-Maleylacetoacetate	4.3634	0.00019949	3.7001	0.0014327
L-Tryptophan	-4.2562	0.00026453	3.5775	0.0018172
1-Palmitoylglycerol 3-phosphate	-4.2311	0.00027612	3.5589	0.0018178
1-Methyladenosine	-4.1094	0.00040482	3.3927	0.0025585
3-Hydroxyanthranilate	-6.0887	0.00042674	3.3698	0.0025933
L-Adrenaline	-3.8816	0.0006982	3.156	0.0040857
3-Dimethylaminopropyl benzoate	4.7859	0.00078949	3.1027	0.004455
Propanil	5.0085	0.00082285	3.0847	0.0044831
Stearoylglycerone phosphate	-3.7659	0.00091976	3.0363	0.0048441
Hypoxanthine	-3.736	0.00098251	3.0077	0.0050076
D-2-Hydroxyisocaproate	3.722	0.0011592	2.9359	0.0054985
6-Hydroxymelatonin	-3.6648	0.0011673	2.9328	0.0054985
Indole-5_6-quinone	3.6726	0.0011832	2.9269	0.0054985
N-Acetylmethionine	3.6107	0.0013535	2.8685	0.0059476
N1-Methyl-2-pyridone-5-carboxamide	-4.2214	0.0013551	2.868	0.0059476
D-Gluconic acid	-3.8235	0.0014258	2.8459	0.0060886
Adenine	-3.787	0.0018606	2.7303	0.0077362
Creatinine	-3.5091	0.0019132	2.7182	0.0077509
Retinol	-3.3348	0.0029065	2.5366	0.011481
5_6-Dihydrothymine	-3.4016	0.0031036	2.5081	0.01196
5-Phosphonoxy-L-lysine	-3.2559	0.0033209	2.4787	0.012493
3-Methyloxindole	-3.2515	0.0042893	2.3676	0.015641

Zeatin	-3.1636	0.0043557	2.3609	0.015641
Adenosine	-3.0758	0.0063492	2.1973	0.022293
Thiocysteine	3.0117	0.0069451	2.1583	0.023855
Inosine	-3.5235	0.0080192	2.0959	0.026958
1_7-Dimethyluric acid	-2.8674	0.0083164	2.0801	0.027375
Glycolithocholate	2.9311	0.0092378	2.0344	0.029787
D-Glucosamine	-3.2818	0.010531	1.9775	0.033279
3-Hydroxyhexobarbital	-2.8883	0.010945	1.9608	0.033907
6-Keto-prostaglandin F1alpha	3.017	0.012337	1.9088	0.036936
Dehydroepiandrosterone sulfate	2.7262	0.01239	1.9069	0.036936
L-Octanoylcarnitine	3.3887	0.0138	1.8601	0.040378
4-Guanidinobutanoate	-2.7708	0.014298	1.8447	0.041073
8Z_11Z_14Z- Icosatrienoic acid	-2.9042	0.016084	1.7936	0.045379

Figure 1

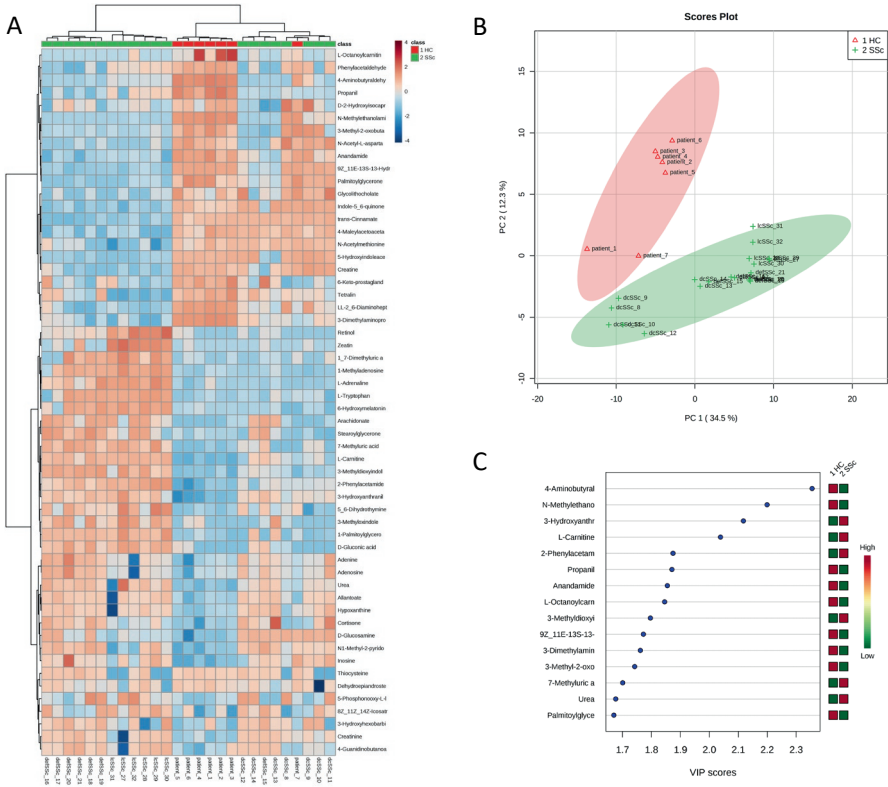


Figure 1. Differentially abundant compounds in plasma from HC and SSc patients. A) Heatmap of the 56 significantly different compounds identified in plasma of HC and SSc patients. **B)** Partial Least Squares Discriminant Analysis of plasma samples from HC and SSc patients. **C)** Variable Importance in Projection score obtained from the Partial Least Squares Discriminant Analysis.

SSc patients have dysregulation of fatty acids and carnitines

Next, we performed the quantitative enrichment analysis script from Metaboanalist.ca pipeline (**Figure 2a**). We found multiple metabolic processes to be altered in the plasma of SSc patients as compared to HC, involving fatty acid (FA) and L-carnitine, such as mitochondrial beta oxidation of short chain saturated FA, FA metabolism, beta oxidation of very long chain FA and carnitine synthesis pathways, to be altered in the plasma of SSc patients as compared to HC. These observations, suggested an inter relation of fatty acids

Figure 2. Fatty acids and Carnitine are altered in SSc. A) Summary Plot for Over Representation Analysis of differentially abundant compounds in plasma from SSc patients and HC. B) On the left quantification of Lauric acid, Myristic acid and Arachidic acid with targeted approach. On the right quantification with untargeted approach. C) On the left quantification of L-carnitine, Isovaleryl-carnitine, Octanoyl-carnitine and Palmitoyl-carnitine with targeted approach. On the right quantification with untargeted approach (Box are represented as 10-90 percentile. *= $P \leq 0.05$, **= $P \leq 0.01$, ***= $P \leq 0.001$, ****= $P \leq 0.0001$).

Carnitine alterations in the immune cells from SSc patients

Further, we investigated if carnitine alterations were also present at the cellular level in SSc patients. Since the role of dendritic cells in SSc pathogenesis is our main focus, we measured the basal level of carnitine in monocytes derived dendritic cells (moDCs), at two different time points (3 and 24 hours). We observed an increase in L-carnitine after 24 hours incubation ($P=0.023$) and L-acetyl-carnitine ($P < 0.0001$ at 3 hours and $P=0.0086$ at 24 hours) in SSc moDCs when compared to HC moDCs (**Figure 3b**). These results further highlight the potential importance of carnitine in the altered metabolism of SSc patients.

Figure 3

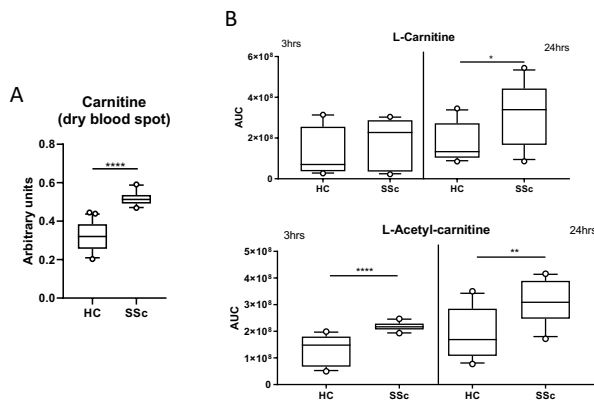


Figure 3. Carnitine is increased in SSc. A) Quantification of L-carnitine in dry blood spot measurement. B) Quantification of L-carnitine and L-Acetyl-carnitine in 4 healthy controls and 4 SSc moDCs executed in triplicate and incubated for 3hrs or 24hrs (AUC: Arbitrary unit count, boxes are represented as 10-90 percentile. *= $P \leq 0.05$, **= $P \leq 0.01$, ***= $P \leq 0.001$, ****= $P \leq 0.0001$).

Fatty acids and carnitine levels in SSc disease subsets

In order to gain more insight on FA and carnitine levels per disease subset we performed

Mann-Whitney t-test per subgroup of ncSSc, lcSSc and dcSSc in plasma and dry bloodspots samples. The comparison was made between the subsets and HC (**Table 3**).

Table 3. Statistical comparisons of fatty acid and carnitine levels in plasma and dry blood spots between ncSSc, lcSSc and dcSSc and healthy controls.

PLASMA FA	ncSSc	lcSSc	dcSSc
Lauric-acid	<i>0.0079</i>	<i>0.0043</i>	<i>0.016</i>
Myristic-acid	<i>0.0079</i>	<i>0.0043</i>	<i>0.11</i>
Arachidic-acid	<i>0.016</i>	<i>0.05</i>	<i>0.29</i>
DRY BLOOD SPOT			
Carnitine	<i><0.0001</i>	<i><0.0001</i>	<i><0.0001</i>
PLASMA CARNITINE			
Carnitine	<i>0.2222</i>	<i>0.0932</i>	<i>0.0159</i>
Isovaleryl-carnitine	<i>0.553</i>	<i>0.0215</i>	<i>0.0159</i>
Octanoyl-carnitine	<i>0.0556</i>	<i>0.1111</i>	<i>0.2857</i>
L-palmitoyl-carnitine	<i>0.1429</i>	<i>0.0671</i>	<i>0.4683</i>

Dysregulation of the Fatty Acid Oxidation and carnitines in SSc patients promotes inflammation and fibrosis.

We hypothesize that the alteration in FA and carnitines observed in SSc patients are a manifestation of dysregulated FAO. Alteration in FAO leads to increase production of pro-inflammatory cytokines and inflammation (19,20). Inflammation is known to induce fibrosis and therefore, promotes a vicious circle which further endorses the FAO (21) (**Figure 4a**).

Inflammation and fibrosis are two main features observed in SSc patients. To test the hypothesis that the FAO is dysregulated in SSc, leading to a vicious circle where inflammation and FAO induce each other, we investigated the role of different carnitine inhibitors (etoposide, thioridazine and mildronate) by testing the production of pro-inflammatory cytokine in immune cells. Etoposide is a molecule with inhibitory effect on the organic cation/carnitine transporter (OCTN2), while thioridazine inhibits peroxisomal oxidation of lipids (22,23) and mildronate is an inhibitor of the mitochondrial carnitine/ acyl-carnitine transporter (24). To study the effect of carnitine inhibitors on the production

of pro-inflammatory cytokines, we used SSc and HC PBMCs. Since PBMCs from SSc patients are known to spontaneously produce pro-inflammatory cytokine such as interleukin (IL-) 6 (25), we used IL-6 as readout of the cytokine production. We observed that etoposide, but not thioridazine and mildronate, was able to significantly reduce the production of IL-6, in PMBCs from HC ($P=0.031$) and SSc patients ($P=0.03$). (**Figure 4b**). Therefore, further experiments were performed using etoposide only. Furthermore etoposide, thioridazine and mildronate did not affect cell viability (**Supplementary Figure 2**).

Etoposide downregulates inflammatory response in SSc moDCs

Next, moDCs generated from HC and SSc were stimulated with Poly(I:C) (TLR3 ligand), and cultured in the presence of etoposide for 24 hours. We observed no induction of IL-6 in healthy moDCs exposed to TLR3 and/or etoposide. Interestingly, we found reduction of IL-6 in SSc moDCs cultured in the presence of etoposide, both, with and without TLR3 stimulation (respectively $P=0.057$ and $P=0.028$) (**Figure 4c**). Our data suggests that etoposide have an anti-inflammatory effect on SSc moDCs. These results open a new avenue to exploit fatty acid inhibition.

Figure 4

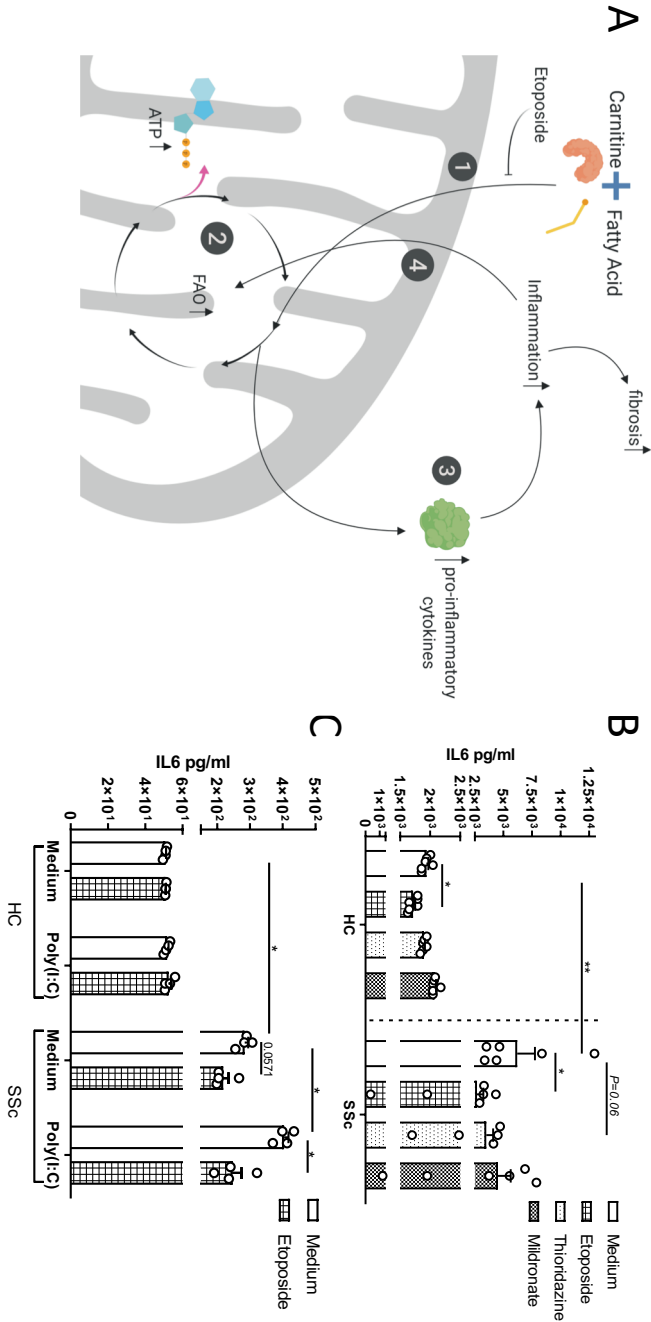


Figure 4. Effect of Etoposide on inflammation and fibrotic genes. **A)** Schematic representation of the FAO and etoposide effect: 1) Carnitine and fatty acid combine to form an acyl-carnitine. This is transported inside the mitochondria. Etoposide, blocking the intake of carnitine limits the formation of acyl-carnitine in the cell. 2) The acyl-carnitine combines with CoA in fatty acyl-CoA, this enters the FAO to generate ATP. 3) FAO can promote the release of pro-inflammatory cytokines, 4) promoting inflammation. Inflammation promotes fibrosis and 5) promotes FAO, generating a vicious circle. Created with Biorender. **B)** IL6 quantification in PBMCs from 6 HC and 6 SSC patients exposed to etoposide or thioridazine. **C)** IL6 quantification in modCs from 4 HC and 4 SSC patients exposed to etoposide or thioridazine. (Bars are represented as mean ±SEM. *=*P*≤0.05, **=*P*≤0.01, ***=*P*≤0.001, ****=*P*≤0.0001).

Discussion

The aim of our study was to identify and explore the potential role of circulatory and intracellular metabolites in the development of inflammation in SSc patients.

We observed an altered FA and carnitines profile both in blood and immune cells (plasma and DCs) of SSc patients. Carnitine is a molecule with a structure similar to amino acids and present in every mammalian species. Carnitine can be both taken up by food or being endogenously produced (26). Carnitine plays an important role in cellular energy metabolism. In fact, carnitine transports fatty acids (as acyl-carnitine) into the mitochondria in order to allow FA to be oxidized (26). Therefore, carnitine and FA via the FAO, are the fundamental key players for the energy metabolism of cells. It has been shown that an altered FA metabolism is reflected by defective composition of acyl-carnitines (27). In line with this, our observations signify an altered energy metabolism in immune cells and plasma of SSc patients reflected by dysregulated FA and carnitine profile including acyl-carnitines. Immune cells with altered metabolism lead to aberrant immune response (28,29). In macrophages, increased FA metabolism triggers disturbed immune response, difficulties in adaptation to the surrounding environment and shifting towards profibrotic M2 phenotype (30,31). Furthermore, studies on T helper cells showed that an altered FA metabolism and a disturbed (micro)environment surrounding the naïve T helper cells, predict the metabolic programming of the cells. Inhibition of FAO shifts the T helper cell differentiation more towards pro-inflammatory T helper 17 phenotype (32). Therefore, in SSc, an increase of the FA metabolic profile of the immune cells, might worsen the disease prognosis by priming a pro-inflammatory programmed immune system. Moreover, dysfunction of FAO was found to play an important role in the direct induction of renal fibrosis development (33). Both, inflammation and FAO amplifies the production of pro-inflammatory cytokines (20,21,34) and thereby substantiates the vicious circle of chronic inflammation and fibrosis.

To better understand the significance of FAO in SSc, we blocked the cellular carnitine intake by inhibiting the OCTN2 transporter using etoposide. Etoposide is a well-known

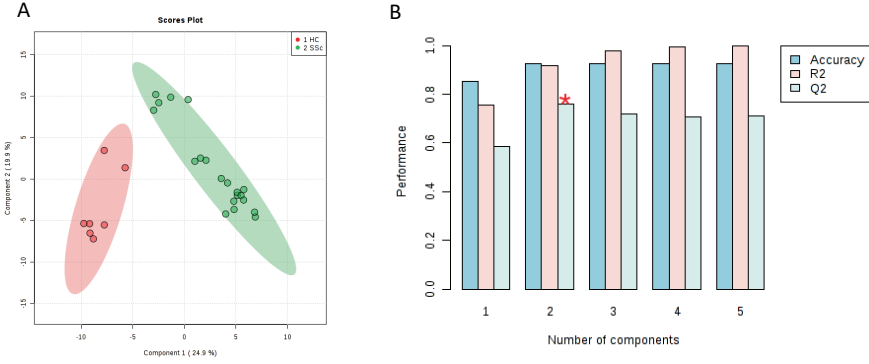
drug available for cancer treatment as in i.e. prostate cancer, small cell lung carcinoma and leukaemia (35,36). Etoposide inhibits carnitine transporter OCTN2 (37) which prevents FAO and subsequently might potentiate the downregulation of proinflammatory immune system. In addition, etoposide has been shown to inhibit topoisomerase II that might impact the experimental results in proliferating cells (38). As monocyte derived dendritic cells do not divide in culture and the incubation time with the inhibitor was short, the expected impact on the experimental results is unlikely to occur.

Furthermore, etoposide is suggested to be used in combination with corticosteroids or other DMARDS in treatment of systemic inflammation in Still's disease (39), which is a rare disease with rheumatoid arthritis-like hallmarks. In our studies, etoposide showed anti-inflammatory properties on DCs from SSc. However, further studies need to be performed to support this hypothesis.

In conclusion, targeted suppression of the FAO metabolism could be helpful to inhibit inflammation in SSc and therefore might offer a novel therapeutic target. While the literature on FAO and carnitine in SSc is rather poor, we believe that our results provide an intriguing and robust foundation to further elucidate the pathogenic mechanisms taking place in SSc immune dysregulation.

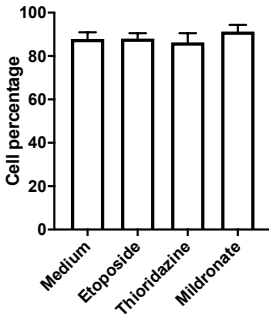
Supplementary Figures

Supplementary Figure 1



Supplementary Figure 1. A) Principal Component Analysis (PCA) of plasma samples from HC and SSc patients. **B)** PLS-DA model evaluation R2/Q2 values.

Supplementary Figure 2



Supplementary Figure 2. Percentage of live cells. FACS analysis expressed as percentage of live cells in annexin V, 7-AAD dead staining of PBMCs exposed to etoposide, thioridazine and mildronate for 24 hours. All data represents mean \pm SEM.



Conflict of Interest

The authors declare that the research was conducted in the absence of any commercial or financial relationships that could be construed as a potential conflict of interest.

Author Contributions

All authors approved the final version after being involved in drafting and revising the article for important intellectual content. A. Ottria and W. Marut had full access to the data and takes responsibility for the accuracy of the performed analysis and the integrity of the data. A. Ottria, T.R.D.J. Radstake and W. Marut were involved in design of the study. Execution and analysis of the results was performed by A. Ottria, A.T. Hoekstra, M. van der Kroef, C.G.K. Wichers, N. Vazirpanah, M. Cossu, E. Chouri, M. Rossato, L. Beretta, R.G. Tieland, E. Stigter, C. Gulersonmez were involved in performing experiments. A. Ottria and M. Cossu were involved in selection of the patients. T.R.D.J. Radstake, L. Beretta and F. Bonte-Mineur were involved in inclusion of SSc patients. All the authors contributed to the review of the manuscript.

Funding

Wioleta Marut obtained funding from Marie Curie Intra-European Fellowship (Proposal number: 624871) and from the NWO VENI (grant number 91919149).

Acknowledgments

Boudewijn M. T. Burgering helped in revising the paper. All the authors listed have made substantial, direct, and intellectual contribution to the work and approved it for publication.

References

- Pattanaik D, Brown M, Postlethwaite BC, Postlethwaite AE. Pathogenesis of Systemic Sclerosis. *Front Immunol* (2015) **6**:272. doi:10.3389/fimmu.2015.00272
2. Alonso A, Julià A, Vinaixa M, Domènech E, Fernández-Nebro A, Cañete JD, Ferrándiz C, Tornero J, Gisbert JP, Nos P, et al. Urine metabolome profiling of immune-mediated inflammatory diseases. *BMC Med* (2016) **14**:133. doi:10.1186/s12916-016-0681-8
 3. Bellocchi C, Fernández-Ochoa Á, Montanelli G, Vigone B, Santaniello A, Quirantes-Piné R, Borrás-Linares I, Gerosa M, Artusi C, Gualtierotti R, et al. Identification of a Shared Microbiomic and Metabolomic Profile in Systemic Autoimmune Diseases. *J Clin Med* (2019) **8**: doi:10.3390/jcm8091291
 4. Poddighe S, Murgia F, Loreface L, Liggi S, Cocco E, Marrosu MG, Atzori L. Metabolomic analysis identifies altered metabolic pathways in Multiple Sclerosis. *Int J Biochem Cell Biol* (2017) **93**:148–155. doi:10.1016/j.biocel.2017.07.004
 5. Wu T, Xie C, Han J, Ye Y, Weiel J, Li Q, Blanco I, Ahn C, Olsen N, Putterman C, et al. Metabolic disturbances associated with systemic lupus erythematosus. *PLoS One* (2012) **7**:e37210. doi:10.1371/journal.pone.0037210
 6. van Wietmarschen HA, Dai W, van der Kooij AJ, Reijmers TH, Schroën Y, Wang M, Xu Z, Wang X, Kong H, Xu G, et al. Characterization of rheumatoid arthritis subtypes using symptom profiles, clinical chemistry and metabolomics measurements. *PLoS One* (2012) **7**:e44331. doi:10.1371/journal.pone.0044331
 7. Deidda M, Piras C, Cadeddu Dessalvi C, Locci E, Barberini L, Orofino S, Musu M, Mura MN, Manconi PE, Finco G, et al. Distinctive metabolomic fingerprint in scleroderma patients with pulmonary arterial hypertension. *Int J Cardiol* (2017) **241**:401–406. doi:10.1016/j.ijcard.2017.04.024
 8. Fernández-Ochoa Á, Quirantes-Piné R, Borrás-Linares I, Gemperline D, PRECISESADS Clinical Consortium, Alarcón Riquelme ME, Beretta L, Segura-Carretero A. Urinary and plasma metabolite differences detected by HPLC-ESI-QTOF-MS in systemic sclerosis patients. *J Pharm Biomed Anal* (2019) **162**:82–90. doi:10.1016/j.jpba.2018.09.021
 9. Murgia F, Svegliati S, Poddighe S, Lussu M, Manzin A, Spadoni T, Fischetti C, Gabrielli A, Atzori L. Metabolomic profile of systemic sclerosis patients. *Sci Rep* (2018) **8**:7626. doi:10.1038/s41598-018-25992-7
 10. Affandi AJ, Carvalheiro T, Ottria A, Broen JC, Bossini-Castillo L, Tieland RG, Bon L van, Chouri E, Rossato M, Mertens JS, et al. Low RUNX3 expression alters dendritic cell function in patients with systemic sclerosis and contributes to enhanced fibrosis. *Ann Rheum Dis* (2019) **78**:1249–1259. doi:10.1136/annrheumdis-2018-214991
 11. van Bon L, Affandi AJ, Broen J, Christmann RB, Marijnissen RJ, Stawski L, Farina GA, Stifano G, Mathes AL, Cossu M, et al. Proteome-wide Analysis and CXCL4 as a Biomarker in Systemic Sclerosis. *N Engl J Med* (2014) **370**:433–443. doi:10.1056/NEJMoa1114576
 12. O'Neill LAJ, Pearce EJ. Immunometabolism governs dendritic cell and macrophage function. *J Exp Med* (2016) doi:10.1084/jem.20151570
 13. Van Den Hoogen F, Khanna D, Fransen J, Johnson SR, Baron M, Tyndall A, Matucci-Cerinic M, Naden RP, Medsger TA, Carreira PE, et al. 2013 classification criteria for systemic sclerosis: An american college of rheumatology/European league against rheumatism collaborative initiative. *Arthritis Rheum* (2013) doi:10.1002/art.38098
 14. de Sain-van der Velden MGM, van der Ham M, Gerrits J, Prinsen HCMT, Willemsen M, Pras-Raves ML, Jans JJ, Verhoeven-Duif NM. Quantification of metabolites in dried blood spots by direct infusion high resolution mass spectrometry. *Anal Chim Acta* (2017) **979**:45–50. doi:10.1016/j.aca.2017.04.038
 15. Rodríguez-Colman MJ, Schewe M, Meerlo M, Stigter E, Gerrits J, Pras-Raves M, Sacchetti A, Hornsveld M, Oost KC, Snippert HJ, et al. Interplay between metabolic identities in the intestinal crypt supports stem cell function. *Nature* (2017) **543**:424–427. doi:10.1038/nature21673
 16. Pluskal T, Castillo S, Villar-Briones A, Orešič M. MZmine 2: Modular framework for processing, visualizing, and analyzing mass spectrometry-based molecular profile

- data. *BMC Bioinformatics* (2010) **11**:395. doi:10.1186/1471-2105-11-395
17. Stigter ECA, Letsiou S, Broek NJF vd, Gerrits J, Ishihara K, Voest EE, Verhoeven-Duif NM, Brenkman AB. Development and validation of a quantitative LC–tandem MS assay for hexadeca-4,7,10,13-tetraenoic acid in human and mouse plasma. *J Chromatogr B* (2013) **925**:16–19. doi:10.1016/j.jchromb.2013.01.012
 18. Silva-Cardoso SC, Affandi AJ, Spel L, Cossu M, van Roon JAG, Boes M, Radstake TRDJ. CXCL4 Exposure Potentiates TLR-Driven Polarization of Human Monocyte-Derived Dendritic Cells and Increases Stimulation of T Cells. *J Immunol* (2017) **199**:253–262. doi:10.4049/jimmunol.1602020
 19. Nicholas DA, Proctor EA, Agrawal M, Belkina AC, Van Nostrand SC, Panneerseelan-Bharath L, Jones AR, Raval F, Ip BC, Zhu M, et al. Fatty Acid Metabolites Combine with Reduced β Oxidation to Activate Th17 Inflammation in Human Type 2 Diabetes. *Cell Metab* (2019) **30**:447-461. e5. doi:10.1016/j.cmet.2019.07.004
 20. Fujieda Y, Manno A, Hayashi Y, Rhodes N, Guo L, Arita M, Bamba T, Fukusaki E. Inflammation and Resolution Are Associated with Upregulation of Fatty Acid β -Oxidation in Zymosan-Induced Peritonitis. *PLoS One* (2013) **8**:e66270. doi:10.1371/journal.pone.0066270
 21. Lee SB, Kalluri R. Mechanistic connection between inflammation and fibrosis. *Kidney Int Suppl* (2010) **S22-6**. doi:10.1038/ki.2010.418
 22. Shi R, Zhang Y, Shi Y, Shi S, Jiang L. Inhibition of peroxisomal β -oxidation by thioridazine increases the amount of VLCFAs and A β generation in the rat brain. *Neurosci Lett* (2012) **528**:6–10. doi:10.1016/j.neulet.2012.08.086
 23. Van den Branden C, Roels F. Thioridazine: a selective inhibitor of peroxisomal β -oxidation in vivo. *FEBS Lett* (1985) **187**:331–333. doi:10.1016/0014-5793(85)81270-9
 24. Oppedisano F, Fanello D, Calvani M, Indiveri C. Interaction of mildronate with the mitochondrial carnitine/acylcarnitine transport protein. *J Biochem Mol Toxicol* (2008) **22**:8–14. doi:10.1002/jbt.20208
 25. Zhu HL, DU Q, Chen WL, Zuo XX, Li QZ, Liu SJ. [Altered serum cytokine expression profile in systemic sclerosis and its regulatory mechanisms]. *Beijing Da Xue Xue Bao* (2019) **51**:716–722. doi:10.19723/j.issn.1671-167X.2019.04.021
 26. Fielding R, Riede L, Lugo J, Bellamine A. L-Carnitine Supplementation in Recovery after Exercise. *Nutrients* (2018) **10**:349. doi:10.3390/nu10030349
 27. Beger RD, Bhattacharyya S, Gill PS, James LP. “Acylcarnitines as Translational Biomarkers of Mitochondrial Dysfunction,” in *Mitochondrial Dysfunction Caused by Drugs and Environmental Toxicants* (Hoboken, NJ, USA: John Wiley & Sons, Inc.), 383–393. doi:10.1002/9781119329725.ch24
 28. Loftus RM, Finlay DK. Immunometabolism: Cellular metabolism turns immune regulator. *J Biol Chem* (2016) **291**. doi:10.1074/jbc.R115.693903
 29. Pearce EJ, Everts B. Dendritic cell metabolism. *Nat Rev Immunol* (2015) doi:10.1038/nri3771
 30. Freerman AJ, Johnson AR, Sacks GN, Milner JJ, Kirk EL, Troester MA, Macintyre AN, Goraksha-Hicks P, Rathmell JC, Makowski L. Metabolic Reprogramming of Macrophages. *J Biol Chem* (2014) **289**:7884–7896. doi:10.1074/jbc.M113.522037
 31. Wang T, Liu H, Lian G, Zhang S-Y, Wang X, Jiang C. HIF1 α -Induced Glycolysis Metabolism Is Essential to the Activation of Inflammatory Macrophages. *Mediators Inflamm* (2017) **2017**:1–10. doi:10.1155/2017/9029327
 32. Slack M, Wang T, Wang R. T cell metabolic reprogramming and plasticity. *Mol Immunol* (2015) **68**:507–512. doi:10.1016/j.molimm.2015.07.036
 33. Allison SJ. Fibrosis: dysfunctional fatty acid oxidation in renal fibrosis. *Nat Rev Nephrol* (2015) **11**:64. doi:10.1038/nrneph.2014.244
 34. Angajala A, Lim S, Phillips JB, Kim J-H, Yates C, You Z, Tan M. Diverse Roles of Mitochondria in Immune Responses: Novel Insights Into Immuno-Metabolism. *Front Immunol* (2018) **9**:1605. doi:10.3389/fimmu.2018.01605
 35. Teicher BA, Silvers T, Selby M, Delosh R, Laudeman J, Ogle C, Reinhart R, Parchment R, Krushkal J, Sonkin D, et al. Small cell

- lung carcinoma cell line screen of etoposide/
carboplatin plus a third agent. *Cancer Med*
(2017) **6**:1952–1964. doi:10.1002/cam4.1131
36. Papiez M, Krzyściak W, Szade K,
Bukowska-Straková K, Bystrowska B,
Jozkowicz A, Dulak J, Kozakowska
M, Hajduk K. Curcumin enhances the
cytogenotoxic effect of etoposide in leukemia
cells through induction of reactive oxygen
species. *Drug Des Devel Ther* (2016)557.
doi:10.2147/DDDT.S92687
37. Hu C, Lancaster CS, Zuo Z, Hu S, Chen
Z, Rubnitz JE, Baker SD, Sparreboom A.
Inhibition of OCTN2-mediated transport
of carnitine by etoposide. *Mol Cancer Ther*
(2012) **11**:921–9. doi:10.1158/1535-7163.
MCT-11-0980
38. Baldwin E, Osheroff N. Etoposide,
Topoisomerase II and Cancer. *Curr
Med Chem Agents* (2005) **5**:363–372.
doi:10.2174/1568011054222364
39. Mitrovic S, Fautrel B. Complications
of adult-onset Still's disease and their
management. *Expert Rev Clin Immunol*
(2018) **14**:351–365. doi:10.1080/174466
6X.2018.1465821

mTOR inhibition by metformin impacts monosodium urate crystal induced inflammation and cell death in gout: a prelude to a new add-on therapy?

N. Vazirpanah¹, A. Ottria¹, M. van der Linden¹, C. Wichers¹, M. Schuiveling¹, E. van Lochem², A. Phipps-Green³, T. R. Merriman³, M. Zimmermann¹, M. Janssen⁴ T. R.D.J. Radstake^{1,5#}, J. C.A. Broen^{1,5#}

¹Laboratory of Translational Immunology, Laboratory of Immunology, University Medical Centre Utrecht, Utrecht, The Netherlands.

²Department of Immunology, Rijnstate Hospital, Arnhem, Netherlands.

³Department of Biochemistry, University of Otago, Dunedin, New Zealand.

⁴Department of Rheumatology, VieCuri Hospital, Venlo, Netherlands.

⁵Department of Rheumatology and Clinical Immunology, University Medical Centre Utrecht, Utrecht, The Netherlands.

#These authors contributed equally

Corresponding author: j.c.a.broen@umcutrecht.nl | phone +31 88 755 1010 | WKZ
Lundlaan 6 KC 02.085.2 P.O. Box 85090; 3508 AB Utrecht|

Keywords: Gout, Monosodium urate crystal, Monocyte, mTOR, Rapamycin, Metformin,

Manuscript published in Annals of the Rheumatic diseases DOI: 10.1136/annrheumdis-2018-214656

Abstract

Objective: Gout is the most common inflammatory arthritis worldwide, patients experience a heavy burden of cardiovascular and metabolic diseases. The inflammation is caused by the deposition of monosodium urate (MSU) crystals in tissues, especially in the joints, triggering immune cells to mount an inflammatory reaction. Recently it was shown that MSU crystals can induce mechanistic target of rapamycin (mTOR) signaling in monocytes encountering these crystals *in vitro*. The mTOR pathway is strongly implicated in cardiovascular and metabolic disease. We hypothesized that inhibiting this pathway in gout might be a novel avenue of treatment in these patients, targeting both inflammation and comorbidities.

Methods: We used a translational approach starting from *ex vivo* to *in vitro* and back to *in vivo*.

Results: We show that *ex vivo* immune cells from gout patients exhibit higher expression of the mTOR pathway, which we can mimic *in vitro* by stimulating healthy immune cells (B lymphocytes, monocytes, T lymphocytes) with MSU crystals. Monocytes are the most prominent *mTOR* expressers. By using live imaging, we demonstrate that monocytes, upon encountering MSU crystals, initiate cell death and release a wide array of pro-inflammatory cytokines. By inhibiting *mTOR* signaling with metformin or rapamycin a reduction of cell death and release of inflammatory mediators was observed. Consistent with this, we show that patients with gout that are treated with the mTOR inhibitor metformin have a lower frequency of gout attacks.

Conclusions: We propose mTOR inhibition as a novel therapeutic target of interest in gout treatment.

Introduction

Gout is the most common inflammatory arthritis affecting approximately 4% of the population in Europe and the United States. The inflammation is caused by the deposition of monosodium urate (MSU) crystals in the joints, which predominantly occurs in hyperuricemia (0.42 mmol/L serum urate). The level of comorbidity in gout patients is high; 74% have hypertension, 71% have chronic kidney disease and more than 10% suffer from either a myocardial infarction, heart failure or a major stroke[1–3]. Gout is associated with senescence and with increased mortality due to cardiovascular- and infectious diseases and cancer[4–7]. Recently it has become apparent that an important driver of inflammation in gout is interleukin-1beta (IL-1 β) mediated NLRP3-inflammasome activation[8–10]. This process is initiated by autophagy of MSU crystals in macrophages, the same effect is observed when stimulating PBMCs or monocytes *in vitro* with MSU crystals[10–12]. In addition, interleukin 8 (IL-8) levels seem to be constitutionally increased in the circulation of gout patients with concomitant cardiovascular disease and diabetes[13].

A recent study showed that stimulating monocytes with MSU crystals *in vitro* leads to a higher expression of mechanistic target of rapamycin (mammalian target of Rapamycin) (mTOR) and increased IL-1 β [10]. The mTOR signaling pathway partially regulates IL-8 production and IL-1 β and therefore might be of interest as a target in inhibiting the chronic inflammation in gout patients[14,15]. The mTOR pathway is well conserved in eukaryotes, and its signaling is tightly entwined with regulation of lymphocyte proliferation, immune-cell activation, autophagy, lipid and glucose metabolism. As a consequence of its central role in cellular signaling, increased mTOR signaling has been implicated in multiple diseases and is a common causative pathway in vascular disease, inflammation, obesity, progressive renal disease and diabetes[16–18]. These comorbidities are a heavy concomitant disease burden in gout, for which contemporary urate-lowering treatments have not been effective. The most potent clinically approved drug that inhibits mTOR is rapamycin, which is used as an immunosuppressant agent in transplant patients and as a coating for coronary stents[19]. In

addition, a number of reports have been published on using rapamycin as an add-on therapy in rheumatoid arthritis, systemic lupus erythematosus and Sjögren's disease[20–22]. A less-well known, weak inhibitor of mTOR, but more widely used is metformin. Metformin inhibits mTOR signaling indirectly through AMPK activation and has been shown to reduce IL-8 production and might be able to reduce inflammasome activation[23,24]. In addition, metformin has been shown to reduce the risk for cardiovascular disease and diabetes development in clinical trials and might have a beneficiary effect on these concomitant diseases in gout [25,26].

In the current translational study, we were interested whether we could find evidence for increased mTOR signaling in patients with gout, to pinpoint the immune-cells mostly involved and to test whether mTOR inhibition might be an approach to reduce MSU crystal-induced inflammation *in vitro* and *in vivo* in patients with gout.

Patients and methods

Demographics of patients and healthy participants

We included 89 Dutch patients with intercritical gout and 89 healthy participants (**Table 1** and **supplementary table 1**). All subjects provided written informed consent. The study was approved by local ethical review committees of the Rijnstate hospital (Nijmegen, the Netherlands) and was performed in accordance to the guidelines of the Declaration of Helsinki.

Table 1. Baseline characteristics of patients with gout and healthy participants.

	Gout (n=89)	Healthy participants (n=89)
Male N (%)	72 (81.5)	77 (85.60)
Age	62.66 ±13.44	47.84 ±17.87
Colchicine (Yes) N (%)	44 (48.9)	-
NSAID (Yes) N (%)	14 (16.20)	-
Allopurinol (Yes) N (%) (Mean 200mg/Day)	76 (84.40)	-
Corticosteroids (Yes) N (%)	40 (44.40)	-
Metformin (Yes) N (%)	23 (25.84)	-
Diabetes (Type 2) (Yes) N (%)	19 (21.35)	-
Stroke (Yes/No) N (%)	5 (5.6)	-
Myocardial Infarction (Non-Fatal) (Yes) N (%)	14 (15.6)	-
Heart Failure (Yes) N (%)	12 (13.30)	-
Angina Pectoris (Yes) N (%)	12 (13.30)	-
Creatinine Level (µmol/L)	95.59 (±31.32)	-
Body Mass Index (Kg/M2) (Mean ± SD)	29.95 (±6.12)	25.79 (±4.18)
Smoking (Yes) N (%)	12 (13.30)	1(1.24)

Serum Urate (Mmol/L)	0.50 (±0.12)	-
Total Number of Flares Per Year (Mean ± SD)	4.41 (±5.17)	-
Presence of Tophi (Yes) N (%)	40 (45)	-
Systolic Blood Pressure Mean (Mm Hg) (SD)	142.65 (±17.37)	-
Diastolic Blood Pressure Mean (Mm Hg) (SD)	85.72 (±10.19)	-

The significance of the association between the 2 classified subgroups of patients with gout and healthy participants was tested using the Mann–Whitney *U* test (non-parametrical continues values) and Fisher’s exact test (categorical values) and ($P < 0.05$). The data are presented as mean ± Standard Deviation (SD).

Cell isolation and culture

Using lithium heparin tubes, peripheral blood of patients and healthy participants was collected. Total peripheral blood mononuclear cells (PBMCs) were isolated using Ficoll (Ficoll-Paque Plus, GE Healthcare).

Monocytes (CD14⁺/CD16⁻) were isolated from total PBMCs of healthy participants (Supplementary table 1) through a monocytes isolation microbead kit (Lot.# 5170817557) by AutoMACS apparatus (Miltenyi) according to the manufacturer guidelines. After 30 minutes of resting in RPMI-1640 (Gibco RPMI 1640 Glutamax medium enriched with 10% Fetal Bovine Serum (FBS) and 1% penicillin/streptavidin, Sigma-Aldrich), 0.5×10^6 monocytes per condition were either kept unstimulated or stimulated with 0.1mg/ml of monosodium urate crystals (MSU) (5mg, Cat. # tlr-msu, InvivoGen,) suspended in sterile phosphate buffered saline (PBS) buffer (Lot # RNBG2264, Sigma-Aldrich life-science), MSU in combination with 10nM rapamycin (Cat. #S1039, Batch # S103911 (Sirolimus)) and MSU in combination with sterile metformin (1gr, Cat. # tlr-metf, InvivoGen) suspended in RPMI medium (as described above) at a final concentration of $38.71 \mu\text{M}$ (1gr, Cat. # tlr-metf, InvivoGen). The study design was optimized and the incubation times were applied according to the readout of the experiment. To exclude bacterial endotoxin contamination within the MSU crystal preparation that might cause activation of the cells during incubations, a Limulus Amebocyte Lysate (LAL) assay (LAL Chromogenic Endotoxin

Quantitation Kit, Cat. # 88282, ThermoFisher Scientific) was performed following the manufacturers' procedure. The quantified endotoxin level (EU/ml) was below the detection limit which excludes any endotoxin contamination in MSU crystals.

Gene expression analysis

RNA was isolated from total PBMCs of patients with gout and healthy individuals (Cat. # /ID: 80204, Qiagen All-prep RNA purification) according to the manufacturer guidelines. Subsequently cDNA was created using the Biorad iScript kit. Quantitative polymerase chain reaction (qPCR) was performed on a Quantstudio QPCR apparatus, with Taqman Beadchip technology (Applied Biosystems) under conditions as specified by the manufacturer. As housekeeping genes, *GUSB* and *GAPDH* were included to normalize expression. The following genes were included in the analyses; protein kinase B (*Akt1*), DEP domain-containing mTOR-interacting protein (*DEPTOR*), glyceraldehyde 3-phosphate dehydrogenase (*GAPDH*), beta-glucuronidase (*GUSB*), interleukin 10 (*IL-10*), (interleukin 6) *IL-6*, mammalian target of rapamycin (*mTOR*), nuclear factor-kappa-B p105 subunit (*NFκB1*), phosphatase and tensin homolog (*PTEN*), rapamycin-insensitive companion of mammalian target of rapamycin (*RICTOR*), regulatory-associated protein of mTOR (*RAPTOR*). These specific genes were chosen due to their involvement in mTOR complex.

The expression level of *mTOR* genes was determined using synthesized cDNA (Biorad iScript kit) from RNA that was extracted from 0.5×10^6 of total PBMCs, T lymphocytes ($CD3^+/CD56^-$), B lymphocytes ($CD19^+$), monocytes ($CD14^+/CD16^-$), Classical, Intermediate and Nonclassical monocytes. The cells were lysed after 6 and 24 hours and consecutively cDNA was generated. Taqman single gene qPCR assays were performed on a Quantstudio apparatus (Applied Biosystems). The Housekeeping *GUSB* and *GAPDH* Genes (HKG) were included to normalize the gene expression.

Fluorescence activated cell sorting (FACS) quantification and analysis

Healthy participants' PBMCs were assessed by fluorescence activated cell sorting (FACS) (FACS Aria_{III}, BD Biosciences) (**Supplementary table 2**). Cellular markers that were included in FACS quantifications were: CD3⁺ (AF700, mouse anti-human, Clone UCHT1 (isotype IgG2a), 1:50 dilution, Cat.# 300424, Biolegend)/CD56⁻ (PE-CF594, mouse anti-human, Clone B159) (isotype IgG1), 1:25 dilution, Cat.# 562328, BD) for T lymphocytes, CD19⁺ (PECy7, mouse anti-human, Clone LT19 (isotype IgG1), 1:40 dilution, Cat.# 130-091-247, Miltenyi) for B lymphocytes, CD14⁺ (BV785, mouse anti-human, Clone M5E2 (isotype IgG2a), 1:100 dilution, Cat.# 301840, Biolegend)/ CD16⁺(FCγRII) (APC, mouse anti-human, Clone ebio-CB16 (isotype IgG1), 1:20 dilution, Cat.# 17-0168-42, eBioscience) monocytes and CD3⁻/CD56⁺ NK cells. The three cell-subsets within the main group of monocytes were differentiated by gating the cells from the CD14⁺/CD16⁺ gate according to the brightness of CD14⁺⁺ (Classical), CD14⁺CD16⁺ (Intermediate) and CD16⁺⁺ (Nonclassical).

The percentage of activation markers of Classical, Intermediate and Nonclassical monocytes' subsets were quantified after gating the CD14⁺/CD16⁺ monocytes, by measuring the expressed CD163⁺ (APC, mouse anti-human, eBioGHI/61 (isotype IgG1), 1:20 dilution, Cat.# 17-1639-42, eBioscience) and CD86⁺ (BV605, mouse anti-human IT2.2 (isotype IgG2b) 1:70 dilution, Cat.# 2127150, Sony Biotechnology) percentage on the surface of the cells. Isolation and stimulation (6 and 24 hours) of the cell-subsets were performed as described above. The cells were subsequently acquired using flow cytometry (FACS Aria_{III}, BD Biosciences).

Intracellular FACS was applied to assess the activation level of intracellular mTOR pathway at the protein level after stimulating monocytes for 15 minutes according to the abovementioned protocol. Monocytes were first stained extracellularly for abovementioned cell marker panel to distinguish Classical, Nonclassical and intermediate monocytes. After being fixed and permeabilised, monocytes were stained for phosphorylated S6 (pS6) with human anti-pS6 antibody (Anti-S6 pS240-FITC human, monoclonal recombinant IgG1,

1:5 dilution, Miltenyi biotec). The pS6 level was quantified and represented as the mean fluorescent intensity (MFI) in monocytes.

Live Imaging technique

The microscopic live imaging technique was utilized to visualize the monocytes over time. In medium rested monocytes (2×10^5 /condition) were administered to the medium (RPMI 1640 (10% FBS, 1% Penicillin-Streptavidin)) containing Hoechst 33342 (20 μ M) for 30 min at 37°C. The cells were then washed and stimulated according to the previously described stimuli/inhibitors in RPMI 1640 (without phenol red) (10% FBS, 1% Penicillin-Streptavidin) containing 4nM Sytox Green (Life Technologies) and plated in pre-coated wells of a 96-well plate (clear bottom) (Ibidi). Monocytes were recorded on the Pathway 855 bio-imaging system (BD Biosciences) with a 20x objective during a period of 5 hours at 5% CO₂ at 37°C. Using an Orca high-resolution CCD camera and four fields of view, every 13 minutes, a set of two images Exc/Em: 350/461 nm (Hoechst) and 504/523 nm (Sytox Green)) was captured. AttoVision software (version 1.7/855) controlled the system.

Monocyte markers

Cytokine measurements by Luminex

Cytokines were quantified utilizing a multiplex Luminex assay. Quantification of the cytokines was done using an in-house developed and further validated (ISO9001 certified) multiplex immunoassay (Laboratory of Translational Immunology, University Medical Center Utrecht) based on Luminex technology (xMAP, Luminex, Austin TX USA). Each sample was a supernatant of 0.5×10^6 monocytes per condition that were left either untreated, incubated with MSU crystals, MSU crystals and rapamycin and MSU crystals and metformin during 6 and 24 hours. The monocytes were centrifuged (300g, 8 min) and the supernatant was collected and kept in -80°C until measured. The cytokine panel included interleukin 1 receptor alpha (IL-1R α), interleukin 1 (IL-1 α), interleukin 1 beta (IL-1 β), interleukin 6 (IL-6), interleukin 8 (IL-8), interleukin 10 (IL-10), interleukin 18 (IL-18),

tumor necrosis factor alpha (TNF- α), interferon gamma (IFN- γ), monocyte chemotactic protein-1 (MCP-1), macrophage inflammatory protein (MIP-1) and interferon gamma-induced Protein 10 (IP-10). A Biorad FlexMAP3D (Biorad laboratories, Hercules USA) in combination with xPONENT software version 4.2 (Luminex) was included to perform the acquisition. To analyze the data, 5-parametric curve fitting using Bio-Plex Manager software version 6.1.1 (biorad) was assessed.

Statistical analysis

Statistical analyses were performed using IBM SPSS Statistics v23 (SPSS, Chicago, IL; 60606 U.S.A.) and Graphpad Prism v6 (GraphPad Software, San Diego, California). Microscopic live imaging captures were analyzed using ImageJ 1.51h program (Java 1.8.0_111, National institutes of Health, USA). Where appropriate testing for significant differences in categorical groups was performed using the student T-test ($P < 0.05$).

Results

Genes of mTOR pathway have a higher relative expression in gout patients compared to healthy controls

Exploiting a custom Taqman gene expression array, we investigated the expression of genes involved in the mTOR pathway (*mTOR*, *Rictor*, *Raptor*, *Deptor*, *AKT1* and *PTEN*) in *ex vivo* PBMCs from 89 crystal proven patients with gout and 89 healthy controls (Table 1). A higher expression of the genes involved in the mTOR complex was observed in patients with gout ($P < 0.0001$). The expression of *PTEN*, an mTOR inhibitor was lower in patients ($P < 0.0001$). Taken together, these results demonstrate an upregulation of various genes involved in mTOR signaling in gout (**Figure 1A**).

Stimulation of PBMCs from healthy subjects with MSU crystals leads to increased mTOR gene expression in vitro

To investigate if the increased expression of mTOR genes in gout patients could be caused by contact with MSU crystals in these patients, we cultured PBMCs from healthy subjects with MSU crystals *in vitro* for 24 hours and quantified mTOR expression. We observed an increase of *mTOR* expression in the PBMCs challenged with MSU crystals ($P = 0.0007$) (**Figure 1B**).

MSU crystal stimulation induces mTOR gene expression in immune cell-subsets in Vitro

The gene expression level of *mTOR* upon (*in vitro*) MSU crystal stimulation was measured in T and B lymphocytes and total monocytes of 10 healthy participants immediately after isolation of the cells (T=0) and after stimulating the cells for 6 and 24 hours. After 6 hours of stimulation, MSU crystals induced *mTOR* gene expression in B lymphocytes ($P = 0.0006$) and monocytes ($P = 0.024$) but not in T lymphocytes ($P = 0.085$). After 24 hours, there was an induction of *mTOR* gene expression in T lymphocytes ($P = 0.0001$), B lymphocytes ($P = 0.0008$) and monocytes ($P < 0.0001$) as compared to the T=0 conditions (**Figure 1C**).

Encountering MSU crystals in vitro substantiates a reduction of monocytes in PBMCs

In order to study the effect of MSU crystal stimulation on immune-cell subsets in more detail, PBMCs were challenged with MSU crystals for 6 and 24 hours (Figure 1D). After 6 hours of stimulation with MSU crystals, there was a significant reduction in the proportion of monocytes within the total PBMCs cultured ($P=0.0002$). Reciprocally, there was an increase in the proportion of T lymphocytes ($P=0.012$). Consistent with this, the proportion of monocytes in the PBMCs that had been incubated for 24 hours showed a further decrease in the proportion of monocytes ($P=0.001$). Accordingly, an increase of the proportion of T lymphocytes ($P=0.0004$) and NK cells ($P<0.0001$) was observed (**Figure 1D**). In order to investigate the immune-cell subsets that might be responsible for mTOR activation and subsequently the inflammatory reaction in patients with gout, we evaluated the ratio of the subsets. In PBMCs of patients with gout and healthy participants, the ratio of the T ($P=0.22$) and B ($P=0.01$) lymphocytes and NK ($P=0.01$) cells was higher in patients with gout as compared to healthy participants. The total monocytes however were lower in patients with gout as compared to healthy participants ($P=0.007$). The percentage of Classical ($P=0.01$) and Intermediate ($P=0.03$) monocytes were lower in patients with gout. There was a similar trend in Nonclassical monocytes ($P=0.05$) (**Supplementary figure 2**). The mean percentages (\pm SD) of the immune cell-subset of patients and healthy participants are presented in **Supplementary table 2**.

Figure 1

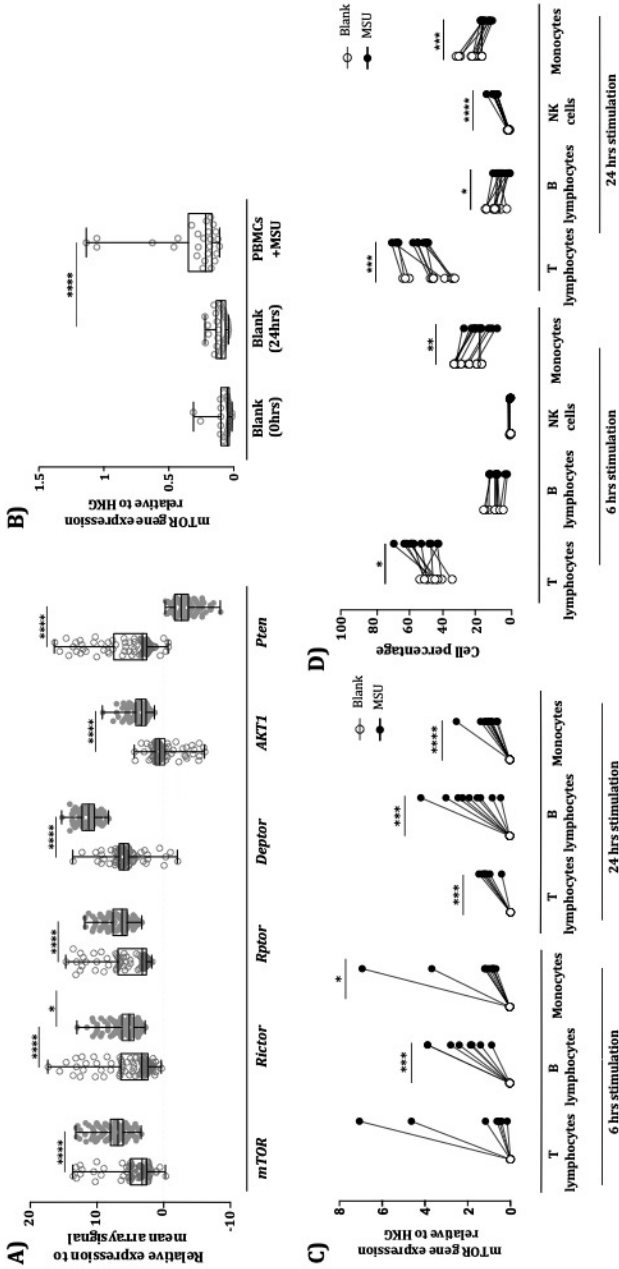


Figure 1(A) The gene expression of mTOR pathway related genes in patients with gout (N=89) and healthy participants (N=89) (filled dots and empty dots respectively). **1(B)** Expression of *mTOR* after stimulating PBMCs of healthy participants with MSU crystals *in vitro* (N=28) **1(C)** Gene expression level of *mTOR* upon MSU stimulation after 6 and 24 hours of stimulation as compared to basal level of the gene at T=0 in immune cell subsets. The gene expression level of *mTOR* is increased in B lymphocytes ($P=0.0006$) and monocytes ($P=0.024$) after 6 hours of stimulation. After 24 hours of stimulation, there was a significant induction of *mTOR* gene expression in T lymphocytes ($P=0.0001$) and monocytes ($P=0.0008$) as compared to the T=0 conditions. **1(D)** After 6 hours of stimulation with MSU crystals, there was a reduction in the proportion of monocytes within the total PBMCs cultured ($P=0.0002$) within the MSU challenged condition compared to the control. Reciprocally, there was an increase in the proportion of T lymphocytes ($P=0.012$). In line with this, the proportion of monocytes in the PBMCs that had been incubated for 24 hours showed a further decrease in the proportion of monocytes ($P=0.001$). Accordingly, an increment of the proportion of T lymphocytes ($P=0.0004$) and NK cells ($P<0.0001$) was observed.

7

Monocytes actively engage MSU crystals and undergo cell death after contact

To better gauge the reaction of monocytes towards MSU crystals, we performed live imaging of CD14⁺ monocytes encountering MSU crystals. We used two dyes, namely, Sytox Green (green color that visualizes dead cells) and Hoechst (blue color that visualizes live cells) to quantify the number of monocytes dying upon encountering MSU crystals. During 7 hours of imaging we observed an active movement of monocytes towards MSU crystals. A large proportion of these monocytes undergo cell death upon encountering these crystals. The full movies are made available on the website of the journal (**Supplementary movies S1 (MP4)**). In **figure 2A** we show representative snapshots made every hour. After 7 hours 61% of the monocytes cultured in medium only were still alive, whereas only 35% of the monocytes stimulated with MSU crystals survived ($P<0.0001$) (**Figure 2B**). The imaging experiment was repeated 8 times with analogous outcomes. The results of the similar assessments and analysis on Classical, Nonclassical and Intermediate monocytes are presented in **Supplementary figure 1**.

Proportions of CD14⁺⁺ (Classical), CD14⁺CD16⁺ (Intermediate) and CD16⁺⁺ (Nonclassical) monocytes within the total PBMCs are all decreased after encountering MSU crystals

After 6 hours of stimulating PBMCs with MSU crystals we quantified the number of monocytes by flow-cytometry and further differentiated the monocytes from the CD14⁺/CD16⁺ gate according to the brightness of CD14⁺⁺ (Classical), CD14⁺CD16⁺ (Intermediate) and CD16⁺⁺ (Nonclassical) monocytes.

After culturing PBMCs for 6 hours with MSU crystals, we observed a significant reduction in proportion of classical monocytes ($P=0.0008$), Nonclassical monocytes ($P=0.02$) and intermediate monocytes ($P=0.04$) within the total PBMC number. The PBMCs that were incubated for 24 hours showed a significant reduction in Classical ($P<0.0001$) and Intermediate ($P=0.001$) monocytes, while the reduction of Nonclassical monocytes ($P=0.34$) was not significant (**Figure 2C**). The mean percentages (\pm SD) of the immune cell-subsets of patients and healthy participants are presented in Supplementary table 2.

mTOR inhibition by rapamycin or metformin reduces MSU crystal induced monocyte death

Since we observed an increased rate of cell death and an increased expression of mTOR in monocytes encountering MSU crystals we investigated whether mTOR inhibition, which promotes autophagy and decreases inflammatory responses and response to apoptotic cells, would have a dampening effect on monocyte death and MSU crystal induced inflammation. First, we evaluated whether the observed increased mTOR gene expression was reflected in the protein level. We measured the phosphorylation of S6 ribosomal protein (S6) at serine 240/244, which is downstream from mTOR activation and therefore commonly used as readout of mTOR activation. After resting, monocytes were stimulated for 15 minutes with MSU crystals and MSU crystals with metformin. As presented in **Figure 2D**, metformin caused a decrease of the pS6 mean fluorescence intensity in total ($P=0.013$), Classical ($P=0.015$) and Nonclassical ($P=0.040$) monocytes within 15 minutes.

To investigate temporal stability of the inhibitory effect of metformin in monocytes we performed titration assays where we quantified the expression level of *mTOR* gene in monocytes (N=5) after 3, 6, 9 and 12 hours of incubation in the presence of MSU crystals. After 3 hour of metformin stimulation in MSU crystal challenged monocytes, we observed a significant decrease in *mTOR* gene expression as compared to MSU crystal challenged monocytes ($P=0.0007$). This inhibitory effect of metformin was stable after 6 hours ($P=0.008$) (**Figure 3D**). The inhibitory effect of metformin in MSU crystal challenged monocytes was until 9 hours of stimulation ($P=0.19$) and reached its minimum after 12 hours of stimulation ($P=0.27$). In the same monocytes and the same setting, *NFkB* gene expression was quantified. After 3 ($P=0.027$) and 9 ($P=0.026$) hour metformin stimulation, there was a significant inhibition of *NFkB* (**Supplementary figure 3a**). Interestingly, metformin had an inhibitory effect on *IL-1 β* in monocytes after 3 ($P=0.023$), 9 ($P=0.024$) and 12 ($P=0.041$) hours. Similarly, after 6 hours ($P=0.063$) there was a trend of inhibitory effect of metformin on monocytes (**Supplementary figure 3b**).

Since we were now able to inhibit mTOR *in vitro* with metformin and rapamycin, we

co-cultured monocytes with medium only, with MSU crystals, with MSU crystals and metformin or with MSU crystals and rapamycin. In addition, we cultured monocytes with rapamycin and metformin without MSU crystals. These conditions were all evaluated alongside live imaging, at the same time, in which monocytes from a healthy participant were cultured in every condition mentioned and analyzed. This experiment was performed 6 times. When we quantified the proportion of cell death by ImageJ, comparing “live cell” dye within each snapshot (Time between each snapshot T=13 minutes), we observed that monocytes co-cultured with MSU crystals and rapamycin (cells alive 56%) or metformin (cells alive 59%) had a significantly lower death rate as compared to monocytes stimulated with MSU crystals only after 7 hours (cells alive 35%) (both $P < 0.0001$). The rate of cell death in the monocytes treated with mTOR inhibitors and MSU crystals was similar to that of monocytes cultured without MSU crystals (61% alive). In **figure 2A** we show representative snapshots made every hour of monocytes cell-culture at T=0 to 7 hours and **figure 2B** shows the number of alive cells per condition over time.

Figure 2

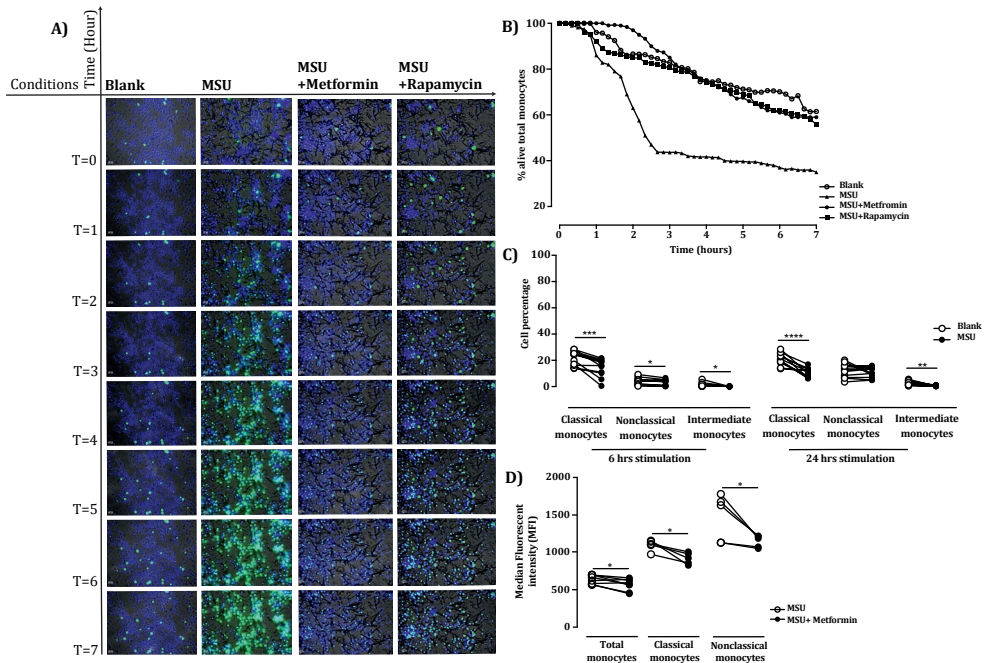


Figure 2 (A) Captures made from monocytes, collected from one healthy participant that were kept unstimulated, stimulated with MSU crystals, MSU crystals with rapamycin and MSU crystals with metformin at the time 0 to 7 hours are demonstrated. (blue is alive cell, green is dead cell). **2(B)** Captures made every 13 minutes from the same cells were analyzed and plotted against the time represented in hours. Treating the monocytes with rapamycin ($P < 0.0001$) and metformin ($P < 0.0001$) upon MSU stimulation induces cell survival as compared to MSU crystal stimulation alone. **2(C)**. *In Vitro*, 6 hours of MSU stimulation of PBMCs showed a reduction in percentage of Classical ($P = 0.0008$), Nonclassical ($P = 0.02$) and Intermediate ($P = 0.04$) cells. After 24 hours stimulation Classical ($P < 0.0001$) and Intermediate ($P = 0.001$) monocytes were significantly reduced. after crystal stimulation, while nonclassical are unchanged ($P = 0.34$) **2(D)**. In monocytes from healthy participants ($N = 10$), metformin gave a significant reduction in phosphorylation of S6 protein after 15 minutes of stimulation with MSU crystals.

mTOR inhibition by metformin or rapamycin reduces pro-inflammatory cytokine release by monocytes upon encountering MSU crystals in vitro

To assess whether *mTOR* inhibition leads to less cytokine production upon monocytes exposure to MSU crystals *in vitro*, we quantified the release of IL-1R α , IL-1 α , IL-1 β , IL-6, IL-8, IL-10, IL-18, TNF- α , IFN- γ , MCP-1, MIP-1 and IP-10 by Luminex in monocytes from eleven donors. Monocytes were cultured with MSU crystals. We compared cytokine levels

between MSU-cultured monocytes with MSU crystals alone or co-cultured with metformin or rapamycin, which are both mTOR inhibitors. The monocytes co-cultured with MSU crystals and rapamycin showed a reduction in levels of IL-1 β ($P=0.02$), IL-6 ($P=0.02$), IL-8 ($P=0.0017$), IL-10 ($P=0.024$), IL-18 ($P=0.0009$), IFN- γ ($P=0.001$), MCP-1 ($P=0.01$), MIP-1 ($P=0.0026$) and IP-10 ($P=0.029$). in the presence of metformin a reduction in levels of IL-1 β ($P=0.02$), IL-6 ($P=0.31$), IL-8 ($P=0.01$), IL-10 ($P=0.0051$), IL-18 ($P=0.045$), TNF- α ($P=0.042$), MCP-1 ($P=0.006$), MIP-1 ($P=0.04$) and IP-10 ($P=0.046$) was observed when compared to the monocytes cultured with MSU crystals alone. The reduced cytokine level after 24 hours of incubation with MSU crystals and rapamycin was IL-1 α ($P=0.027$), IL-8 ($P=0.02$), IL-10 ($P=0.005$), MCP-1 ($P=0.0032$) and MIP-1 ($P=0.005$). Reduced cytokine levels in monocytes incubated with metformin and crystal stimulation after 24 hours was IL-1 α ($P=0.032$), IL-1 β ($P=0.04$), IL-6 ($P=0.034$), IL-10 ($P=0.015$), TNF- α ($P=0.0024$), MCP-1 ($P=0.008$) and MIP-1 ($P=0.04$). The quantified values are represented on a logarithmic scale (**Figure 3A**). Color heat-maps represent the effect of stimuli and inhibitors on the cells (**Figure 3B**).

Metformin treatment associates with low flare frequency in patients with gout

To scrutinize whether mTOR inhibition through metformin in gout patients leads to a lower frequency of gout flares we performed a retrospective cohort analyses in 23 Caucasian patients with gout and metformin use in comparison to 19 patients with gout and diabetes without using metformin. As diabetic comedication insulin use was allowed. Patients were selected from the Dutch cohort (**Table 1**) and Caucasian gout patients from New Zealand (**Supplementary table 3**). Our analysis demonstrates that patients with gout who were treated with a combination of metformin and allopurinol have significantly lower percentage of attack frequency as compared to patients who were treated with allopurinol alone ($P=0.010$) (**Figure 3E**).

Figure 3

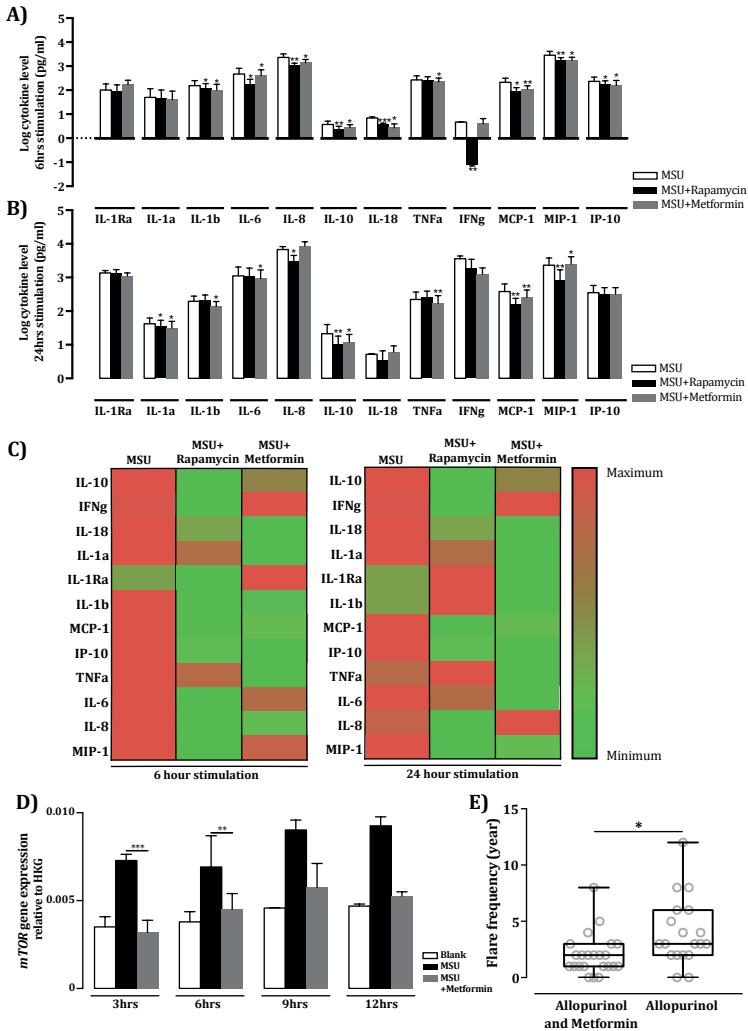


Figure 3 (A, B) Differential cytokine expression in monocytes stimulated with MSU crystals with and without mTOR inhibition by metformin or rapamycin. The cytokines that were significantly differently secreted from monocytes treated with MSU crystals and rapamycin as compared to MSU only after respectively 6 and 24 hours. **3(C)** Heatmap representing the changes in monocytes' cytokine expression upon stimulation with MSU crystals only, MSU crystals with rapamycin and MSU crystals with metformin. **3(D)** Inhibitory effect over time of metformin on *mTOR* gene expression (normalized for Housekeeping Gene (HKG) expression) in MSU challenged monocytes. In monocytes of healthy participants (N=5). Blank condition contains unstimulated monocytes that have the same incubation time as the stimulated conditions. **3(E)** Patients with gout treated with a combination of allopurinol and metformin have significantly less recurrent flairs as compared to patients treated only with allopurinol ($P=0.010$).

Discussion

The main conclusion of this study is that PBMCs from patients with gout have a signature of increased mTOR signaling as compared to healthy participants. By performing *in vitro* experiments we showed that MSU crystals provoke upregulation of mTOR pathways gene expression, IL-1 β IL-6, IL-8, IL-18 release and cell death in monocytes. We were able to inhibit these phenomena by adding mTOR inhibitors rapamycin and metformin. When we analyzed the effect of metformin on gout flares in a retrospective analysis of patients with gout with diabetes stratified according to metformin treatment, we observed significantly lower gout attack frequency as compared to patients not treated with metformin.

An interesting finding of our study is the active engagement of monocytes towards MSU crystals, which induces a form of acute cell death. It is well known that there is an overlap in apoptosis and necrosis *in vivo* when immune cells encounter strong danger signals[27]. It is established that necrosis leads to NACHT, LRR and PYD domains-containing protein 3 (NLRP3) activation and increased IL1 β production, an important feature of gout and also observed in our study. Interestingly, mTOR activation enhances the process of necrosis[28]. To apply this to gout and our study, it is conceivable that necrosis of monocytes when encountering MSU crystals leads to activation of the inflammasome pathway and release of pro-inflammatory cytokines, as we demonstrate. The high expression of mTOR within monocytes further facilitates the pro-necrotic state within gout patients. When mTOR is inhibited there is a lower tendency towards cell death and consequently less inflammasome activity and inflammation, as we display in our study as well. Hence, the very start of the gout attack might lie in the encounter of monocytes with MSU crystals and seems to be modulated by mTOR.

Our findings are in line with a recent study also showing that stimulation of monocytes with MSU crystals enhances mTOR activation[10]. Very little research has been performed within the field of mTOR inhibition and gout, however, most available data concern the effects of metformin treatment in gout disease activity. A large retrospective case-control study

(N=7536) in diabetes patients showed that the use of metformin decreases the odd ratios for developing gout compared to patients not using metformin[29]. The authors, however, mainly focused on the finding that poorly controlled diabetes as defined by HbA1c levels is correlated with a decreased incidence of gout. Two small scale studies conducted in Russia (N=30 and N=26) in non-diabetic patients with gout showed that metformin reduces the frequency of gout attacks, lowers uric acid and led to normo-uricemia in 11 patients[30,31]. Of interest is the observation that metformin is able to interfere directly with the purine pathway, which might be the mode of action for the lowering of uric acid levels, the latter however has not yet been clearly proven [32,33].

The evidence for an anti-inflammatory effect of metformin has been mounting over the past years. It is known that metformin activates AMPK (5' adenosine monophosphate-activated protein kinase) to inhibit NF- κ B via the PI3K (Phosphoinositide 3-kinase)-Akt1 pathway and reduces the production of NO (nitric oxide), prostaglandin E2, and pro-inflammatory cytokines (IL-1 β , IL8, IL-6 and TNF- α) in monocytes and macrophages[34,35]. One study that included over 4000 pre-diabetic patients showed a significant reduction of CRP levels when treated with metformin as compared to placebo after 12 months[36]. Moreover, in monocyte-derived macrophages, metformin seemed to interfere directly with the inflammasome, orchestrating an inhibition of IL-1 β maturation in patients with type 2 diabetes treated with metformin[37]. Patients with gout are typified by inflammasome induction and high circulating IL-8 levels and metformin is likely to be a suitable treatment for these patients since it is an effective inflammasome and IL-8 suppressor.

Metformin is the first-choice drug for treating type 2 diabetes, it is effective in reducing the hyperglycemic state decreases insulin resistance. Less obvious, but well-proven is the fact that metformin reduces the cardiovascular risk in patients with diabetes. The UK Prospective Diabetes Study (N=5500) demonstrated a substantial beneficial effect of metformin therapy on cardiovascular disease outcomes, with a 36% relative risk reduction in all-cause mortality and a 39% relative risk reduction in myocardial infarction[38]. The

exact mechanism of action by which metformin protects the vasculature is not known, but it is thought to be a combination of improving lipid metabolism, AMPK induction and reduction of reactive oxygen species. Of interest for the gout population, which is at high risk to have or develop diabetes, metformin reduced the incidence of diabetes in high risk groups[39].

Our study has strengths and weaknesses, the strength of our study lies in the fact that we started from *ex vivo* patient material and observations, which we translated in an *in vitro* model and validated retrospectively in an *in vivo* observation. This chain of experimental settings makes our findings more robust to translation to the clinical setting. Our experiments were performed in parallel on the same apparatus and analyzed by the same algorithms to avoid mistakes or bias by measurement or observer. Another strength is that the observations were made on both gene expression and protein level with various techniques. All patients included in *the ex vivo* study had crystal proven gout, which is the golden standard of diagnosis. Moreover, the concentrations of metformin and rapamycin used in our experimental settings were derived from real life plasma concentrations of these drugs in patients being treated with these drugs in clinical practice. This makes the results more relevant to clinical use. A weakness of our study is the small cohort in which we performed a retrospective analysis on the effects of metformin on the frequency of gout attacks. Although highly informative in the light of our study, these results need to be confirmed in a larger prospective study to make way for use of metformin in gout clinical practice. In our retrospective study we did not have longitudinal data on glucose status, kidney function, treatment adherence and dose escalation, therefore these results should be regarded with caution for direct extrapolation to clinical practice without further prospective and preferably randomized clinical trials.

As described above, metformin has many potential beneficial effects on the disease course in gout. It has properties that inhibit inflammation through the mTOR and NLRP3 pathways, it decreases cardiovascular risk and it potentially might be able to directly decrease uric acid

levels and gout flares. The currently available drugs are well able to target one of these domains, (e.g. allopurinol/colchicine in uric acid lowering, canakinumab for inflammasome targeting), however, none of them are able to target all three domains. Up till now, it is not clear if any of the currently used drugs reduce cardiovascular and metabolic risk.

A large body of evidence shows that metformin reduces cardiovascular risk and increases insulin-sensitivity, reducing the burden of diabetes. Hence, taking also into account the favorable drug profile and our observations, we advocate to investigate metformin as an add-on therapy for patients with gout in a prospective study to clarify whether metformin is able to reduce the burden of gout flares and comorbidities.

Acknowledgements

J.C.B. is supported by a VENI Award from the Netherlands Organization for Scientific Research (N.W.O. project number 91614041). Multiplex Luminex immunoassays were in-house developed by W. De Jager, H. te Velthuis, B.J. Prakken, W. Kuis, G.T. Rijkers, validated and performed at the Multiplex core facility of the Laboratory for Translational Immunology (LTI) of the University Medical Center Utrecht

Author contribution

All authors approved the final version after being involved in drafting and revising the article for important intellectual content. As the corresponding author, N. Vazirpanah had full access to the data and takes responsibility for the accuracy of the performed analysis and the integrity of the data. N. Vazirpanah, TRDJ Radstake and J.C.A. Broen were involved in design of the study. Execution, analysis and writing of the manuscript was performed by N. Vazirpanah. A. Ottria, M. van der Linden respectively contributed in FACS and Live Imaging of this study. C. Wichers was involved in performing gene arrays. M. Schuiveling and M. Zimmerman thought along on rapamycin and metformin stimulations. E. Van Lochem and M. Jansen were involved in inclusion of Dutch gout patients and T. Merriman participated by including patients with gout from the New Zealand.

Supplementary files

Supplementary table 1. Baseline characteristics of healthy individuals participating in functional experiments

	Male n (%)	Age
Healthy participants (n=30)	27 (90)	48 ± 13.88

The data are presented as mean ± SD.

Supplementary table 2. Percentages of T and B lymphocytes, NK cells, total monocytes, Classical, Nonclassical and Intermediate monocytes in patients with gout, healthy participants in *in Vivo* and healthy PBMCs stimulated *in Vitro*.

	T lymphocytes	B lymphocytes	NK cells	Total monocytes	Classical monocytes	Nonclassical monocytes	Intermediate monocytes
Gout	61.80 (±17.30)	23.24 (±11.55)	10.50 (±2.41)	10.48 (±7.69)	3.90 (±2.50)	8.86 (±7.76)	0.04 (±0.05)
Healthy individuals	54.23 (±4.50)	7.76 (±4.39)	0.70 (±0.19)	35.20 (±7.02)	18.88 (±4.77)	18.88 (±4.77)	1.22 (±0.4)
6 hours MSU stimulation	54.82 (±8.47)	8.93 (±3.33)	0.84 (±0.35)	18.6 (±5.61)	14.42 (±6.81)	2.86 (±2.39)	0.11 (±0.09)
6 hours unstimulated	45.84 (±5.25)	9.96 (±3.67)	0.81 (±0.25)	27.43 (±6.27)	21.71 (±5.56)	3.80 (±2.86)	1.29 (±1.69)
24 hours MSU stimulation	58.15 (±8.18)	5.56 (±3.30)	9.47 (±1.80)	15.58 (±2.42)	10.65 (±3.47)	10.86 (±4.07)	0.55 (±0.36)
24 hours unstimulated	46.75 (±11.17)	10.14 (±3.89)	1.15 (±0.46)	23.63 (±5.29)	21.12 (±4.69)	12.19 (±5.37)	2.66 (±1.62)

The data are presented as mean of the percentages ± SD

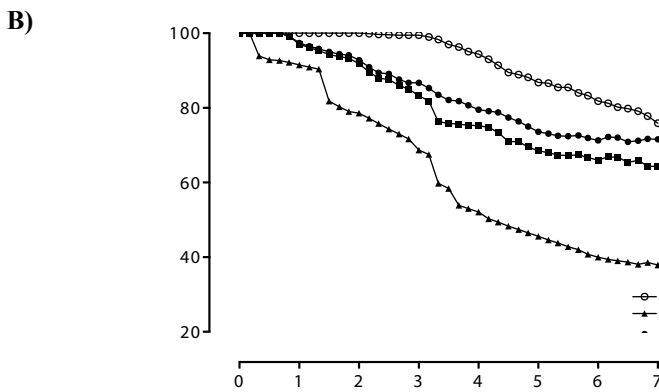
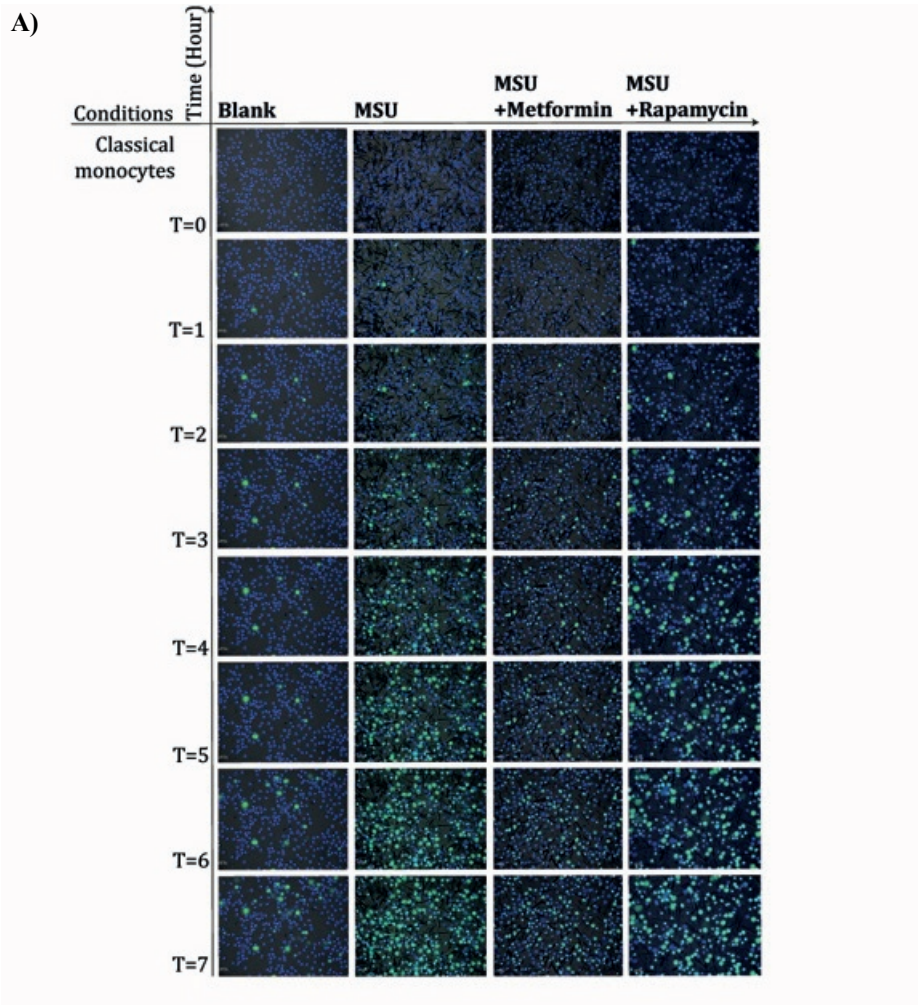


Supplementary table 3. Baseline characteristics of patients with gout from New Zealand.

	Male n (%)	Age	Allopurinol (yes) n (%) (mean 200mg/day)	Metformin (yes) n (%) (mean x mg/day)	Diabetes (type 2) (yes) n (%)	Creatinine level (µmol/L)	Body mass index (kg/m ²) (mean ± SD)	Serum urate (mmol/L)	Total number of flares per year (mean ± SD)	Presence of tophi (yes) n (%)
Gout (n=9)	7(77.8)	67.33 ± 8.15	7 (87.50)	5 (55.60)	9(100)	145.38 (± 48.18)	32.09 (± 6.20)	0.52 (± 0.12)	2.22± (1.86)	9 (100)

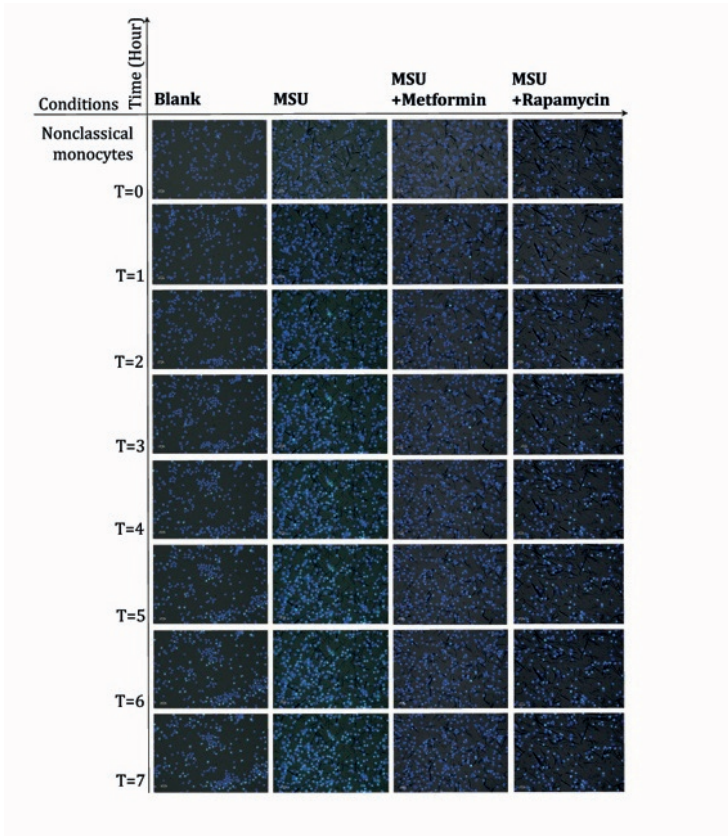
The data are presented as mean ± SD.

Supplementary Figure 1

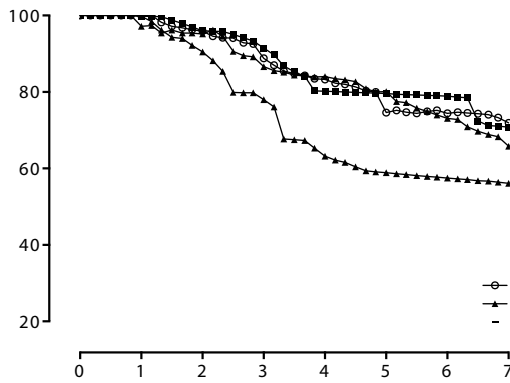


7

C)

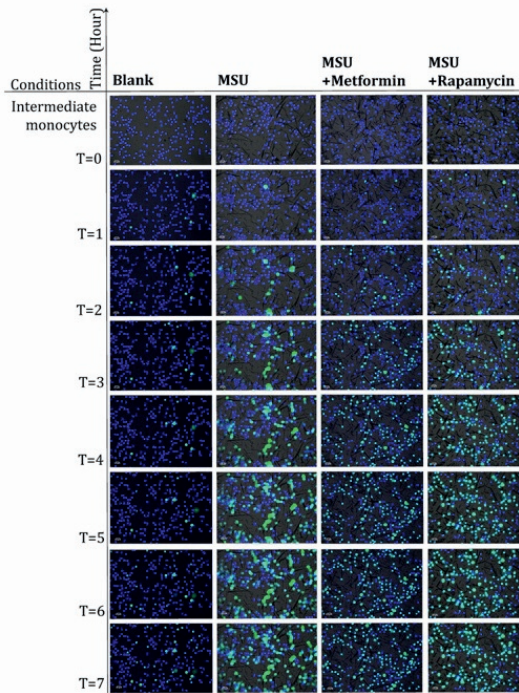


D)

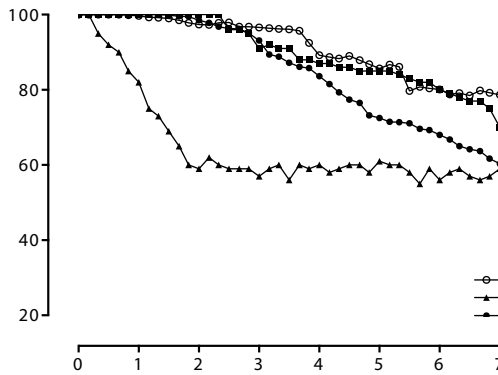


7

E)



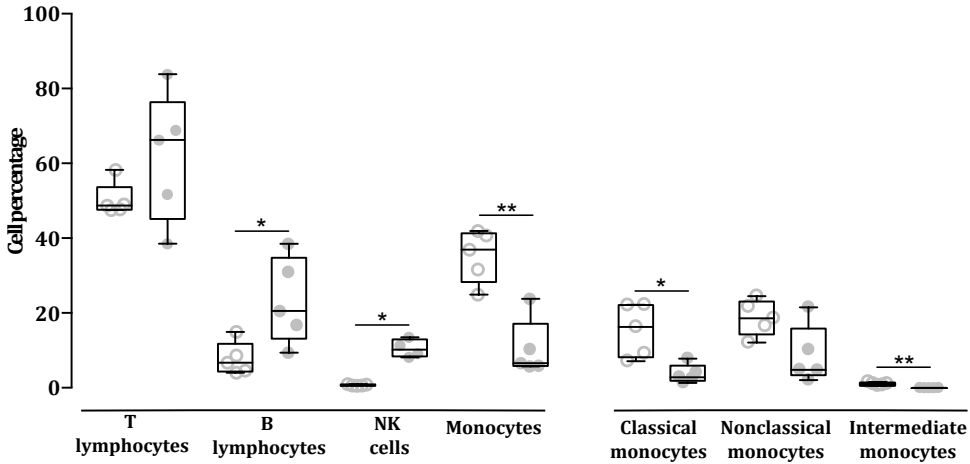
F)



Supplementary Figure 1. Live imaging demonstrates an induction in mortality of monocytes upon MSU crystal stimulation which is compensated by treating the cells with rapamycin or metformin. Captures made from (A) Classical, (C) Nonclassical and (E) intermediate monocytes collected from one healthy participant that were kept unstimulated, stimulated with MSU crystals, MSU crystals with rapamycin and MSU crystals with metformin at the time 0 to 7 hours are demonstrated. Captures made every 13 minutes from the same cells were analyzed and plotted against the time represented in hours. (B) In Classical monocytes, the survival percentage of untreated, stimulated with MSU crystals only and stimulated with combination of MSU crystals and rapamycin or metformin was respectively 39.9%, 41.2%, 51.2%, 24.9%. This difference as compared to MSU crystal challenged cells was significant ($P < 0.0001$). (D) The Nonclassical monocytes that were unstimulated and stimulated with MSU crystals and rapamycin or metformin had a cell survival of 57.4%, 40.2% and 50.4% and were all significantly

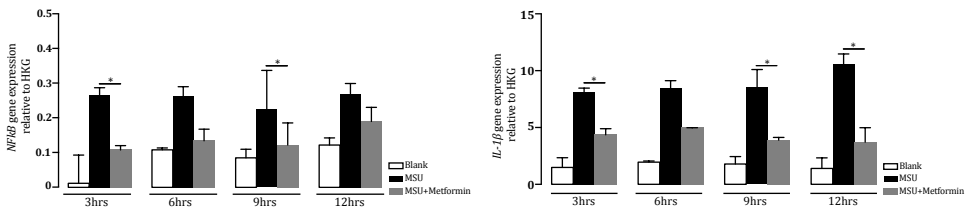
higher as compared to MSU crystal stimulation alone (32.2%) ($P < 0.0001$). (F) Intermediate monocytes that were left untreated (31.6%) or treated with a combination of MSU crystals and rapamycin (50%) or metformin (43.2%) had a significant higher survival percentage as compared to MSU crystal only (24%) ($P < 0.0001$).

Supplementary Figure 2



Supplementary Figure 2. Effect of MSU crystals on immune cell subsets of patients with gout and healthy participants, *in ex-vivo* condition. (A) The percentage of the B lymphocytes ($P=0.01$) and NK cells ($P=0.01$) are higher in patients with gout ($N=5$) (filled dots). The percentage of total monocytes ($P=0.007$), Classical monocytes ($P=0.01$) and Intermediate monocytes ($P=0.03$) are reduced in gout patients as compared to healthy participants ($N=5$) (empty dots).

Supplementary Figure 3



Supplementary Figure 3. Temporal effect of metformin on *NFkB* and *IL-1β* gene expression in MSU challenged monocytes. In monocytes of healthy participants ($N=5$) (A) metformin had an inhibitory effect on *NFkB* in 3 ($P=0.027$) and 9 ($P=0.026$) hour stimulation with a trend after 6 ($P=0.38$) and 12 ($P=0.07$) hour stimulation. Monocytes had an exponentially induced gene expression level of *IL-1β* upon MSU crystal challenge. Metformin reduced this induction significantly in 3 ($P=0.023$), 9 ($P=0.024$) and 12 ($P=0.041$) hour stimulations. After 6 hours of stimulation the effect was not significant ($P=0.063$). White bar represents the monocyte blank condition, black bar represents MSU crystal condition and gray bar represents the monocyte samples that were challenged with MSU crystal and stimulated with metformin simultaneously.



References

- 1 Vazirpanah N, Kienhorst LBE, Van Lochem E, *et al.* Patients with gout have short telomeres compared with healthy participants: Association of telomere length with flare frequency and cardiovascular disease in gout. *Ann Rheum Dis* 2017;**76**. doi:10.1136/annrheumdis-2016-210538
- 2 Dalbeth N, Haskard DO. Mechanisms of inflammation in gout. *Rheumatology (Oxford)* 2005;**44**:1090–6. doi:10.1093/rheumatology/keh640
- 3 Bardin T, Richette P. Impact of comorbidities on gout and hyperuricaemia: an update on prevalence and treatment options. *BMC Med* 2017;**15**:123. doi:10.1186/s12916-017-0890-9
- 4 Kuo C-F, See L-C, Luo S-F, *et al.* Gout: an independent risk factor for all-cause and cardiovascular mortality. *Rheumatology* 2010;**49**:141–6. doi:10.1093/rheumatology/kep364
- 5 Kuo CF, Yu KH, See LC, *et al.* Elevated risk of mortality among gout patients: A comparison with the National Population in Taiwan. *Jt Bone Spine* 2011;**78**:577–80. doi:10.1016/j.jbspin.2011.01.007
- 6 Krishnan E, Svendsen K, Neaton JD, *et al.* Long-term cardiovascular mortality among middle-aged men with gout. *Arch Intern Med* 2008;**168**:1104–10. doi:10.1001/archinte.168.10.1104
- 7 Perez-Ruiz F, Martínez-Indart L, Carmona L, *et al.* Tophaceous gout and high level of hyperuricaemia are both associated with increased risk of mortality in patients with gout. *Ann Rheum Dis* 2014;**73**:177–82. doi:10.1136/annrheumdis-2012-202421
- 8 Cris TO. Uric acid priming in human monocytes is driven by the AKT – PRAS40 autophagy pathway. 2017;**114**:5485–90. doi:10.1073/pnas.1620910114
- 9 Martinon F, Pétrilli V, Mayor A, *et al.* Gout-associated uric acid crystals activate the NALP3 inflammasome. *Nature* 2006;**440**:237–41. doi:10.1038/nature04516
- 10 Chung YH, Kim DH, Lee WW. Monosodium urate crystal-induced pro-interleukin-1 β production is post-transcriptionally regulated via the p38 signaling pathway in human monocytes. *Sci Rep* 2016;**6**:1–15. doi:10.1038/srep34533
- 11 Mylona EE, Mouktaroudi M, Crisan TO, *et al.* Enhanced interleukin-1 β production of PBMCs from patients with gout after stimulation with Toll-like receptor-2 ligands and urate crystals. *Arthritis Res Ther* 2012;**14**:R158. doi:10.1186/ar3898
- 12 Crisan TO, Cleophas MCP, Novakovic B, *et al.* Uric acid priming in human monocytes is driven by the AKT–PRAS40 autophagy pathway. *Proc Natl Acad Sci* 2017;**114**:5485–90. doi:10.1073/pnas.1620910114
- 13 Kienhorst LBE, Van Lochem E, Kievit W, *et al.* Gout is a chronic inflammatory disease in which high levels of interleukin-8 (CXCL8), myeloid-related protein 8/myeloid-related protein 14 complex, and an altered proteome are associated with diabetes mellitus and cardiovascular disease. *Arthritis Rheumatol* 2015;**67**:3303–13. doi:10.1002/art.39318
- 14 Lin HYH, Chang KT, Hung CC, *et al.* Effects of the mTOR inhibitor Rapamycin on Monocyte-Secreted Chemokines. *BMC Immunol* 2014;**15**:1–9. doi:10.1186/s12865-014-0037-0
- 15 Castranova V, Asgharian B, Sayre P, *et al.* HHS Public Access. 2016;**118**:1922–2013. doi:10.1080/10937404.2015.1051611. INHALATION
- 16 De Vita V, Melnik BC. Activation of mechanistic target of rapamycin complex 1: the common link between rheumatoid arthritis and diabetes mellitus. *Rheumatology* 2018;**1**:1–3. doi:10.1093/rheumatology/key038
- 17 Saxton RA, Sabatini DM. mTOR Signaling in Growth, Metabolism, and Disease. *Cell* 2017;**168**:960–76. doi:10.1016/j.cell.2017.02.004
- 18 Johnson SC, Rabinovitch PS, Kaeberlein M. MTOR is a key modulator of ageing and age-related disease. *Nature* 2013;**493**:338–45. doi:10.1038/nature11861
- 19 Zivelonghi C, van Kuijk JP, Nijenhuis V, *et al.* First report of the use of long-tapered sirolimus-eluting coronary stent for the treatment of chronic total occlusions with the hybrid algorithm. *Catheter Cardiovasc Interv* Published Online First: 2018. doi:10.1002/ccd.27539
- 20 Shao P, Ma L, Ren Y, *et al.* Modulation of the immune response in rheumatoid arthritis

- with strategically released rapamycin. *Mol Med Rep* 2017;**16**:5257–62. doi:10.3892/mmr.2017.7285
- 21 Koganesawa M, Yamamoto S, Kaneko R, *et al.* Utility of the attached sample blood for quality control of long-Term cryopreserved umbilical cord blood for hematopoietic cell transplantation. *J Showa Med Assoc* 2016;**76**:199–206. doi:10.1016/j.pestbp.2011.02.012.Investigations
- 22 Kato H, Perl A. Blockade of Treg Cell Differentiation and Function by the Interleukin-21-Mechanistic Target of Rapamycin Axis Via Suppression of Autophagy in Patients With Systemic Lupus Erythematosus. *Arthritis Rheumatol* 2018;**70**:427–38. doi:10.1002/art.40380
- 23 Li A, Zhang S, Li J, *et al.* Metformin and resveratrol inhibit Drp1-mediated mitochondrial fission and prevent ER stress-associated NLRP3 inflammasome activation in the adipose tissue of diabetic mice. *Mol Cell Endocrinol* 2016;**434**:36–47. doi:10.1016/j.mce.2016.06.008
- 24 Rotondi M, Coperchini F, Pignatti P, *et al.* Metformin reverts the secretion of CXCL8 induced by TNF- α in primary cultures of human thyroid cells: An additional indirect anti-tumor effect of the drug. *J Clin Endocrinol Metab* 2015;**100**:E427–32. doi:10.1210/jc.2014-3045
- 25 Maruthur NM, Tseng E, Hutfless S, *et al.* Diabetes medications as monotherapy or metformin-based combination therapy for type 2 diabetes: A systematic review and meta-analysis. *Ann Intern Med* 2016;**164**:740–51. doi:10.7326/M15-2650
- 26 Mazzotti A, Caletti MT, Marchignoli F, *et al.* Which treatment for type 2 diabetes associated with non-alcoholic fatty liver disease? *Dig Liver Dis* 2017;**49**:235–40. doi:10.1016/j.dld.2016.12.028
- 27 Nikolettou V, Markaki M, Palikaras K, *et al.* Crosstalk between apoptosis, necrosis and autophagy. *Biochim Biophys Acta - Mol Cell Res* 2013;**1833**:3448–59. doi:10.1016/j.bbamer.2013.06.001
- 28 Wu YT, Tan HL, Huang Q, *et al.* Activation of the PI3K-Akt-mTOR signaling pathway promotes necrotic cell death via suppression of autophagy. *Autophagy* 2009;**5**:824–34. doi:10.4161/auto.9099
- 29 Bruderer SG, Bodmer M, Jick SS, *et al.* Poorly controlled type 2 diabetes mellitus is associated with a decreased risk of incident gout: A population-based case-control study. *Ann Rheum Dis* 2015;**74**:1651–8. doi:10.1136/annrheumdis-2014-205337
- 30 Barskova VG, Eliseev MS, Nasonov EL, *et al.* [Use of metformin (siofor) in patients with gout and insulin resistance (pilot 6-month results)]. *Ter Arkh* 2005;**77**:44–9. <https://www.ncbi.nlm.nih.gov.proxy.library.uu.nl/pubmed/?term=16514819>
- 31 Barskova VG, Eliseev MS, Kudaeva FM, *et al.* [Effect of metformin on the clinical course of gout and insulin resistance]. *Klin Med (Mosk)* 2009;**87**:41–6. <https://www.ncbi.nlm.nih.gov.proxy.library.uu.nl/pubmed/19705791>
- 32 Scotland S, Saland E, Skuli N, *et al.* Mitochondrial energetic and AKT status mediate metabolic effects and apoptosis of metformin in human leukemic cells. *Leukemia* 2013;**27**:2129–38. doi:10.1038/leu.2013.107
- 33 Schuiveling M, Vazirpanah N, Radstake TRDJ, *et al.* Metformin, A New Era for an Old Drug in the Treatment of Immune Mediated Disease? *Curr Drug Targets* 2018;**19**:945–59. doi:10.2174/1389450118666170613081730
- 34 Vasamsetti SB, Karnewar S, Kanugula AK, *et al.* Metformin inhibits monocyte- To-macrophage differentiation via AMPK-mediated inhibition of STAT3 activation: Potential role in atherosclerosis. *Diabetes* 2015;**64**:2028–41. doi:10.2337/db14-1225
- 35 Hattori Y, Suzuki K, Hattori S, *et al.* Metformin inhibits cytokine-induced nuclear factor κ B activation via AMP-activated protein kinase activation in vascular endothelial cells. *Hypertension* 2006;**47**:1183–8. doi:10.1161/01.HYP.0000221429.94591.72
- 36 Haffner S, Temprosa M, Crandall J, *et al.* Intensive Lifestyle Intervention or Metformin on. 2005;**54**.
- 37 Lee H-M, Kim J-J, Kim HJ, *et al.* Upregulated NLRP3 Inflammasome Activation in Patients With Type 2 Diabetes. *Diabetes* 2013;**62**:194–204. doi:10.2337/db12-0420
- 38 Anonymous. U.K. Prospective diabetes study

- 16: Overview of 6 years' therapy of type II diabetes: A progressive disease. *Diabetes* 1995;44:1249–58.
- 39 Knowler WC, Barrett-Connor E, Fowler SE, *et al.* Reduction in the incidence of type 2 diabetes with lifestyle intervention or metformin. *N Engl J Med* 2002;**346**:393–403. doi:10.1056/NEJMoa012512

Discussion

The aim of the first part of this thesis was to identify the mechanism(s) underling the aberrant CXCL4 production and the role of CXCL4 in fibrosis in patients with SSc. In **Chapter 2** and **Chapter 3** we showed how hypoxia together with endogenous TLR stimulation induces CXCL4 production in pDCs and moDCs. In **Chapter 2** we showed that the combination of hypoxia and TLR9 led to an increase of mtROS and consequent stabilization of HIF-2 α in pDCs. It is known that mtROS are molecules involved in intracellular signalling and are capable to induce the production of pro-inflammatory cytokines¹. In line with the findings, in **Chapter 2**, mtROS are shown to stabilize HIFs^{2,3}. The HIF factors are involved in different cellular processes and they play a crucial role in the immune response⁴. For example, HIF-1 α has been positively correlated with the production level of pro-inflammatory cytokines such IL-6, IL-8 and TNF α ⁵. In contrary to HIF-1 α , the role of HIF-2 α in pro-inflammatory cytokine production has been poorly studied and recent literature indicates its role in immunity and in particular the production of cytokines such as TNF α ^{6,7}.

In **Chapter 2** we showed that HIF-2 α , but not HIF-1 α is fundamental for the production of CXCL4 in healthy pDCs. There is no literature indicating the role of HIF-2 α in pro-inflammatory cytokine production in human and the available insights are limited to TNF α production in mouse models⁷. Here for the first time, we showed the involvement of HIF-2 α in CXCL4 cytokine production level in pDCs. Also, we showed that oxidative state and mtROS are increased in patients with SSc. Moreover, a reduction in mtDNA copy numbers and an increase in mRNA level of antioxidant factors was observed. These observations further corroborate the already known presence of a disbalance in SSc oxidative omeostasis⁸⁻¹⁴. Furthermore, HIF-2 α was increased in SSc pDCs both on mRNA and protein level.

For the first time, our studies demonstrate an increase of HIF-2 α in SSc pDCs. We believe that this confirms and could be explained by chronic hypoxia present in patients with SSc,

as HIF-2 α , rather than HIF-1 α , orchestrates the response to prolonged hypoxia¹⁵. In this chapter, we showed that the inhibition of mtROS via mitoQ, a specific mtROS inhibitor, reduces HIF-2 α which downstream reduces CXCL4 production. Accordingly, our results demonstrate and pinpoint HIF-2 α as an underlying mechanism responsible for CXCL4 production in SSc and healthy pDCs.

In **Chapter 3** we demonstrated that moDCs are also able to produce CXCL4. After being co-exposed to hypoxia and TLR3, healthy moDCs produced CXCL4. Following this observation, we speculated that moDCs might rely on a different mechanism to orchestrate CXCL4 production than the pDCs. In line with our speculation, our results showed that in healthy moDCs, a combination of mtROS and both HIF-1 α and HIF-2 α followed CXCL4 production. It is known that regulation and distribution of HIFs is tissue and cell specific¹⁶. For instance, type II pneumocytes rely only on HIF-2 α , while HIF-1 α is not detectable¹⁷. Similarly, subtypes of dendritic cells seem to have differences in HIF-1 α and HIF-2 α mechanism of action since in pDCs, HIF-2 α appears to be responsible for CXCL4 production while in moDCs a combination of HIF-1 α and HIF-2 α is required to orchestrate CXCL4 production. Further in this chapter, we showed that in contrast to pDCs, CXCL4 production by SSc moDCs is mtROS independent. This observation could be explained by hypoxia induced epigenetic modifications during the early phases of the disease.

Speculating on our results in SSc moDCs, the involvement of both, HIF-1 α and HIF-2 α in CXCL4 production could depend on a different modulatory mechanism. We observed that HIF activity is decisive for CXCL4 production level since stabilization of HIF-1 α abate the quantity of CXCL4 production level.

Taking into account the emerging role of HIF-2 α in modulating CXCL4 cytokine production, we further explored the effect of HIF-2 α on proinflammatory cytokine production in SSc. In **Chapter 4** we showed that in healthy pDCs, HIF-2 α orchestrates IFN α and TNF α production, independently of HIF-1 α . In SSc pDCs however, a combination of HIF-1 α and HIF-2 α stimulation elicit IFN α , TNF α and IL-8 production. Besides, IL-6 production was

elevated upon HIF-2 α only. These observations underline the important role of mtROS, HIF-2 α alone and in combination with HIF-1 α in pro-inflammatory cytokine production in SSc. Therefore, it is likely to assume that suppressing this mechanism might potentially provide a therapeutic target in reducing proinflammatory cytokine production. Interestingly, mitoQ and HIF-2 α inhibitors are already available on the market. For instance, mitoQ is applied in an investigational study to prohibit the accumulation of mtROS during aging¹⁸. Also, PT2385 (inhibitor of HIF-2 α) has been safely used to treat clear cell carcinoma in human patients with a promising outcome¹⁹.

So far, **Chapter 2, 3 and 4** provided an overview of hypoxia induced proinflammatory cytokine production through HIF stabilization consequence in particular, and increase in production levels of CXCL4, IFN α , TNF α , IL-8 and IL-6 in DCs of patients with SSc. Following this line of thought, in **Chapter 5**, we provided the first proof of concept for targeting CXCL4 as pro-fibrotic chemokine. CXCL4 induces collagen production and expression of myofibroblast's markers in endothelial cells, pericytes, adipose stem cell as well as fibroblasts. Moreover, upon CXCL4 exposure, endothelial cells and pericytes differentiate towards myofibroblasts and initiate collagen production. Also, adipocyte stem cells initiate the differentiation towards myofibroblast like cells when exposed to CXCL4 which might be one of the factors leading to the typical intradermal fat loss observed in SSc patients. It is known in literature that hypoxia induces a pro-fibrotic phenotype in fibroblasts via HIF induced epigenetic modifications²⁰. Similarly, hypoxia via HIFs can epigenetically reprogram monocytes and shift their metabolism in order to prime these cells to react more promptly by orchestrating pro-inflammatory immune response²¹. Therefore, overlooking the literature and our findings, it is likely to assume that the immune cells in SSc are primed in a pro-inflammatory environment. As result, pro-fibrotic and pro-inflammatory immune cells are therefore overproducing cytokines such CXCL4 (as observed in pDCs and moDCs) and IL-8 (in moDCs), even in absence of stimuli. Furthermore, as discussed in **Chapter 3** mtROS could modulate a regulatory mechanism leading to an aberrant overproduction of CXCL4 by immune cells. In line with this Cardoso *et al.*, showed that moDCs differentiated

in the presence of CXCL4 are subjected to a priming towards a more mature phenotype with augmented responsiveness to TLRs²². Therefore, we speculated that high levels of CXCL4 present in the circulation of patients with SSc induces the fibrotic process on one hand and on the other hand primes the immune cells to express a more pro-inflammatory phenotype²³. Consequently, a vicious circle is established where hypoxia and inflammation induce CXCL4 that maintains the inflammation and promotes HIFs activation which in return elevates CXCL4 production.

Taken together, in the first part of this thesis we demonstrated the relevance of CXCL4 in inflammation and fibrosis, and therefore we believe that downregulation of CXCL4 by inhibiting HIF-2 α would reduce pro-inflammatory cytokine production and as a consequence, fibrosis in SSc.

In the second part of this thesis, we focused on the metabolism of SSc patients. In **Chapter 6** we studied the potential role of circulatory and intracellular metabolites in the development of inflammation in SSc. After analysing the plasma from a cohort of twenty patients with SSc, we observed multiple metabolic processes to be altered in SSc. The majority of those were involving pathways that take place within the mitochondria, such as the mitochondrial beta oxidation of short chain fatty acid (FA) and the beta oxidation of FA. This observation supports the central role of mitochondria in the pathophysiology of SSc as already suggested in literature²⁴ and have been emphasized within the first part of this thesis. Furthermore, our results signified that the carnitine synthesis pathway is altered in patients with SSc. As discussed in the introduction, carnitine plays a fundamental role in the cellular energetic metabolism allowing FA to enter mitochondria and generate ATP through fatty acid oxidation (FAO) pathway²⁵. Furthermore, there is a disbalance in the ratio of carnitines in the cellular lysates of SSc moDCs as compared with healthy moDCs. According to the literature, altered FA metabolism correlate to an altered acyl-carnitine composition²⁶, which could explain the aberrant FA metabolism in moDCs derived from SSc monocytes.

In **Chapter 6**, mass spectrometry analysis on plasma and moDCs lysates of SSc patients signified and altered carnitine and FA metabolism. An altered FA metabolism can modulate the immune cell's function towards a proinflammatory setting. According to the literature, inhibition of FAO in T helper cells, directs the cell differentiation towards pro-inflammatory T helper 17²⁷. Similarly, in monocytes, FA excess can induce a pro-inflammatory phenotype whereby the cells become less flexible to the surrounding environment and lose their adaptation and plasticity characteristics^{28,29}. Therefore, an altered FA metabolism, as observed in SSc, could worsen the disease prognosis and prime a pro-inflammatory set of immune cells. In line with this, dysfunction in FAO metabolism has been observed to promote renal fibrosis³⁰. Inflammation and FAO, both promote the production of pro-inflammatory mediators³¹⁻³³, and could thereby lead to chronic inflammation and consequent fibrosis.

Further in **Chapter 6**, we showed that etoposide-induced interference with the carnitine intake, could substantiate a reduction in pro-inflammatory cytokine production by immune cells. Etoposide, even if known for its use as anti-cancer drug, is capable to inhibit the carnitine transporter OCTN2³⁴, blocking the carnitine uptake and inhibiting the carnitine dependent part of the FAO. Furthermore, recent evidences on etoposide promote administration of this drug in combination with corticosteroids or disease modifying anti rheumatic drugs (DMARDs) for the treatment of Still's disease, a condition with rheumatoid arthritis-like features³⁵. Taken together, in **Chapter 6** we showed that targeting FAO metabolism could provide treatment strategy in order to inhibit the chronic inflammation in SSc.

In **Chapter 7** we studied the inhibitory effect of the mammalian target of rapamycin (mTOR) in MSU crystals stimulated monocytes and whether this could reduce pro-inflammatory cytokine production in monocytes. Exposing monocytes to MSU crystal induced the expression of mTOR and subsequent upregulation of pro-inflammatory mediators such as IL-1 β , IL-6, IL-8 and IL-18. Following, MSU crystals induced acute cell death in monocytes and activated pro-inflammatory immune response. According to our findings, mTOR inhibition by metformin reduced cell death and pro-inflammatory cytokine production

emphasizing the role of mTOR in the pro-inflammatory response. Metformin is a drug commonly used to treat diabetes type 2. But, recent evidences showed that metformin can inhibit NF- κ B via the PI3K-Akt1 pathway and reduce pro-inflammatory cytokine (IL-1 β , IL8, IL-6 and TNF α) production in monocytes and macrophages^{36,37}. Interestingly, mTOR is known to activate HIF-1 α via Akt1^{38,39}, therefore, it is interesting to speculate on the beneficial effects of metformin in downregulation of chronic inflammation in SSc, given its regulatory effect on inflammation via mTOR downstream on HIF-1 α . It is known that mTOR governs the glucose metabolism via HIF-1 α stabilization⁴⁰ which in differentiating monocytes results in establishment of a pro-inflammatory cell-phenotype²⁹. The beneficial effect of metabolic reprogramming has already been indicated by Yiming *et al.*, in Lupus. More precisely, inhibition of glycolysis and mTOR pathway with 2-DG and metformin, Yiming *et al.*, observed downregulating effects on disease phenotype in mice⁴¹. Therefore, anti-inflammatory properties of metformin via mTOR inhibition and its potential effect on HIF-1 α might be interesting in downregulation of chronic inflammation in patients with SSc. Metformin has been already used in a bleomycin model of SSc and showed promising anti-fibrotic effect⁴², but its effect in SSc patients remains to be studied.

Taken together, the second part of this thesis delineates the importance and the effect of metabolic disturbance in immune cells and eventually on immune response. On one hand in **Chapter 6** we demonstrate FA and carnitine dysregulation in patients with SSc and that the inhibition of FAO could reduce pro-inflammatory cytokines production. On the other hand, in **Chapter 7** we demonstrated the beneficial effect of mTOR inhibition on cytokine production level in stimulated immune cells. Finally, in the second part of this thesis we further pinpoint the importance of the metabolism in orchestrating pro-inflammatory immune response.

Future prospective

Inhibition of CXCL4 production represents an important potential target in SSc therapy, as the actual therapy is solely based on treating the symptoms and downregulating the proinflammatory response. Novel approaches including the immune suppressive therapies are introducing molecules capable to interfere with cell signalling such as Tofacitinib, an inhibitor of the JAK-STAT signalling pathway. The findings introduced in this thesis pinpointing the major role of HIF-2 α in orchestrating immune response elucidates its potential role as a potential therapeutic target. Considering that the small molecules designed to target HIF-2 α are already available and are introduced in clinical trials in cancer treatment. Notably, the safety of inhibiting HIF-2 α requires further investigations since it might potentially interfere with other metabolic pathways within the immune cells. In this regard, recent studies on metformin, a drug with many metabolical effects, showed its potential role in diminishing fibrosis in bleomycin mice model. Furthermore, metformin interferes with mTOR, a fundamental key player of the immune metabolism that is also linked to HIF activation. Therefore, future studies signifying the effect of metformin on HIFs regulatory mechanism in immune cells could be of fundamental contribution for the treatment of SSc which could diminish the prevalence of disease associated complications, increase patient's quality of life and reduce the burden of economic health costs.

Taken together, when initiating the research presented in this thesis, our aim was to study the mechanism underlying CXCL4 production in order to delineate strategies capable of suppressing CXCL4 production. Intriguingly we observed that blocking HIF interferes with metabolic pathways responsible for CXCL4 production within immune cells. In line with this, this approach also inhibited the production of other pro-inflammatory cytokines *in Vitro*. Although anti HIF therapy have already showed promising results in cancer, this approach requires further investigations in SSc and similar immune associated diseases.

References

1. Agod Z, Fekete T, Budai MM, et al. Regulation of type I interferon responses by mitochondria-derived reactive oxygen species in plasmacytoid dendritic cells. *Redox Biol.* 2017;13:633–645.
2. Shida M, Kitajima Y, Nakamura J, et al. Impaired mitophagy activates mtROS/HIF-1 α interplay and increases cancer aggressiveness in gastric cancer cells under hypoxia. *Int. J. Oncol.* 2016;
3. Mansfield KD, Guzy RD, Pan Y, et al. Mitochondrial dysfunction resulting from loss of cytochrome c impairs cellular oxygen sensing and hypoxic HIF- α activation. *Cell Metab.* 2005;1(6):393–399.
4. Bosco MC, Varesio L. Dendritic cell reprogramming by the hypoxic environment. *Immunobiology.* 2012;217(12):1241–1249.
5. Jeong HJ, Chung HS, Lee BR, et al. Expression of proinflammatory cytokines via HIF-1 α and NF- κ B activation on desferrioxamine-stimulated HMC-1 cells. *Biochem. Biophys. Res. Commun.* 2003;306(4):805–811.
6. Ryu JH, Chae CS, Kwak JS, et al. Hypoxia-Inducible Factor-2 α Is an Essential Catabolic Regulator of Inflammatory Rheumatoid Arthritis. *PLoS Biol.* 2014;12(6):1–16.
7. Imtiyaz HZ, Williams EP, Hickey MM, et al. Hypoxia-inducible factor 2 α regulates macrophage function in mouse models of acute and tumor inflammation. *J. Clin. Invest.* 2010;120(8):2699–2714.
8. Zhu H, Chen W, Liu D, Luo H. The role of metabolism in the pathogenesis of systemic sclerosis. *Metabolism.* 2019;93:44–51.
9. Ogawa F, Shimizu K, Muroi E, et al. Serum levels of 8-isoprostane, a marker of oxidative stress, are elevated in patients with systemic sclerosis. *Rheumatology.* 2006;45(7):815–818.
10. Böger RH, Maas R, Schulze F, Schwedhelm E. Elevated levels of asymmetric dimethylarginine (ADMA) as a marker for cardiovascular disease and mortality. *Clin. Chem. Lab. Med.* 2005;43(10):1124–1129.
11. Ricciari V, Spadaro A, Fuksa L, et al. Specific oxidative stress parameters differently correlate with nailfold capillaroscopy changes and organ involvement in systemic sclerosis. *Clin. Rheumatol.* 2008;27(2):225–230.
12. Tikly M, Channa K, Theodorou P, Gulumian M. Lipid peroxidation and trace elements in systemic sclerosis. *Clin. Rheumatol.* 2006;25(3):320–324.
13. Luo JY, Liu X, Jiang M, Zhao HP, Zhao JJ. Oxidative stress markers in blood in systemic sclerosis: A meta-analysis. *Mod. Rheumatol.* 2017;27(2):306–314.
14. Murrell DF. A radical proposal for the pathogenesis of scleroderma. *J. Am. Acad. Dermatol.* 1993;28(1):78–85.
15. Martin SK, Diamond P, Gronthos S, Peet DJ, Zannettino ACW. The emerging role of hypoxia, HIF-1 and HIF-2 in multiple myeloma. *Leukemia.* 2011;25(10):1533–1542.
16. Patel SA, Simon MC. Biology of hypoxia-inducible factor-2 α in development and disease. *Cell Death Differ.* 2008;15(4):628–634.
17. WIESENER MS, JÜRGENSEN JS, ROSENBERGER C, et al. Widespread hypoxia-inducible expression of HIF-2 α in distinct cell populations of different organs. *FASEB J.* 2003;17(2):271–273.
18. Rossman MJ, Santos-Parker JR, Steward CAC, et al. Chronic Supplementation With a Mitochondrial Antioxidant (MitoQ) Improves Vascular Function in Healthy Older Adults. *Hypertension.* 2018;71(6):1056–1063.
19. Courtney KD, Infante JR, Lam ET, et al. Phase I Dose-Escalation Trial of PT2385, a First-in-Class Hypoxia-Inducible Factor-2 α Antagonist in Patients With Previously Treated Advanced Clear Cell Renal Cell Carcinoma. *J. Clin. Oncol.* 2018;36(9):867–874.
20. Watson CJ, Collier P, Tea I, et al. Hypoxia-induced epigenetic modifications are associated with cardiac tissue fibrosis and the development of a myofibroblast-like phenotype. *Hum. Mol. Genet.* 2014;23(8):2176–2188.
21. Cheng SC, Quintin J, Cramer RA, et al. MTOR- and HIF-1 α -mediated aerobic glycolysis as metabolic basis for trained immunity. *Science (80-).* 2014;345(6204):.
22. Silva-Cardoso SC, Affandi AJ, Spel L, et al.

- CXCL4 Exposure Potentiates TLR-Driven Polarization of Human Monocyte-Derived Dendritic Cells and Increases Stimulation of T Cells. *J. Immunol.* 2017;199(1):253–262.
23. van Bon L, Affandi AJ, Broen J, et al. Proteome-wide Analysis and CXCL4 as a Biomarker in Systemic Sclerosis. *N. Engl. J. Med.* 2014;370(5):433–443.
 24. Luckhardt TR, Thannickal VJ. Systemic sclerosis-associated fibrosis: An accelerated aging phenotype? *Curr. Opin. Rheumatol.* 2015;27(6):571–576.
 25. Fielding R, Riede L, Lugo JP, Bellamine A. L-carnitine supplementation in recovery after exercise. *Nutrients.* 2018;10(3):349.
 26. Beger RD, Bhattacharyya S, Gill PS, James LP. Acylcarnitines as Translational Biomarkers of Mitochondrial Dysfunction. *Mitochondrial Dysfunct. Caused by Drugs Environ. Toxicants.* 2018;1–2:383–393.
 27. Slack M, Wang T, Wang R. T cell metabolic reprogramming and plasticity. *Mol. Immunol.* 2015;68(2):507–512.
 28. Freemerman AJ, Johnson AR, Sacks GN, et al. Metabolic reprogramming of macrophages: Glucose transporter 1 (GLUT1)-mediated glucose metabolism drives a proinflammatory phenotype. *J. Biol. Chem.* 2014;289(11):7884–7896.
 29. Wang T, Liu H, Lian G, et al. HIF1 α -Induced Glycolysis Metabolism Is Essential to the Activation of Inflammatory Macrophages. *Mediators Inflamm.* 2017;2017:1–10.
 30. Allison SJ. Dysfunctional fatty acid oxidation in renal fibrosis. *Nat. Rev. Nephrol.* 2015;11(2):64.
 31. Angajala A, Lim S, Phillips JB, et al. Diverse Roles of Mitochondria in Immune Responses: Novel Insights Into Immuno-Metabolism. *Front. Immunol.* 2018;9:1605.
 32. Fujieda Y, Manno A, Hayashi Y, et al. Inflammation and Resolution Are Associated with Upregulation of Fatty Acid β -Oxidation in Zymosan-Induced Peritonitis. *PLoS One.* 2013;8(6):e66270.
 33. Lee SB, Kalluri R. Mechanistic connection between inflammation and fibrosis. *Kidney Int.* 2010;78(SUPPL. 119):S22-6.
 34. Hu C, Lancaster CS, Zuo Z, et al. Inhibition of OCTN2-mediated transport of carnitine by etoposide. *Mol. Cancer Ther.* 2012;11(4):921–929.
 35. Mitrovic S, Fautrel B. Complications of adult-onset Still's disease and their management. *Expert Rev. Clin. Immunol.* 2018;14(5):351–365.
 36. Vasamsetti SB, Karnewar S, Kanugula AK, et al. Metformin inhibits monocyte- To-macrophage differentiation via AMPK-mediated inhibition of STAT3 activation: Potential role in atherosclerosis. *Diabetes.* 2015;64(6):2028–2041.
 37. Hattori Y, Suzuki K, Hattori S, Kasai K. Metformin inhibits cytokine-induced nuclear factor κ B activation via AMP-activated protein kinase activation in vascular endothelial cells. *Hypertension.* 2006;47(6):1183–1188.
 38. Harada H, Itasaka S, Kizaka-Kondoh S, et al. The Akt/mTOR pathway assures the synthesis of HIF-1 α protein in a glucose- and reoxygenation-dependent manner in irradiated tumors. *J. Biol. Chem.* 2009;284(8):5332–5342.
 39. Pan C, Liu Q, Wu X. Hif1 α /mir-520a-3p/akt1/mTOR feedback promotes the proliferation and glycolysis of gastric cancer cells. *Cancer Manag. Res.* 2019;11:10145–10156.
 40. Salmond RJ. mTOR regulation of glycolytic metabolism in T cells. *Front. Cell Dev. Biol.* 2018;6(SEP):
 41. Yin Y, Choi SC, Xu Z, et al. Normalization of CD4+ T cell metabolism reverses lupus. *Sci. Transl. Med.* 2015;7(274):274ra18.
 42. Ursini F, Grembale RD, D'Antona L, et al. Oral Metformin Ameliorates Bleomycin-Induced Skin Fibrosis. *J. Invest. Dermatol.* 2016;136(9):1892–1894.

Summary

Background

Systemic sclerosis is a rare autoimmune disease with heterogeneous symptoms and presentation. The hallmarks of SSc are immune alteration, vascular abnormalities, fibrosis and hypoxia. SSc is a poorly understood disease with no available effective cure and an unknown pathophysiology. It is generally accepted that an aberrant TLR activation and endothelial damage are the first events. Recent studies on SSc identified CXCL4, a chemokine mainly produced by pDCs, as a potential biomarker of the disease. CXCL4 has also been shown to play an important role in multiple autoimmune diseases and cancer, where it has been shown to have pro-inflammatory role.

Immunometabolism is the study of biochemical reactions ongoing within the immune cells and recently this field gained interest due to its potential applications. One important metabolical pathway in immune cells is the fatty acid oxidation (consumption of fatty acids by the cells in order to create energy). Recent studies showed the decisive properties of this pathway on polarisation of immune cell development towards a pro- or anti-inflammatory phenotype and response. Furthermore, recent knowledge in this field showed that SSc could be characterized by an alteration in the fat metabolism.

In this thesis we studied the mechanisms leading to CXCL4 production and its role in the fibrotic processes. Furthermore, we looked into the metabolic status of immune cells in SSc and assessed pro-inflammatory cytokine production after interfering with cellular metabolism.

Aim of this thesis

The aim of this thesis is to determine the underlying mechanisms in aberrant CXCL4 production and its role in fibrotic processes in SSc. Furthermore, we aimed to further investigate on the metabolic status in pathophysiology of SSc.

Summary of findings

In the first part of this thesis we focussed on the mechanisms responsible for the increased CXCL4 production and the role of CXCL4 in fibrotic processes in SSc. In **Chapter 2** and **3** we studied the function of pDCs and moDCs exposed to hypoxia and TLR triggers. We observed that hypoxia in combination with endosomal TLR (TLR9 for pDCs and TLR3 for moDCs) was responsible for CXCL4 production. Furthermore, we observed that in healthy cells the production of CXCL4 depends on mitochondrial reactive oxygen species (mtROS) increase and hypoxia inducible factor (HIF)-2 α stabilization. In **Chapter 2** we studied the function of SSc pDCs, where we observed that these cells spontaneously produce mtROS, HIF-2 α and CXCL4. Both in SSc pDCs as well as in healthy cells, we observed that the inhibition of either mtROS or HIF-2 α reduces CXCL4 production level. In this chapter we demonstrated the importance of mtROS and HIF-2 α in CXCL4 production in patients with SSc. In **Chapter 3** we focussed on moDCs, where we demonstrate that healthy moDCs (in contrary to pDCs) were able to produce CXCL4 already after being challenged with solely hypoxia. We also observed that both HIF-1 α and HIF-2 α played a role in CXCL4 production. Furthermore, we studied the function of SSc moDCs. We observed that SSc moDCs produced high level of CXCL4 and, in contrary to healthy moDCs, were not mtROS dependant in production of CXCL4. Similarly, to healthy moDCs, CXCL4 production in SSc moDCs was HIF-1 α and HIF-2 α dependant. In this study we underlined the role of HIF-1 α and HIF-2 α in CXCL4 production level and hypothesized the presence of epigenetic modification in SSc moDCs leading to constitutive stabilisation of HIF-1 α and HIF-2 α as responsible mechanism for elevated CXCL4 production.

Following these findings on HIF-1 α and HIF-2 α in SSc, in **Chapter 4** we studied their role in pro-inflammatory cytokines production in pDCs. We observed that TNF α and IFN α were both exclusively HIF-2 α dependant in healthy pDCs, while SSc pDCs production of TNF α , IFN α and IL-8 required both HIF-1 α and HIF-2 α stimulation. Interestingly, IL-6 production in SSc pDCs was found to be only HIF-2 α dependant. This study pinpoints the

role of both HIFs on cytokine production and confirmed the potential features of HIF-2 α as a therapy target in treatment of SSc.

Finally, in **Chapter 5** we studied the effect of CXCL4 on different precursor cells such as fibroblasts, endothelial and pericytes. Furthermore, we investigated the role of CXCL4 in different in vivo mice models such as bleomycin and transverse aortic constriction models.

In the second part of the thesis we focussed on the metabolic status of SSc. In **Chapter 6** we demonstrated that fatty acids and carnitine composition were altered in SSc and this alteration was observed both, in SSc plasma and in moDCs lysates. Furthermore, we observed that inhibition of fatty acid oxidation with etoposide shows promising abilities in reduction of pro-inflammatory cytokine production in SSc immune cells. Taking these observations into consideration, we further studied whether inflammation and fatty acid oxidation create a positive feedback loop orchestrating chronic inflammation in SSc.

To further show the importance of metabolism in immune regulation, in **Chapter 7** we studied the effect of mammalian target of rapamycin (mTOR), a fundamental regulator of the metabolism in immune cells, inhibition on stimulated monocytes. We observed that inhibition of mTOR with metformin reduces pro-inflammatory cytokine production such as IL-1 β , IL-6 and TNF α , signifying the potential therapeutic effect of metabolic mediators in immune cells.

Concluding remarks

Taken together, the findings of this thesis demonstrate how increased production of pro-inflammatory cytokines, with the focus on the CXCL4 can be reduced by HIFs interference. Furthermore, showing the pro-fibrotic effect of CXCL4 in precursor cells and in different in vivo mice models, we pinpoint the potential beneficial effect of blocking this chemokine in the treatment of SSc (**Figure 1**). Finally, we showed that SSc is potentially characterized by a disbalance in the fat metabolism and showed potential areas of intervention for therapies.

Figure 1

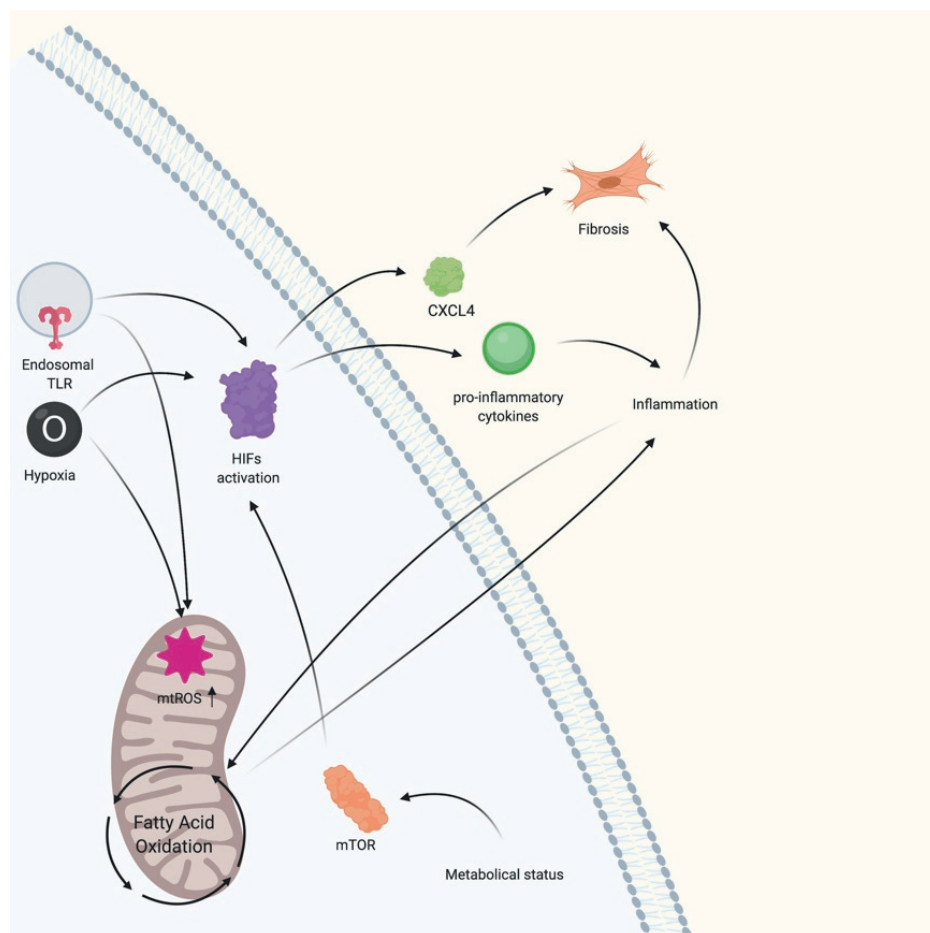


Figure 1: schematic representation of the main findings of this thesis

Nederlandse Samenvatting

Achtergrond

Systemische sclerose is een zeldzame auto-immuunziekte met heterogene symptomen en presentatie. De kenmerken van SSc zijn immuunverandering, vaatafwijkingen, fibrose en hypoxie. SSc is een slecht begrepen ziekte zonder beschikbare effectieve remedie en een onbekende pathofysiologie. Het is algemeen aanvaard dat een afwijkende TLR-activering en endotheliale schade de eerste gebeurtenissen zijn. Recente studies over SSc identificeerden CXCL4, een chemokine die voornamelijk wordt geproduceerd door pDC's, als een potentiële biomarker van de ziekte. Van CXCL4 is ook aangetoond dat het een belangrijke rol speelt bij meerdere auto-immuunziekten en kanker, waarvan is aangetoond dat het een pro-inflammatoire rol speelt.

Immunometabolisme is de studie van biochemische reacties die gaande zijn in de immuuncellen en recent heeft dit veld belangstelling gekregen vanwege de mogelijke toepassingen. Een belangrijke metabole route in immuuncellen is de vetzuuroxidatie (consumptie van vetzuren door de cellen om energie te creëren). Recente studies toonden de beslissende eigenschappen van deze route op polarisatie van de ontwikkeling van de immuuncel naar een pro- of ontstekingsremmend fenotype en respons. Bovendien heeft recente kennis op dit gebied aangetoond dat SSc kan worden gekenmerkt door een verandering in het vetmetabolisme.

In dit proefschrift hebben we de mechanismen bestudeerd die leiden tot de productie van CXCL4 en zijn rol in de fibrotische processen. Verder onderzochten we de metabolische status van immuuncellen in SSc en beoordeelden pro-inflammatoire cytokineproductie na interfereren met cellulair metabolisme.

Doel van dit proefschrift

Het doel van dit proefschrift is het bepalen van de onderliggende mechanismen in afwijkende

CXCL4-productie en de rol ervan in fibrotische processen in SSc. Verder wilden we verder onderzoek doen naar de metabole status in de pathofysiologie van SSc.

Samenvatting van Bevindingen

In het eerste deel van dit proefschrift hebben we ons gericht op de mechanismen die verantwoordelijk zijn voor de verhoogde productie van CXCL4 en de rol van CXCL4 in fibrotische processen in SSc. In **hoofdstuk 2** en **3** hebben we de functie bestudeerd van pDC's en moDC's die zijn blootgesteld aan hypoxie en TLR-triggers. We zagen dat hypoxie in combinatie met endosomale TLR (TLR9 voor pDC's en TLR3 voor moDC's) verantwoordelijk was voor de productie van CXCL4. Verder hebben we geconstateerd dat in gezonde cellen de productie van CXCL4 afhankelijk is van toename van mitochondriale reactieve zuurstofspecies (mtROS) en hypoxia induceerbare factor (HIF) -2 α stabilisatie. In **hoofdstuk 2** hebben we de functie van SSc pDC's bestudeerd, waarbij we zagen dat deze cellen spontaan mtROS, HIF-2 α en CXCL4 produceren. Zowel in SSc pDC's als in gezonde cellen hebben we vastgesteld dat de remming van mtROS of HIF-2 α het productieniveau van CXCL4 vermindert. In dit hoofdstuk hebben we het belang aangetoond van mtROS en HIF-2 α bij de productie van CXCL4 bij patiënten met SSc. In **hoofdstuk 3** hebben we ons gericht op moDC's, waar we aantonen dat gezonde moDC's (in tegenstelling tot pDC's) al in staat waren om CXCL4 te produceren nadat ze alleen met hypoxie werden uitgedaagd. We zagen ook dat zowel HIF-1 α als HIF-2 α een rol speelden bij de productie van CXCL4. Verder hebben we de functie van SSc moDC's bestudeerd. We hebben vastgesteld dat SSc-moDC's een hoog CXCL4-niveau produceerden en, in tegenstelling tot gezonde moDC's, niet afhankelijk waren van mtROS bij de productie van CXCL4. Evenzo was de productie van CXCL4 in SSc-moDC's voor gezonde moDC's HIF-1 α en HIF-2 α afhankelijk. In deze studie onderstreepten we de rol van HIF-1 α en HIF-2 α in het CXCL4-productieniveau en veronderstelden we de aanwezigheid van epigenetische modificatie in SSc moDC's die leiden tot constitutieve stabilisatie van HIF-1 α en HIF-2 α als verantwoordelijk mechanisme voor verhoogde CXCL4-productie.

Naar aanleiding van deze bevindingen over HIF-1 α en HIF-2 α in SSc, bestudeerden we in **hoofdstuk 4** hun rol bij de productie van ontstekingsbevorderende cytokines in pDC's. We zagen dat TNF α en IFN α beide uitsluitend HIF-2 α -afhankelijk waren in gezonde pDC's, terwijl SSc pDC's-productie van TNF α , IFN α en IL-8 zowel HIF-1 α - als HIF-2 α -stimulatie vereiste. Interessant is dat IL-6-productie in SSc-pDC's alleen HIF-2 α -afhankelijk bleek te zijn. Deze studie wijst op de rol van beide HIF's op de productie van cytokine en bevestigde de potentiële kenmerken van HIF-2 α als een therapiedoel bij de behandeling van SSc.

Tot slot hebben we in **hoofdstuk 5** het effect van CXCL4 op verschillende voorlopercellen, zoals fibroblasten, endotheel en pericyten, bestudeerd. Verder onderzochten we de rol van CXCL4 in verschillende in vivo muizenmodellen zoals bleomycine en transversale aorta constrictie modellen.

In het eerste deel van dit proefschrift hebben we ons gericht op de mechanismen die verantwoordelijk zijn voor de verhoogde productie van CXCL4 en de rol van CXCL4 in fibrotische processen in SSc. In **hoofdstuk 2** en **3** hebben we de functie bestudeerd van pDC's en moDC's die zijn blootgesteld aan hypoxie en TLR-triggers. We zagen dat hypoxie in combinatie met endosomale TLR (TLR9 voor pDC's en TLR3 voor moDC's) verantwoordelijk was voor de productie van CXCL4. Verder hebben we geconstateerd dat in gezonde cellen de productie van CXCL4 afhankelijk is van toename van mitochondriale reactieve zuurstofspecies (mtROS) en hypoxia induceerbare factor (HIF) -2 α stabilisatie. In **hoofdstuk 2** hebben we de functie van SSc pDC's bestudeerd, waarbij we zagen dat deze cellen spontaan mtROS, HIF-2 α en CXCL4 produceren. Zowel in SSc pDC's als in gezonde cellen hebben we vastgesteld dat de remming van mtROS of HIF-2 α het productieniveau van CXCL4 vermindert. In dit hoofdstuk hebben we het belang aangetoond van mtROS en HIF-2 α bij de productie van CXCL4 bij patiënten met SSc. In **hoofdstuk 3** hebben we ons gericht op moDC's, waar we aantonen dat gezonde moDC's (in tegenstelling tot pDC's) al in staat waren om CXCL4 te produceren nadat ze alleen met hypoxie werden uitgedaagd. We zagen ook dat zowel HIF-1 α als HIF-2 α een rol speelden bij de productie van CXCL4.

Verder hebben we de functie van SSc moDC's bestudeerd. We hebben vastgesteld dat SSc-moDC's een hoog CXCL4-niveau produceerden en, in tegenstelling tot gezonde moDC's, niet afhankelijk waren van mtROS bij de productie van CXCL4. Evenzo was de productie van CXCL4 in SSc-moDC's voor gezonde moDC's HIF-1 α en HIF-2 α afhankelijk. In deze studie onderstreepten we de rol van HIF-1 α en HIF-2 α in het CXCL4-productieniveau en veronderstelden we de aanwezigheid van epigenetische modificatie in SSc moDC's die leiden tot constitutieve stabilisatie van HIF-1 α en HIF-2 α als verantwoordelijk mechanisme voor verhoogde CXCL4-productie.

Naar aanleiding van deze bevindingen over HIF-1 α en HIF-2 α in SSc, bestudeerden we in **hoofdstuk 4** hun rol bij de productie van ontstekingsbevorderende cytokines in pDC's. We zagen dat TNF α en IFN α beide uitsluitend HIF-2 α -afhankelijk waren in gezonde pDC's, terwijl SSc pDC's-productie van TNF α , IFN α en IL-8 zowel HIF-1 α als HIF-2 α stimulatie vereiste. Interessant is dat IL-6-productie in SSc-pDC's alleen HIF-2 α afhankelijk bleek te zijn. Deze studie wijst op de rol van beide HIF's op de productie van cytokine en bevestigde de potentiële kenmerken van HIF-2 α als een therapiedoel bij de behandeling van SSc.

Tot slot hebben we in **hoofdstuk 5** het effect van CXCL4 op verschillende voorlopercellen, zoals fibroblasten, endotheel en pericyten, bestudeerd. Verder onderzochten we de rol van CXCL4 in verschillende in vivo muizenmodellen zoals bleomycine en transversale aorta constrictie modellen.

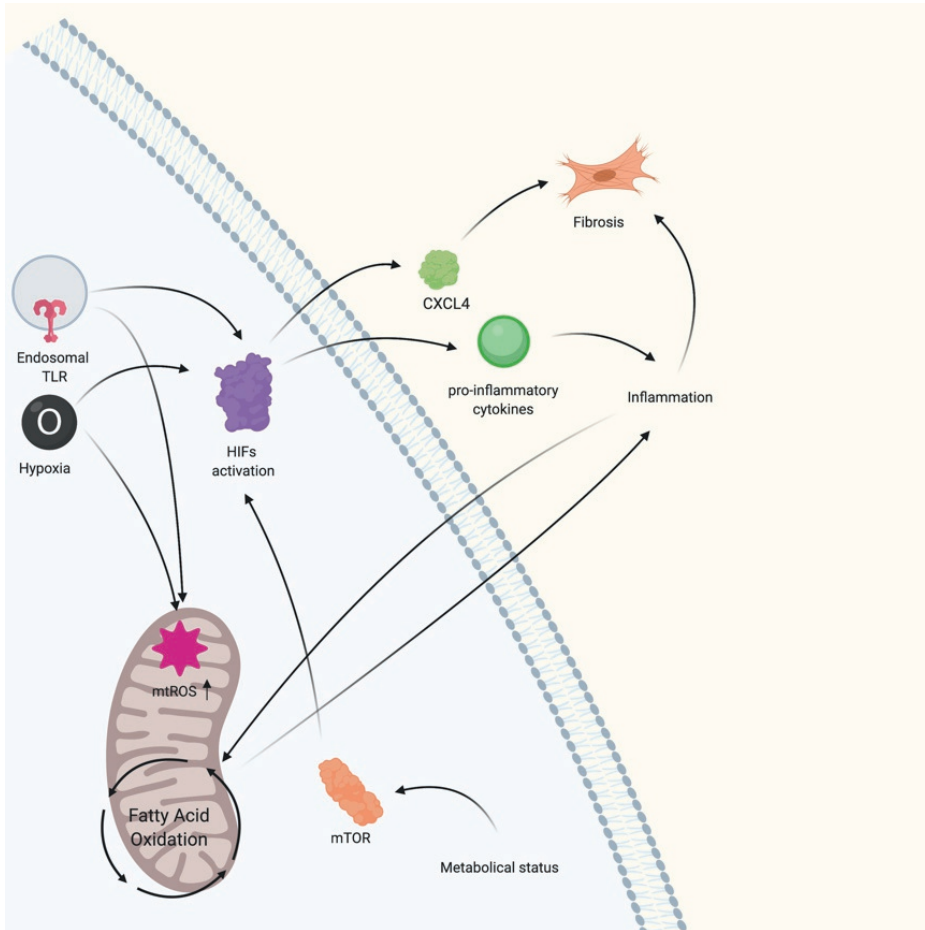
In het tweede deel van het proefschrift hebben we ons gericht op de metabole status van SSc. In **hoofdstuk 6** hebben we aangetoond dat vetzuren en carnitinesamenstelling in SSc zijn veranderd en deze wijziging is zowel in SSc-plasma als in lysaten van moDC's waargenomen. Verder stelden we vast dat remming van vetzuuroxidatie met etoposide veelbelovende eigenschappen vertoont in vermindering van pro-inflammatoire cytokineproductie in SSc-immuuncellen. Rekening houdend met deze waarnemingen hebben we verder onderzocht of ontsteking en vetzuuroxidatie een positieve feedbacklus creëren die chronische ontsteking orkestreert in SSc.

Om het belang van metabolisme in immuunregulatie verder aan te tonen, hebben we in **hoofdstuk 7** het effect bestudeerd van zoogdierdoelwit van rapamycine (mTOR), een fundamentele regulator van het metabolisme in immuuncellen, remming van gestimuleerde monocytten. We hebben geconstateerd dat remming van mTOR met metformine pro-inflammatoire cytokineproductie zoals IL-1 β , IL-6 en TNF α vermindert, wat het potentiële therapeutische effect van metabole mediators in immuuncellen betekent.

Slotopmerkingen

Samengevat laten de bevindingen van dit proefschrift zien hoe verhoogde productie van pro-inflammatoire cytokines, met de focus op de CXCL4, kan worden verminderd door HIF-interferentie. Verder laten we het pro-fibrotische effect van CXCL4 in voorlopercellen en in verschillende in vivo muizenmodellen zien, wijzen we op het potentiële gunstige effect van het blokkeren van deze chemokine bij de behandeling van SSc (figuur 1). Ten slotte hebben we aangetoond dat SSc mogelijk wordt gekenmerkt door een disbalans in het vetmetabolisme en mogelijke interventiegebieden voor therapieën laten zien.

Figuur 1



Figuur 1: schematische weergave van de belangrijkste bevindingen van dit proefschrift

Dankwoorden

I would like to thank Viola and Tim that gave me the opportunity to start my PhD trajectory. With Viola we had our up and downs, but we managed always to find a way out. I am very thankful to you for the time and energy you invested in me, as also for all the support. You are a kind-hearted woman and a cat lover, never change that.

Tim, as the boss of the former Radstake group you were also a sort of foster parent for everyone in the group. Always updated, working day and night and traveling more than Marco Polo. I still believe you have some clones that you send around to do all these things. You have been an inspiration for me for what I wanted to achieve and a lead in the world of science.

Maili, italiana acquisita, sempre gentile e disponibile ad aiutare, grazie per tutte le volte che mi hai aiutato con gli esperimenti e le chiacchierate in italiano

Aridaman, our guru for everything about biostatistics, but also often for life. I learned something really important from you while playing laser-game: you can win the game while walking, you don't need to run! Thanks for everything

Tiago, Jorre, Ralph, Alsya, the boys from Marut group, thanks for the many scientific discussions and inputs, but also for the cultural, football, series, movies and videogame discussion topics

Alsya, Emmerik, Maarten K, Jonas, the Madeira boys, the first Dutch person I ever met in my life and the first future new colleagues I met in Madeira, thanks for the marvellous time spent there during those days, but also each time we had a chat or could discuss about anything during my PhD days.

Samu and Bea, our Spanish team, always talking loud and warming people with a smile, thank you for the scientific discussions and experimental help.

Chiara, Sandra, Luuk, Lotte, Elena, we were office mates for just a week or two, thanks Chiara for the Italian chats, Lotte for being the game master, Luuk for teaching me scheldwoorden, Sandra for all the help and Elena for making me deaf with the missing low volume trigger, but always ready to help and support. Thank you guys!

Sofie, you were like a role-model, always calm and on the topic, knowing what you were doing, and full of advices, I learned a lot from you, thank you.

Maarten K, oh Martino, I never could get a grasp of your mood, but I understood something, you have a big hart and you are always willing to help people out. Thank you for all the chats, support and help.

Maarten H, thank you for all the jokes, you are a stand-up comedian with the brain of a scientist. Thanks for always making us laugh with your jokes.

Ana, together with Tiago, Sandra, Ines and Ruben our Portuguese people, you are always willing to help and helped me many times. Thank you for everything.

Kamil, we stated our PhD almost together and we finish it almost together, always polite and nice to everyone. Thanks a lot!

Pawel, a really sweet guy with the face of a hard one, you are a great scientist and I learned a lot from you. Thank you.

Ruben and Maarten vd Linde, I missed you guys from the moment you left the LTI, you were really two nice colleagues trying to help everyone whenever needed. Thank you very much!

Marta, oh Marta, sempre carica di lavoro, colei che mi ha insegnato a screenare i pazienti per la ricerca, grazie per tutti i suggerimenti che mi hai dato negli anni.

Tao, Ninke, Lotte2, Ellen, Doron, Judith, Jin mei, my room-mates, thank you for all the time you helped me while struggling and for the chats we had about everything. Doron, my indoor football promotor, I loved playing football with you guys. Thanks for every chat and

football match we had

Giulio, sempre sorridente e allegro, presente all'addio al celibato e paraninph per questa avventura, grazie per tutte le risate che ci siamo fatti in questi tempi di dottorato

Alsya, Madeira boy, colleague and paraninph, a great person with a big heart, always ready to help everyone, someone I am proud to call friend, thanks for all the help you provided me since I know you. Thank you Alsya for being Alsya

Michiel (Linde), thank you for all the time you helped me learning Dutch, you have a wonderful way of teaching!

Edwin and Can, guys thank you super for all the times we discussed about metabolomics and all the time you listened to me and my thousand questions and requests for experiments. I appreciate it.

Barbara, mi hai insegnato tantissimo, sempre ordinata e pronta ad aiutare tutti, grazie per tutto

Sarita, Rina, Cornelis, Sanne, Michiel and Ralph our technicians, always there to solve the impossible when an experiment doesn't want to work and super resourceful, knowing where the secret stocks are and super helpful in case of difficulties, thanks for your support guys!

All the Radstake group and the CTI people, thank you all for all the support and constructive talks we had during my PhD, you have been a great help. Saskia and the other office managers, you are the backbone of everything that is going on in the LTI, sorry CTI. You are the glue that holds the whole structure together! Thank you

Janneke, jij gaf me een kans om weer de praktische kunst van geneeskunde toe te passen. Jij had vertrouwen in mij en je hielp mij om te herinneren dat ik een arts ben. Ik ben enorm dankbaar voor de talloze overleggen dat we over patiënten hadden. Bedankt voor alles Janneke.

Mamma e Papà, di certo un'ispirazione ed un punto di riferimento. Ho imparato le basi della vita da voi. Mi avete sempre cresciuto ed amato incondizionatamente. Vi sono eternamente grato perché è anche grazie a voi se sono riuscito a completare questo passo della mia vita. Grazie di esistere e dell'immenso supporto che mi date sempre. Vi voglio tanto bene mamma e papà

Mimì o madame la chat come mi piace chiamarla sempre dolce ed affettuosa con me, ma strombola con chiunque altro, grazie per tutte le giornate di studio in cui hai dormito sulle mie gambe o sui miei libri.

Mama en Papa, daste shoma dard nakone mamane o babae man. Jullie zijn mijn nieuwe familie en bedankt dat jullie mij geaccepteerd hebben zoals jullie eigen zoon en bedankt dat jullie er altijd voor mij zijn. Ik hou van jullie

Naz bedankt voor mijn zusje te zijn, jij bent een fantastisch zusje, altijd vrijgevig en met een glimlach, de kunstenaressen van de familie. Bedankt dat je als een echt zusje altijd voor mij klaar staat en bedankt voor het tekenen van de Cover van mijn Proefschrift, het is zoals altijd een prachtige kunst en ik bof ermee

Lily en Lola, my "hairy cat daughters" mao mio miao miao meow maramao miew miao, that in human language should sound like, thanks for keeping our company and fill our days with love, thanks for sleeping next to us and on our books and computers and thanks for always coming helping typing when most needed

Nadia, my lovely wife, eshgham jij bent de licht van het huis, jouw glimlach geef kleur aan mijn wereld. Jij bent mijn steun en mijn kracht, wie altijd naar me luistert en bijstaat. Jij bent mijn trots en mijn geluk. Jij maakt me compleet. Ik bof om jou als mijn vrouw in mijn leven te hebben! Bedankt voor de persoon die jij bent, Ik hou van jou.

دوستت دارم لبالب
میسوزه عشقم از تب
پر میشم از اسم تو
هر ثانیه هر شب

List of publication

- Carvalheiro T, Malvar Fernández B, **Ottria A**, Giovannone B, Marut W, Reedquist KA, Garcia S, Radstake TR. Extracellular SPARC cooperates with TGF- β signalling to induce pro-fibrotic activation of systemic sclerosis patient dermal fibroblasts. *Rheumatology (Oxford)*. 2019 Dec 16. pii: kez583. doi: 10.1093/rheumatology/kez583. [Epub ahead of print] PubMed PMID: 31840182.
- Carvalheiro T, Affandi AJ, Malvar-Fernández B, Dullemond I, Cossu M, **Ottria A**, Mertens JS, Giovannone B, Bonte-Mineur F, Kok MR, Marut W, Reedquist KA, Radstake TR, García S. Induction of Inflammation and Fibrosis by Semaphorin 4A in Systemic Sclerosis. *Arthritis Rheumatol*. 2019 Oct;71(10):1711-1722. doi: 10.1002/art.40915. Epub 2019 Aug 27. PubMed PMID: 31012544; PubMed Central PMCID: PMC6790618.
- Affandi AJ, Carvalheiro T, **Ottria A**, Broen JC, Bossini-Castillo L, Tieland RG, Bon LV, Chouri E, Rossato M, Mertens JS, Garcia S, Pandit A, de Kroon LM, Christmann RB, Martin J, van Roon JA, Radstake TR, Marut W. Low RUNX3 expression alters dendritic cell function in patients with systemic sclerosis and contributes to enhanced fibrosis. *Ann Rheum Dis*. 2019 Sep;78(9):1249-1259. doi: 10.1136/annrheumdis-2018-214991. Epub 2019 May 24. PubMed PMID: 31126957.
- Vazirpanah N, **Ottria A**, van der Linden M, Wichers CGK, Schuiveling M, van Lochem E, Phipps-Green A, Merriman T, Zimmermann M, Jansen M, Radstake TRDJ, Broen JCA. mTOR inhibition by metformin impacts monosodium urate crystal-induced inflammation and cell death in gout: a prelude to a new add-on therapy? *Ann Rheum Dis*. 2019 May;78(5):663-671. doi: 10.1136/annrheumdis-2018-214656. Epub 2019 Feb 27. PubMed PMID: 30814053.

- Paardekooper LM, Bendix MB, **Ottria A**, de Haer LW, Ter Beest M, Radstake TRDJ, Marut W, van den Bogaart G. Hypoxia potentiates monocyte-derived dendritic cells for release of tumor necrosis factor α via MAP3K8. *Biosci Rep*. 2018 Dec 14;38(6). pii: BSR20182019. doi: 10.1042/BSR20182019. Print 2018 Dec 21. PubMed PMID: 30463908; PubMed Central PMCID: PMC6294625.
- Dolcino M, **Ottria A**, Barbieri A, Patuzzo G, Tinazzi E, Argentino G, Beri R, Lunardi C, Puccetti A. Gene Expression Profiling in Peripheral Blood Cells and Synovial Membranes of Patients with Psoriatic Arthritis. *PLoS One*. 2015 Jun 18;10(6):e0128262. doi: 10.1371/journal.pone.0128262. eCollection 2015. PubMed PMID: 26086874; PubMed Central PMCID: PMC4473102.
- Barbieri A, Dolcino M, Tinazzi E, Rigo A, Argentino G, Patuzzo G, **Ottria A**, Beri R, Puccetti A, Lunardi C. Characterization of CD30/CD30L(+) Cells in Peripheral Blood and Synovial Fluid of Patients with Rheumatoid Arthritis. *J Immunol Res*. 2015;2015:729654. doi: 10.1155/2015/729654. Epub 2015 May 19. PubMed PMID: 26090498; PubMed Central PMCID: PMC4452350.
- Elisa T, Antonio P, Giuseppe P, Alessandro B, Giuseppe A, Federico C, Marzia D, Ruggero B, Giacomo M, **Andrea O**, Daniela R, Mariaelisa R, Claudio L. Endothelin Receptors Expressed by Immune Cells Are Involved in Modulation of Inflammation and in Fibrosis: Relevance to the Pathogenesis of Systemic Sclerosis. *J Immunol Res*. 2015;2015:147616. doi: 10.1155/2015/147616. Epub 2015 May 18. PubMed PMID: 26090478; PubMed Central PMCID: PMC4451773.
- Dolcino M, Lunardi C, **Ottria A**, Tinazzi E, Patuzzo G, Puccetti A. Crossreactive autoantibodies directed against cutaneous and joint antigens are present in psoriatic arthritis. *PLoS One*. 2014 Dec 16;9(12):e115424. doi: 10.1371/journal.pone.0115424. eCollection 2014. PubMed PMID: 25514237; PubMed Central PMCID: PMC4267814.
- Dolcino M, Puccetti A, **Ottria A**, Barbieri A, Patuzzo G, Lunardi C. Modulation of

adaptive immune response following intravenous immunoglobulin therapy in common variable immunodeficiency. *Isr Med Assoc J.* 2014 Oct;16(10):648-50. PubMed PMID: 25438459.

- Dolcino M, Patuzzo G, Barbieri A, Tinazzi E, Rizzi M, Beri R, Argentino G, **Ottria A**, Lunardi C, Puccetti A. Gene expression profiling in peripheral blood mononuclear cells of patients with common variable immunodeficiency: modulation of adaptive immune response following intravenous immunoglobulin therapy. *PLoS One.* 2014 May 15;9(5):e97571. doi: 10.1371/journal.pone.0097571. eCollection 2014. PubMed PMID: 24831519; PubMed Central PMCID: PMC4022614.

Curriculum vitae



Name: Andrea Ottria, MD.
Address: Tweede Oosterparklaan 235; 3544 AS
Utrecht. The Netherlands
Email: andrea.ottria@gmail.com
LinkedIn: <https://it.linkedin.com/pub/andrea-ottria/b5/a56/b79>
Date of birth: 05 April 1987
Place of birth: Genova, Italy
Nationality: Italian
Gender: Male

Personal skills

Ambitious, perseverant, creative, eye for detail, reliable, lucky, good planner

Education

- ❖ 2015-2020
PhD student in Rheumatology at UMC Utrecht
Thesis: “The role of hypoxia and metabolism in the pathogenesis of systemic sclerosis” (Thesis defense date 10-6-2020)
- ❖ 2019
Taalvaardigheid Nederlands voor artsen certificate
- ❖ 2015
Course on Laboratory Animal Science (Utrecht University), Certification for permit to work with animals (art.9)
- ❖ 2008-2014
Master’s Degree in Medicine (Università degli Studi of Genova)
Graduation topic: “Finding of a serological marker of Psoriatic Arthritis: the presence of autoantibodies cross reacting against cutaneous and articular antigens”
Graduated with 110/110 summa cum laude and honour

❖ 2006-2008

Master's Degree in Pharmacy (Università degli studi di Genova)

❖ 2001-2006

Liceo Scientifico Leonardo Da Vinci Genova (high school)

Graduated with 100/100

Work experience

❖ January 2018- December 2019

Voluntary attendance at UMC Utrecht poli reumatologie under the supervision of Dr. Janneke Tekstra

❖ July 2016- December 2019

Responsible for the selection and inclusion of patients for research studies

Contact person for patients involved in research studies

Responsible of the clinical database for research studies

❖ October 2015- September 2019

PhD student at the UMC Utrecht, Utrecht University

Manuscripts in preparation and published:

- HIF-2 α stabilization by hypoxia and Toll-like receptor activation as the key mechanism for CXCL4 production (submitted manuscript)
- Targeting elevated fatty acid oxidation in Systemic Sclerosis: a novel add-on oxidative stress lowering therapy? (submitted manuscript)
- Indole as a potential remedy to prevent fibrosis formation in Systemic Sclerosis (in preparation)
- Localized scleroderma and eosinophil fasciitis, a metabolomic approach (in preparation)
- A distinct energy metabolism in monocyte derived dendritic cells of patients with Systemic Sclerosis; explaining an enhanced immune activity? (in preparation)
- CXCL4 drives fibrosis by promoting several key cellular and molecular processes in precursor cells. (submitted manuscript)

- mTOR inhibition by metformin impacts monosodium urate crystal induced inflammation and cell death in gout: a prelude to a new add-on therapy? (published)
- Hypoxia potentiates monocyte-derived dendritic cells for release of tumour necrosis factor α via MAP3K8. (published)
- Low RUNX3 expression alters dendritic cell function in patients with systemic sclerosis and contributes to enhanced fibrosis. (published)
- Semaphorin4A co-ordinately induces inflammation and fibrosis in systemic sclerosis. (published)

Techniques used:

- Elisa
- Cell culture (primary and cell line)
- Cell culture in hypoxic environment
- *In vitro* cell differentiation (pDCs from umbilical cord blood derived CD34+ cells)
- FACS (until 20 colours)
- PBMCs isolation
- Cell subset isolation with Automacs
- Cell transfection
- qPCR
- Western Blot
- Seahorse
- Mass Spec data analysis
- Optogenetic approach to induce mitochondrial ROS production in DCs

❖ September 2008- February 2014

Voluntary attendance as medical student at IRCCS Azienda Ospedaliera Universitaria San Martino (average 25% of working days)

❖ September 2008-July 2014

Training student at Department of experimental medicine at IRCCS Azienda Ospedaliera Universitaria San Martino IST (25 to 30% of working days)

Manuscripts published:

- Cross-reactive autoantibodies directed against cutaneous and joint antigens are present in psoriatic arthritis. (co-author)
- Gene expression profiling in peripheral blood cells and synovial membranes of patients with psoriatic arthritis. (co-main author)
- Gene expression profiling in peripheral blood mononuclear cells of patients with common variable immunodeficiency: modulation of adaptive immune response following intravenous immunoglobulin therapy. (co-author).
- Modulation of adaptive immune response following intravenous immunoglobulin therapy in common variable immunodeficiency. (co-author)
- Characterization of CD30/CD30L(+) Cells in Peripheral Blood and Synovial Fluid of Patients with Rheumatoid Arthritis. (co-author)
- Endothelin Receptors Expressed by Immune Cells Are Involved in Modulation of Inflammation and in Fibrosis: Relevance to the Pathogenesis of Systemic Sclerosis. (co-author)

Techniques used:

- Elisa
- Cell culture (primary and cell line)
- FACS
- PBMCs isolation

Awards

NVR Najaarsdagen 2019 - Best poster award

Additional skills

MS Office, windows and mac platform, basics in software programming, computer maintenance, Graphpad Prism, IBM SPSS, Adobe Photoshop, Adobe Illustrator, Adobe Indesign, HIX patient's system, Medicom patient system

Languages

Fluent in Italian (Native language), English (advanced), Dutch (advanced)

Hobbies

Videogaming, Do-it-yourself projects, Cooking, Sports (sailing and soccer)

In few words

Systemic sclerosis (SSc) is a rare autoimmune disease with heterogeneous symptoms and characterized by immune alteration, vascular abnormalities, fibrosis and hypoxia. SSc is a poorly understood disease with no available effective cure and an unknown pathophysiology. Recent studies identified chemokine (C-X-C-motif) ligand-4 (CXCL4) as a potential biomarker produced by pro-inflammatory immune-cells. Besides, alteration in fat metabolism has been shown to elicit immune-cell polarisation in SSc.

The aim of this thesis is to explore the augmented production of CXCL4 and its role in aberrant fibrogenesis in patients with SSc. Moreover, the metabolic status of fat biology in pathophysiology of SSc was further inquired.

In healthy immune-cells CXCL4-production depends on mitochondrial reactive oxygen species and hypoxia inducible factor (HIF)-2 α stabilization. We observed that Toll-Like receptor (TLR) triggered upon hypoxic environment is responsible for augmented CXCL4-production in SSc. Also, we pinpointed the potential beneficial role of HIF-2 α stabilization on cytokine production and confirmed its potential features as a therapeutic target in SSc treatment. Besides, we demonstrated that fatty acids and carnitine composition were altered in SSc and demonstrated that inhibiting fatty acid oxidation abates pro-inflammatory cytokine production in immune-cells of SSc patients. Finally, we observed that inhibition of mammalian target of rapamycin (mTOR), with metformin reduces pro-inflammatory cytokine production, signifying the potential therapeutic effect of metabolic mediators in immune cells.

Taken together, targeting TLR stimulation, HIF-2 α stabilization and fatty acid oxidation inhibits aberrant cytokine and CXCL4-production in immune cells and metformin treatment can contribute in reducing pro-inflammatory cytokine production in patients with SSc.

In het kort

Systemische sclerose (SSc) is een zeldzame auto-immuunziekte met heterogene symptomen en wordt gekenmerkt door immuun veranderingen, vaatafwijkingen, fibrose en hypoxie. SSc is een aandoening zonder effectieve genezing met een onbekende pathofysiologie. Recente studies hebben chemokine (C-X-C-motief) ligand-4 (CXCL4) geïdentificeerd als een potentiële biomarker die wordt geproduceerd door pro-inflammatoire immuuncellen. Bovendien is aangetoond dat veranderingen in het vetmetabolisme de polarisatie van immuuncellen in SSc opwekken.

Het doel van dit proefschrift is om de verhoogde productie van CXCL4 en zijn rol in afwijkende fibrogenesis bij patiënten met SSc te onderzoeken. Daarnaast, werd de metabole status van vetbiologie in de pathofysiologie van SSc nader onderzocht.

In gezonde immuuncellen is de CXCL4-productie afhankelijk van mitochondriale reactieve zuurstofspecie en hypoxie-induceerbare factor (HIF) -2 α -stabilisatie. We hebben waargenomen dat Toll-Like receptor (TLR) die wordt geactiveerd in een hypoxische omgeving verantwoordelijk is voor een verhoogde CXCL4-productie in SSc. We hebben ook de potentiële gunstige rol van HIF-2 α -stabilisatie op de cytokineproductie vastgesteld en de potentiële kenmerken ervan als therapeutisch mogelijkheid bij SSc-behandeling aangetoond. Daarnaast hebben we bewezen dat vetzuren en carnitine-samenstelling in SSc zijn veranderd en dat het remmen van vetzuuroxidatie de pro-inflammatoire cytokineproductie in immuuncellen van SSc-patiënten vermindert. Tenslotte hebben we vastgesteld dat remmen van het mammalian target van rapamycine (mTOR) met metformine de pro-inflammatoire cytokineproductie vermindert, wat het potentiële therapeutische effect van metabole mediators in immuuncellen aangeeft.

Samengenomen, reguleren van TLR-stimulatie, HIF-2 α -stabilisatie en vetzuuroxidatie remt afwijkende cytokine- en CXCL4-productie in immuuncellen en behandeling met metformine kan bijdragen aan het verminderen van pro-inflammatoire cytokineproductie bij patiënten met SSc.